Modeling decision-making in social systems: a network dynamical systems approach

Author: Camilla Ancona

UNIVERSITÀ
DEGLI STUDI
DI BERGAMO

UNIVERSITÀ DEGLI STUDI DI NAPOLI
FEDERICO II

Tutor: Prof. Pietro De Lellis

Supervisor: Prof. Francesco Lo Iudice

Abstract

The aim of this thesis is to advance our ability to model the decision making-process in social systems, with the overarching goal of helping policymakers and government bodies take mathematically backed decisions. Toward this aim, we adapted a complex network approach, leveraging tools from network science, control theory, and social science which altogether offers a powerful and multidisciplinary approach to tackle the complexity that pervades social dynamics. We explored the conditions under which we can confer given controllability and observability properties to complex networks of dynamical systems, so to have an insight on our ability to steer or monitor their collective behaviors in the presence of realistic constraints. Then, we studied the opinion dynamics in groups of interconnected individuals discussing on a given topic, that is, we analyzed the evolution over time of their opinions under the effect of social ties and other psychological traits, such as stubbornness or the tendency to conform. Opinions dynamics models enable us to describe the collective behaviors that occur in real world social groups and to unveil how the social interactions, namely the peer pressure and other biases, shape our opinion formation and result in the group exhibiting behaviors such as consensus, disagreement, or polarization of opinions. In particular, we analyzed how external influences, such as the ones exerted by opinion leaders (the so-called influencers) can steer the opinion profile of a social group towards a desired state at steady state. To this aim, we borrowed a tool from network control, namely pinning control, to show how agents with relatively few connections can exploit the structure of the social interconnections to diffuse their influence throughout the social group. Using heuristic approaches and leveraging theoretical and graphical knowledge of the network dynamical systems under investigation, we showed that a smart selection of the individuals to directly influence allows to maximize the effect of persuading actions of opinion leaders. Finally, we illustrated how the model we proposed can provide quantitative predictions on opinions' distribution in a given population, which in turn can be used to gauge the effectiveness of different awareness campaigns strategies aimed at mitigating vaccine hesitancy.

List of Figures

List of Tables

Acknowledgements

Abbreviations

DT Discrete-time

CT Continuous-time

OD Opinion dynamics

NLP Natural Language Processing

ODE Ordinary Differencial Equation

DDE Discrete Difference Equation

SCC Strongly Connected Component

DAG Directed Acyclic Graph

RSCC Root Strongly Connected Component

WS Watts and Strogatz

ER Erdős-Rényi

EC Eigenvector Centrality

DC Degree Centrality

BC Betweenness Centrality

F-J Friedkin-Johnsen

CODA Continuous Opinions Discrete Actions

GDM Group Decision Making

PBH Popov-Belevitch-Hautus

LTI Linear Time-Invariant

Contents

Introduction

In the last decades, modeling and controlling of complex dynamical systems has drawn great attention from the scientific community because of the need to capture the increasing complexity that pervades a wide variety of fields such as business and management, social sciences, information technology, finance, and especially those where an analytical framework can support decision-making process [3–6]. For example, let us reckon on enterprises having to cope with growing complexity originating from an extremely competitive economy, the higher demand of sophisticated and customizable products and the unpredictability of online purchases. The same challenges must be made by governments when dealing with events, such as pandemics, wars, economic crises, that have a global impact and require the coordination of many entities and decisions to be readily made. These are only a few of the examples that motivate the attempt made in this thesis to endow policymakers and government bodies of tools to allow taking mathematically backed decisions. Indeed, the overarching goal is to use a comprehensive quantitative approach that can help describe, analyze and then smartly act on dynamical process within a general framework, that can support decision-making in a wide range of application.

Schooling of fishes, fleets of robots, social groups, power grids, what they have in common? At first glance, one could answer "nothing" as they belong to very different environments, but actually they are all examples of networks of dynamical systems, that share some key aspects: a dynamical nature, that is the evolution over time of their characteristics, both at an individual level and on a collective one, and an underlying structure that describes in which ways their components interact to each other, namely the network of interconnections, which plays a fundamental role in determining the dynamics of the whole.

Complexity theory is the mathematical tool that enable us to study how such interconnected dynamical systems can give a rise to collective mechanisms that we can observe in real life. "Complex" does not mean necessarily "complicated": a complex system is made up with simple elements among which there are strong local interactions, that lead to an emergent and unexpected global behavior of the system in a whole self-organized way, that is, without any central control unit. Typically, complexity does not refer to the individuals' dynamics, but to their interconnections among each other and with their environment. An effective way to represent an ensemble of connected dynamical systems is in terms of a network, where a graph describes the interactions among the individuals.

Studying complex systems as networks provide a cross-disciplinary framework that allows to analyze, monitor, control, and predict the evolution over time of different types

of network systems because, thanks to their similar topological properties, they tend to exhibit similar non-trivial collective behaviors such as synchronization, consensus, organization in hierarchical structures.

Complexity theory has been the methodological backbone of this thesis, which is organized in two parts. Part I focused on expanding the theory on control of network dynamical systems with the goal of investigating sufficient conditions for unilateral controllability and observability, to complex networks of Linear Time-Invariant (LTI) dynamical systems. Addressing these problems can help us to unveil under which conditions we can effectively act and monitor these network dynamical systems under realistic constraints that make control and observe them a tough goal, to ultimately support decision-making process on how to allocate limited resources such as sensors and actuators.

The second part, instead, focused on a specific complex system of interest, namely social systems. Specifically, in complex networks of social systems, the object of study are the opinion dynamics in groups of individuals sharing information on a given topic through a network of interaction. Their social ties among the individuals, as well as their intrinsic characteristics, such as stubbornness or susceptibility to social pressure, contribute to the dynamical diffusive process of opinion formation, which results in interesting collective behaviors such as consensus, disagreement, and polarization. In this thesis, we have revisited classic opinion dynamics models to also describe the decisions associated to the opinions, trying to uncover which are the mechanisms that influence opinion formation and decision-making in large social groups.

Finally, we leveraged pinning control, a classic control strategy for network systems, to model how opinion leaders (aka influencers) shape the action of social groups, uncovering topological factors that can be exploited to maximize their (beneficial or detrimental) effect on the outcome of a discussion. This mathematical description allowed a quantitative understanding on how opinion diffuse on social media, an understanding that can help policymakers to test the effectiveness of potential initiatives. Finally, we took a step forward to bridge the gap between explanatory models and applications, by providing a method to tune the parameters of these models. In this way, models can provide, beyond a qualitative description of the social phenomenon under analysis, also the ability of predicting future scenarios. To demonstrate our approach, we have considered as a paradigmatic example the controversial debate on vaccines during Covid-19 pandemic, where we have used an opinion dynamics model tuned on survey data to evaluate the effectiveness of different awareness campaign strategies to tackle vaccine hesitancy on a group of Italian citizens.
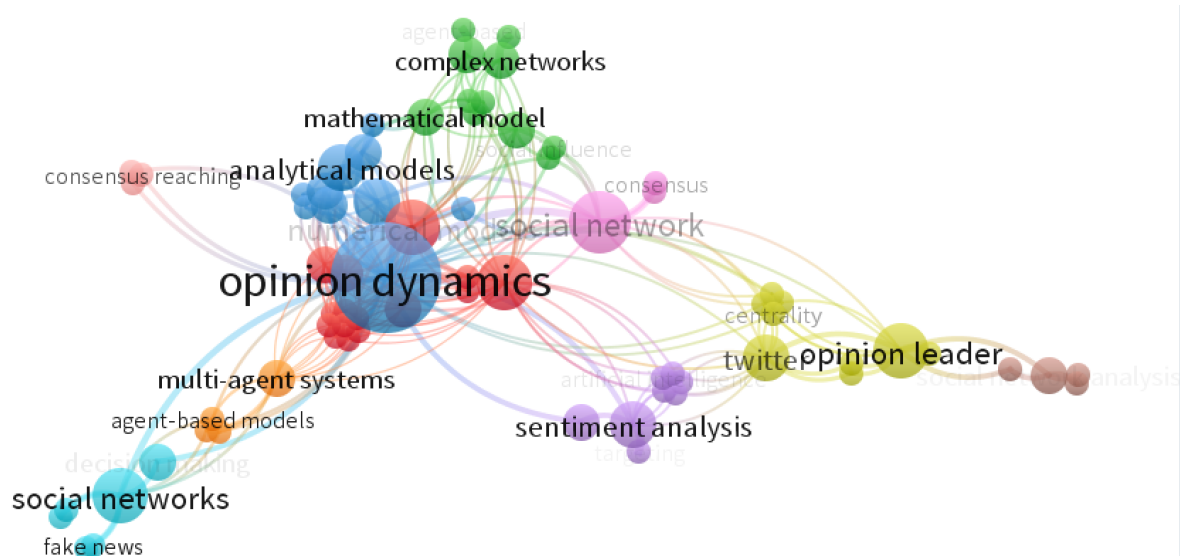
Figure 0.1. Co-occurence graph of keywords of articles included in this thesis.

Thesis outline

The thesis is divided in three parts:

 I. theoretical background,

 II. literature review,

 III. contributions.

In part I, we introduce the key concepts of graph theory, the main complex networks topologies and their properties that have been considered in the works presented below. Then, we provide theoretical background on the most commonly studied emerging behaviors in the context of complex networks of dynamical systems, with emphasis on synchronization and consensus. Next, we tackle the problem of controlling these network dynamical systems, first from the standpoint of conferring given controllability and observability properties and then focusing on structural approach and pinning control as mathematical tools to achieve control goals.

Part II presents a comprehensive taxonomy of the literature on opinion dynamics, providing a critical overview highlighting gaps, limitations, and potential future directions in this field of application of complex dynamical networks.

Part III consists of edited versions of four contributions, with additional unpublished analyses and considerations.

Then, conclusions and open problems are discussed. Finally, the thesis also includes two appendices:

 – Appendix A collects the printed version of journal papers co-written by the author of this thesis.

 – Appendix B gives a brief introduction to Natural Language Processing tasks and methods.

Part I

Theoretical Background

CHAPTER 1

Complex networks of dynamical systems

Studying complexity by means of networks of dynamical systems has been inspired by two seminal articles: one by Watts and Strogatz on Small-World networks [7] and the other by Barabási on Scale-Free networks [8] which both investigated structural properties of complex networks. The network structure is essential in modeling interactions among single systems, as they lead to the emergence of interesting macroscopic behaviors of the ensemble that cannot be deduced from the microscopic properties of its parts. On the other hand, another key aspect to investigate is the dynamical nature of such systems, that is how the state, i.e., the set of variables that best characterize the interconnected system, changes over time. Since then, a series of metrics have been proposed to quantify and compare the properties of these types of networks with real-world ones, to link topological features with given interesting behaviors. Indeed, nature offers a lot of examples of collective behaviors such as flocking of birds, flashing of fireflies, self-organization in ants colonies. When we consider an ensemble of dynamical systems that are decoupled, their dynamics is simply the sum of individuals' dynamics. Let us think about some people in a room without any visual or verbal communication tie: they think exactly the same as if they were alone. Whereas, when they interact with each other, there may be the emergence of collective behaviors, such as synchronization, consensus, coordination, polarization, that cannot be explained only looking at the individual dynamics. Hence, we want to learn from nature how the feedback paradigm and so the interconnection between systems is crucial to the emergence of an observed (analysis problem) or desired (control problem) collective behavior to better comprehend these fascinating phenomena and become able to replicate/induce them also in real-world ap-
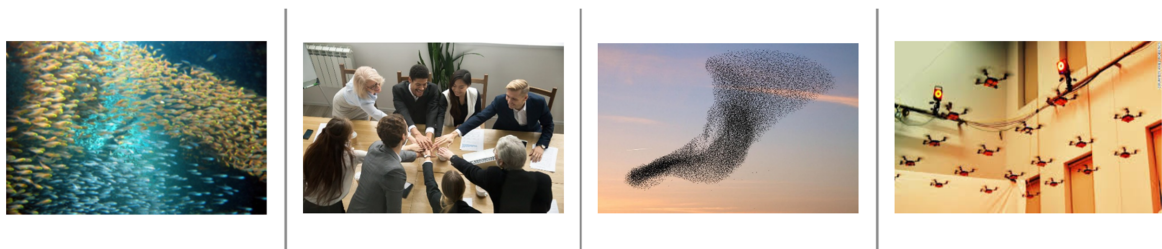
Figure 1.1. Examples of complex systems: from the left school of fishes, social systems, flock of birds, fleets of drones.

plications such as formation in robotics, time-synchronization in power grids, consensus in opinion dynamics, see Figure 1.1.

The mathematical models considered in this thesis will describe complex networks of dynamical systems assumed made up by nodes which represent single dynamical systems coupled with a given interaction protocol occurring onto a certain network topology. The general network model is described by the following set of ordinary differential equations (ODEs):

$$\dot{x}_i = f_i(x_i) + g_i(u_i(x_i, x_j)) \quad \forall i, j = 1, \ldots, N \tag{1.1}$$

Note that an analogous model can be given in discrete-time, i.e.,

$$x_i(k+1) = \phi_i(x_i(k)) + g_i(u_i(x_i, x_j)) \quad \forall i = 1, \ldots, N \tag{1.2}$$

Therefore, we can identify the following three key ingredients to characterize a complex network model:

(a) The interconnection structure that represents network topology and can be described by the adjacency matrix $A := a_{ij} \in \mathbb{R}_{\geq 0}, i, j = 1, \ldots, N$.

(b) A model of the intrinsic dynamics of each agent i. The dynamical system can be represented in Continuous-time (CT) or in Discrete-time (DT). In CT, it has the form of an Ordinary Differencial Equation (ODE)

$$\dot{x}_i = f_i(x_i), \forall i = 1, \ldots, N$$

where $x_i \in \mathbb{R}^n$ represents the vector of the state variables of each system, say n, and thus the network state will be the stack vector $x \in \mathbb{R}^{n \times N}$, and $f_i(x_i)$ is the i-th component of the smooth vector field $f : \mathbb{R}^n \to \mathbb{R}^N$.

In compact form, we have in CT, a set of ODEs

$$\dot{x} = f(x),$$

and analogously, in DT, we have a set of Discrete Difference Equation (DDE)s

$$x(k+1) = \phi(x(k)), \quad k = 1, \ldots, N,$$

where $\phi : \mathbb{R}^n \to \mathbb{R}^N$.

(c) The interaction protocol $g_i(u_i(x_i, x_j))$ defines how the single entities interact with each others: the most common framework in the literature is the linear diffusive interaction protocol where $g_i(\cdot)$ is the identity matrix and $u_i = \sigma_i \sum_{J=1}^{N} a_{ij} [h(x_j) - h(x_i)]$, where σ_i represents the coupling strength or gain associated to agent i, a_{ij} is the generic element of the adjacency matrix A, and $h(\cdot)$ is a function of the state variables $x_i \ \forall i = 1, \ldots, N$.

For simplicity, some assumptions are usually made:

- The agents are homogeneous, that is, all nodes are identical and share the same dynamics $f_i(x) = f_j(x) = f(x)$

- All the states are measurable: $h(j) = x(j)$

- The network is static: σ and A are time-invariant

With these assumptions, the model simplifies as follows:

$$\dot{x}_i = f\left(x_i\right) + \sigma \sum_{j \in N_i} a_{ij}\left(x_j - x_i\right) \quad \forall i = 1, \ldots, N \tag{1.3}$$

In this framework, a complex network is made up of many entities, or nodes, each of which represents a dynamical system. For a single nonlinear dynamical system, we can write its state space model as

$$\dot{x}(t) = f(t, x(t), u(t); \Theta) \tag{1.4a}$$
$$y(t) = h(t, x(t), u(t); \Theta) \tag{1.4b}$$

where the vector $x \in \mathbb{R}^N$ represents the state of the system at time t, the input vector $u \in \mathbb{R}^M$ captures the known input signals, and the output vector $y \in \mathbb{R}^P$ is the set of measures. The functions $f(\cdot)$ and $h(\cdot)$ are generally nonlinear, and Θ is the set of system's parameters. Equations (1.4a) and (1.4b) are called the state and output equations, respectively.

If $f(\cdot)$ and $h(\cdot)$ are linear and the parameters are time-invariant, we can define the class of LTI systems:

$$\dot{x}(t) = Ax(t) + Bu(t); \tag{1.5a}$$
$$y(t) = Cx(t) \tag{1.5b}$$

The matrices $A \in \mathbb{R}^{N \times N}$, $B \in \mathbb{R}^{N \times M}$, $C \in \mathbb{R}^{P \times N}$ in Eq. (1.5) admit two different interpretations depending on whether we refer to a dynamical system or a network of N dynamical systems. In the first case the matrix A defines the system dynamics, the matrix B represents the effect of M inputs in the vector u on the N state variables x and the matrix C defines which P linear combinations of state variables are measured and form the output vector y. In the second interpretation, $A = \{a_{ij}\}_{i,j=1}^N$ is the network adjacency matrix associated to a graph. Its ij-th element is different from zero if the dynamics of the state x_i of node i is affected by the state x_j of node j. The elements on the diagonal a_{ii} capture the intrinsic node dynamics and are represented as self-loops (i.e., connections from a node to itself) in the graph. In this second scenario, the matrix B identifies the nodes where the M input signals are injected, the actuators or driver nodes. Along the same lines, the matrix C indicates the sensor nodes, i.e., the nodes whose state we are able to directly measure.

In the next subsection, some fundamental concepts of graph theory and network science will be given in order to better understand the link between dynamical systems and complex networks.

1.1   Graph theory

A very intuitive way of describing how entities are interconnected forming a network is visualizing their communication ties by means of a graph and its properties. In the following, some definitions are given:

Definition 1. *A graph $\mathcal{G} = \{\mathcal{V}, \mathcal{E}\}$ is a pair of sets, where $\mathcal{V} = \{1, \dots, N\}$ is the set of vertices or nodes and $\mathcal{E} \subset \mathcal{V} \times \mathcal{V}$ is the set of edges $(i, j) \in \mathcal{E} : i, j \in \mathcal{V}$ connecting node i and j.*
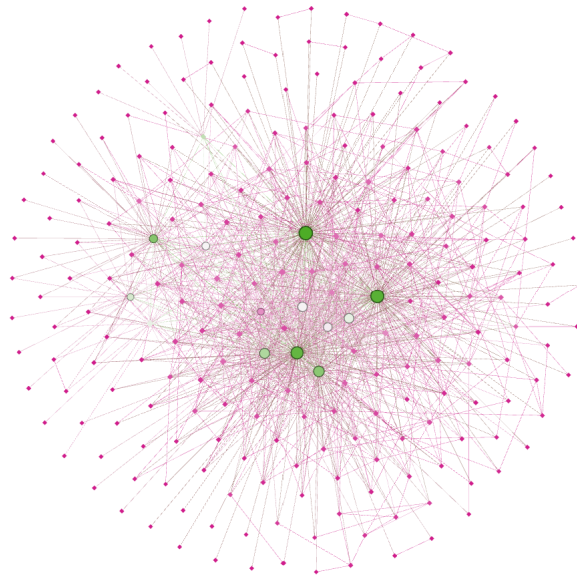
Figure 1.2. Example of the real network of US airports. The nodes size and color are related to their centrality: the nodes in green are the hubs, the ones with higher average degree.

Definition 2. *A graph is called undirected when the direction of the edges is not specified, that is $(i, j) = (j, i) \in \mathcal{E}$.*

Definition 3. *A directed graph or digraph is a graph where the edges are a set of ordered pairs, that is, $(i, j) \neq (j, i) \in \mathcal{E}$.*

Definition 4. *Given a pair of nodes (i, j) we say that i and j are connected if $(i, j) \in \mathcal{E}$. The set of neighbors of node i is: $\mathcal{N}_i = \{j : (i, j) \in \mathcal{E}\} \subset \mathcal{V}$.*
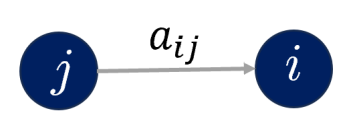
Figure 1.3. Our "influence" convention for edge notation for directed graphs.

Definition 5. *A weighted graph is the triplet $\mathcal{G} = \{\mathcal{V}, \mathcal{E}, \mathcal{W}\}$, where $\mathcal{V}$ is the set of nodes, $\mathcal{E} \subseteq \mathcal{V} \times \mathcal{V}$ is the set of edges, and $\mathcal{W}$ is the set weight function that associates to every edge $(i, j) \in \mathcal{E}$ a positive weight w_{ji}.*

Definition 6. *Given a subset $\mathcal{V}_s \subset \mathcal{V}$ of the nodes of graph $\mathcal{G}$, we define the* subgraph *$\mathcal{G}_s$ of $\mathcal{G}$ as the pair $(\mathcal{V}_s, \mathcal{E}_s)$, where $\mathcal{E}_s := \mathcal{E} \cap (\mathcal{V}_s \times \mathcal{V}_s)$.*

Definition 7. *Given two vertices, say i and j, i is* reachable *from j if there exists a directed path from j to i. If this holds, i is in the* downstream *of j and j is in the* upstream *of i.*

Definition 8. *For an undirected graph $\mathcal{G}$, a path between nodes i and $j (i, j \in \mathcal{V})$ is a sequence of distinct nodes $k_1, \ldots, k_\ell \in \mathcal{V}$ such that all consecutive pairs are edges of $\mathcal{G} : (j, k_1), (k_1, k_2), \ldots, (k_\ell, i) \in \mathcal{E}$.*

Definition 9. *For a digraph $\mathcal{G}$ a (directed) path between i and j is a sequence of distinct nodes $k_1, \ldots, k_\ell \in \mathcal{V}$ such that all consecutive pairs are directed edges of $\mathcal{G} : (j, k_1), (k_1, k_2), \ldots, (k_\ell, i) \in \mathcal{E}$ (the directed path is $j \to k_1 \to \ldots \to k_\ell \to i$).*

Definition 10. *A (directed or undirected) path that begins and ends at the same node is called a* cycle. *A graph is said acyclic if it contains no cycle.*

Definition 11. *A graph is called covered by a subgraph if they have the same set of vertices.*

Definition 12. *A state vertex is called source if it has only edges that come out from it.*

Definition 13. *A state vertex is called sink if it has only edges that enter in it.*

Definition 14. *A stem is an elementary path in which its start node is a source and its end node is a sink.*

Definition 15. *A bud is a cycle with an additional edge that ends but not begins in a vertex contained in the cycle itself.*

Definition 16. *We define a* stem-cycle disjoint subgraph *as a subgraph of $\mathcal{G}$ composed of disjoint stems and cycles. We say that a* stem-cycle disjoint subgraph *spans from a given set of nodes, if the source node of each stem in the subgraph is encompassed in this set.*

Definition 17. *A state vertex is called inaccessible if there isn't any direct path from drivers to it.*

Definition 18. *A (undirected) graph $\mathcal{G}$ is connected if there is am (undirected) path between any two nodes.*

Definition 19. *A digraph is strongly-connected if for any vertex pair (i, j) there exist either a directed path from vertex j to vertex i or a directed path from vertex i to vertex j.*

Definition 20. *A SCC of a directed graph is a maximal strongly connected subgraph.*

Definition 21. *A Root Strongly Connected Component (RSCC) is an SCC whose nodes have incoming edges only from nodes of the same SCC.*

Definition 22. *A condensation of a graph say $\mathcal{C}$, is a DAG that is a directed graph $\mathcal{G}'$, whose vertices are strongly connected components of G, and the edge in $\mathcal{G}'$ is present only if there exists at least one edge between the vertices of corresponding connected components.*
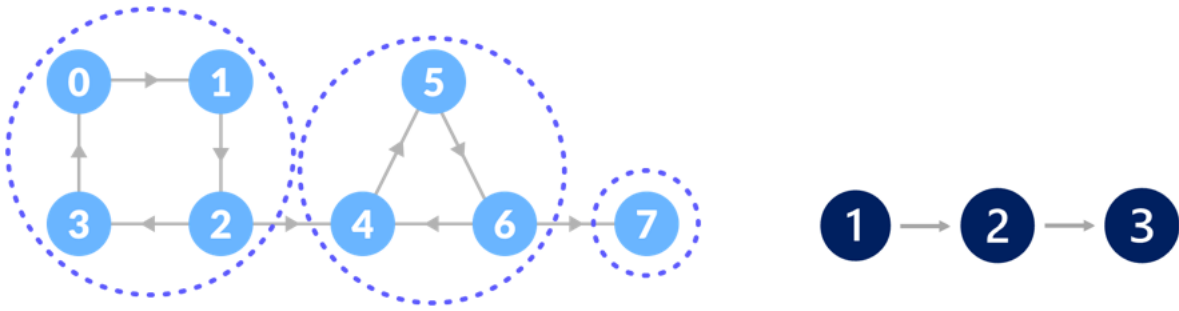
Figure 1.4. On the left panel we have a graph in which we can identify 3 SCC, on the right the DAG of this graph.

Definition 23. *For an undirected graph, the degree of a node i is the number of its neighbors $\delta(i) = |\mathcal{N}_i|$.*

Definition 24. *For digraphs, for a given node i, we define the node in-degree (out-degree) δ_i^{in} (δ_i^{out}) as the number of inbounding (outgoing) edges of i, $k_i^{\text{in}} := |\mathcal{N}_i^{\text{in}}|(k_i^{\text{out}} := |\mathcal{N}_i^{\text{out}}|)$. Then the* degree *of node i is defined as $k_i := \delta_i^{\text{in}} + \delta_i^{\text{out}}$. Note that for any graph holds that $|\mathcal{E}| = \sum_i \delta^{\text{in}}(i) = \sum_i \delta^{\text{out}}(i)$.*
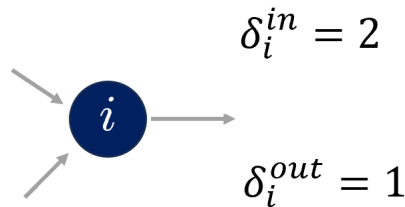
Figure 1.5. In-degree and out-degree of node i

Definition 25. *A node with zero in-degree is called a root while one with zero out-degree is called a leaf of $\mathcal{G}$.*

Definition 26. *The weighted in/out-degree are computed in terms of the weights of matrix W :*

$$\delta_w^{\text{in}}(i) \quad = \sum_{j=1}^{n} w_{ij}$$

$$\delta_w^{\text{out}}(i) \quad = \sum_{j=1}^{n} w_{ji}$$

Definition 27. *The degree distribution $P(k)$ is defined as the probability that a randomly chosen node has degree k or, equivalently, as the fraction of nodes in the network that have degree k.*

Definition 28. *The in-degree distribution $P(k_{\text{in}})$ of a digraph is a function that associates to each integer $k_{in} \in [0, \infty)$ the fraction of nodes having in-degree equals to k_{in}.*

Definition 29. *The out-degree distribution $P(k_{\text{out}})$ of a digraph is a function that associates to each integer $k_{\text{out}} \in [0, \infty)$ the fraction of nodes having out-degree equals to k_{out}.*

The network topology is the structure accordingly to which the links and nodes of a network are arranged to be interconnected; however, if the number of nodes explodes, then, graphs are not as informative as before, thus it is more convenient to describe the interconnections with an associated matrix

Definition 30. *Considering a matrix R, it is defined as non-negative if all of its entries r_{ij} are non-negative, that is $r_{ij} \geq 0$.*

Definition 31. *An adjacency matrix $A = \{a_{ij}\}_{i,j=1}^{N}$ is a non-negative matrix which synthesizes the information on the interaction among the nodes of the network. It is a square matrix with nodes both on the rows and columns $A \in \mathbb{R}^{N \times N}$ whose ij-th element $a_{ij} \geq 0$ with $i \neq j$ if there is an edge connecting the node j to the node i. If the matrix A is symmetric, the graph is undirected.*

Definition 32. *A graph is strongly connected if and only if the matrix associated to it is irreducible. [9].*

Definition 33. *A non-negative matrix R is said to be row-stochastic if, for all $i = 1, \ldots, n$, there holds that $\sum_{j=1}^{n} r_{ij} = 1$ whereas it is said to be doubly-stochastic if $\sum_{j=1}^{n} r_{ij} = 1$ and $\sum_{i=1}^{n} r_{ij} = 1$.*

Definition 34. *A non-negative square matrix $R \in \mathbb{R}^{n \times n}$ is primitive if there exists $k \in \mathbb{N}$ such that $R^k > 0$.*

Definition 35. *An irreducible matrix is a matrix in which the sum of the power k of R is strictly greater than zero: $\sum_{k=0}^{n-1} R^k > 0$.*

Definition 36. *The Laplacian matrix $\mathcal{L} = D - A$ is the difference between the degree matrix, which on the super diagonal has the degree of each node and zero otherwise, and the adjacency matrix.*

Definition 37. *Given a matrix, say F, we denote its rank by $\rho(F)$.*

1.2   Complex network topologies

Complexity stands for the nontrivial structure of interconnection among the entities considered. In the literature, some models of artificial topologies of complex networks have been proposed, each of which resembles some feature observed in real-world networks. In a spectrum ranging from the most human-made to the most realistic, let us give a brief insight on regular lattices, random, small world and Scale Free networks.

Traditionally, the connection structure was modeled either completely regular (each node is linked to a fixed, known a priori number of neighbors) or completely random graphs. Random networks were theorized in 1960 by Erdős-Rényi [10] defined as networks whose degree distribution follows a Poisson distribution with a single parameter *lambda* that corresponds both to its first and second moment, that is, is expected value and its variance

$$p_k = \frac{\lambda^{k_{\max}}}{k_{\max}!} e^{-\lambda}.$$

Both in nature and in engineered networks there are a lot of examples of interconnections that do not fall in neither of these two categories, as they are provided with non-trivial topological features. Therefore, there is the effort to find new network models that could mimic the structural properties of real networks, namely the complex networks.

In 1998, Watts and Strogatz [11] investigated in particular two network features: the characteristic path length L that is the length of the shortest path between any two nodes averaged over all possible pairs, and the clustering coefficient C_c that measures the cliquishness of a typical neighborhood (that is the likelihood that given three nodes they form a triangle of interconnections). They assessed that regular networks are characterized by high L and low C_c, random networks exhibit both low L and C_c but, instead, most of the real networks did not lie in these two simple categories, but stayed somewhere in the middle, being characterized by low mean characteristic path length but high clustering coefficient. Hence, starting from a regular graph, they thought of randomly rewiring a fraction of edges accordingly to a probability p : the more p is increasing the more the network becomes random, generating a new topology model called Small World or Watts and Strogatz (WS) network. It has been proved that a rewiring probability of 0.15 is sufficient to reveal WS features.

Even if the small world networks have been a huge step forward in modeling real networks, they are still characterized by a certain homogeneity of degree, however as Barábasi and Albert noted in 1999 [12], studying the features of the World Wide Web or of genetic networks, many real networks are characterized by a scale-free power law degree distribution.

A Scale-Free network is defined as a network whose degree distribution follows a power law $p_k = Ck^{-\gamma}$ that provides that a node has exactly k links. For a scale-free network, the nth moment of the degree distribution is: $\langle k^n \rangle = C \frac{k_{\max}^{n-\gamma+1} - k_{\min}^{n-\gamma+1}}{n-\gamma+1}$

For many scale-free networks, the degree exponent γ is between 2 and 3. Hence, for these in the $n \to \infty$ limit, the first moment $\langle k \rangle$ is finite but the second and higher moments go to infinity. This divergence helps us understand the origin of the "scale-free" term. Indeed, if the degrees follow a normal distribution, then the degree of a randomly chosen node is typically in the range $k = \langle k \rangle \pm \lambda k$. For power law distributions with $\gamma < 3$, instead, when we randomly choose a node, we do not know what to expect: the selected node's degree could be low or arbitrarily large. Hence, networks with $\gamma < 3$ do not have a meaningful internal scale but are "scale-free".

Comparing Erdős-Rényi and Scale-Free networks, it can be noted that:

- For small k, a scale-free network has a large number of small degree nodes, most of which are absent in a random network.

- For $k \approx \langle k \rangle$ in a random network there is an excess of nodes with degree $k \approx \langle k \rangle$.

- For large, k the probability of observing a high-degree node, or hub, is hugely higher in a scale free than in a random network.

Generation algorithms for synthetic networks

Random networks can be generated by following few simple steps:

- start with N disconnected nodes,

- draw from a uniform distribution a pair of nodes to be connected,

- generate a link between the selected nodes unless they are already connected or they are the same node

These steps must be repeated until the network has a predefined number of edges $|\mathcal{E}|$. Small world networks start from a regular network (ring lattice) of N nodes of mean degree k. Each node is connected to its $k/2$ nearest neighbors on either side. For each node in the graph, a target edge is rewired with probability p. The rewired edge cannot
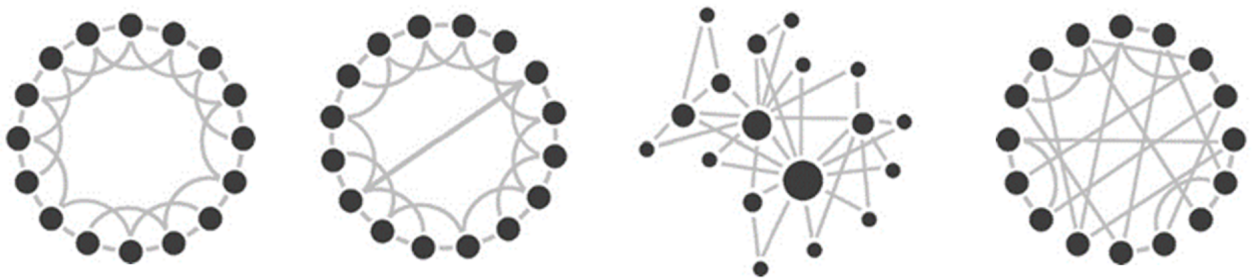
Figure 1.6. Increasing disorder in graph topologies: from left to right, regular, small-world, scale-free and random graphs.
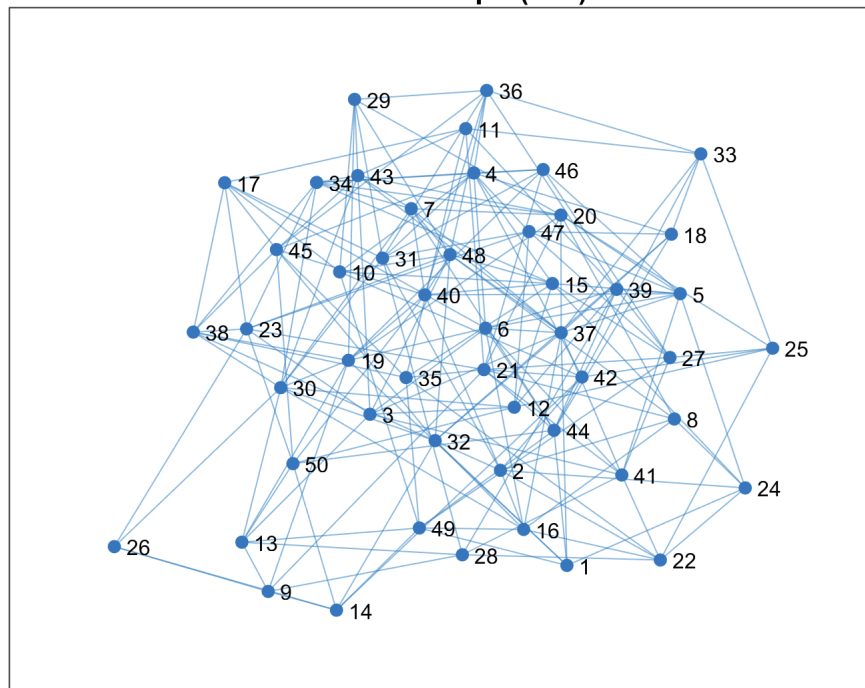
Figure 1.7. Example of a random network of 50 nodes.

be a duplicate or self-loop. So when $p = 0$, no edges are rewired and the model returns a ring lattice. In contrast, when $p = 1$, all the edges are rewired and the ring lattice is transformed into a random graph. When $0 < p < 1$ the features of a small world graph can be appreciated.

Barábasi and Albert realized that two aspects of generation of real networks were not incorporated in these models. First, both models assume that we start with a fixed number N of vertices that are then randomly connected (Erdős-Rényi (ER) model), or reconnected (WS model), without modifying N. In contrast, most real world networks form themselves by adding new nodes that are connected to the vertices already present in the network, thus the number of vertices N increases during the time. Moreover, the random network models assume that the probability that two vertices are connected is random and uniform. In truth, there is a higher probability that the new node will be linked to a vertex that already has numerous connections. These ideas concentrate in two concepts: growth and preferential attachment.

The steps of the algorithm to generate a scale free network are: start with a small number, say m_0, of vertices, at every time step add a new vertex with $m \leq m_0$ edges that link the new vertex to m different vertices already present in the system. The probability π that a new vertex will be connected to vertex i depends on the connectivity k_i of that vertex, so that $\pi(k_i) = \frac{k_i}{\sum_j k_j}$. After t time steps, the model leads to a scale-free network with $t + m_0$ vertices and mt edges. The algorithms presented above were used to generate undirected random, small world and scale free graphs.

In the following several procedures to generate directed graphs are illustrated.
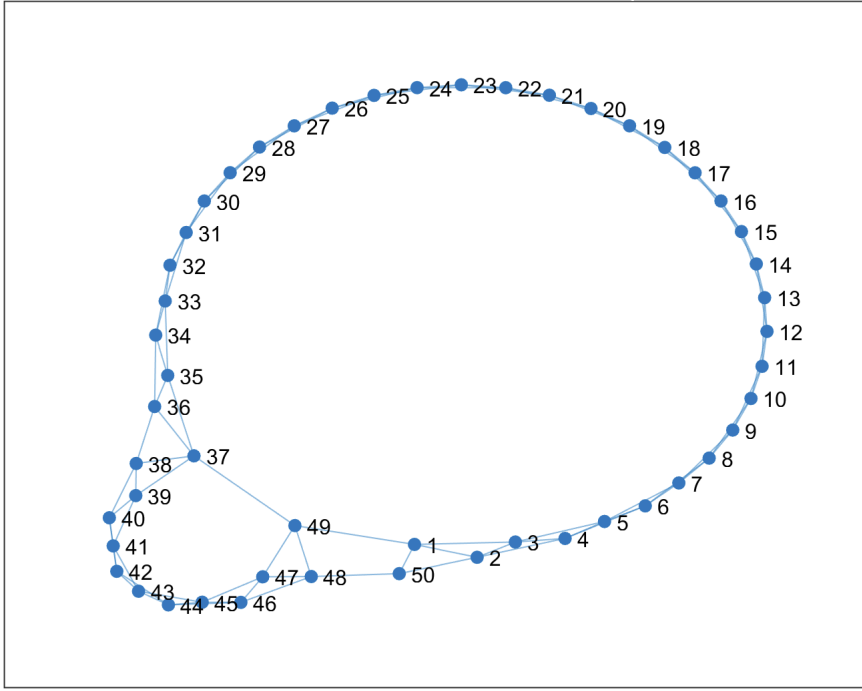
Figure 1.8. Example of small world network with a rewiring probability of $p = 0.16$.

Scale-free networks were generated by means of the directed version of the static model [13]. The static model steps to generate a directed network are: consider N vertices, which are indexed by an integer $i = 1, \ldots, N$. Assign two weights $p_i = i^{-\alpha_{out}}$ and $q_i = i^{-\alpha_{in}}$ to each vertex for outgoing and incoming edges, respectively. Both control parameters α_{out} and α_{in} are in the interval $[0, 1)$. Then two different vertices (i, j) are selected with probabilities, $p_i / \sum_k p_k$ and $q_i / \sum_k q_k$, respectively, and an edge from the vertex i to j is created with an arrow, i $\rightarrow$> j unless one exist already. This process is repeated until mN edges are created. Then, the mean degree is $2m$. The scale free networks generated have both out-degree and in-degree distributions that follow a power law with the exponents γ_{out} and γ_{in}, respectively. They are given as $\gamma_{\text{out}} = (1 + \alpha_{\text{out}}/\alpha_{\text{out}}$ and $\gamma_{\text{in}} = (1 + \alpha_{in}) / \alpha_{\text{in}}$. Thus, choosing various values of α_{out} and α_{in}, we can determine different exponents γ_{out} and γ_{in}.

Random networks were generated by means of the configuration model [8]. In the network generated by this model, each node has a pre-defined degree k_i, but otherwise the network is wired randomly. The probability to have a link between nodes of degree k_i and k_j is $p_{ij} = \frac{k_i k_j}{2L-1}$. The configuration model steps are assigning a degree to each node, represented as stubs or half-links. The degree sequence is generated analytically from a Poisson distribution. We must start from an even number of stubs, otherwise we are left with unpaired stubs. Randomly select a pair of stubs and connect them. Then, randomly choose another pair from the remaining $2L - 2$ stubs and connect them. This procedure is repeated until all stubs are paired up. Depending on the order in which the stubs are chosen, we obtain different networks. Some networks include cycles, others
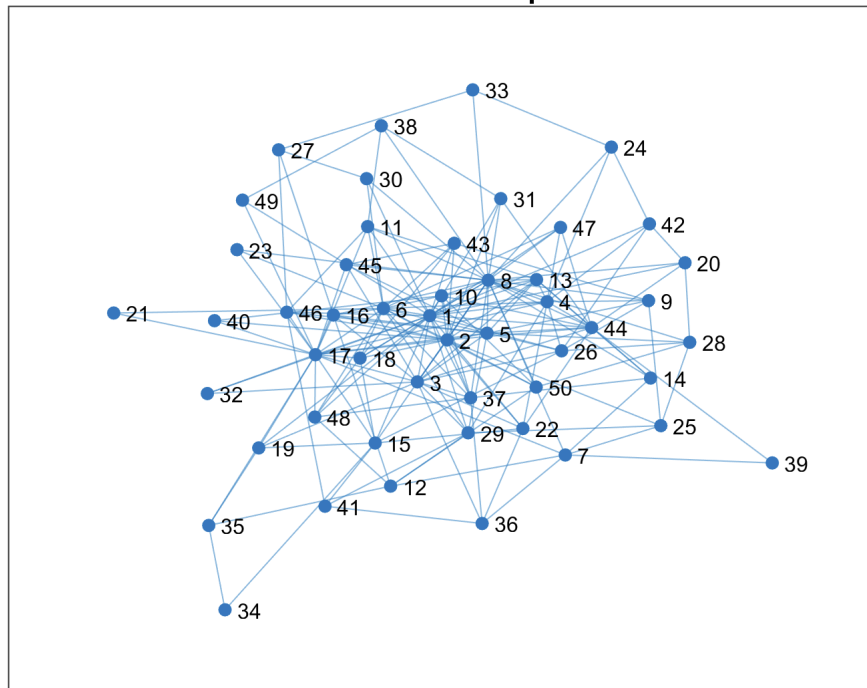
Figure 1.9. Example of a scale-free network of 50 nodes.

self-loops or multi-links. Yet, the expected number of self-loops and multi-links goes to zero in the $N \to \infty$ limit. By repeatedly applying this procedure to the same degree sequence, different networks with the same p_k can be generated.

Network centrality metrics

When networks are generated through these advanced and realistic algorithms, their nodes do not share the same importance in diffusing a process through the network: centrality metrics quantifies how important, or central, the different nodes of a network are. There have been proposed numerous centrality metrics in the literature [14–16], but why is it relevant? Because these metrics can measure and thus identify how influential a node is in propagating the process occurring on the network: for instance, its opinion or social norm if considering individuals discussing on a topic, or an illness if the network models the contacts in an epidemic outbreak, or, more in general, if we want to act individually on the network to stop/promote a certain behavior globally, and we want to find which node is better to target to efficiently do the task.

Centrality metrics are based on the knowledge of some characteristics of the connectivity of each node:

- Degree Centrality (DC), for undirected graphs, counts how many social connections (aka, the number of neighbors) a node has: $DC_i := \sum_j^N a_{ij}$. In a digraph, it can be defined both for in-neighbors and out-neighbors. For weighted networks, the

sum of the edge weights is used rather than the number of connecting edges. The limitation is that it relies only on local information at one step.

- Betweenness Centrality (BC) measures how often each graph node appears on the shortest path between two nodes in the graph. Since there can be several shortest paths between two graph nodes s and t, the centrality of node i is: $BC(i) = \sum_{s,t \neq i} \frac{n(i)_{st}}{N_{st}}$ where $n(i)_{st}$ is the number of shortest paths from s to t that pass through node i, and N_{st} is the total number of shortest paths from s to t.

- Eigenvector Centrality (EC) is a positive multiple of the sum of adjacent centralities. Relative scores are assigned to all nodes in a network based on an assumption that connections to high-scoring nodes contribute more to the score of the node than connections to low-scoring nodes. It uses the eigenvector corresponding to the largest eigenvalue of the graph adjacency matrix, and it is defined as $EC(i) = k_1^{-1} \sum_j a_{ij} x_j$, with the constant $k_1 \in \mathbb{R}$.

- Pagerank centrality results from a random walk of the network. The centrality score is the average time spent at each node during the random walk: at each node in the graph, the next node is chosen with a certain probability from the set of successors of the current node in digraphs (neighbors for the undirected case). It is criticized because it does not deal with acyclic graphs.

- Hubs/authority centrality are two linked centrality measures that are recursive. The hubs score of a node is the sum of the authorities scores of all its successors. Similarly, the authorities score is the sum of the hubs scores of all its predecessors. The sum of all hubs scores is 1 and the sum of all authorities scores is 1.

1.3 Emerging collective behaviors

Collective behavior in complex dynamical systems networks represents an emerging phenomenon in which 'coordinated motion' is driven by local interactions that occur in communication ties between entities. The way in network nodes interact is influenced by various constraints, both physical and biological, but the most important is the way in which the network of interconnection is perceived from the single entity, that is, the definition of neighborhood. These phenomena are called emergent because they arise naturally in a wide range of real-world groups, including fish, birds, and humans, without a control unit that dictates how the single entity must behave in order to get a desired coordinated behavior of the whole.

Every emerging collective behavior can be seen in the broadest sense as a coordination among entities to reach a certain state of the whole only by means of local interactions. There are a lot of examples from biological, economics, epidemiological, and social networks, only to mention a few, that surround us:

- flocks of birds often exhibit coordinated movements, maintaining a specific formation. This behavior helps them optimize their flight efficiency and avoid predators.

- synchronization of fireflies exhibiting synchronized flashing patterns. When fireflies in proximity synchronize their flashing, it can create mesmerizing light shows in nature;

- neuronal synchronization: in the brain, groups of neurons can synchronize their firing patterns, leading to the emergence of specific brain rhythms like alpha, beta, or gamma oscillations. These rhythms are associated with different cognitive functions;

- stock market bubbles and crashes: financial markets are influenced by the collective behavior of traders and investors. The emergence of stock market bubbles, followed by sharp crashes, is a classic example of how collective behavior such as herding or imitation can impact economic systems;

- disease spread: the diffusion of diseases in populations, such as the transmission of infectious diseases like COVID-19, is an example of collective behavior within epidemiological networks;

- Information cascades: in social media networks, such as Twitter or Facebook, information or trends can spread rapidly as users share and repost content. This can lead to viral phenomena where a piece of information becomes widely adopted in a short period.

Here, we define more formally two of the main categories of collective behaviors that have been extensively studied in the literature, namely synchronization and consensus, due to the fact that understanding them and under which circumstances they arise have practical implications in our society.

When the collective behavior consists in achieving a common and time-varying final state for all the agents, it can be deemed as synchronization. Consensus is the particular case of synchronization when the final common state is a constant trajectory, namely a point in the state space.

Synchronization and consensus

Given a complex network, synchronization implies convergence of all nodes to the same asymptotic time-varying solution $x_s(t)$ (i.e., common limit cycle or chaotic attractor). We recall that $x_s(t)$ is unknown a priori. There are different types of synchronization [17]:

if all agents are homogeneous, we can reach perfect synchronization, which implies that all nodes trajectories contract onto the synchronous manifold, i.e.,

$$\lim_{t\to\infty} x_i(t) = x_s(t) \Leftrightarrow |x_i - x_j| = 0.$$

One of the reasons diffusive coupling has been the most studied in the literature is that the completely synchronized state $x_1(t) = x_2(t) = \cdots = x_N(t) = s(t)$ is a natural solution of Eq. (1.3). It defines a linear invariant manifold, the synchronization manifold, where all agents evolve synchronously as $\dot{s} = f(s)$. Note that $s(t)$ may be an equilibrium point (in this case, it translates into a consensus problem), a periodic orbit, or even a chaotic solution.

When the agents are not identical, generalized synchronization is addressed, and it implies that there is a function Φ such that, when $t \to \infty, x_i = \Phi x_j$ which means that the dynamics of one system is dependent on the other. Perfect synchronization is the particular case of generalized synchronization when Φ is the identity.

Bounded synchronization [18] implies that the mismatch between the trajectories of individual agents are upper limited by a small scalar ε

$$\lim_{t\to\infty} x_i(t) = x_s(t) \Leftrightarrow |x_i - x_j| \leq \varepsilon.$$

When the dynamics of the i-th node is

$$\dot{x}_i = f(x_i) + \sigma \sum_{j \in N_i} \mathcal{L}_{ij} x_j \quad i = 1, \ldots, N$$

then, synchronizing the network means finding the range of values of σ so that all systems in the network evolve asymptotically along the same trajectory $x_s(t)$.

Consensus is a particular case of synchronization, typically studied for linear dynamical systems, and it defines a condition in which the ensemble of interconnected agents reaches, asymptotically, a constant steady-state [19].

Mathematically, it can be defined as

$$\lim_{t\to\infty} x_i(t) = c \in \mathbb{R} \qquad \forall t. \tag{1.6}$$

The difference with respect to synchronization is that the solution to which the system
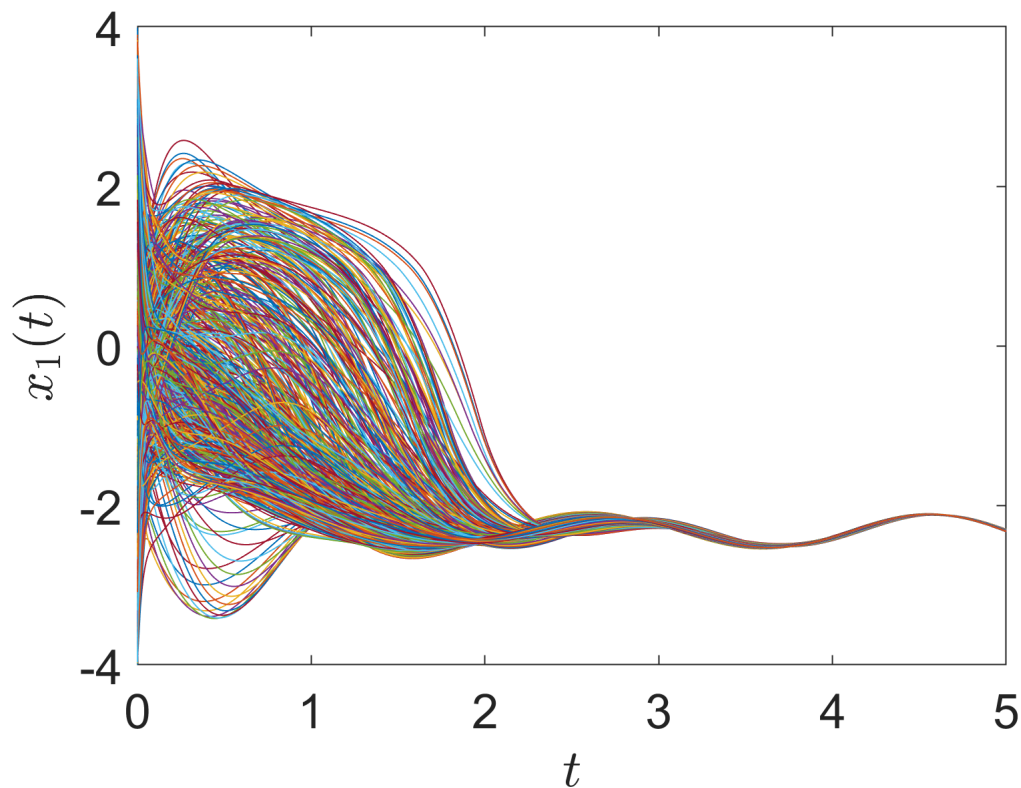
Figure 1.10. Example of a coupled Chua's circuit network [1] of 100 nodes synchronizing on a time-varying trajectory.

converges cannot be time-varying, as the individual dynamics of each agent is often neglected for these systems [20].

Consensus emerges when the dynamical matrix that governs the networked systems has a single zero eigenvalue that corresponds to the unitary eigenvector, the agreement subspace, and thus we can appreciate how the structure determines the emergence of collective behaviors. Consensus problems in multi-agent systems have gained significant research attention due to their applications in fields like aerial vehicles, air traffic control, wireless sensor networks, and decision-making. The master stability function has been useful for studying synchronization over static networks, while pinning control schemes have been explored to induce synchronization. [21]

1.4   Control of complex network of dynamical systems

Once we have assessed that complexity is an integral part of most of the systems that surround us, a question arises: how can we tame complexity, that is, control systems
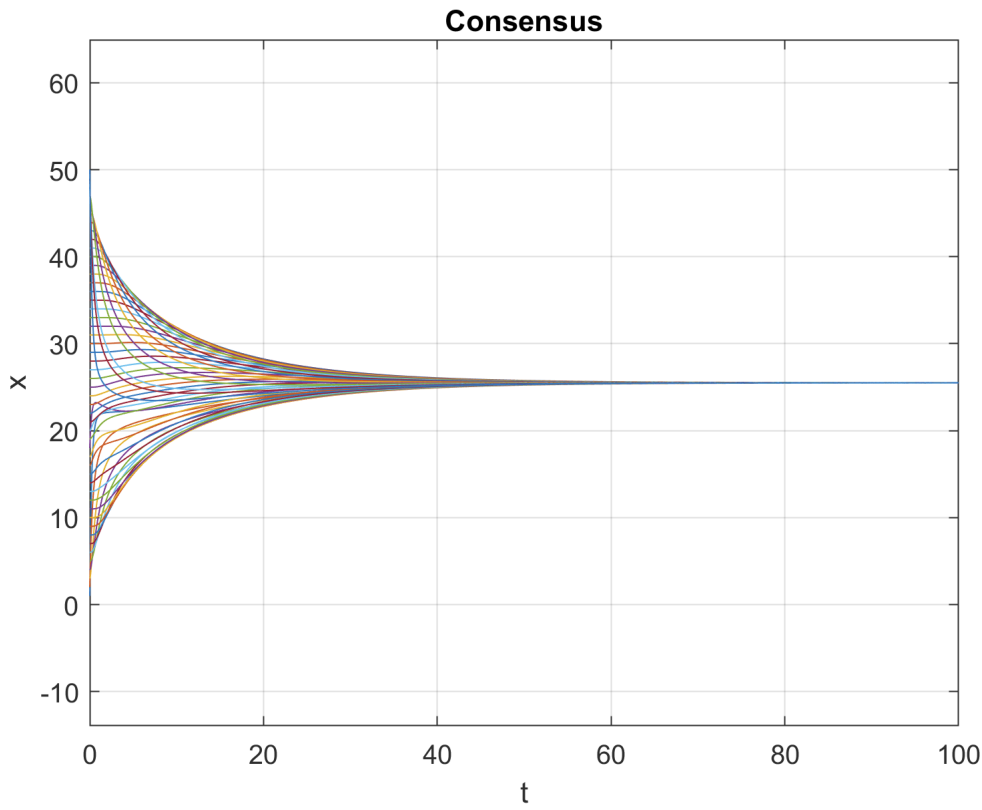
Figure 1.11. Example of 100 nodes reaching consensus, i.e., synchronizing on a constant trajectory.

to make them exhibit desired collective behaviors onto a predefined solution known a priori? Control theory provides the theoretical tools to determine how to influence the behavior of a network of dynamical systems, choosing which and how many inputs must be injected so that the system's outputs reach a desired trajectory or final state. The key idea in control is feedback, that is, applying a function of the error, expressed as the difference between the actual and desired output, to the system as an input, forcing the system's output to converge to the reference.

Controllability and observability

Before proposing a control scheme for a system or a network of dynamical systems, we need some conditions under which we are guaranteed that the control is feasible.

Controllability is a prerequisite for the implementation of a control strategy in a network of dynamical systems [22].

Definition 38. *A complex network of dynamical systems is controllable if it is possible to steer the states associated to all the nodes from any initial condition to zero in finite time.*

Definition 39. *An LTI DT system is controllable to the origin in k steps if $\forall x_0 \in \mathbb{R}^n$ there exists a sequence $u(0), \ldots, u(k-1) \in \mathbb{R}^m$ such that $0 = A^k x_0 + \sum_{j=0}^{k-1} A^j B u(k-1-j)$*

This implies that we can move the state variable of each node of a network to a predefined value, corresponding to the system's desired position in the state space. Our ability to do so is largely determined by the network topology.

Controllability has been mostly studied in the case of linear dynamical systems for different reasons: first, linear systems offer an accurate model for some real problems, such as consensus in multi-agent networks; second, also when there are nonlinear interactions between the components, the first step in any control challenge is to establish the controllability of the locally linearized system. Finally, as the complex network topology adds a new layer of complexity to the controllability problem, focusing on the linear case allows understanding the impact of the topological characteristics on our ability to control, regardless of their nonlinear dynamics.

Definition 40. *A dynamical system is reachable if it is possible to reach any state in finite time, starting from zero initial conditions.*

Definition 41. *An LTI DT system is reachable if $\forall x_1, x_2 \in \mathbb{R}^n$ there exist $k \in \mathbb{N}$ and $u(0), \ldots, u(k-1) \in \mathbb{R}^m$ such that $x_2 = A^k x_1 + \sum_{j=0}^{k-1} A^j B u(k-1-j)$*

Note that analogous definition can be given for LTI systems in continuous time, for which the controllability and reachability properties are equivalent [23].

For what concerns nonlinear dynamical systems, many tried to generalize the concept of controllability; however, it has not been possible to overcome mathematical issues. Instead, a weaker form of controllability, called accessibility, has been proposed.

Definition 42. *Accessibility concerns the possibility of reaching or accessing an open set of states in the state space from a given initial state. If the system is locally accessible from an initial state x_0, then we can reach or access the neighborhood of x_0 through trajectories that are within the neighborhood of x_0.*

This is the reason most nonlinear systems are studied in the neighborhood of their equilibrium points: studying the controllability properties of its linearization around an equilibrium point or along a trajectory can often offer an efficient test of local nonlinear controllability.

Thus, in the case in which the network is composed of linear time-invariant systems, then some algebraic criteria have been proposed in the literature:

- Kalman test: The pair (A, B) is controllable if and only if the controllability matrix

$$K = [B \quad AB \quad A^2 B \ldots A^{N-1} B], \qquad (1.7)$$

  has full rank $\rho(K) = N$.

- Popov-Belevitch-Hautus (PBH) test: $\rho([sI - AB]) = N \quad \forall s \in \lambda(A)$

Note that the PBH test and Kalman's rank condition are equivalent. Yet, the former connects the controllability of the pair (A, B) to the eigenvalues and eigenvectors of the state matrix A.

Any feedback control action assumes that the state of the system or a network of dynamical systems is known (or at least a reliable estimate of it) for each time instant. This translates into assuming a prerequisite, dual to controllability, called observability.

Definition 43. *A system is said to be observable if it is possible to recover the state of the whole system from the measured inputs and outputs.*

When a system is observable, it means that we can estimate the state variables of each unit $x(t)$ by some measurements of its outputs $y(t)$. Instead of monitoring each node of the network with sensors, a fact that could be unfeasible or not convenient, we rely on a subset of nodes and then exploit the network structure. In fact, it is possible to do so exactly because systems are interconnected and so the state of some nodes depends on the state of their neighbors, thus it is possible to reconstruct their states even though they are not directly measured. So, a system is observable if there is a known relation between the outputs $y(t)$, the state vector $x(t)$, and the inputs $u(t)$ such that the system's initial state $x(0)$ can be inferred.

For linear systems, observability and controllability are mathematically dual concepts. Indeed, considering an LTI system

$$\dot{x}(t) = Ax(t) + Bu(t),$$
$$y(t) = Cx(t).$$

the duality principle states that the triple (A, B, C) is observable if and only if its dual system $\left(A^{\mathrm{T}}, C^{\mathrm{T}}, B^{\mathrm{T}}\right)$ is controllable. Graphically, this translates in studying the controllability properties of the transposed network defined by A^{T}, which is obtained by flipping the direction of each link in $\mathcal{G}(A)$.

Thus, we can use a dual Kalman test for observability.

Definition 44. *the system (A, B, C) is observable if and only if the observability matrix*

$$O = \begin{bmatrix} C \\ CA \\ CA^2 \\ \vdots \\ CA^{N-1} \end{bmatrix}$$

has full rank, i.e., $\rho(O) = N$

In this case, the N rows of the observability matrix O are linearly independent, thus the N state variables can be recovered by linearly combining the output variables $y(t)$.

Target controllability and observability

When for physical or economical constraints there are not enough actuators to guarantee the complete controllability or more generally, if we want to exert control only onto a subset of nodes, the so-called targets, we can pose the controllability problem of how can we smartly select a subset of nodes to directly control with a fixed cardinality in order to obtain the largest controllable subnetwork. This problem has been addressed in [24] and solved by adapting the graphical interpretation of Hosoe's theorem [25] to the optimization problem under investigation. As in partial controllability, dually we could settle for observing only a fraction of the state variables of the system, the targets. In case those target variables cannot be directly measured, we can refer to target observability to optimally select the nodes to be sensors that can infer the state of the target variables. Analogously to optimal driver selection, this optimization problem can be tackled by means of a graphical approach, recalling that

Definition 45.

The state of a target node x_t can be observed from a sensor node x_s only if there is a directed path from x_s to x_t.
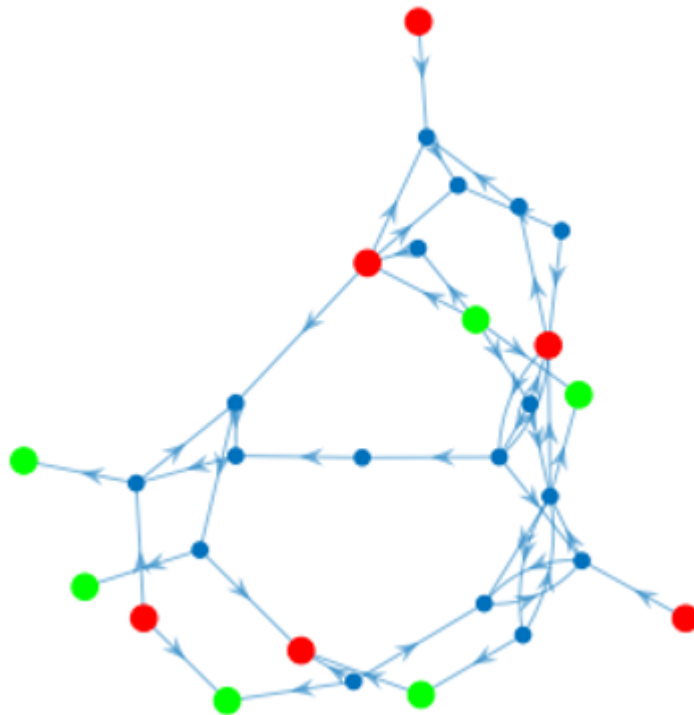
Figure 1.12. Driver/sensor node selection example: actuator nodes in red and sensor nodes in green.

Parameter identification

A particularly relevant observability problem is the so-called parameter identification problem (PI) in control theory [26]. In most models, it assumed that the system parameters are known. Yet, this is not the case for most complex systems, in which the parameters are unknown or known only approximately. Under which conditions can we infer the parameters from the knowledge of the inputs and the outputs of the system? If we consider the system parameters Θ as constant state variables and extend the state vector to include a larger them, i.e., $(x(t), \Theta)$, we can check the observability of the extended system with the traditional tool, thus the identifiability problem could be recast as an observer design problem [27]

Structural controllability

Any complex network of dynamical LTI systems is controllable if we control each node individually with an independent signal. However, this approach is unfeasible for large complex systems. Hence, the literature has focused on solving the so-called minimal controllability problems, that is, finding the minimum set of pivotal nodes, namely driver nodes, that if injected with control inputs, can guarantee controllability of the entire network, exploiting the network structure to permeate the control action. In this thesis, when we refer to this problem we intend to find a matrix $B \in \mathbb{R}^{N \times N}$ whose columns are a subset of that of the N-dimensional identity matrix and that has as the minimum number of columns such that the network is controllable. Namely we assume that each control input u_i can directly control only one node (aka state variable). Structural controllability provides a feasible, easy-to-use and computationally efficient methodology to solve such controllability problem.

Conversely, Kalman and PBH tests imply the knowledge of all the parameters of the equations that describe the LTI system, an assumption that deos not always holds. Moreover, the Kalman criterion is suitable when the dimension of the controllability matrix is small, otherwise there are computational problems. Hence, for large complex systems, there is the need of a novel approach that does not require numerically calculating the rank of the controllability matrix. Thus, there have been some advances to overcome these difficulties, by mapping the control problem into well-studied network problems, like matching, and borrowing some tools from statistical physics like the cavity method, that were traditionally beyond the scope of control theory [28].

Structural controllability deals with structural linear systems [29, 30], whose triplet (A, B, C) is composed by structured matrices.

Definition 46. *A* structured matrix *is defined as a matrix with either independent (free) parameters or fixed zeros.*

Definition 47. *The pair (A, B) is structurally controllable if we can set the nonzero elements in A and B such that the resulting system is controllable in the usual sense.*

The power of structural controllability comes from the fact that if a system is structurally controllable, then it is controllable for almost all (except for Lebesgue measure's cases) possible parameter realizations. Thanks to the graphical interpretation of Lin's structural controllability theorem, this approach provides conditions to test the structural controllability of a network of dynamical systems without expensive matrix operations.

Definition 48. *A digraph contains a dilation if there exists a subset of nodes $\mathcal{S} \subset \mathcal{V}$ such that the neighborhood set of S, denoted as $\mathcal{T}(S)$, has fewer nodes than $\mathcal{S}$ itself. Here, $\mathcal{T}(S)$ is the set of vertices j for which there is a directed edge from j to some other vertex in $\mathcal{S}$. Note that the input vertices are not allowed to belong to $\mathcal{S}$ but may belong to $\mathcal{T}(S)$.*

Definition 49. *A cactus is a subgraph defined recursively as follows. A stem is a cactus. The union of a stem S_0 and buds $B_1, B_2, \ldots, B_l$ then $S_0 \cup B_1 \cup B_2 \cup, \ldots, B_l$ is a cactus if for every $i(1 \leq i \leq 1)$ the initial vertex of the distinguished edge of B_i is not the terminal vertex of S_0 and is the only vertex belonging at the same time to B_i and $S_0 \cup B_1 \cup B_2 \cup, \ldots, \cup B_{i-l}$. A set of vertex disjoint cacti is called a cactus.*
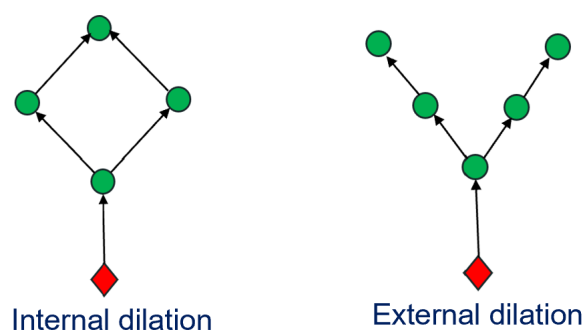
Figure 1.13. Example of internal and external dilation, respectively, on the left and right. Red diamonds are driver nodes, namely, the nodes where the control input is directly injected.
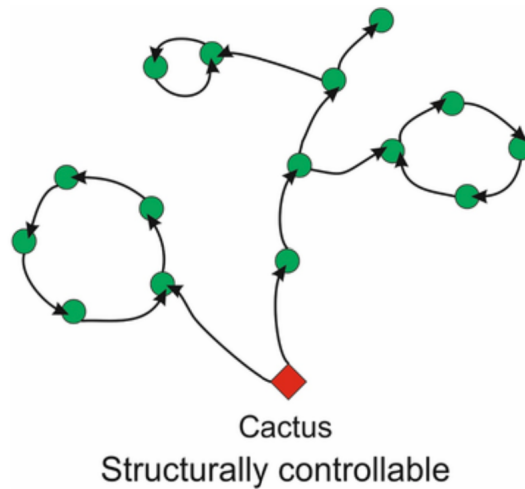
Figure 1.14. An example of a cactus.

It is the minimal structure which contains neither inaccessible nodes nor dilations. In this analysis a cactus is always a set of stems and buds linked to the stems which must be originated by a driver.

Theorem 1. *The following three statements are equivalent:*

1. *An LTI system (A, B) is structurally controllable.*

2. *The digraph $G(A, B)$ contains no inaccessible nodes.*

3. *The digraph $G(A, B)$ contains no dilations.*
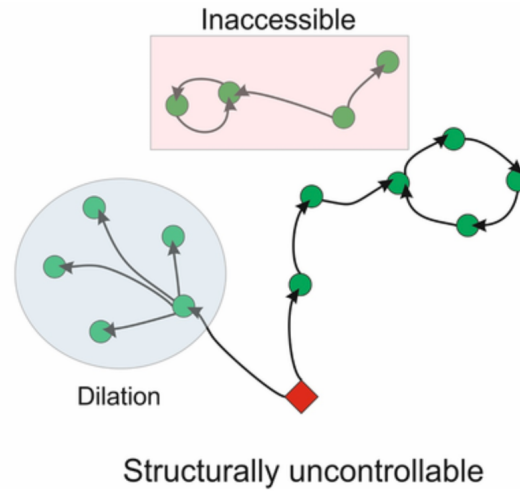
Figure 1.15. An example of uncontrollable network due to the presence of inaccessible nodes.

4. $G(A, B)$ is spanned by a cactus

This theorem has mathematical consequences because in structurally controllable networks the structured matrix $[A; B]$ is irreducible and has full generic rank. Indeed, the presence of inaccessible state vertices means that the structured matrix $[A; B]$ is reducible, i.e., there exists a permutation matrix P such that:

$$PAP^{-1} = \begin{bmatrix} A_{11} & 0 \\ A_{21} & A_{22} \end{bmatrix} \text{ and } PB = \begin{bmatrix} 0 \\ B_2 \end{bmatrix}$$

where $A11 \in R^{K \times K}$, $A_{21} \in R^{(N-K) \times K}$, $A_{22} \in R^{(N-K) \times (N-K)}$, and $B_2 \in R^{(N-K) \times M}$ with $1 \leq K \leq N$.

Furthermore, the presence of a dilation is equivalent to the statement that the structured matrix $[A; B]$ has generic rank less than N : $\text{rank}_g[A; B] < N$ where the generic rank is the maximum rank that the matrix attains as a function of the free parameters.

Basically, this theorem allows saying that a system is structural controllable if and only if it doesn't have any inaccessible nodes because they couldn't be influenced by the input control and if it does not have any dilations, i.e., any expansion of the graph in which there are more sinks than sources, because two subordinates can't be independently controlled if they share one superior. These two statements are equal to the third one, that is that the graph is spanned by a cactus, because a cactus is the minimum structure which does not contain neither inaccessibility nor dilations.

Pinning control

If we want to steer the agents' dynamics towards a desired solution, we can think of controlling their behavior adding some feedback control input, but where? The simplest strategy could be to act on each node (i.e., each dynamical system) in centralized fashion. However, this approach is unfeasible when we are facing large-scale networks. Going

towards distributed decentralized control, the idea is to exploit the strong dependence between the dynamics of the network and the network structure: this concept is the basis of pinning control [31, 32], where, by means of an additional dynamical system (i.e., a node), whose trajectory acts as reference, called pinner, the feedback control action is directly injected in a small fraction of nodes of the network, the pinned nodes. The pinner plays the role of a leader, and it is connected only to the pinned nodes, the followers, but taking advantage of the network topology, the control action can permeate through all the nodes, achieving the control goal. Pinning control is also known as leader-follower control, as the pinner exerts a leadership within interconnected groups that significantly influences the collective behavior of the whole. In this scenario, leaders have more information than their followers or other "special" characteristics. If a network cannot synchronize/reach consensus spontaneously, we can design controllers that, applied to a subset of pinned nodes, help achieving the collective goal. This procedure, known as pinning control, is fundamentally different from spontaneous synchronization, where we do not specify the synchronized trajectory $s(t)$. Hence, the system "self-organizes" into the synchronized trajectory under appropriate conditions. In pinning control, we choose the desired trajectory $s(t)$, aiming to achieve some desired control objective, and this trajectory must be explicitly taken into account in the feedback controller design. Thus, the design of the control scheme must take into account the dynamical characteristics of each component as well as the network's topology.

A pinning control problem mathematically translates into a closed-loop dynamics where the network is no longer homogeneous because we have M pinned nodes and $N - M$ uncontrolled ones:

$$\begin{cases} \dot{x}_i = f\left(x_i\right) - \sigma \sum_j \mathcal{L}_{ij} h\left(x_j\right) + \tilde{u}_i & i = 1, \dots, M \\ \dot{x}_i = f\left(x_i\right) - \sigma \sum_j \mathcal{L}_{ij} h\left(x_j\right) & i = M+1, \dots, N \end{cases}$$

If the goal is that all nodes synchronize asymptotically onto a desired trajectory $x_s(t)$, one can think of an additional proportional control action where σ is the coupling strength of pinning control:

$$\tilde{u}_i = \sigma \left[x_s(t) - x_i(t)\right]$$

Finally, the closed loop network equation will be:

$$\dot{x}_i = f\left(x_i\right) - \sigma \sum_j \mathcal{L}_{ij} h\left(x_j\right) + \delta_i \sigma \left[x_s(t) - x_i(t)\right] \quad i = 1, \dots, N \qquad (1.8)$$
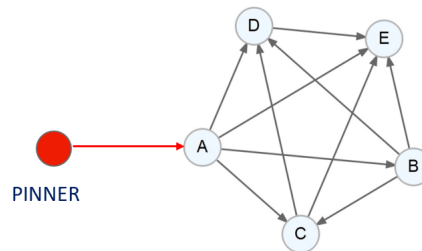
Figure 1.16. A network example in which the red node is the pinner.

where δ_i is an indicator function which is 1 for the pinned nodes and 0 otherwise.

The pinner has its own dynamics, described in Eq. 1.9, that is not influenced by the other agents, and defines the desired trajectory.

$$\begin{cases} \dot{s} = f(s,t) \\ s(0) = s_0 \end{cases} \tag{1.9}$$

If the pinner's goal is to guide the group to a common state, this translates in a specialized consensus problem known as leader-follower consensus [21]. In any case, the pinning control problem consists not only in designing the strength of the pinner control action, but also in determining which and how many nodes need to be pinned.

Analogously to other control problems, before delving into the control scheme, we need some conditions of pinning controllability.

As the nodes' dynamics is inhomogeneous, the Master Stability Function approach cannot be directly applied to the pinning controlled network. However, extending the network to $N+1$ nodes, so that $y_1 = x_1,..., y_N = x_N$ and $y_{N+1} = s$. The dynamics of the i-th agent

$$\dot{x}_i = f(x_i,t) - \sigma \sum_{j=1}^{N} l_{ij} h(x_j) + u_i \tag{1.10}$$

becomes

$$\dot{y}_i = f(y_i,t) - \sigma \sum_{j=1}^{N+1} m_{ij} h(y_j) \ \forall i = 1,..,N+1 \tag{1.11}$$

where m_{ij} is the (i,j) element of a $N+1$ dimensional square matrix M:

$$\begin{pmatrix} l_{11} + \delta_1 k_1 & \dots & l_{1N} & -\delta_1 k_1 \\ \vdots & \ddots & \vdots & \vdots \\ l_{N_1} & \dots & l_{NN} + \delta_N k_N & -\delta_N k_N \\ 0 & \dots & 0 & 0 \end{pmatrix}. \tag{1.12}$$

Here, M is the effective coupling matrix of the $(N+1)$-dimensional extended system. As $M = (m_{ij})_{(N+1)\times(N+1)}$ is a zero row-sum matrix, we can sort its eigenvalues as $0 = \lambda_1 \leq \text{Re}\{\lambda_2\} \leq \cdots \leq \text{Re}\{\lambda_{N+1}\}$ and apply the MSF approach to numerically explore the local stability of the synchronization manifold of the controlled network. The role of the control and coupling gain, and the number and the selection of pinned nodes has on local pinning controllability has been systematically studied [32]. For example, under some assumption on f and h, the network can be controlled through only one pinned node. In particular, if the graph is undirected and connected or directed and strongly-connected, it is possible to reach synchronization by pinning just one randomly selected node. If the graph is directed and its condensation has a spanning tree, the pinned node should belong to its root. On the other hand, if the condensation has multiple-sources, more than just one node must be pinned. Considering that the number of connections of the pinner can be limited, it is not always possible to control all the nodes. Hence,

the partial pinning control problem [33] is considered. It consists in identifying the combination of the pinned nodes that maximize the number of vertices that are able to slide towards the pinner's trajectory.

To control digraphs, some assumptions on the individual dynamics, such as the QUAD assumption, need to be made. If we consider N-dimensional dynamical systems of the form $\dot{x} = f(x, t)$ where $x \in \mathbb{R}^N$ is the state of the system and the vector field $f : \mathbb{R}^N \times \mathbb{R}^+ \to \mathbb{R}^N$ the QUAD assumption can be defined:

A function $f : \mathbb{R}^N \times \mathbb{R}^+ \to \mathbb{R}^N$ is QUAD(Δ, w) if and only if for any $x, y \in \mathbb{R}^N$

$(x-y)^T[f(x,t)-f(y,t)]-(x-y)^T\Delta(x-y) \leq -w(x-y)^T(x-y)$ where Δ is a diagonal matrix and w is a scalar. If we look at y as the reference trajectory where we want to converge, the QUAD assumption means that the differences between vector fields in the left hand-side are always upper limited by the product between the mismatch of state variables and a constant w, this implies that the coupling effect can be made stronger than the vector field mismatch. The QUAD condition is an assumption on the vector field usually made in the literature to prove global network synchronizability by means of appropriate Lyapunov function because as it has a quadratic form, and as it is an upper bound it ensures the existence of an appropriate Lyapunov function.

While in undirected networks the pinned nodes can be chosen arbitrarily, even if there are of course some optimal choice in selecting them in order to minimize the control effort, in directed network it is necessary to pin at least one node in each (RSCC) of the network [34]. Theorem 1 of [33] guarantees that the DAG condensation of the network is pinning controllable if we pin at least a node in each RSCC and if the coupling gain σ and the control gain K are large enough. Generally, it has been shown that, in the case of diffusive coupling, counterintuitively, for undirected networks pinning the nodes with low degree, instead of hubs, is more convenient when the coupling strength σ is small, whereas, for directed networks, nodes with very small in-degree or large out-degree should be pinned first [35]. We will see that this is not the case when the coupling is not linear but saturated (See Paper C).

In all the contributions presented in this thesis, control problems on complex networks of dynamical systems have been proposed, and the methodologies presented in this section have been used to give theoretical conditions under which the problem formulations could be solved.

Regarding the problem formulations, all the works focused on control problems in the context of opinion dynamics (see next section for an overview). Even though talking about control of opinions might have ethics implication, many phenomena like fake news, targeted advertising, propaganda, awareness campaigns, daily affect our opinion formation in everyday life. An intuitive way to capture, and thus understand, the influence of these factors is modelling them as controllers. Hence, exploiting the role of control in opinion dynamics can be useful to deeply understand how opinions' influence can be exerted in order to apply some countermeasures against malicious agents or instead helping promote initiatives for the well-being of social groups. Indeed, possible control goals in such context could be

- Reach/prevent consensus (to take a collective decision or to preserve diversity)

- Disagreement containment (compromise)

- Steer the opinion of the majority of the agents toward a desired value (Media, Propaganda)

- (Discourage)Promote (un)healthy social norms (campaigns)

- Mitigate adversarial influences (fake news, bot)

and some of them have been addressed in this dissertation.
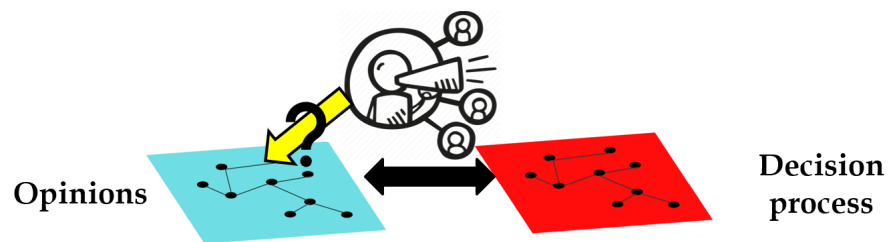
Figure 1.17. Our framework idea of bridging the gap between opinions, decision-making, and the role of influencers and policymakers in social systems.

Part II

Literature Review

Complex networks of social systems: opinion dynamics models

Opinion dynamics (OD) is a multidisciplinary research field that combines tools and knowledge from different scientific areas such as social sciences, control theory, applied mathematics and computer science. Its aim is to study the process of opinion formation of a single individual as the output of the interaction of a group of agents that resembles a complex system [36]. Opinion dynamics deals with the development and analysis of dynamical models that capture how individuals in a social network interact and exchange opinions; an individual's opinion may evolve over time as a result of becoming aware of the opinions of their neighbors and considering them (to a certain extent) to update his own opinion. Opinion dynamics models can be aggregated, that is referred to a community or a category of people, or agent-based where each individual is represented by an agent and the opinion of an individual on a topic is represented by a numerical value, evolving in time. In the latter case, the one considered in this thesis, the network of interactions between individuals is conveniently captured by a graph, where a node represents an individual, while edges represent a communication tie between two individuals. Agent-based opinion dynamics models are examples of how single dynamics, if interconnected on a network, can lead to interesting emergent global behaviors that reflect real social phenomena, like consensus, polarization, or persistent disagreement [37].

In the literature, there have been proposed numerous opinion dynamics models, differing on the opinion state space, the opinion evolution rule chosen and the nature of the time period in which the evolution occurs, for an overview see [38, 39]. Therefore, a first categorization can be made of how the opinion is mathematically translated.

- Discrete-state opinion models inspired by physics phenomena, such as Sznajd model [40] and the Voter model [41], where the opinion is represented by a discrete number, commonly -1 or 1 to indicate the disagreement/agreement towards a certain topic;

- Continuous-state opinion models such as the DeGroot model [42], the Friedkin-Johnsen model [43], the Deffuant and Weisbuch model [44,45] and the Hegselmann-Krause model [46] in which opinions are real numbers that lie in the range $[0, 1]$,
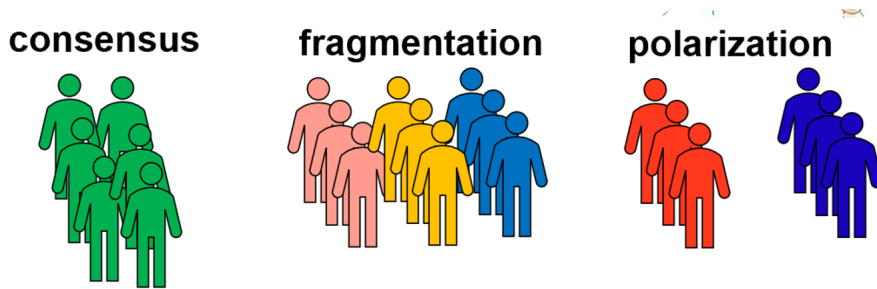
Figure 2.1. Sketch of the 3 main social emerging phenomena in opinion dynamics: from left to right, consensus corresponds to the exact agreement onto a single opinion of the whole group, fragmentation refers to the persistent disagreement on more than two opinions and polarization concerns with the phenomenon of extremization of the opinions of the groups towards two opposite opinions.

expressing the intensity towards two extremes of a spectrum regarding a certain topic.

2.1 Discrete state space models

When it is necessary to represent situations with two (or more) alternatives, it may be convenient to associate with each agent a discrete opinion, $x_i \in \mathbb{Z}$.

The Voter, Galam and Snajzd models are the most popular discrete opinion state models [40, 47, 48]. They all share a basic mechanism:

- at each iteration, a pair of neighboring nodes is randomly selected,

- if their opinions are different, one of them changes it accordingly to an updating rule,

- the updating stops when it reaches a steady state: consensus or stalemate

The Voter model was introduced in [49] and is called like that due to its political applications. This model describes the social dynamics of public choices on social issues. In the Voter model, all agents are placed in regular lattices, each agent's opinion (or choice) is denoted as a binary variable, and an agent updates his/her opinion based on that of a randomly selected neighbor.

More formally, $\forall i$, $x_i(k) \in [\pm 1]$. The agent i will randomly select an agent j among the four neighbors of the lattice and follow his/her opinion $=> x_i(k+1) = x_j(k)$.

Galam model is based on the local majority rule, that is, in a small social group, individuals always reach consensus as the minority subordinate to the majority. Agents have discrete opinions ± 1 and can interact with all other agents in an all-to-all graph. At each time step, a group of r agents is selected randomly, and they all take the most preferred opinion within the group. Defined $\tilde{x}$ as the mode of the opinions of a neighborhood, Galam model prescribes

$x_i(k+1) = \tilde{x}_j(k), \forall i = 1, \ldots, r, \forall j \in \mathcal{N}_i$.

Snajzd model employs the theory of social impact [40] based on the consideration that a group of individuals with the same opinion can influence their neighbors more than one single individual. At each time step, a pair of neighboring agents is selected and, if their opinion coincides, all their neighbors take that opinion. Otherwise, the neighbors take contrasting opinions.

Formally,

- In each iteration, a pair of agents i and $i+1$ is selected to influence their nearest neighbors, i.e., the agents $i-1$ and $i+2$.

- If $x_i(k) = x_{i+1}(k)$, then $x_{i-1}(k+1) = x_{i+2}(k+1) = x_i(k)$

- If $x_i(k) = -x_{i+1}(k)$, then $x_{i-1}(k+1) = x_i(k)$ and $x_{i+2}(k+1) = x_{i+1}(k)$

These three models share a very intuitive modeling framework that is suitable to represent discussion on a topic that involves few alternatives, such as political referendum or product adoption. However, discrete opinion state models they are very simplistic as they consider a predefined update rule that is not inspired by real world mechanisms but is mostly random and overlooks the role of complex topology in determining the opinion dynamics of the individuals. Moreover, they do not lend themselves to being mathematically analyzed, they do not allow investigating transient dynamics because they are not provided of any inertia mechanism. They are memory-less as updating rule is based only on the current state of the agents, thus they cannot consider how intrinsic beliefs influence agents in the opinion formation process. Finally, they cannot describe the intensity of opinions towards a certain topic but only their preferences among different alternatives.

2.2   Continuous state space models

For a more refined modeling of the opinion formation process, continuous state space models have been proposed in the literature, as their nature of associating a real value of an opinion from 0 to 1 lends itself to take into account an intensity of belief, rather than a simple preference among options. They can be enriched by a set of parameters to capture psychological traits of agents and can be studied not only to replicate collective behaviors, but also for analyzing all the evolution of opinion formation process. In figure 2.2

2.3   Averaging linear models

The literature of opinion dynamics dates back to 1956 when the psychologist French [50] proposed a mathematical model to represent social power, intended as the ability of an
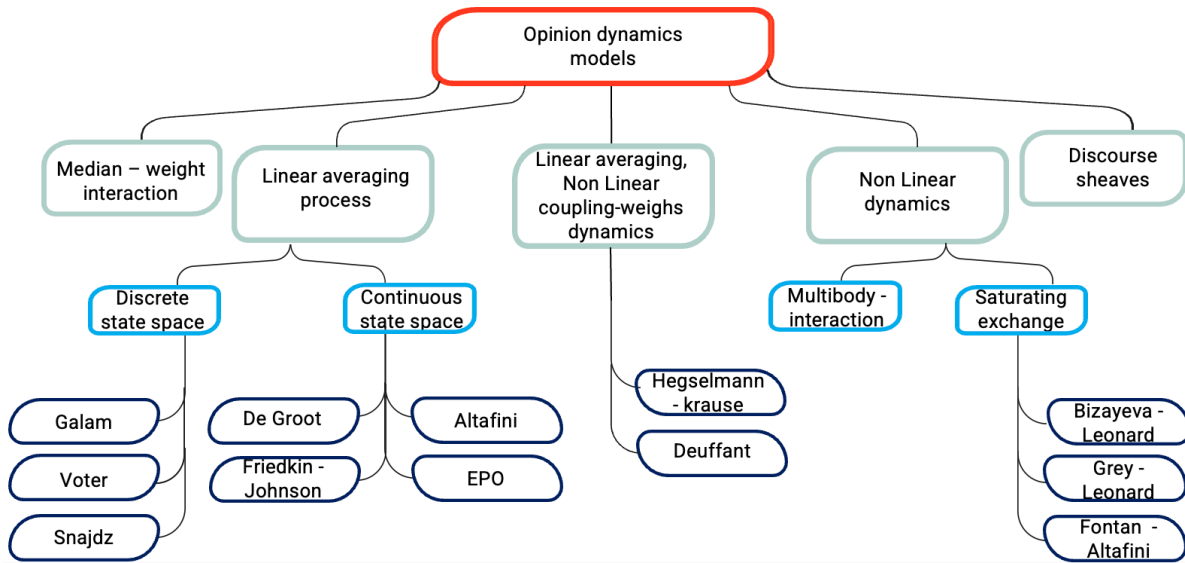
Figure 2.2. Taxonomy of the main opinion dynamics models categorized on the basis of opinions' update rules.

individual to influence the behavior of a social group. Then, about 20 years later, the statistician DeGroot [42] revived the interest towards social systems presenting a very similar model, called "iterative opinion pooling", where the focus was shifted to study how consensus can emerge in a group of people with different opinions. The model proposed, in fact, is a decentralized iterative averaging algorithm in which each agent modifies its opinion averaging the opinions of its neighbors, with no global knowledge of the opinion profile, that is the opinion of all the group at a certain time instant.

From this groundbreaking model stems the entire category of models of opinion dynamics based on the averaging process, a process of "compromise" in which opinions of neighbors are attracted to each other to become more similar.

DeGroot

The evolution over time of the opinion of agent i can be described by means of an averaging rule in the following way:

$$x_i(t+1) = w_{i1}x_1(t) + w_{i2}x_2(t) + \ldots + w_{in}x_n(t) \tag{2.1}$$

That is, agent i updates his opinion $x_i(t+1)$ at time $t+1$ by taking a weighted average of all the opinion of all other agents j at time t, where the weight that agent i gives to the opinion of agent j is denoted by w_{ij}. If w_{ij} is 0, then the agent i is not influenced by agent j in forming its opinion. The element $w_{ii} \geq 0$ represents the openness of agent i to others' opinions: if $w_{ii} = 0$ there is no self-reinforce of its opinion and the opinion formation completely relies on the others' opinions, whereas the agent with $w_{ii} = 1$ is a stubborn

or so-called zealot agent, that remains anchored to its initial opinion $x_i(t) = x_i(0) \forall t$. In matrix form, Eq. (2.1) rewrites as

$$x(t+1) = Wx(t) \qquad t = \{0, 1, \ldots, T\} \tag{2.2}$$

where W is a weighted non-negative row-stochastic adjacency matrix. Note that $x_i(t) \in \mathbb{R}_{\geq 0}$, thus, the vector $x(t) = [x_1(t), \ldots, x_N(t)] \in \mathbb{R}^N$ represents the opinion profile at time t of all N interconnected agents.

According to Perron-Frobenius theorem [9], if the matrix W is primitive and row-stochastic the system is marginally stable, then the opinion profile at steady state will be a consensus on the weighted-average of the initial opinions of the agents. If W is doubly-stochastic, the consensus value will be exactly the average of the initial opinions. In this sense, the system is said to have a "memory", because the equilibrium point of the agreement subspace, towards which the system converges to, is determined by the initial conditions.
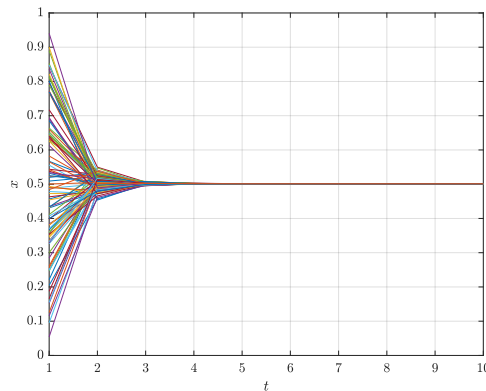
Figure 2.3. Evolution over time of opinions according to DeGroot model.

2.4   Beyond consensus

In classical engineering applications, such as fleets of drones, wireless sensor networks, power grids, the main focus has been deriving under which condition synchronization or consensus could emerge because the control tasks were mostly coordinating the entities in order to achieve a collective task. Even in real complex systems such as small groups of individuals, ant colonies, honeybees, or school of fishes, the emergent behavior is cooperation towards a common goal. However, when we shift towards a large-scale networked system such as social networks encompassing millions of users or entire populations, the emergent behaviors that we can observe are not always intended to collaboration or compromise. Instead, many scientific studies have stressed the increment of social phenomena like group polarization or anti-conformism, persistent disagreement (or known

as fragmentation), manipulation or spreading of misinformation. These findings motivate how important it is to model other phenomena beyond consensus that can capture also antagonism or disagreement over social ties, and also stress how important is the way in which information is conveyed and shares among peers.

Friedkin-Johnsen model

To make the study of opinion formation more adherent to the reality, variations of the DeGroot model have been proposed during the last decades to investigate how different social phenomena may arise. This has been done by encompassing in the agents' dynamics some additional psychological traits involved in an individual's opinion formation process. Whereas DeGroot model captures how a group of interconnected individuals can reach consensus of opinions via an averaging mechanism modelling conformism, reaching consensus in real situations is not that common, especially when considering a large social group, it can happen that different opinions coexist at steady state. This phenomenon is called fragmentation.

The Friedkin-Johnsen (F-J) model is an extension of the DeGroot model, in which each individual is assumed to be attached to its intrinsic belief with a certain intensity, namely it could be more or less stubborn. In the seminal paper of Friedkin and Johnsen [43], these prejudices of the agents are imagined being generated by some exogenous conditions in the past.

In the classical version of F-J model [43], the interconnection among individuals is represented by an undirected connected graph $\mathcal{G} = \{\mathcal{V}, \mathcal{E}, \mathcal{W}\}$ where $\mathcal{V}$ is the set of the N nodes or individuals, $\mathcal{E} = \{(i, j) \subseteq \mathcal{V} \times \mathcal{V}\}$ is the set of edges, namely the links connecting individuals and $\mathcal{W}$ are the weights associated to each link in $\mathcal{E}$. The opinion x_i of the i-th agent at each time instant t evolves as follows:

$$x_i(t+1) = \lambda_i \sum_{j \in N_i} w_{ij} x_j(t) + (1 - \lambda_i) x_i(0) \qquad (2.3)$$

where $\lambda_i \in [0, 1]$ is the phycological trait of being susceptible to the social pressure of the agent i, namely it represents the complement to the stubbornness of the agent: the more susceptible is to the opinion of other neighbors the less stubborn is and vice versa. The averaging occurs over the set of the neighbors of agent $i : \mathcal{N}_i = \{i \in \mathcal{V} : (i, j) \in \mathcal{E}\}$, and $w_{ij} = \frac{1}{|\mathcal{N}_i|}$ weighs the opinion of neighbor j, where $|\cdot|$ denotes the cardinality of a set. Finally $x_i(0)$, that is, the opinion of agent i at the beginning, represent its prejudice toward a certain topic of discussion.

In matrix form, the model translates in:

$$x(t+1) = \Lambda W x(t) + (I_n - \Lambda) x(0) \qquad (2.4)$$

where $\Lambda = \text{diag}\{\lambda\}$ is the diagonal matrix of the susceptibilities of each individual, I_N is the identity matrix of size N, W is the row-stochastic matrix whose element w_{ij}

is how much agent i weighs the opinion of agent j, and $x(0)$ is the state vector of the initial opinions of the network.

Assuming that $\Lambda \neq I_n$, that is, there exists at least one non-stubborn agent, the opinions of the agents will converge [51] at steady-state toward $\bar{x} = [\bar{x}_1, \ldots, \bar{x}_n]^T$:

$$\bar{x} = (I_n - \Lambda W)^{-1}(I_n - \Lambda)x(0) \tag{2.5}$$

It can be shown that this equilibrium point $\bar{x}$ is globally asymptotically stable [52] and belongs to the convex hull of the initial conditions $bar x \in co(x(0))$, modelling the fact that the discussion among people yields the opinions to get closer to each other, namely shrinking the opinion profile even though the steady state is not consensus in general, i.e. $\bar{x}_i \neq \bar{x}_j$.

As for the previous model, in the Friedkin-Johnsen there is a "memory effect" of the initial opinions in the outcome of the interaction process among the agents by considering inhomogeneous terms, functions of the initial conditions. Different from the majority of opinion dynamics models proposed in the literature, this model has been experimentally validated for small and medium-size groups, as reported in [53–55].Thus, this F-J enables to model a well-known sociological behavior that emerges in real-world communication.
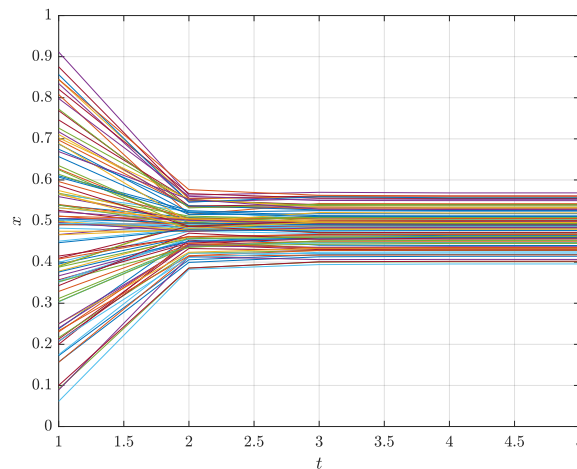
Figure 2.4. Evolution over time of opinions according to F-J model.

2.5 Modelling sophisticated social traits with nonlinear coupling

Stubbornness is not the only psychological trait that influences the opinion formation process, resulting in disagreement. Also, competitiveness or cognitive biases can (mis)guide

us in interacting with other people on a certain topic. Among the different updating rules proposed to capture disagreement, we recall the following well-established ones: antagonistic interactions [56–58], interacting only people with similar opinions [46, 59], imitation or herding [37, 60].

In the following, there is a brief description of some emblematic averaging models with nonlinear coupling-weight dynamics.

Altafini model

In order to encompass also negative ties that links interconnected people such as competitiveness or antagonism, Altafini in 2012 [56, 61] proposed an opinion dynamics model that occurs on a signed graph based on the following intuitive assumption: if positive edges correspond to collaboration, trust, or cooperation among the agents, then negative edges should correspond to antagonism, mistrust, or rivalry. He extended the consensus algorithm to the case where there are antagonistic interactions, considering structurally balanced graphs. Moreover, these negative ties can lead to boomerang effects, first described in [62]: in the process of persuasion, opinions (even close to each other initially) can become opposite. we define a structurally balanced graph as a network that can be partitioned into two vertex subsets, such that intra-group edges are all positive and inter-group edges are all negative. When a graph is structurally balance, we can achieve the so-called bipartite consensus where agents are split into two disjoint subcommunities $\mathcal{V}_1, \mathcal{V}_2 : \mathcal{V}_1 + \mathcal{V}_2 = \mathcal{V}$

$$|x(k)| \overset{k \to \infty}{\longrightarrow} x^* \to \begin{cases} x_i(k) \overset{k \to \infty}{\longrightarrow} x^* \in \mathcal{V}_1 \\ x_j(k) \overset{k \to \infty}{\longrightarrow} -x^* \in \mathcal{V}_2 \end{cases}$$
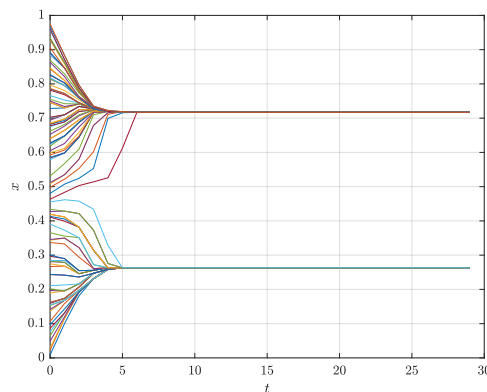
Figure 2.5. Evolution over time of opinions according to Altafini model.

Bounded confidence models

Disagreement cannot persist only when there are antagonistic ties. Another way of modelling this phenomenon is reflecting upon the fact that individuals are more likely to weigh positively opinions of like-minded individuals and to discard the ones that are too far away from its own, this bias is known in psychology as biased assimilation [59]. The opinion dynamics models that focuses on how people tend to group together with similar individuals, aka homophily [63], are called bounded confidence models [44, 46].

Hegselmann-Krause model

The Hegselmann-Krause (H-K) model [46] is quite similar to the DeGroot, the subtle yet significant difference is the set of neighbors of each agent i is time-varying as it is defined in the basis of the opinions at each time instant: each individual is connected only with the ones whose opinions differ from them by no more than a certain confidence level ϵ. In this model, the opinion $x_i(t)$ is a real number $\in [0, 1]$, and two opinions are similar if the absolute value of their difference $|x_i(t) - x_j(t)|$ is smaller than the threshold $\epsilon \in \mathbb{R}$.

The resulting time-varying non-linear opinions updating rule is

$$x_i(t+1) = \frac{1}{\sum_{j=1}^{n} w_{ij}(x_i(t))} \sum_{j=1}^{n} w_{ij}(x_i(t))x_j(t) \tag{2.6}$$

$$\begin{cases} w_{ij}(x(t)) = 1 & if \ |x_i(t) - x_j(t)| \leq \epsilon \\ w_{ij}(x(t)) = 0 & \text{otherwise} \end{cases}$$

This model is able to capture what in literature is called "strong diversity" that is the opinion profile at steady-state will converge to a configuration of persistent disagreement or fragmentation, with a range of different opinion values. However, in H-K model if an agent i disregards the opinion of agent j because they do not fall in their confidence bound, a split in their connection occurs and cannot be reestablished, a fact that is it not so common in real world. Agent i interacts only with like-minded agents defined by a certain confidence level ε.

For each agent i we denote a confidence set as

$$D(i, x) = \{1 \leq j \leq n, |x_i - x_j| \leq \varepsilon\}$$

The update rule consists in an average of the trusted agent opinions

$$x_i(k+1) = |D(i, x(k))|^{-1} \sum_{j \in D(i,x(k))} x_j(k)$$

The possible asymptotic behaviors are three: fragmentation, polarization (fragmentation in only to groups) or consensus, depending on ε.
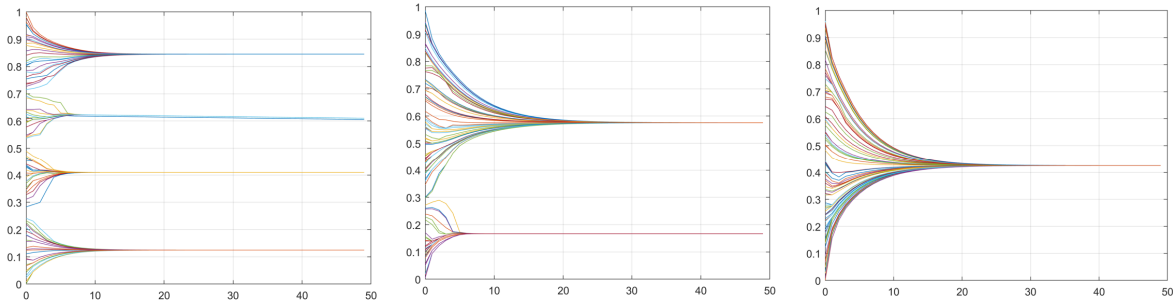
Figure 2.6. Evolution over time of opinions according to H-K model at varying ε.

Deffuant-Weisbuch model

The Deffuant-Weisbuch model is very similar to the HK model and it is defined by the following updating rule:

$$x_i\left(k+1\right) = x_i\left(k\right) + \mu(x_j\left(k\right) - x_i(k)) \tag{2.7a}$$
$$x_j\left(k+1\right) = x_j\left(k\right) + \mu(x_i\left(k\right) - x_j(k)) \tag{2.7b}$$

where μ is the so-called learning rate that usually lies in $(0, \ 0.5]$ to avoid crossover. The update takes place only if $|x_i(k) - x_j(k)| \leq \varepsilon$. The main difference is that the update is not synchronous for all agents: at each time instant, two agents are randomly chosen from the set of all individuals. Depending on the parameters and μ, a consensus, polarization, or fragmentation of opinion distribution will be obtained.

2.6   Cutting-edge models

Beyond the classical opinion dynamics models that laid the foundations of this research field, a lot of new models have been proposed in the literature recently [64–71]. They revisit and combine well-established models or propose new frameworks to take into account more complex mechanisms such as accounting for multiple opinions simultaneously onto different topics (multidimensional opinion state space), multi-body interactions going beyond peer-to-peer communication ties, sequential topic discussion, discrepancies in what we think and what we say etc. In the following, some interesting examples of these cutting-edge models are briefly reported, also to show how they rely on the classical models in their main mechanisms.

Expressed and private opinion (EPO) model

To take into account that more often than not individuals tend not to be completely sincere about what they think, due to peer pressure, shame, willingness to conform, the

author of [37] proposed an opinion dynamics model to study the discrepancy between private and expressed opinion can arise in social groups.

Each individual in the network has both a private and an expressed opinion: an individual's private opinion evolves under social influence of the average of the expressed opinions of its neighbors, whereas the agent updates its expressed opinion modifying his private opinion under the pressure to conform to the average of the expressed opinions of its neighbors.

Formally, private opinion of agent i, $x_i(t)$ evolves as

$$x_i(t+1) = \lambda_i w_{ii} x_i(t) + \lambda_i \sum_{i \neq j}^{n} w_{ij} \hat{x_i}(t) + (1 - \lambda_i) x_i(0) \qquad (2.8)$$

and expressed opinion $\hat{x}_i(t)$ is updated according to

$$\hat{x}_i(t+1) = \phi_i x_i(t) + (1 - \phi_i) \hat{x}_{avg}(t) \qquad (2.9)$$

where $\hat{x}_{avg}(t) = \frac{\sum_{i=1}^{n} x_i(t)}{n}$ is called the public opinion and $\phi_i \in [0, 1]$ is a resilience parameter, that is the ability for individual to withstand group pressure.

We can observe that an individual's expressed opinion is a convex combination of his/her private opinion and the public opinion in the previous round of discussion. The private opinion evolves according to the F-J with the peculiarity that only the expressed opinions are known (observable) by each agent.
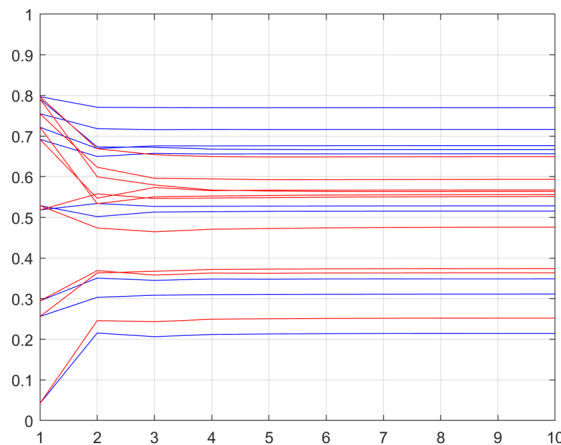
Figure 2.7. Evolution over time of opinions according to EPO model.

Continuous Opinions Discrete Actions model

The Continuous Opinions Discrete Actions (CODA) model proposed by Martins [72] is a hybrid model where each individual is only aware of the (discrete) choices of other individuals, whereas their (continuous) opinions remains private. It has been initially

proposed to explain the emergence of extreme opinions in the population, but it is also the first attempt to model simultaneously the evolution of opinions and decisions. This model consists of three key ingredients:

- opinions are continuous variables bounded between 0 and 1, and they are private (unobservable)

- individuals can take binary actions that are observable;

- individuals update opinions by incorporating peer behavior using a Bayesian update rule;

Initially, agent i has a given opinion $p_i(0) \in (0,1)$ about which decision q_i is better. The action value $q_i(k) \in \{0,1\}$ is a quantized version of $p_i(k)$ defined by:

$$q_i(k) = \begin{cases} 0 & \text{if} p_i(k) < 0.5 \\ 0 & \text{if} p_i(k) = 0.5 \text{and} p_i(k-1) < 0.5 \\ 1 & \text{otherwise} \end{cases}$$

Each agent has access only to the action of its neighbors. The opinion of agent i updates according to the following rule:

$$p_i(k+1) = p_i(k) + \frac{p_i(k)\,(1-p_i(k))}{n_i} \sum_{j \in N_i} (q_j(k) - p_i(k))$$

The model can capture different behaviors observed in networks of social groups such as dissensus, clustering, oscillations, opinion propagation [73].

Nonlinear opinion dynamics model

Recently, in [74], has been proposed a model that claims to be a generalization of most of the classical models presented in the previous section, and still to avoid a paradox that constitutes a limitation of averaging linear models. Indeed, this mechanism implies that the strength of the coupling between the opinions of two individuals increase linearly with their difference. It means that the more divergent the two agents'opinions are, the more strongly they will be attracted to each other. This is not the case in many real cases, where two individuals with too divergent opinions will rarely compromise to agree on the same opinion, indeed this consideration is the one that has inspired bounded confidence models.

This recent model presents a generalized framework in which the opinion update process is nonlinear, introducing a saturation of the opinion exchange, meaning that, given an agent i and its neighbors $j \in \mathcal{N}_i$, there is a certain threshold onto the difference of opinions $x_i - x_j$ beyond which the influence that the others can have on the opinion of agent i is limited.

The general formulation of the multi-option model is quite complicated. Thus, let us first introduce some quantities

- $N_o \geq 2$ is the number of available options

- N_a is the number of agents

- $Z_i = (z_{ij}, i = 1, \ldots, N_a, j = 1, \ldots, N_o)$ is the vector of state variable associated to agent i

- $Z = (Z_1, \ldots, Z_{N_a}) =$ is the whole system state matrix

- $d_i > 0$ weighs the linear resistance term

- $u_i \geq 0$ weighs the social influence term

- b_{ij} is the input (bias) of agent i on option j

When the resistance parameter d_i dominates the attention parameter u_i, it means that the agent is weakly susceptible to other agents' opinions. When u_i dominates d_i, the agent is strongly attentive to other agents' opinions. A shift from a weakly attentive to a strongly attentive state can be induced, for instance, by a time urgency (election day approaching) or a spatial-urgency (target getting closer) to form an informed collective opinion. Then, we have four gains of the couplings $\alpha_i, \beta_i, \gamma_{ik}, \delta_{ik}$ $\boldsymbol{i \neq k}$

- α_i intra-agent same option coupling

- β_i intra-agent inter-option coupling

- δ_{ik} inter-agent same option coupling

- γ_{ik} inter-agent inter-option coupling

Note that $\alpha_i \geq 0$ as options are self-reinforcing, $\beta_i < 0$ as options are mutually exclusive, if $(\gamma_{ik} - \delta_{ik}) > 0$ agents cooperate because agent i give credit to agent k 's preference, otherwise $(\gamma_{ik} - \delta_{ik}) < 0$ agents compete because agent i prefers what agent k dislike.

Now we can provide the general formulation

$$\dot{Z}_i = P_0 F_{ij}(z)$$

$$F_{ij}(z) = -d_i z_{ij} + u_i \left(S_1 \left(\alpha_i z_{ij} + \sum_{\substack{k=1 \\ k \neq i}}^{N_a} \gamma_{ik} z_{kj} \right) + \sum_{\substack{l=1 \\ l \neq j}}^{N_o} S_2 \left(\beta_i z_{il} + \sum_{\substack{k=1 \\ k \neq i}}^{N_a} \delta_{ik} z_{kl} \right) \right) + b_{ij}$$

Furthermore, let us note that the larger d_i is, the more resistance the agent has in forming an opinion. If all the other terms are zero, then it drives the systems towards the neutral point, the indecisiveness. Moreover, the social influence term can act only in a bounded way in either direction, as opinion exchanges are saturated. Finally, note that if u_i is small it means that inertia dominates thus, the system behaves linearly
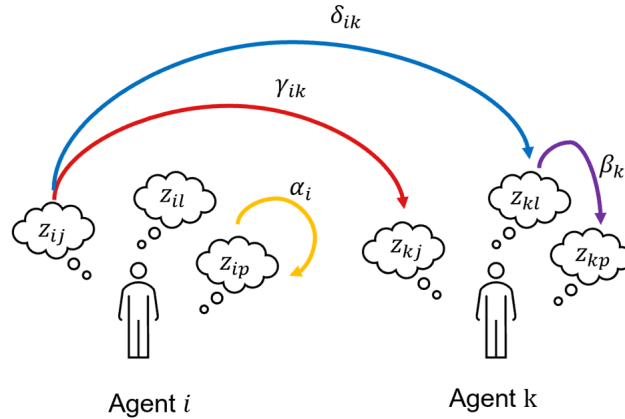
Figure 2.8. Representation of the four couplings of the general version of this model.

$z_i \approx b_{ij}$. Otherwise, if u_i is large, social pressure dominates, hence the system behaves non linearly $|z_i| \gg |b_{ij}|$.

This model prescribes a particular single dynamics such as $\dot{x}_i = -d_i x_i + u_i \mathcal{S}(x_i)$

Hence, this intrinsic dynamics of opinion formation can give a rise to a bifurcation, even in the absence of inputs, as long as the attention parameter is sufficiently high, that is the opinions at steady state can be more extreme than the initial ones.
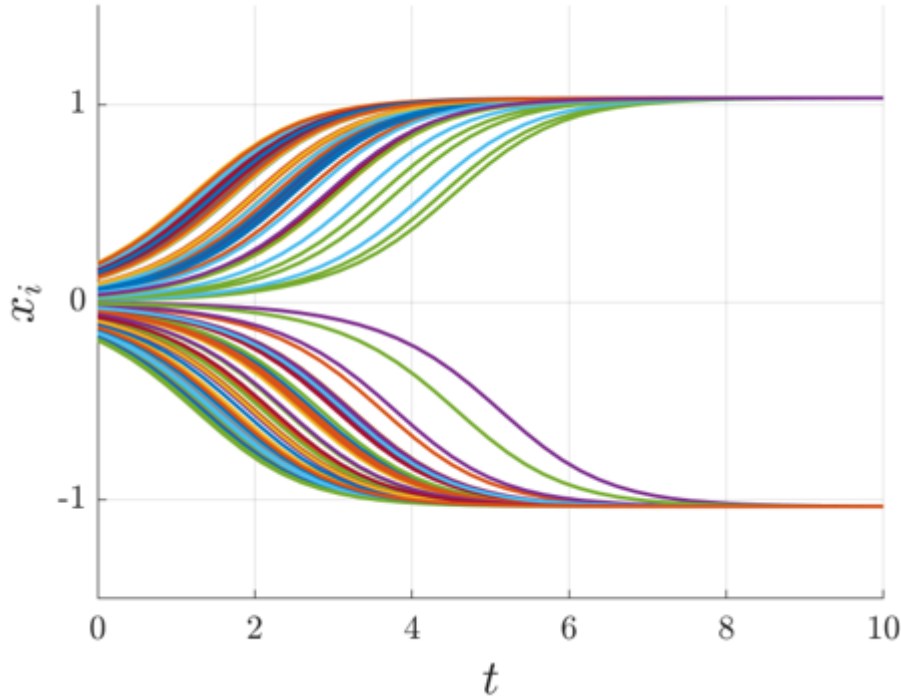
Figure 2.9. Evolution over time of the opinion of a single agent at varying its initial conditions.

Beyond capturing opinion formation starting from indecisiveness, this model, adding a nonlinear coupling, is able to replicate behaviors of the classical opinion dynamics

models as simplified subcases and a rich ensemble of properties that cannot be captured by linear models such as multistable agreement and disagreement, tunable sensitivity to input, robustness to disturbance, opinion cascades. In continuous time linear models, consensus on non-zeros values and dissensus are never exponentially asymptotically stable because the Jacobian of these models have a zero eigenvalue. Saturating opinion exchanges makes the model structurally stable, the equilibria hyperbolic, and it weakens the conditions for stable disagreements in steady states (e.g., balanced coupling of network graph or time-varying structure). Non-linearity enables the coexistence and simultaneous stability of many consensus and dissensus equilibria.

In the case of the classical two-options model, at steady state we have bistability with two stable equilibria and the neutral state as unstable equilibria

More formally, the two-options model is

$$\dot{x}_i = -d_i x_i + u_i \hat{S}\left(\alpha_i x_i + \sum_{\substack{k=1 \\ k \neq i}}^{n} \gamma_{i,k} x_k\right) + b_i \tag{2.10}$$
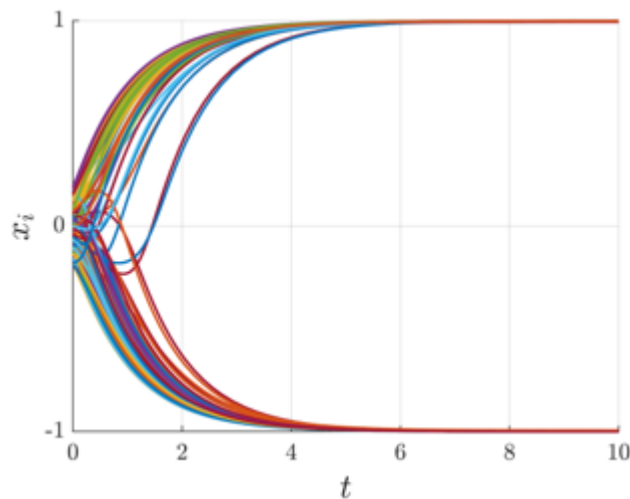
Figure 2.10. Evolution over time of opinions according to the two-option model in a network of 100 individuals.

2.7   Critical overview

Wanting to contribute to a critical insight of the wide literature on opinion dynamics, here I try to briefly state what has been done up to now and what are the gaps and the new perspectives that I found to be the most relevant underlining, among them, the ones I tried to address by means of my research work. Indeed, my attempt in this thesis has been developing a modeling framework for the coevolution of opinion dynamics and collective decision-making in complex social systems that could

1. be representative of the dynamics over time of large social networks;

2. bridge the gap between opinion dynamics and decision-making;

3. capture the role of influencers in opinion formation;

4. be tuned on data.

Network control theory has brought new life to the opinion dynamics literature, rooted in 1950, because, thanks to its mathematical tools, it enables us to model, analyze in rigorous fashion and replicate some collective behaviors that occurs in real-world situations that encompass social groups. Opinion dynamics models helped to shed some light on the underlying mechanisms that regulate social interaction and opinion formation over time: it helped comprehend how people in a society or network influence each other's opinions, gain insights into human behavior, collective decision-making, and the emergence of shared norms and beliefs, understand how network structures influence the likelihood of consensus or polarization, together with network theory helps us understand how the topology of connections affects the speed of information spread, provide insights into the mechanisms behind the dissemination of information, rumors, and news, provide valuable insights for policymakers, social scientists, and organizations when considering potential outcomes of different interventions or strategies, provide insights into strategies to mitigate the negative consequences of extreme polarization while fostering healthy debate. As stated in [75] "Idealized models of opinions dynamics are useful as proofs of concept to test the consistency of descriptive theories of collective behavior, and to explore the potential outcomes of sociopolitical scenarios based on simplified hypotheses of human interaction." However, there are still some gaps that need to be filled in order to exploit the full potentiality of opinion dynamics.

Issue 1 Indeed, a lot of work has been devoted to study in which conditions consensus can emerge or be induced. Consensus formation has attracted most of the attention from the researchers because of its practical usefulness in some societal-relevant applications. It has been thought that reaching consensus was critical in a decision-making process ranging from politics to health education to economics. However, nowadays, the amount of interconnections and also the way how people can interact with each other has changed so drastically that consensus might not be the most interesting regime state that systems may reach [76]. In fact, if we consider large complex networks of individuals, it is quite unrealistic that they all agree on a topic, as it is evident from social networks debates

daily. Fragmentation and polarization are the most common scenarios that we can observe in reality. Some studies like [77, 78] tried to replicate or minimize polarization. In this thesis, we wanted to unveil the mechanism of influencing opinions so to exploit the knowledge of such collective behaviors and take them into account when trying to diffuse some idea in the network in support of vaccine willingness or product adoption.

Issue 2 The study of dynamical models of opinion evolution on social networks has drawn the interest also of the control community because as stated in [39]

> "Opinions and beliefs are at the basis of behavior, and can be seen as the internal state of individuals that *drives* a certain action. Hence understanding opinion formation and evolution is key to explaining human choices. Opinion formation is a complex process depending on the information that we collect from peers or other external sources, among which *mass media* are certainly the most predominant. Hence, understanding how these different forces interact can give insight into how complex non-trivial collective human behavior emerges and how well formulated information may *drive* individuals toward a virtuous behavior."

With the development of information and network technology, opinion dynamics on social network is often an integral part of large-scale decision-making [79]. Many works point out that a bridge lacks between opinion dynamics and Group Decision Making (GDM) research: for example, on one hand, deploying complex networks topologies (e.g., Erdős-Rényi random graph or the scale-free network) to represent the relationships among decision makers, has been a tool overlooked in GDM literature. On the other hand, there are only few works trying to model at the same time how the opinion disagreement translates into agents' decisions. Moreover, Noorazar in [76] highlighted the need to study more deeply the presence of non-cooperative agents. Indeed, the premise at the base of all the literature on consensus formation was that the people were cooperative and willing to compromise in order to get cohesion on a topic, an assumption that seems reasonable for example when considering small groups of people in a meeting trying to come up with new ideas or initiatives, but this is not the case of public discussions.

Issue 3 Strictly linked to the previous point, there is the issue of how opinion formation processes can be (intentionally) influenced: some individuals may manipulate the opinions and relationships towards an established purpose. Indeed, even though the majority of individuals in a society have quite similar behaviors, say *ordinary*, there exist a minority of individuals with specific characteristics such as opinion leaders, informed agents, stubborn agents or zealots and contrarians. Opinion leaders can be defined as individuals who have a great amount of influence on the decision-making of other people [80]. The influencers have a crucial role in determining the opinion formation of other agents. Identifying influencers can be key in different fields of applications such as in marketing to efficiently promote the adoption of new products by means of targeted advertising [81]; political science where opinion leaders propagate their beliefs and norms to the population arena [82]; public health that support the adoption of evidence-based

healthcare initiatives [83];education in which they can actively contribute to enhancing teaching quality, shaping student perspectives [84]. A plethora of methods to detect influencers in social networks have been proposed in the past 40 years, being different based on the research field of origin. They can be mainly classified into centrality measures, link topological ranking measures, entropy measures, and node embedding measures [85,86]. The effort in this thesis is to link influencer detection, opinion dynamics and control theory to model the effect of this "particular individuals" in the opinion formation and decision-making process.

Issue 4 Even though agent-based opinion dynamics models have a powerful explanatory nature, their predictive one is rather limited by parameter tuning that still represents a significant challenge: in [87] it is claimed that "there is a striking imbalance between empirical evidence and theoretical modelization, in favor of the latter". Generally, studies in opinion dynamics devote a lot of attention to simulation analyses, but the data sets used are often from random data in simulations, and there are few studies involving the opinion dynamics simulations analysis with real data [38]. Moreover, transient dynamics and the memory effect of social interaction have been overlooked [88] and more complete datasets could enable also the tuning of the timescale of the evolution over time of opinions, namely giving a real estimate of how long the time step and the transient are and thus how long it takes to reach the steady state predicted by the model. This motivates our attempt to use real data from surveys or social networks to provide of an empirical validation of these interesting models that have not been fully exploited in all their potential.

Different from other types of data, gathering empirical data on opinions poses challenges, as it requires transforming opinions expressed in words into measurable quantities suitable for mathematical modeling. Moreover, there is the problem of how to collect these data. The two major sources are surveys and online social media data, and both are not free of limitations: surveys are the most intuitive way of collecting opinions of people, as they come from a design of experiment in which what and how to ask is carefully decided to retrieve data reliably. Surveys are easy to interpret as they are made for acquiring information and can be statistically representative even if administrated to a small group of people as individuals can be selected to have a sample stratified for categories as age, income, educational background etcetera. However, they come with some drawbacks, as they are costly and time-consuming both in the design and informtion collection phases. Furthermore, there is risk of biased answers due to boredom, willing not to express opinions that are perceived as minority. Finally, surveys do not provide information on how opinions have formed. On the other hand, online social networks could seem like a goldmine of freely expression of individuals' ideas, and it is also possible to investigate how people change opinions over time and how they interact with other users. However retrieving data from social media requires automated data processing tools which do not guarantee that the translation from words to numbers is reliable and free of noise. Moreover, the population that "lives" on social networks may not be representative of the one in real life. Thus, it is desirable to use both sources of information carefully, being aware of their potential and their limitations.

Anyhow, this difficulty in collecting reliable data has led to the dominance of mod-

eling and simulation at the expenses of experimental works in the field. Sociological theories are translated into mathematical rules, often relying on common sense rather than empirical validation [88], even though the relevance of these models of probing scenarios, testing theoretical consistency, and exploring emergent behaviors [75] remains indubitable.

Part III

Contributions

Contributions

In the following a summary of each work included in this thesis is presented.

Paper A – Partial Controllability of Network Dynamical Systems With Unilateral Inputs

Paper A is a reformatted version of

Summary: Our ability to control network dynamical systems is often hindered by constraints on the number and nature of the available control actions, which make controlling the whole network unfeasible. In this letter, we focus on the case where unilateral inputs are exerted on a subset of the network nodes. Leveraging the observation that, different from the case of subsystems, unilateral node reachability and controllability are equivalent, we provide conditions for a given node subset to be unilaterally controllable. The theoretical findings are then employed to develop a computationally efficient heuristic to select the nodes where the unilateral inputs should be injected.

Authors' contributions: The author of this thesis contributed with the other authors to theoretical derivations and to the drafting of the manuscript. Numerical simulations were devised and implemented by the author of the thesis.

Paper B – Partial observability of complex networks

Paper B is a draft version of an ongoing work

Summary: The study of the controllability properties of complex networks has been the focus of numerous researchers in the past decade. When a network is considered as a whole, indeed all controllability results extend to the case of observability as well. However, when controllability and observability are sought of only a fraction of the network nodes, or in other words of a given subnetwork, then the subtle yet significant differences between a network and a large-scale dynamical system arise, leading to the surprising observation that the theoretical tools used to study subnetwork controllability do not extend to subnetwork observability. In this work we show that this *loss of duality* between controllability and observability of complex networks reflects into a substantial difference in our ability of controlling and observing complex subnetworks and it brings out the need of finding a novel strategy to place sensor nodes with respect to the well-established one for driver nodes selection.

Authors' contributions: The author of this thesis contributed with the other authors to the devise of heuristic algorithms and to the drafting of the manuscript. Numerical simulations were devised and implemented by the author of the thesis.

Paper C – Influencing Opinions in a Nonlinear Pinning Control Model

Paper C is a reformatted version of

Summary: This letter studies how opinions and subsequent actions of groups of individuals are shaped by opinion leaders, nowadays denoted influencers. We model an influencer as a pinner that exerts a control input on a small subset of individuals, and leverages the interaction network to affect the action of a large fraction of individuals. We provide sufficient conditions so that a given agent takes the same action as the pinner. Based on these conditions, we design a heuristic for the pinned node selection that maximizes the number of nodes taking the action elected by the pinner. The performance of the heuristic is then numerically tested against standard pinning strategies.

Authors' contributions: The author of this thesis contributed with the other authors to theoretical derivations and to the drafting of the manuscript. Numerical simulations were devised and implemented by the author of the thesis.

Paper D – A model-based opinion dynamics approach to tackle vaccine hesitancy

Paper D is a reformatted version of

Summary: Uncovering the mechanisms underlying the diffusion of vaccine hesitancy is crucial in fighting epidemic spreading. Toward this ambitious goal, we treat vaccine hesitancy as an opinion, whose diffusion in a social group can be shaped over time by the influence of personal beliefs, social pressure, and other exogenous actions, such as pro-vaccine campaigns. We propose a simple mathematical model that, calibrated on survey data, can predict the modification of the pre-existing individual willingness to be vaccinated and estimate the fraction of a population that is expected to adhere to an immunization program. This work paves the way for enabling tools from network control towards the simulation of different intervention plans and the design of more effective targeted pro-vaccine campaigns. Compared to traditional mass media alternatives, these model-based campaigns can exploit the structural properties of social networks to provide a potentially pivotal advantage in epidemic mitigation.

Authors' contributions: The author of this thesis contributed with the other authors to theoretical derivations and to the drafting of the manuscript. Numerical simulations were devised and implemented by the author of the thesis.

In this thesis, different models and problem formulations have been considered, nevertheless all of them aim to investigate how the complexity and control theory tools can help modelling, analyzing and validating what-if scenarios of collective behaviors that can emerge in groups of interconnected individuals to ultimately provide a support for decision-making processes in social systems.

In Paper A, we analyze the controllability property of a simple LTI model and consider economic and physical constraints to the available control inputs. Nameluy, the inputs are assumed to be limited in number and unilateral, i.e., they can take either positive or negative values but not both. This scenario is reasonable when trying to steer the states of a large scale network of dynamical systems towards a desired equilibrium. Considering the context of shaping the opinion formation process of a large group of interconnected individuals, we can think of government bodies that want to ensure that a new initiative will bring the expected outcome, considering the limited budget and the fact that they can provide an incentive/fee but not both on the same issue, or a company that, not being allowed to make comparative advertising as in Italy, can only promote its products and want to know how effective could be its campaign in convincing people to buy its products. Thus, having at disposal a theoretical framework that can provide conditions on effectiveness of their measure can represent a competitive advantage on the market.

Paper B tackles the problem of conferring observability to the largest subnetwork of a complex network of LTI dynamical systems in case the number of sensors at disposal is strictly smaller than the one required to observe all the nodes of the network. We highlight the differences in considering subsystems and subnetworks and propose a heuristic to maximize the number of observable nodes in the network. If we interpret the LTI network systems as a social group discussing on the adoption of a product, we can translate the ability to observe the network dynamics in practical implications like reconstructing the behavior of consumers to have feedback on effectiveness of targeted advertising promoted by some company or monitoring the acceptance of a certain social norm furthered by government bodies.

Paper C investigates the role of opinion leaders in influencing the opinion and thus the action of a group of interconnected individuals. To do so, a nonlinear opinion dynamics model, one of the most recent and complete available in the literature, is studied in the presence of a virtual node, a pinner, that exert its influence on a subset of individuals with the goal of convincing them to take its own action. This phenomenon is what can be seen on social media, like Twitter, where an individual that has gained social power is not influenced by the other in the community but tends to promote a certain action (for instance, a stance in a political referendum or a preference among similar product of different brands). Theoretical conditions are derived so that an individual takes the same action as the pinner, and they are leveraged to devise a strategy to maximize the number of people that follow the opinion leader.

In Paper D, we consider a classic opinion dynamics model, that by Friedkin-Johnsen, that can capture the attachment of each individual towards an intrinsic belief, and try to make a step in bridging the gap between the descriptive capability of opinion dynamics models and the predictive potential that these models have by tuning its parameters on

survey data. To do so, we consider the paradigmatic example of COVID-19 vaccination to capture how on one hand, the fragmentation of opinions towards this divisive topic is related to taking an actual action (agent-based decision-making process), and on the other hand, how having a model could benefit the government bodies, who promoted the awareness vaccination campaigns, to decide towards who they should devote their effort to gain the largest increase in vaccination acceptance. To do so, methods from parametric identification have been used as well as data sources from surveys on vaccine willingness of a representative sample of Italian citizen at the beginning of the vaccination campaign together with a network of interactions borrowed from Facebook. On this testbed the effectiveness of different vaccination campaigns differing for the criterion with which individuals were targeted to diffuse vaccine acceptance was evaluated in what-if scenarios.

Papers A, C, D have been already published in Q1-ranked journals, whereas paper B is a draft version of a paper in the process of being submitted soon.

On controllability and observability of subnetwork of dynamical systems

Introduction and Motivation

For what concerns the theoretical-oriented works in this thesis, they address the analysis of complex dynamical networks properties such as controllability and observability. Being able to control and observe the complex network of dynamical systems is an essential goal because it enables us respectively to bring the network's elements from any initial state to a target one or to reconstruct any initial states thanks to known inputs and measured outputs. Control and observation are key issues in most complex networks related problems because the ultimate proof of deeply understanding the dynamics of interaction between elements of a certain system is, on one hand, to be able to influence their behavior towards to a desired one and on the other hand to monitoring if abovementioned control is actually effective. Conferring these desired properties to networks of interest could be cumbersome when feasibility constraints hold [89], such as when we can deploy only unilateral inputs, that is inputs can assume only positive or negative values, for example just think of international trade networks: economic policies such as import restrictions and tolls as well as subsidies of the domestic production acts as one-sided controls. The paper [90] addresses this particular issue, providing both theoretical results and heuristic solutions to find the maximal complex dynamical subnetworks when both limited number of actuators and unilateral control inputs are the only available. Indeed, another common and relevant issue in real large-scale applications is that of the availability and the selection of actuators/sensors to control/monitor the network of interactions is constrained by both economical and physical limitations [24]. Hence, there is the need to select actuators/sensors in an optimal way to confer desired properties to the largest subnetwork possible. Analytical and heuristic solutions has been already proposed in the literature for ensuring the controllability and observability of the whole network, however, being often an unfeasible problem for large-scale networks, our article aim to fill the gap for what concerns the partial framework, namely the controllability and observability of the largest subnetwork. In particular, the work entitled "Observabil-

ity of complex dynamical networks" deals with the partial observability problem, that is observing the largest subnetwork possible, proposing a smart sensor node selection in order to maximize our ability to observe a complex network in case of a limited number of sensors available. This work lends itself to market-oriented applications or more generally to all the cases in which there is the need of monitoring the evolution over time of some dynamics occurring on a network or the effectiveness of some designed campaigns: for example, the potential could be to dynamically observe the customers preferences, in order to give the company a competitive advantage, enabling it to use the reconstructed tastes as an input to improve the design process of new products or existing items or to estimate the perception of people on a key societal issue related to education or health to collect information that could drive the decision-making onto next initiatives. Sticking with the former example, the ultimate goal would be that of creating a dynamical feedback loop between product innovation and customers preferences in order to update the real needs and desires of the consumer. The idea of reconstructing costumer preferences is not brand new because companies already monitor our navigation data to reconstruct our purchases preferences as we can notice each time a site ask us for the cookie consent. The innovation of our approach stands in an agent-based modeling approach, that is, looking at the customers who share their purchases preferences as a network where the node represents the customer and the link between them represent their interaction. Thanks to opinion dynamics theory, we can model the opinions' evolution as a dynamical system, to which we can apply the tools of control theory to observe and predict how opinions change over time. This could strongly support the design or rethinking of products in order to dynamically adapt them to the customers' needs, reducing the gap between demand and offer.

3.1   Paper A - Partial controllability of network dynamical systems with unilateral inputs

In the last decade, since the publication of Liu's work [28] revived the interest towards classical control problems in the complex network framework, a lot of work have been devoted to modeling, mathematically analyze and derive conditions under which network complex systems can be controlled [91–96], with a particular attention to design decentralized control strategies to induce the emergence of collective behaviors, mostly synchronization and consensus [97–100]. However, as we stated in Section 1, controllability is a prerequisite of control design, thus many works focused on translating the concept of controllability of dynamical systems to the complex networks of dynamical systems' framework, solving the minimal controllability problem, that is finding the minimum set of driver nodes, that, if injected with control inputs, can guarantee complete controllability [101, 102], minimum energy problems that take into account also the energy required to make the network controllable [103–105]. the next step has been the one to address more realistic scenario that account for the fact that achieving complete network controllability can be unnecessary or unfeasible, due to the limited amount of actuators and thus the problem of *partial* controllability, namely controlling the largest subnetwork, arise [24, 106].

A further restriction on the nature of control inputs, typically overlooked in the literature on network control, is their sign over time, namely only unilateral inputs are available [107, 108]. Application areas with naturally unilateral control inputs include the optimal power flow problem in power grids, where nodes are either loads that absorbs power or generators producing it and not vice versa [109, 110], in biological networks with nodes corresponding to molecular components, a drug acting on a molecule constitutes a control action that can inhibit or activate genes but not both simultaneously [111], control of wire-driven parallel robots that can be only pushed or pulled on a plane [112, 113], marketing campaigns where comparative advertising is forbidden thus it is not possible to simultaneously promote a product and discourage the adoption of the competitors [114], Other examples of unilateral controls can be found in mobility networks transport measures like traffic lights or speed limitations, in international trade networks trade policies such as import restrictions and tolls as well as subsidies of the domestic production, in water distribution networks, pumps and valves [108].

The first articles tackling the problem of considering constrained control inputs dealt with null-controllability of dynamical systems [115, 116], but recently the same problem has been addressed in the network dynamical systems' framework. In [108] the minimal input problem have been mathematically solved to make the whole network unilaterally controllable. The literature gap that we filled with this work has been tackling the controllability problem of a subset of the network nodes with unilateral inputs. This translates to a control design problem to select the actuator nodes to maximize the number of nodes unilaterally controllable. When considering unilateral inputs, the network controllability cannot be studied through structural approaches, nor through classical

Figure 3.1. Application areas where unilateral inputs naturally exists.
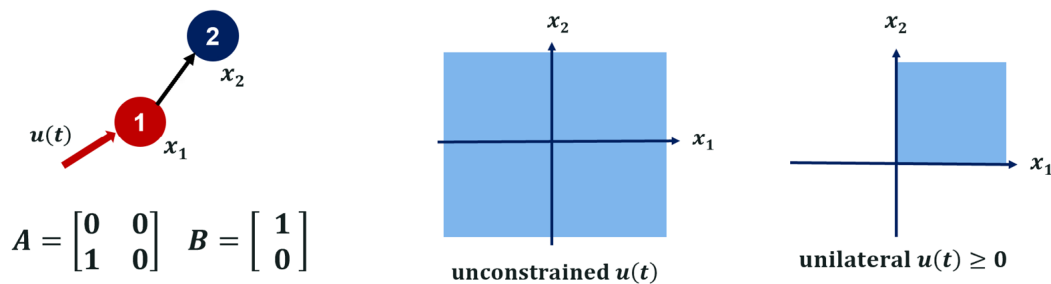
Figure 3.2. Disposing of only unilateral control hinder our ability of conferring controllability to networks: in this toy example with a two-node network where we control node 1 with a positive input, differently from the unconstrained case, we cannot control the whole network.

algebraic controllability tests for LTI systems. Having at disposal less theoretical tools to solve this particular controllability problem makes it more challenging than the unconstrained case, see Fig. 3.2. We tackled this problem by first characterizing the part of the state space that is unilaterally controllable, namely the convex cone containing the unilaterally controllable subspace, which we show to differ from the one containing the unilaterally reachable states. Then, by means of a suitable projection, we translated these results for network dynamical systems, to finally derive the conditions for unilateral reachability and controllability of a node subset that we showed to be equivalent for networks. To solve the minimal driver node selection strategy for maximizing the unilaterally controllable subnetwork we proposed a greedy heuristic based on the theoretical findings, which provided a suboptimal solution to the NP-hard problem of maximizing the number of unilaterally controllable nodes.

Preliminaries

Some preliminaries on vectors, matrices and geometric definitions are provided in addition to the theoretical background in section 1.1 for the sake of clarity.

Let us recall that a real matrix $M \in \mathbb{R}^{m \times m}$ is diagonalizable if and only if all of its eigenvalues are semisimple, that is, their algebraic and geometric multiplicity coincide. Given a set $\mathcal{H}$, we denote by $|\mathcal{H}|$ its cardinality, and given a vector space, we denote by 0 its origin. Given a real vector space $\mathbb{R}^n$, we denote by $\mathbb{R}^n_{\geq 0}$ ($\mathbb{R}^n_{\leq 0}$) the set of vectors in $\mathbb{R}^n$ with nonnegative entries. Let $\mathcal{D}$ be a set of $|\mathcal{D}| = k$ vectors $d_1, \ldots, d_k$ in $\mathbb{R}^n$, $\mathrm{Span}(\mathcal{D})$ is the set of all linear combinations of the vectors in $\mathcal{D}$. Additionally, the *positive span* $\mathrm{Span}^+(\mathcal{D})$ of $\mathcal{D}$ is the set of all linear combinations with nonnegative coefficients, that is, $\mathrm{Span}^+(\mathcal{D}) = \{\sum_{i=1}^k \alpha_i d_i \mid \alpha_i \in \mathbb{R}_{\geq 0}\}$, which constitutes a polyhedral convex cone [117]. If $\mathcal{D}$ is a singleton, then $\mathrm{Span}^+(\mathcal{D})$ is called a ray. Note that all the rays and the singleton $\mathcal{O} = \{0\}$ are degenerate cones. Given a convex polyhedral cone $\mathcal{C}$, we define its dimension $|\mathcal{C}|$ as the number of vectors required to generate it. The lineality space of a convex cone $\mathcal{C}$ is defined as the largest subspace $\mathcal{X}^l := \mathcal{C} \cap -\mathcal{C}$ contained in $\mathcal{C}$, whose dimension is the so-called lineality of $\mathcal{C}$ [118]. Next, let us denote by $\mathfrak{e}_i$ the i-th versor in $\mathbb{R}^n$. Given an index set $\mathcal{K}$, we define $\mathcal{X}_\mathcal{K}$ as the subspace linearly spanned by $\cup_{i \in \mathcal{K}} \{\mathfrak{e}_i\}$. Furthermore, given a vector $d \in \mathbb{R}^n$, we denote by $\mathrm{proj}_{\mathcal{X}_\mathcal{K}}(d) = \sum_{i \in \mathcal{K}} \left(d^{\mathrm{T}} \mathfrak{e}_i\right) \mathfrak{e}_i$ the orthogonal projection of d along $\mathcal{X}_\mathcal{K}$. Finally, given a real matrix $M \in \mathbb{R}^{m \times m}$, we denote by $\mathrm{spec}(M)$ its spectrum, and, given a complex vector $c \in \mathbb{C}^n$, we denote by $\mathrm{Re}(c)$ and $\mathrm{Im}(c)$ its real and imaginary parts, respectively.

Problem formulation

Let us consider a linear dynamical network on a graph $\mathcal{G} = \{\mathcal{V}, \mathcal{E}\}$. Defining the network state $x = [x_1, \ldots, x_n]^{\mathrm{T}}$, with $x_i \in \mathbb{R}$ being the state of the i-th node, the network dynamics are given by

$$\dot{x}(t) = Ax(t) + Bu(t), \tag{3.1}$$

where $A \in \mathbb{R}^{n \times n}$ is the adjacency matrix of $\mathcal{G}$, whose ij-th entry, denoted a_{ij}, is one if $(i, j) \in \mathcal{E}$ and zero otherwise; matrix A encapsulates both the individual dynamics and the interaction between the network nodes, which are encoded by the diagonal and off-diagonal elements of A, respectively; matrix $B \in \mathbb{R}^{n \times m}$ is the input matrix, whose ij-th element modulates the effect the *unilateral* input u_j has on the dynamics of node i.

Here, we consider the case in which the inputs are unilateral.

Definition 50. *The input $u(t)$ to network (3.1) is called unilateral if $(u(t) \in \mathbb{R}^m_{\geq 0}, \forall t)$ or $(u(t) \in \mathbb{R}^m_{\leq 0}, \forall t)$.*

In what follows, without loss of generality, we consider only nonnegative inputs, whereby their sign will be determined by the selection of matrix B. More specifically, we make the following assumptions on network (3.1):

Assumption 1. *Matrix A is diagonalizable and $u(t) \in \mathbb{R}_{\geq 0}^m$ for all t.*

Assumption 2. *[108] Each column of matrix B belongs to the set $\mathcal{B} = \{\mathfrak{e}_i, \ -\mathfrak{e}_i, i = 1, \ldots, n\}$.*

Note that 1 is made only for the sake of clarity and brevity, but the results hold for negative inputs and can be easily extended to the case of non-diagonalizable dynamics matrix A. Regarding 2, it means that we aim to minimize the number of dedicated actuator nodes that receive independent input signals. One signal can drive only one actuator node.

In what follows, we focus on the case in which unilateral controllability of the whole network is not feasible due to a limitation on the number of inputs available, whereby the conditions given in [108] do not hold. The problem then arises of selecting the input so that the state of a subset of the network nodes can be steered towards any desired value. Before formally stating this problem, we need to formally define unilateral reachability and controllability of a node subset $\mathcal{V}_s$, whose associated state x_s is the vector stacking the states of all nodes in $\mathcal{V}_s$.

Definition 51. *A node subset $\mathcal{V}_s \subset \mathcal{V}$ is unilaterally reachable if the state of its nodes x_s can be steered from 0 to any target value in finite time, through an appropriate selection of a unilateral input $u(t)$.*

Definition 52. *A node subset $\mathcal{V}_s \subset \mathcal{V}$ is unilaterally controllable if, for all initial conditions $x_s(0)$, the state of its nodes can be steered towards any target value in finite time through an appropriate selection of the unilateral control actions $u(t)$.*

Given the adjacency matrix A, the controllability problem is that of designing the input matrix B fulfilling Assumption 2 that maximizes the cardinality of the set $\mathcal{V}_s = \mathcal{V}_s(B)$ of unilaterally controllable nodes, that is,

$$\max_{B \subset \mathcal{B}} \quad |\mathcal{V}_s| \tag{3.2a}$$

subject to

$$\sum_{i,j} |b_{ij}| = m \tag{3.2b}$$

$$\mathcal{V}_s \text{ unilaterally controllable} \tag{3.2c}$$

Solving problem (3.2) requires first finding the conditions that allow to define when a set of nodes is unilaterally controllable given a set of control inputs of cardinality m, and then devising an input placement algorithm that finds a unilaterally controllable node subset of maximal dimension.

Unilateral reachability and controllability of a node subset

Here, we start by characterizing the set of unilaterally reachable states, to then find the (non-unique) unilaterally controllable node subsets. Then, we characterize unilateral controllability to show that, different from the case of subsystems, node reachability and controllability are equivalent. Before giving our main results, we need to introduce the following definitions. We characterize the set of unilaterally reachable states: as matrix A is supposed to be diagonalizable we will have n semi-simple eigenvalues associated to n left and right eigenvectors linearly independent chosen to maximize the number of those orthogonal to the columns of matrix B. Then we can define the reachable cone as the positive span of the set $\{\gamma_i\}$ where γ_i is defined based on the product between l_i and B following the PBH test.

Let $\mathcal{L} := \{l_1, \ldots, l_n\}$ be a set of (unit norm) linearly independent left eigenvectors of A with maximal number of elements orthogonal to the columns of the matrix B, and $\gamma_i = \gamma_i(l_i^{\mathrm{T}} B)$ the vector

$$
\gamma_i =
\begin{cases}
0, & \text{if } l_i^{\mathrm{T}} B = 0, \operatorname{Im}\{\{l_i\}\} = 0, & (3.3a) \\
\{r_i, -r_i\}, & \text{if } l_i^{\mathrm{T}} B \notin (\mathbb{R}_{\geq 0}^m \cup \mathbb{R}_{\leq 0}^m \setminus \mathcal{O}), \operatorname{Im}\{\{l_i\}\} = 0, & (3.3b) \\
r_i, & \text{if } l_i^{\mathrm{T}} B \in (\mathbb{R}_{\geq 0}^m \setminus \mathcal{O}), \operatorname{Im}\{\{l_i\}\} = 0, & (3.3c) \\
-r_i, & \text{if } l_i^{\mathrm{T}} B \in (\mathbb{R}_{\leq 0}^m \setminus \mathcal{O}), \operatorname{Im}\{\{l_i\}\} = 0, & (3.3d) \\
\left\{ \operatorname{Re}\{r_i\}, -\operatorname{Re}\{r_i\}, \operatorname{Im}\{r_i\}, -\operatorname{Im}\{r_i\} \right\}, & \text{otherwise}, & (3.3e)
\end{cases}
$$

for $i = 1, \ldots, n$. Additionally, we denote by $\mathcal{C}_r(B)$ the positive span of the set of all γ_i-s, that is,

$$
\mathcal{C}_r(B) := \operatorname{Span}^+(\{\gamma_1, \ldots, \gamma_n\}). \tag{3.4}
$$

Theorem 2. *If Assumption 1 holds, then*

(i) the cone $\mathcal{C}_r(B)$ is the set of unilaterally reachable states of the pair (A, B);
(ii) the lineality space $\mathcal{X}^l$ of $\mathcal{C}_r(B)$ is the largest unilaterally reachable subspace of the pair (A, B).

Proof.
    *S*tatement (i). Let us consider the transformation $z = Tx$, where T is the matrix obtained by juxtaposing row-wise the vectors in $\mathcal{L}$. As A is diagonalizable, we can write $A = T^{-1}\Lambda T$, where $\Lambda = \operatorname{diag}\{\lambda_1, \ldots, \lambda_n\}$, with λ_i being the i-th eigenvalue of A. In these new coordinates, the dynamics of network (3.1) become

$$
\dot{z}(t) = \Lambda z(t) + TBu(t).
$$

By setting $z(0) = 0$, we obtain its forced dynamics as

$$
z(t) = \int_0^t \exp(\Lambda(t - \tau))TBu(\tau)d\tau,
$$

whose i-th component can be expressed as

$$
\begin{aligned}
z_i(t) &= \int_0^t \exp(\lambda_i(t - \tau)) \sum_{j=1}^m l_i^\mathrm{T} b_j u_j(\tau) d\tau \\
&= \sum_{j=1}^m l_i^\mathrm{T} b_j \eta_j(u_j),
\end{aligned}
\tag{3.5}
$$

where $\eta_j(u_j) = \int_0^t \exp(\lambda_i(t - \tau))u_j(\tau)d\tau$. Since $x = T^{-1}z$, and as the columns of $T^{-1} = T^\mathrm{T}$ are the right eigenvectors $r_1, \ldots, r_n$ of A, $z_i(t)$ represents the dynamics along the eigenvector r_i, for all $i = 1, \ldots, n$. Let us now distinguish the case in which r_i is associated to a real or to a complex eigenvalue, respectively:

Case (a): $\mathrm{Im}(\lambda_i) = 0$. From Assumption 1, we have that $\eta_j(u_j) \geq 0$ for all j. Next, we distinguish 4 subcases depending on the product $l_i^\mathrm{T} B$:

- if $l_i^\mathrm{T} B = 0$, then any $\tilde{x} \in \mathrm{Span}(\{r_i\})$ is unreachable;

- if $l_i^\mathrm{T} B \in (\mathbb{R}_{\geq 0}^m \cup \mathbb{R}_{\leq 0}^m \setminus \mathcal{O})$, then there exist j, m such that $l_i^\mathrm{T} b_j \eta_j(u_j) < 0$ and $l_i^\mathrm{T} b_m \eta_m(u_m) > 0$. Hence, any $\tilde{x} \in \mathrm{Span}(\{r_i\})$ is unilaterally reachable;

- if $l_i^\mathrm{T} B \in (\mathbb{R}_{\geq 0}^m \setminus \mathcal{O})$, then any $\tilde{x} \in \mathrm{Span}^+(\{r_i\})$ is unilaterally reachable;

- if $l_i^\mathrm{T} B \in (\mathbb{R}_{\leq 0}^m \setminus \mathcal{O})$, then any $\tilde{x} \in \mathrm{Span}^+(\{-r_i\})$ is unilaterally reachable.

Case (b): $\mathrm{Im}(\lambda_i) \neq 0$. As A is a real matrix, each complex eigenvalue will have a complex conjugate. Therefore, the modal dynamics associated to λ_i and its complex conjugate occur along the two dimensional subspace $\widetilde{\mathcal{X}} = \mathrm{Span}(\mathrm{Re}\{r_i\}, \mathrm{Im}\{r_i\})$ of $\mathbb{R}^n$ and, according to the Euler's formula, can be expressed as a sum of sinusoidal functions. Hence, all the states belonging to $\widetilde{\mathcal{X}}$ are reachable if there exists an index j such that $\mathrm{proj}_{\widetilde{\mathcal{X}}} l_i^\mathrm{T} b_j \neq 0$. If, instead, such an index did not exist, then no state would be unilaterally reachable. Finally, considering that (i) if two (or more) states are unilaterally reachable, then any positive combination of the these states is also unilaterally reachable, and (ii) any linear combination involving an unreachable state defines another unreachable state, Statement (i) follows.

Statement (ii). From Statement (i), no state outside $\mathcal{C}_r(B)$ is reachable. Therefore, Statement (ii) follows.   □

Recall that controllability property can be defined as being able to move the system from an initial state $x(1)$ to any other state $x(2)$, and reachability as the ability to get from the origin $x(0) = 0$ to any other state $x(2)$ and null-controllability to get from an initial state $x(1)$ to the origin 0. Hence, being able to get from any state $x(1)$ to any state $x(1)$ (thus controllability) implies reachability as you can select the origin as $x(1)$ and being able to reach any state $x(2)$. Indeed, reaching $x(2)$ from $x(1)$ is equivalent to reaching from 0 to $x(2) \exp(At)x(1)$. Since all the states are reachable from 0, this implies controllability. This is not true anymore for unilateral inputs: different from the general case of systems, unilateral reachability does not imply unilateral controllability.

Lemma 1. *Let Assumption 2 hold, then the set of controllable states is $\mathcal{C}_c(B) := \mathcal{X}^l(B) \cup \{x \in \mathbb{R}^n : -\exp(At)x \in \mathcal{C}_r(B)\}$.*

Proof. The thesis follows from the consideration that a point $\bar{x}$ is controllable if and only if $-\exp(At)\bar{x}$ is reachable. $\qquad\square$

Even though the set of reachable states differs from that of controllable states, For node subsets instead the equivalence between controllability and reachability is preserved, even under the assumption of unilateral inputs. The next section will show these theoretical findings.

Node subset unilateral reachability

When studying partial unilateral controllability of network dynamical systems, we need to preserve the association between state variables and network nodes. Therefore, we now provide the following theorems and corollaries characterizing the unilateral reachability and controllability of a node subset.

Theorem 3. *Given network (3.1) and a node subset $\mathcal{V}_s \subset \mathcal{V}$, if Assumption 1 holds and $\mathrm{proj}_{\mathcal{X}_{\mathcal{V}_s}}(\mathcal{C}_r(B)) = \mathcal{X}_{\mathcal{V}_s}$, then $\mathcal{V}_s$ is unilaterally reachable.*

Proof. From Definition 51, for a node subset $\mathcal{V}_s$ to be reachable, for all $\bar{x}_s \in \mathbb{R}^{|\mathcal{V}_s|}$ and $x(0) : x_s(0) = 0$ there must exists a unilateral input $u(t)$ that steers the network towards a state $\bar{x}$ such that the projection of $\bar{x}$ on the subspace $\mathcal{X}_{\mathcal{V}_s}$ spanned by the versors $\{\mathfrak{e}_i \,|\, i \in \mathcal{V}_s\}$, is $\bar{x}_s$. This is equivalent to the existence of a point $\bar{\bar{x}} \in \mathcal{C}_r(B)$ such that

$$\mathrm{proj}_{\mathcal{X}_{\mathcal{V}_s}} \bar{\bar{x}} = \bar{x}_s - \mathrm{proj}_{\mathcal{X}_{\mathcal{V}_s}} \exp(At)x(0). \tag{3.6}$$

As from Theorem 2 $\mathcal{C}_r(B)$ is the unilaterally reachable cone, and $\mathrm{proj}_{\mathcal{X}_{\mathcal{V}_s}}(\mathcal{C}_r(B)) = \mathcal{X}_{\mathcal{V}_s}$ by hypothesis, a point $\bar{\bar{x}}$ fulfilling (3.6) exists for all $\bar{x}_s$ and $x(0) : x_s(0) = 0$, and thus the thesis follows. $\qquad\square$

Interestingly, we note that the number of unilaterally reachable nodes may be larger than the dimension of the largest unilaterally reachable subspace.

Node subset unilateral controllability

Theorem 4. *Given network (3.1), if Assumption 1 holds, then a node subset $\mathcal{V}_s$ is unilaterally reachable if and only if it is unilaterally controllable.*

Proof. Unilateral controllability of a node subset trivially implies its unilateral reachability, see Definitions 51 and 52. Hence, let us focus on proving that the viceversa holds. From Definition 52, for a node subset $\mathcal{V}_s$ to be controllable, for all $\bar{x}_s$ and $x(0)$ there must exists a unilateral input $u(t)$ that steers the network towards a state $\bar{x}$ such that
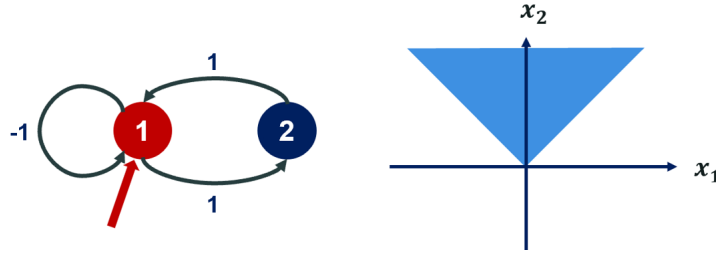
Figure 3.3. In this toy example, there are no reachable directions, however node 1 is controllable as in its direction there are two nonzero projection of opposite signs. The dimension of the largest unilaterally controllable node subset can be larger than the unilaterally reachable subspace.

the projection of $\bar{x}$ on the subspace $\mathcal{X}_{\mathcal{V}_s}$ is $\bar{x}_s$. This is equivalent to the existence of a point $\bar{\bar{x}} \in \mathcal{C}_r(B)$ such that

$$\text{proj}_{\mathcal{X}_{\mathcal{V}_s}} \bar{\bar{x}} = \bar{x}_s - \text{proj}_{\mathcal{X}_{\mathcal{V}_s}} \exp(At)x(0). \tag{3.7}$$

As from Theorem 3 if $\mathcal{V}_s$ is unilaterally reachable then $\text{proj}_{\mathcal{X}_{V_s}} \mathcal{C}_r(B) = \mathcal{X}_{V_s}$, by hypothesis a point $\bar{\bar{x}}$ fulfilling (3.7) exists for all $\bar{x}_s$ and $x(0)$. Hence, $\mathcal{V}_s$ is unilaterally controllable. $\square$

The equivalence between unilateral reachability and controllability of node subsets allows to derive a set of corollaries that characterize partial unilateral controllability of network systems.

Corollary 1. *Given network* (3.1) *and a node subset* $\mathcal{V}_s \subset \mathcal{V}$, *if Assumption 1 holds and* $\text{proj}_{\mathcal{X}_{\mathcal{V}_s}}(\mathcal{C}_r(B)) = \mathcal{X}_{\mathcal{V}_s}$, *then* $\mathcal{V}_s$ *is unilaterally controllable.*

Proof. Combining Theorems 3 and 4, the thesis follows. $\square$

Corollary 2. *Let* $\mathcal{C}_r(B)$ *be the unilaterally reachable set of the pair* (A, B). *There exists a controllable node subset* $\mathcal{V}_s$ *such that* $|\mathcal{V}_s| \geq |\mathcal{X}^l(B)|$.

Proof. From Theorem 2 we know that if $\mathcal{C}_r(B)$ is the unilaterally reachable set, this implies that $\mathcal{X}^l(B)$ is its lineality space of dimension $|\mathcal{X}^l(B)|$. Moreover, considering that, for a given subspace $\mathcal{X}$ there always exists a set of indices $\mathcal{K}$ and the associated subspace $\bar{\mathcal{X}} = \text{Span}(\cup_{i \in \mathcal{K}} \{\mathfrak{e}_i\})$ such that $\text{proj}_{\bar{\mathcal{X}}} \mathcal{X} = \bar{\mathcal{X}}$, this holds also for $\mathcal{X} = \mathcal{X}^l(B)$. Therefore, from Theorem 2 there exists a unilaterally reachable node subset $\mathcal{V}_s$ of dimension at least equal to $|\mathcal{V}_s| = |\mathcal{X}^l(B)|$, that, from Theorem (4), is also unilaterally controllable. $\square$

The next corollary provides a sufficient condition guaranteeing that there exists a unilaterally controllable node subset $\mathcal{V}_s$ that contains a given node i.

Corollary 3. *Given an integer* $i \leq n$, *if there exist two indices* j *and* l *such that* $r_j^T \mathfrak{e}_i > 0$, $r_l^T \mathfrak{e}_i < 0$, *and* $r_j \cup r_l \in \mathcal{C}_r(B)$, *then there exists a unilaterally controllable node subset* $\mathcal{V}_s$ *such that* $i \in \mathcal{V}_s$.

Proof. Considering that $\text{proj}_{\mathfrak{e}_i} \mathcal{C}_r(B) = \mathfrak{e}_i$, the thesis follows from Corollary 1. $\square$

Greedy Algorithm

In what follows, we shall leverage the theoretical findings of Section 3.1 to design a heuristic for solving problem (3.2). Before illustrating the derivation of the algorithm, we need to introduce the spanning set $\mathcal{W}(B)$ of the lineality space $\mathcal{X}^l(B) \in \mathcal{C}_r(B)$, which can be computed as

$$\mathcal{W}(B) = \bigcup_{i=0}^{|\mathcal{X}^l(B)|} w_i, \tag{3.8}$$

where

$$w_i = \begin{cases} \{r_i\}, & \text{if } l_i^\mathrm{T} B \notin (\mathbb{R}_{\geq 0}^m \cup \mathbb{R}_{\leq 0}^m \setminus \mathcal{O}), \mathrm{Im}\{\{l_i\}\} = 0, \\ \left\{ \mathrm{Re}\{r_i\}, \ \mathrm{Im}\{r_i\} \right\}, & \text{if } l_i^\mathrm{T} B \neq 0, \mathrm{Im}\{\{l_i\}\} \neq 0, \\ 0, & \text{otherwise.} \end{cases} \tag{3.9}$$

Furthermore, let $\mathcal{S}$ be the set of all subspaces of $\mathbb{R}^n$ such that

$$\mathrm{proj}_{\mathcal{X}} \mathcal{C}_r(B) = \mathcal{X}, \quad \forall \mathcal{X} \in \mathcal{S}.$$

From Theorem 2, solving problem (3.2), that is, finding a maximal unilaterally controllable node subset, is equivalent to finding the matrix $B^\star$ that maximizes the cardinality of the largest subspace in $\mathcal{S}$. Namely,

$$B^\star := \arg\max_B \left(\max_{\mathcal{X} \in \mathcal{S}} |\mathrm{proj}_{\mathcal{X}} \mathcal{C}_r(B)| \right). \tag{3.10}$$

Unfortunately, (3.10) is a combinatorial problem that can only be solved through extensive search, which is unfeasible even for a network of a handful of nodes.

Since finding an exact solution of (3.10) is typically unfeasible, we propose a two-step procedure for the selection of matrix B. In Step 1, we seek for a heuristic approach that tries to maximize the lineality $|\mathcal{X}^l(B)|$, which from Corollary 2 is a lower bound for the cardinality $|\mathcal{V}_s|$ of the unilaterally controllable node subset $\mathcal{V}_s$. Then, Step 2 attempts to add to $\mathcal{V}_s$ the nodes fulfilling the sufficient condition for node unilateral controllability given in Corollary 3.

Step 1. Heuristic maximizing $|\mathcal{X}^l(B)|$.

Here, we seek for the suboptimal solution

$$\widetilde{B}^\star := \arg\max_B \left(\max_{\mathcal{X}^l} |\mathrm{proj}_{\mathcal{X}^l} \mathcal{C}_r(B)| \right) \tag{3.11}$$

to problem (3.10). The heuristic we propose (Step 1) takes as inputs matrix A, its spectrum, the set of left eigenvectors $\mathcal{L}$, and the corresponding set of right eigenvectors $\mathcal{R}$. Denoting B_k the $\widetilde{B}$ selected at the k-th iteration, the algorithm starts with $B_0 = 0_{n \times m}$. Then, at each iteration, one or two columns are added to $\widetilde{B}$. Defining $\Delta(\beta) := |\mathcal{X}^l([B_{k-1}, \beta])| - |\mathcal{X}^l(B_{k-1})|$, where $\beta \in \mathcal{B}$, we can now distinguish two different cases:

1. If there exists $\beta \in \mathcal{B}$ such that $\Delta(\mathcal{B}) > 0$, then only one column is added at step k, that is,

$$B_k = [B_{k-1}, \beta^\star],$$

where

$$\beta^\star = \begin{cases} \arg\max_{\beta \in \mathcal{B}} |\mathcal{X}^l(B_k)|, \text{if } \exists! \arg\max_{\beta \in \mathcal{B}} |\mathcal{X}^l(B_k)|, & (3.12a) \\ \arg\max_{\beta \in \mathcal{B}} |\mathcal{C}(B_k)|, \text{ if } \nexists! \arg\max_{\beta \in \mathcal{B}} |\mathcal{X}^l(B_k)|^1. & (3.12b) \end{cases}$$

2. If, instead, a $\beta \in \mathcal{B}$ such that $\Delta(\mathcal{B}) > 0$ does not exist, we add two columns to B_{k-1} at step k, that is,

$$B_k = [B_{k-1}, \beta^{\star\star}, -\beta^{\star\star}],$$

where

$$\beta^{\star\star} = \arg\max_{\beta \in \mathcal{B}} |\mathcal{X}^l([B_{k-1}, \ \beta, \ -\beta])|. \tag{3.13}$$

Summing up, at each step k our updating rule attempts to add the input that maximizes the lineality $|\mathcal{X}^l(B_k)|$. When such an input is not unique, it selects the input that adds the largest number of rays in $\mathcal{C}_r(B_k)$. If instead we cannot find a β such that $\Delta(\beta)$ is positive, then we add the two inputs that maximize $|\mathcal{X}^l(B_k)|$. The algorithm stops when $B_k \in \mathbb{R}^{n \times m}$. Once we computed $\widetilde{B} = B_m$, we need to identify one of the unilaterally controllable node subsets $\mathcal{V}_s^1$ corresponding to $\widetilde{B}$. To this aim, we leverage Corollary 2, which states that there exists a unilaterally controllable node subset $\mathcal{V}_s^1$ with $|\mathcal{V}_s^1| = |\mathcal{X}^l(\widetilde{B})|$ such that $\text{proj}_{\mathcal{X}_{\mathcal{V}_s^1}} \mathcal{X}_l(\widetilde{B}) = \mathcal{X}_{\mathcal{V}_s^1}$. To identify such a node subset, we compute the set $\mathcal{W}(\widetilde{B})$ according to (3.8)-(3.9). Then, we build the set $\mathcal{V}_s^1$ so that the elements of the sets $\mathcal{V}_s^1$ and $\mathcal{W}(\widetilde{B})$ can be associated into $|\mathcal{V}_s^1|$ pairs (v_j, w_i) such that (i) no pairs share a common element and (ii) each pair (v_j, w_i) is such that $\mathfrak{e}_{v_j}^{\mathrm{T}} w_i \neq 0$. To do so, we associate a binary variable y_{ij} to all possible pairs $(i, j) \in \mathcal{Y}$, where

$$\mathcal{Y} = \{(i, j) | \mathfrak{e}_i^{\mathrm{T}} w_j \neq 0 \ \wedge \ w_j \in \mathcal{W}(\widetilde{B})\},$$

and solve the following optimization problem

$$\max \sum_{(i,j) \in \mathcal{Y}} y_{ij} \tag{3.14a}$$

subject to

$$\sum_{i: \exists (i,j) \in \mathcal{Y}} y_{ij} \leq 1, \ \forall j \tag{3.14b}$$

$$\sum_{j: \exists (i,j) \in \mathcal{Y}} y_{ij} \leq 1, \ \forall i \tag{3.14c}$$

$$y_{ij} \in \{0, 1\} \tag{3.14d}$$

---

[1]With a slight abuse of notation, here we mean that such a β exists but is not unique.

Then, the controllable node subset can be obtained as $\mathcal{V}_s^1 := \{i : y_{ij} = 1\}$. Note that, albeit problem (3.14) is formulated as an integer linear problem, it can be solved in polynomial time as the constraints in (3.14b) and (3.14c) define a totally uni-modular matrix.

Step 2. Enlarging the unilaterally controllable node subset.

In the second step, we enrich the unilaterally controllable node subset $\mathcal{V}_s^1$ by exploiting the set $\mathcal{C}_r(\widetilde{B}) \setminus \mathcal{X}^l(\widetilde{B})$. To do so, let us define the set

$$
\begin{aligned}
\mathcal{Q}(\widetilde{B}) :=&\{r_j : r_j \in \mathcal{C}_r(\widetilde{B}), -r_j \notin \mathcal{C}_r(\widetilde{B})\}\cup \\
&\{-r_j : -r_j \in \mathcal{C}_r(\widetilde{B}), r_j \notin \mathcal{C}_r(\widetilde{B})\}
\end{aligned}
\tag{3.15}
$$

whose positive span is $\mathcal{C}_r(\widetilde{B}) \setminus \mathcal{X}^l(\widetilde{B})$. We can then leverage Corollary 3 to add a node, say i, to $\mathcal{V}_s^1$ for each triplet $(q_j, q_l, \mathfrak{e}_i)$ such that $(q_j, q_l) \in \mathcal{Q}(\widetilde{B})$, $\mathfrak{e}_i : i \notin \mathcal{V}_s^1$, and $\operatorname{sgn} \mathfrak{e}_i^\mathrm{T} q_j = - \operatorname{sgn} \mathfrak{e}_i^\mathrm{T} q_l$, as specified in Step 2.

Step 1 Maximizing the lineality $|\mathcal{X}^l(B)|$.

  Inputs: A, Λ, m
  procedure INITIALIZATION($B_0 = \varnothing$, $\mathcal{X}^l(B_0) = \mathcal{O}$, $\mathcal{W}(B_0) = \varnothing$)
    while $k \leq m - 1$ **do**
      if $\exists \beta \in \mathcal{B} : |\mathcal{X}^l([B_{k-1},\ \beta])| > |\mathcal{X}^l(B_{k-1})|$ **then**
        compute $\beta^\star$ as in (3.12a), (3.12b)
        set $B_k = [B_{k-1},\ \beta^\star]$
        compute $\mathcal{W}(B_k)$
        $k = k + 1$
      else
        compute $\beta^{\star\star}$ as in (3.13)
        set $B_k = [B_{k-1},\ \beta^{\star\star},\ -\beta^{\star\star}]$
        compute $\mathcal{W}(B_k)$
        $k = k + 2$
      end if
    end while
    if $k = m$ **then**
      compute $\beta^\star$ as in (3.12a), (3.12b)
      set $B_k = [B_{k-1}, \beta^\star]$
      compute $\mathcal{W}(B_k)$
    end if
  end procedure
  Outputs: $\widetilde{B} = B_m$, $\mathcal{W}(\widetilde{B})$

Application on a sample network

To illustrate our heuristic, we consider a linear network dynamical system on the graph $\mathcal{G}$ depicted in Fig. 1, whose dynamics is regulated by matrix

$$A = \begin{bmatrix} 1 & -4 & 0 & 0 & 0 & 0 & 0 \\ 4 & 1 & 0 & 0 & 0 & 0 & 0 \\ 1 & 0 & 3 & 0 & 0 & 0 & 0 \\ 0 & 0 & 1 & 4 & 0 & 0 & 3 \\ 0 & 0 & 0 & 0 & 2 & -3 & 0 \\ 0 & 0 & 0 & 0 & 3 & 2 & 0 \\ 0 & 0 & 0 & 0 & -3 & 0 & 0 \end{bmatrix},$$

with spectrum $\{4, 3, 0, 1 + 4i, 1 - 4i, 2 + 3i, 2 - 3i\}$. Let us assume that we can inject $m = 2$ unilateral control. The input matrix $\widetilde{B}$ is designed following Step 1, that is, by maximizing the lineality $|\mathcal{X}^l(\widetilde{B})|$. At $k = 1$, four possible selections of β ($\mathfrak{e}_2$, $\mathfrak{e}_6$, $-\mathfrak{e}_2$ and $-\mathfrak{e}_6$) yield the same (positive) $\Delta(\beta)$. Hence, $\beta^\star$ should be selected among these four according to Eq. (3.12b). However, since all selections would yield the same $|\mathcal{C}(B_1)|$, the selection is performed randomly, and we set $B_1 = -\mathfrak{e}_6$, with the set $\mathcal{W}(B_1)$ being $[r_6, r_7]$. At $k = 2$, $-\mathfrak{e}_2$ is the unique β returning $\Delta(\beta) > 0$. Hence, we select node 2 as the second and last node where a control signal is injected, i.e., we set $\widetilde{B} = B_2 = [-\mathfrak{e}_6; -\mathfrak{e}_2]$ and $\mathcal{W}(\widetilde{B}) = [r_1, r_4, r_5, r_6, r_7]$.

Having selected the matrix B, we now turn to finding one of the possibly multiple unilaterally controllable node subsets $\mathcal{V}_s^1$ such that

$$|\mathcal{V}_s^1| = |\mathcal{X}^l(\widetilde{B})|$$

by solving the optimization problem (3.14). Among the multiple equivalent solutions to this ILP, we randomly pick $\mathcal{V}_s^1 = \{v_2, v_3, v_4, v_5, v_6\}$.

Finally, considering that, from (3.15), $Q(\widetilde{B}) = \{r_2, -r_3\}$, and as there does not exist a triplet $\{j, l, \mathfrak{e}_i\}$ such that $q_j, q_l \in \mathcal{Q}(\widetilde{B})$, $\mathfrak{e}_i : i \notin \mathcal{V}_s^1$, from Step 2 of the proposed heuristic we cannot further extend the unilaterally controllable node subset, i.e., $\mathcal{V}_s = \mathcal{V}_s^1 = \{v_2, v_3, v_4, v_5, v_6\}$.

Step 2 Enlarging the unilaterally controllable node subset associated to $\widetilde{B}$

    Inputs: $\mathcal{V}_s^1$
    compute the set $\mathcal{Q}(\widetilde{B})$ as in (3.15)
    while $\exists\{j, l, \mathfrak{e}_i\} : q_j, q_l \in \mathcal{Q}(\widetilde{B}), \mathfrak{e}_i : i \notin \mathcal{V}_s^1$ **do**
        if $\operatorname{sgn} \mathfrak{e}_i^{\mathrm{T}} q_j = -\operatorname{sgn} \mathfrak{e}_i^{\mathrm{T}} q_l$ **then**
            Set $\mathcal{V}_s^1 = \mathcal{V}_s^1 \cup \{i\}$
            Set $\mathcal{Q}(\widetilde{B}) = \mathcal{Q}(\widetilde{B}) \setminus \{q_j, q_l\}$
        end if
    end while
    Output: $\mathcal{V}_s = \mathcal{V}_s^1$.
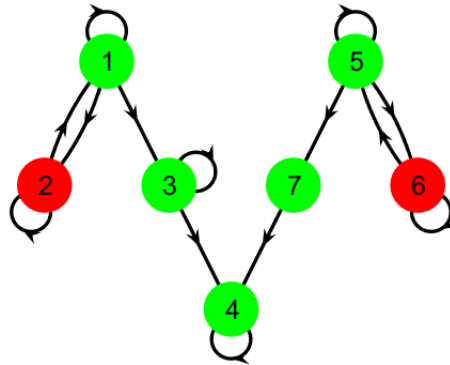
Figure 3.4. Network topology: the nodes in red are the driver nodes where, according to the proposed heuristic, the negative unilateral control inputs are injected, © 2022 IEEE.

Conclusion

In this letter, we tackled the problem of studying the controllability of network of LTI dynamical systems when the control inputs are both constrained in number and in sign, namely unilateral. Specifically, we focused on the realistic case where the constraint on the number and type of inputs, for physical or economic limitations, prevents the achievement of complete controllability of the network system, whereby only a node subset can be made controllable. In this constrained framework, we have characterized the reachable and controllable subset of an LTI system, that, for the particular nature of the control inputs, is a cone and not a subspace as always. Then, we characterized the largest unilaterally reachable subspace contained in the unilaterally reachable cone, and the controllability subspace, showing that reachability do not imply controllability in subsystems. Then, looking at a network dynamical system, we identified theoretical conditions under which unilateral reachability and controllability of a node set hold, and we showed that these two properties are equivalent for subnetworks, different from the general case of subsystems.

These theoretical findings enabled us to give a (suboptimal) solution to the problem of finding the largest subnetwork unilaterally controllable given a fixed number of control inputs, strictly smaller than the one needed to fully control the whole network with unilateral inputs, problem solved in [108] After showing that maximizing the size of a unilaterally controllable nodes' subset is a combinatorial problem, we have leveraged the theoretical findings on unilateral controllability to build a heuristic that can find a suboptimal solution to this problem in polynomial time, as illustrated on a sample network. Our work has laid the foundations of partial controllability under unilateral inputs, thus paving the ways for future studies in this area of research that aims to take into account some constraints in the availability and feasibility of control actions in real-worlds scenario to bridge the gap between theoretical findings and practical applications. However, the work is not free of limitations: first, the heuristic proposed does not guarantee any optimality in the driver node selection, thus, alternative heuristic approaches

may be developed and tested against the one proposed in this manuscript. Moreover, once partial controllability has been guaranteed, the problem of evaluating the energy associated to the control action arises, thereby minimum energy control problems could be formulated in this setting.

3.2   Paper B - Partial observability of complex networks

Introduction

Since Nature and PNAS published the works [119, 120], the study of the controllability and observability properties of complex networks of dynamical systems has attracted remarkable interest among the scientific community [22, 24, 121–124]. One of the main differences between systems and networks is that controllability and observability are properties that must be conferred to a network, rather than verified. Many works tackled the problem of smartly selecting the set of drivers/ sensor nodes to ensure complete controllability/observability [119, 125, 126]. However, achieving these two goals is often unfeasible in real applications, due to physical and economical constraints that limit the actual number of driver and sensor nodes available. As a matter of fact, in most cases guaranteeing controllability and observability of only a fraction of the network nodes, a subnetwork from now on, is sufficient to achieve the desired control goal [127, 128]. Nevertheless, it has been recently highlighted [121] that, when the controllability and observability properties of a subnetwork are considered, then the subtle yet critical differences between networks and dynamical systems emerge. Indeed, as the state of a subnetwork is the collection of the state of its nodes, then we cannot perform any projection, that is, a change of basis to evaluate whether a subnetwork is controllable and/or observable, without losing the association between states and nodes.

Even though this inability to perform a state transformation does not preclude to leverage structural controllability theory to optimally select driver nodes, this is no longer true when we seek to ensuring subnetwork observability [121]. This theoretical finding has the direct consequence that the strategies proposed in the literature for solving the minimum input problem given a fixed number of driver nodes cannot be used by duality when addressing the sensor node selection problem. Hence, this remains an overlooked problem in the literature.

The aim of this work is twofold: first, we want to show that, with the same number of sensors and drivers to place, subnetworks are much harder to be observed than to be controlled, due to theoretical differences between systems and network which have practical consequences in hindering our observability ability. Second, we illustrate through numerical analyses that the existing tools to optimally select driver nodes are not suitable for sensor node selection, especially for Erdős-Rényinetworks, as they lead to a relevant loss in terms of the size of the subnetwork we can make observable. Thus, the need of finding a novel sensor nodes selection strategy arises and indeed an efficient heuristic is presented as a result of the exploitation of the knowledge of key topological features of the network.

Theoretical background

In this work, we will refer to structured linear systems/networks [29, 30], whose triplet (A, B, C) is composed by structured matrices. As we address the problem of partial controllability/observability we define

Definition 53. *The controllable subspace as the set of all vectors $x \in \mathbb{R}^N$ that can be reached from the origin.*

Definition 54. *The unobservable subspace as the set of all nonzero initial conditions $x(0) \in \mathbb{R}^N$ that produce a zero free response.*

With a slight abuse of notation, we will refer to the generic rank $\rho_g(K)$ $(\rho_g(O))$ of the controllability and observability matrices K and O in the sense that, given the triplet (A, B, C), the ranks decreases only for a set of Lebesgue measure zero of the values of the free entries of the triplet. Different from the case of complete controllability/observability, when we study *subnetwork* controllability/ observability, that is when we have at our disposal only a fixed number M of driver (sensor) nodes not large enough to control/observe all the network, the duality between the two properties is lost [121]. Although $\rho_g(K)$ $(\rho_g(O))$ coincides with the dimension of the controllable subspace (orthogonal complement of the unobservable subspace) this correspondence is no longer true when considering subnetworks. Indeed, while the dimension of the controllable subnetwork $|\mathcal{G}_c(M)|$ is equals to $\rho_g(K)$, $\rho_g(O)$ constitutes only an *upper bound* for the dimension of the observable subnetwork $|\mathcal{G}_o^T(M)|$. Hence, while revisiting structural controllability tools [25, 30, 129] and exploiting that maximizing $|\mathcal{G}_c(M)|$ is equivalent to maximizing $\rho_g(K)$ allows to find the largest controllable subnetwork $|\mathcal{G}_c^*(M)|$ [128], this approach is no longer applicable to find the largest observable subnetwork $|\mathcal{G}_o^{*T}(M)|$ due to the theoretical differences mentioned above.

In [121] it has been shown that $|\mathcal{G}_o^T(M)|$ is actually equals to the largest number of elements n_1 of the canonical basis $\mathcal{N}$ that are encompassed in the orthogonal complement to the unobservable subspace of the pair (A, C). However, a graphical translation of this geometrical condition still lacks, and thus the problem of optimally selecting sensor nodes can only be solved by means of an exhaustive search, unfeasible for large-scale networks.

Problem Formulation

The first goal of this work is to uncover the practical consequences of the theoretical differences between controllability/observability properties when the driver (sensor) nodes at our disposal constitute a set Ω_S of cardinality $|\Omega_S| = M < N_S$ where N_S is the number of driver (sensor) nodes that ensures complete controllability (observability). In this scenario, we want to quantify how harder it is to make a subnetwork observable rather than controllable in terms of the difference between the size of the controllable or observable subnetworks defined as $\Delta(M) := |\mathcal{G}_c(M)| - |\mathcal{G}_o^T(M)|$. In order to analyze

$\Delta(M)$ regardless of the number of driver (sensor) nodes M, we introduce a parameter, inspired by the permeability index in [128] that, in the thermodynamic limit $N \to \infty$ is defined as

$$\mu_\Delta := \frac{\int_0^{\overline{M}} \Delta(M) \ dM}{\int_0^{\overline{M}} (|\mathcal{G}_c(M)| - M) \ dM}. \tag{3.16}$$

Roughly speaking, μ_Δ is a measure of the average ratio between the actual $\Delta(M)$ and the $\Delta(M)$ given the sequence $|\mathcal{G}_c(M)|$. Note that $\Delta(M) = 0$ for all $M \geq N_s$. Note that μ_Δ is well-defined only if $\int_0^{\overline{M}} (|\mathcal{G}_c(M)| - M) \ dM \neq 0$ consistently with the fact that if this integral is zero, then $\Delta(M)$ cannot be different from zero. Moreover, μ_Δ is equals to 0 if the observable subnetwork coincides with the controllable one and is equals to 1 if $|\mathcal{G}_o^T(M)| = M$ for all M.

A first method used to assess how harder it is to observe a subnetwork rather than control it is to evaluate μ_Δ considering the set of driver nodes Ω_D onto $\mathcal{G}$ as a set of sensor nodes Ω_S onto $\mathcal{G}^T$. We will analyze two alternative strategies to select Ω_S: the set could be built randomly or optimally. If we choose to select Ω_S in an optimal way, we can recast the problem of quantifying how limited our ability is to observe a subnetwork rather than control it, into solving the following optimization problem:

$$\min_{\Omega_S(M)} \quad \mu_\Delta \qquad \forall M = 1, ..., \overline{M} \tag{3.17}$$

$$\Omega_D(M) \text{ given}$$

that implies finding the optimal $\Delta^*(M) := |\mathcal{G}_c^*(M)| - |\mathcal{G}_o^{*T}(M)|$. Even if a geometrical condition to evaluate the dimension of the observable subnetwork $|\mathcal{G}_o^{*T}(M)|$ exists, as it does not map into a graphical condition, this opimization problem can only be solved by means of an exhaustive search, unfeasible for large-scale networks. Thus, the need of building an effective heuristic for the sensor nodes selection arises and the first question that this paper wants to answer is if the driver nodes selection tools could perform decently even in maximizing $|\mathcal{G}_o^T(M)|$.

Finding controllable and observable subnetworks

Before delving deeper into the reasons behind this crucial difference between network controllability and observability, let us give our first contribution, that is, let us show that this theoretical difference reflects into subnetworks being much harder to be made observable rather than controllable.

We considered two datasets of 1000 nodes directed synthetic networks, the first one encompassing Erdős-Rényi (ER) networks generated by means of the configuration model [130], and the second one made of Scale-Free (SF) networks generated by means of the directed version of the static model [131]. Each dataset encompasses 9 subsets of 10 network topologies differing from each other for the value of the network average degree $\langle k \rangle$ in the range of $2, \dots, 10$. For each network in each dataset we deployed the strategy in [128] to select an optimal sequence of sets of drivers, i.e., a sequence of

matrices $B(M)$ that maximizes $|\mathcal{G}_c(M)|$ for all values of M. Then, we evaluated the corresponding sequence of dimensions of the observable subnetwork $|\mathcal{G}_o^T(M)|$ where the sensor sets are defined by the matrices $B(M)^T$. We find that the network topology has a substantial influence on the quantity $\Delta(M)$, an influence that can become dramatic depending on the network degree distribution. Namely, as shown in Figure 3.5 in panels (a) and (b), $\Delta(M)$ is much smaller for SF networks rather than for ER networks. This is due to the fact that, increasing M, in Erdős-Rényi networks we tend to observe an explosive (first order) phase transition both in $|\mathcal{G}_c(M)|$ and $|\mathcal{G}_o^T(M)|$, but with the explosion from $|\cdot| << 1$ to $|\cdot| \approx 1$ occurring much later in the case of $|\mathcal{G}_o^T(M)|$ than in the case of $|\mathcal{G}_c(M)|$. On the other hand, in Scale Free networks we observe a smooth (second order) phase transition both in $|\mathcal{G}_c(M)|$ and $|\mathcal{G}_o^T(M)|$ with the transition of the former being a little faster than that of the latter. Hence, we can state that the homogeneity of Erdős-Rényi networks induces a delay in the explosion of $|\mathcal{G}_o^T(M)|$ with respect to $|\mathcal{G}_c(M)|$. Moreover, as shown in Figure3.5(c), we find a positive correlation between μ_Δ and the network average degree, with the increase in μ_Δ with $\langle k \rangle$ being much more significant for ER networks rather than for SF networks. Summing up, our analysis suggests that for degree heterogeneous networks the difference between $|\mathcal{G}_c(M)|$ and $|\mathcal{G}_o^T(M)|$ is limited regardless of the average degree, and existing driver node selection tools can be used also to achieve efficient sensor nodes placement. On the other hand, for homogeneous networks $\Delta(M)$ is usually large, and it becomes larger as the average degree increases. The latter class of networks motivate us to look for a better sensor node selection strategy than simply applying to the case of subnetwork observability the algorithms devised for subnetwork controllability.

((a))   ((b))

((c))
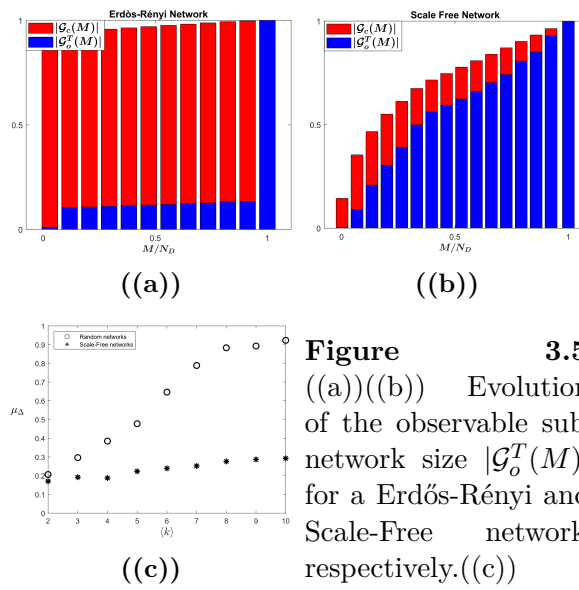
Figure   3.5.
((a))((b))   Evolution
of the observable sub-
network size $|\mathcal{G}_o^T(M)|$
for a Erdős-Rényi and
Scale-Free   network,
respectively.((c))
shows   the   evolution
of μ_Δ as a function
of   average   indegree
$\langle k \rangle$ related   the   two
datasets   described
above.

Topological Considerations

The fact that the topological properties influence the ability of controlling or observing a network is not surprising: for example, Liu et al [119] showed how sparsity and heterogeneity make networks more difficult to control. Dealing with observability instead, it seems that degree homogeneity combined with high density negatively influences our ability to observe a subnetwork. Hence, dense and homogeneous networks like Erdős-Rényi ones are much harder to observe rather than to control. Why observing a subnetwork is more challenging than controlling it? One network motif that can play a crucial role in hindering our ability to observe a subnetwork is the presence of dilations. We recall that a digraph contains a *dilation* if $\exists \, \mathcal{S} \subset \mathcal{V} : |\mathcal{T}(\mathcal{S})| \leq |\mathcal{S}|$ with $\mathcal{T}(\mathcal{S}) = \{v_j | (v_j \to v_i) \in \mathcal{E}(\mathcal{G}), v_i \in \mathcal{S}\}$. In other words, a dilation is a region of the graph where there is an expansion, that is it can be identified a subset of nodes whose cardinality is smaller than the one of its neighbors. Moreover, in the structural controllability framework, we know that, in absence of cycles, a node can control/observe at most one of its direct neighbors, but when there is a dilation a node has, for definition, more than one neighbor: this phenomenon has different effects on controllability and observability. Let us show them in a simple example of a three-node dilation:
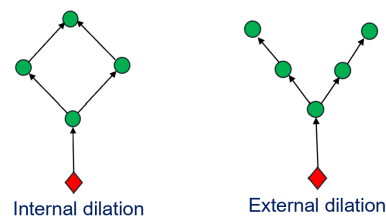
Figure 3.6. Three-node dilation example in controllability case (a) and observability case (b) where node 1 is respectively a driver or a sensor

Looking at this simple dilation in the context of controllability (Figure 3.6*a*), if node 1 is selected as driver node, either node 2 or node 3 can be considered controllable, with the downside that the other node is perturbed,i.e., it is dragged to a point of the state space that cannot be assigned a priori [121]. Nevertheless, if we look at the same dilation in the observability context (Figure 3.6*b*), that is if we select as a sensor node 1, neither node 2 nor 3 can be observed, as the only information we can reconstruct is a linear combination of their states. Generalizing this exemplification to a large-scale network, the dilations become numerous and they would involve a relevant number of nodes, thus our ability to observe the network is extremely reduced compared to the controllability case.

Once pointed out the key role of dilations in hindering our ability of observe a subnetwork, let us explain why this effect is even more dramatic in a specific class of synthetic networks such as the Erdős-Rényi. We recall that, in general, a digraph can be decomposed into different structures: the giant strongly connected component (GSCC), in which any node is reachable from any other node by means of a directed path and

whose dimension scales with network size, the giant IN-component (GIN), formed by the nodes from which it is possible to reach the GSCC (and analogously the giant OUT-component GOUT), the tendrils that are the nodes that cannot reach or be reached by the GSCC (among them, the tubes that connect the GIN and GOUT) and finally a set of disconnected components (DC) [132]. In [133], [134] has been proved that, as the average degree $k \geq 2$, the GSCC arises both in Erdős-Rényi and Scale Free networks. Nevertheless, the homogeneity that characterizes the random networks entails that, as the average degree increases, the upstream of the sensor nodes grows but it is also more likely to include more dilations which involve the nodes in the GSCC. In heterogeneous networks, instead, dilations are more concentrated around the hubs nodes, thus they encompass a limited number of nodes provoking a less remarkable effect in reducing $|\mathcal{G}_o^T(M)|$.

Geometrically, this translates into the fact that, as the average degree increases, the dimension of the orthogonal complement to the unobservable subspace likely increases, as well as the directions of the canonical basis that have nonzero orthogonal projection on the orthogonal complement of the unobservable subspace, reducing the number of elements e_i of the canonical basis and as a result the actual number of the observable nodes. Thus, differently from the case of controllability where our unique goal was to find the biggest stem-cycle disjoint partition which spans from the drivers (i.e. maximizing $\rho_g(K)$), in the case of partial observability, maximizing $\rho_g(O)$ is not enough because it constitutes only an upper bound for the number of observable nodes. Consequently, a more efficient heuristic must exploit the knowledge of this pivotal network motif in order to place a fraction of the M sensor nodes available trying to solve part of the dilations. Recalling that Lin's structural controllability theorem [30] ensures that a digraph is structurally controllable/observable if it contains no dilations, hence all dilations can be solved only relying on $M = N_S$ sensor nodes available. However, the scenario of partial observability implies that $M < N_S$, thus a question arises: which dilation could give us the larger improvement when solved, that is which criterion should we use to place sensor nodes in order to prioritize the removal of certain dilations? In fact, let us stress that not all the dilations have the same effect: some are more damaging than the other (as they encompass more nodes), that is that solving certain specific dilations can lead to a larger increment in the ability of observing the subnetwork. Our conjecture is that the dilations that involve the most connected nodes, i.e. the nodes in the giant strongly connected component, hinder the observability properties of Erdős-Rényi networks the nmost and thus an heuristic built to solve them will be more efficient.

A novel sensor nodes selection strategy

Exploiting the previous topological considerations regarding the role of dilations, here we propose a novel heuristic algorithm to better select sensor nodes, i.e. to increase the dimension of the achievable observable subnetwork $|\mathcal{G}_o^T(M)|$, with respect to choosing sensors likewise to driver nodes. Summing up, a trade-off has to be found in order to obtain the biggest sensor nodes upstream possible that encompasses no dilations: on one

hand, we want to select sensor nodes in order to maximize $\rho_g(O)$ because a node can be observable only if it is included in the stem-cycle disjoint partition that ends in the sensor nodes and, on the other hand, we want to place a fraction of the M sensor nodes at our disposal to solve some dilations, in particular the ones that involve the nodes of the GSCC.

The sensor selection strategy that we propose here is a constructive heuristic that consists in comparing, at each iteration in the range of $M = 2, \ldots, N_S - 1$ (thus except for the first one), alternative ways to add a sensor to the set Ω_S and choosing the one that leads to the larger $|\mathcal{G}_o^T(M)|$. Let us note that the first sensor node is selected maximizing $\rho_g(O)$. In order to recast this geometrical condition into a graphical approach we revisited the strategy in [128]: a weighted augmented graph $\mathcal{G}'(\mathcal{V}', \mathcal{P}', \mathcal{W}')^T$ is built in which the M output variables that we measure in the network are represented as one additional node called $N + 1$. $N + 1$ is initially connected to every other node of $\mathcal{G}^T$ with edges of unit weight, and have zero weight edges coming from each node of $\mathcal{G}'^T$ that is also a node of $\mathcal{G}^T$. The edges entering $N + 1$ node allow the state measurement of any nodes of the network, while the outbounding edges allow M cycles to be closed. Then, the goal is to find the biggest stem-cycle disjoint partition of $\mathcal{G}'^T$: we associate a binary decision variable y_{ij} to each edge p'_{ij} of $\mathcal{G}'^T$. Next, we associate a unit weight w'_{ij} to each decision variable y_{ij} that is linked to either an edge p_{ij} of $\mathcal{G}'^T$ that is also an edge of $\mathcal{G}^T$ or an edge p_{ij} of $\mathcal{G}'^T$ that enters $N + 1$ node. All the edges already existing in the graph $\mathcal{G}'^T$ are considered with unit weight. The optimization problem of maximizing $\rho_g(O)$ can now be translated into a problem on the graph $\mathcal{G}'$. This problem translates into a *polynomial* Integer Linear Program (ILP) problem in which we must select, among all the partitions of $\mathcal{G}'$ in disjoint cycles, the one that encompasses the maximum number of edges with unit weight and satisfies the following constraints:

$$\max_{y} \quad \sum_i \sum_j w'_{ij} y_{ij} \tag{3.18}$$

subject   to

$$y_{ij} \in \{0, 1\} \quad \forall i, j | p'_{ij} \in \mathcal{P}' \tag{3.19}$$

$$\sum_j y_{ij} = 1 \quad \forall i = 1, ..., N \tag{3.20}$$

$$\sum_i y_{ij} = 1 \quad \forall j = 1, ..., N \tag{3.21}$$

$$\sum_j y_{N+1,j} = M \tag{3.22}$$

$$\sum_i y_{j,N+1} = M \tag{3.23}$$

$$\sum_{j \in RSCC \subset GOUT} y_{N+1,j} \geq 1 \tag{3.24}$$

Here (3.19), a binary decision variable y_{ij} is associated with each edge p'_{ij} of the graph G'; if $y_{ij} = 1$, then the corresponding edge p'_{ij} will be part of the cycle partition.

The product $w'_{ij}y_{ij}$ will return a unit cost only either when the selected edge of $\mathcal{G}'^T$ is also an edge of $\mathcal{G}$ or if the edge enters $N + 1$. Hence, (3.18) represents the maximal achievable dimension of the observable subnetwork $|\mathcal{G}_o^T(M)|$ with that choice of sensor nodes. Eqs. (3.20) and (3.21) guarantee that the solution be a cycle partition of $\mathcal{G}'^T$ by forcing each one of its vertices to have exactly one inbounding and one outgoing edge. Let us note that we identify as a root strongly connected component (RSCC) a SCC whose nodes have incoming edges only from nodes belonging to the same SCC. Eq. (3.24) guarantee that we select at least a sensor among the RSCCs $\subset$ GOUT in order to ensure that the GSCC is encompassed in the sensor nodes upstream as it encompasses a large number of cycles that should be included in the solution in order to maximize $|\mathcal{G}_o^T(M)|$. Furthermore, let us note that it has to be ensured that all the nodes of the the stem-cycle disjoint partition that ends in the sensor nodes are accessible from at least one of the sensor node. This can be guaranteed by pruning the network from the inaccessible nodes relative to that choice of sensor nodes at each iteration. Finally, we obtain the largest stem-cycle disjoint subgraph of $\mathcal{G}$ that ends in M sensor nodes. At this point we have to evaluate $|\mathcal{G}_o^T(M)|$: a condition to prove the observability of a node is to verify that, adding that node as a sensor, that is adding an element e_i of the canonical basis in the matrix $B^T = C$ (and thus in O), the size of the orthogonal complement of the unobservable subspace does not increase, because that would mean that e_i was already included in it. Therefore, we implement the ILP, adding, in a iteratively way, a new node as a sensor to $\mathcal{G}'^T$, in a way that it must be included in the solution of the optimization problem and verifying if the size of the orthogonal complement of the unobservable subspace would increase or not.

From the second iteration on, the sensor node can be chosen with three alternative strategies: the former is the one just described, the second follows the same strategy of the former, thus maximizes $\rho_g(O)$ but at each iteration only adds a single sensor node F to the current set of sensors Ω_S rather than M as in the first strategy, the third alternative, instead, aims to exploit the knowledge of dilations role to better place sensor nodes. In particular, some candidate sensors Ω_Q are selected among the nodes which are not encompassed by Σ that is the stem-cycle disjoint partition that ends in the sensor nodes placed up to the previous iteration. These candidates are a subset of the unobservable nodes set Ω_U that are in dilations with at least a node in the upstream of the sensors already placed. At each iteration the dimension of the observable subnetwork is evaluated for both strategies. Finally the new sensor node is selected as the one yielding the largest increment on the dimension of the observable subnetwork $|\mathcal{G}_o^T(M)|$. These steps are iterated until all the $N_D - 1$ sensors available are placed.

Heuristic Steps

Let us consider a certain network where we want to place iteratively the M sensor nodes at our disposal in order to achieve the largest observable subnetwork possible. Then, the

---

[3]through Tarjan's depth-first search algorithm [135] which runs in polynomial time linearly with the number of nodes and edges $\mathcal{O}(|\mathcal{V}| + |\mathcal{E}|)$.

Step 3 Sensor Node Selection Algorithm

> **Network pre-processing:**
> Decompose $\mathcal{G}(A^T)$ in its SCCs. [3]
> Identify the GSCC and its downstream GOUT.
> Find the RSCCs $\subset$ GOUT.
>
> **Inputs:** $A^T \in \mathbb{R}^{N \times N}$, $\Omega = 1, \ldots, N$, N_S, $\Omega_S \in \mathbb{R}^{N_S - 1}$, $M = |\Omega_S|$, RSCCs $\subset$ GOUT
>
> **procedure** INITIALIZATION(O is empty, Ω_S is empty, Ω_U is empty, Ω_Q is empty, $\Sigma \equiv \Omega$)
>> **while** $M < N_S$ **do**
>>> Select M nodes $\Omega_M \subset (\Omega \setminus \Omega_S)$ as sensors solving the ILP in 3.2
>>> Evaluate $|\mathcal{G}_o^T(\Omega_M)|$ solving the ILP in 3.2
>>> Select a node $L \in (\Omega \setminus \Omega_S)$ as a sensor solving the ILP in 3.2
>>> Evaluate $|\mathcal{G}_o^T(\Omega_S \cup L)|$
>>> Evaluate O
>>> Select a set of candidate sensors $\Omega_Q \subset (\Omega_U \not\subset \Sigma) := \sum_{i=1,\ldots,|\Omega_U|} O(\Omega_Q, i) = 1$
>>> **if** $\Omega_Q \neq \emptyset$ **then**
>>>> Select as a sensor $Q^* \in \Omega_Q = \arg \max |\mathcal{G}_o^T(\Omega_Q)|$ where $|\mathcal{G}_o^T(\Omega_Q)|$ is evaluated solving the ILP in 3.2
>>>
>>> **else**
>>>> $Q^* = \emptyset \Rightarrow |\mathcal{G}_o^T(\Omega_S \cup Q^*)| = 0$
>>>
>>> **end if**
>>> **if** $|\mathcal{G}_o^T(\Omega_S \cup Q^*)| > |\mathcal{G}_o^T(\Omega_M)|$ **then**
>>>> $\Omega_S = \{\Omega_S \cup Q^*\}$
>>>
>>> **else if** $|\mathcal{G}_o^T(\Omega_S \cup L)| > |\mathcal{G}_o^T(\Omega_M)|$ **then**
>>>> $\Omega_S = \{\Omega_S \cup L\}$
>>>
>>> **else**
>>>> $\Omega_S = \Omega_M$
>>>
>>> **end if**
>>> $M = M + 1$
>>
>> **end while**
>
> **end procedure**

---

steps required to implement the strategy proposed in the previous section are presented in Algorithm 3.

Results

Solving iteratively the heuristic presented above for $M = 1, \ldots, N_S - 1$, the sequence of sets of selected sensor nodes Ω_S and the corresponding cardinality of the observable subnetwork $|\mathcal{G}_o^T(M)|$ can be obtained. Then, we compared these results with the ones

obtained by means of the first strategy of only maximizing the upper bound $\rho_g(O)$ presented in the 3.5(c) in terms of the μ_Δ index regarding only the Erdős-Rényi dataset. As we can see in Fig.3.7, placing sensor nodes exploiting the key role of dilations that involve the most connected nodes, allows us to have an improvement of the order of 25% on average in our ability to observe a subnetwork. In particular, can be noted that as long as the average degree $\langle k \rangle < 7$, the improvement is significant, then, it seems that with average degree $\langle k \rangle \geq 8$, the dimension of the GSCC become larger (up to 95% of the dimension of the network) and the dramatic effect of the dilations prevails.

Investigating more in detail the evolution of $|\mathcal{G}_o^T(M)|$ in function of the number of sensor nodes placed for a specific Erdős-Rényi network with $\langle k \rangle = 6$, we can appreciate how the second strategy (in green) allow us to anticipate the explosion of $|\mathcal{G}_o^T(M)|$ with respect to one that follows the same logic of driver nodes placement (in blue). More specifically, the ability of observing the subnetwork improves significantly when a third of the N_D sensor is at disposal. This "inertia" is due to the fact that in order to have a significant improvement firstly we have to make the sensors upstream large enough to encompass a relevant number of the nodes composing the network.

Conclusions

Starting from the theoretical differences between partial controllability and observability of subsystems and subnetworks highlighted in [121], we showed their practical consequences in our ability of observing a subnetwork, namely observe the largest node subset with a fixed limited number of sensor nodes at disposal, for two of the most relevant classes of synthetic networks, Erdős-Rényi and Scale Free networks. Then, we stressed how conferring observability to a subnetwork is way more challenging than conferring controllability, highlighting which topological properties play a key role in hindering our ability to observe a subnetwork. Then, we numerically implemented a sensors selection heuristic strategy, and demonstrated that it performs better than selecting sensors in the same way we select driver nodes. We found that exploiting the understanding of dilations in hindering partial observability, we can achieve a relevant improvement in the number of observable nodes, placing the same number of sensor nodes. Nevertheless, as a graphical mapping of the geometric observability condition still lacks, future work should be focused, on one hand, on finding a theoretical upper bound for the dimension of the observable subnetwork given a fixed number of sensor nodes to be placed and on the other hand, on identifying which are the topological features of large observable subnetworks.
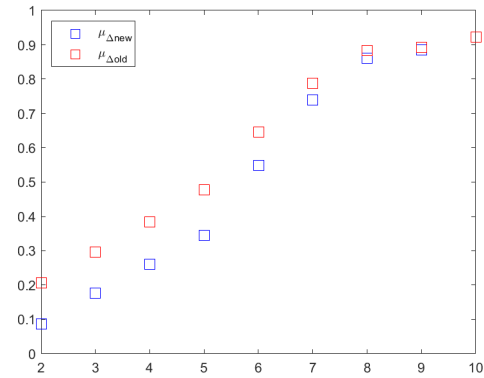
Figure 3.7. Comparison of the evolution of μ_Δ as a function of the average degree $\langle k \rangle$ between the former (in red) and latter (in blue) strategy
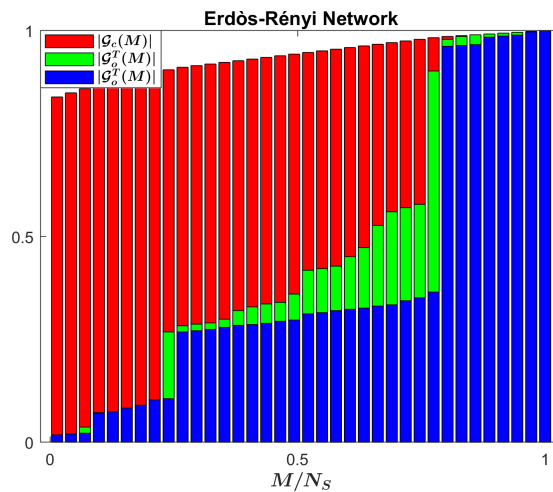
Figure 3.8. Observable subnetwork dimension evolution with regards to the improved strategy (in green) presented in 3 for a Erdős- Rényi network with average degree $\langle k \rangle = 6$.

CHAPTER 4

On opinions' fragmentation in decision-making of large social networks

Conferring controllability and observability to complex networks of dynamical systems is a way to understand under which conditions our ability of controlling a network holds true. Hence, it constitutes a prerequisite for control complex networks of dynamical systems, a problem that has been tackled in the previous two works in chapter 3. The following papers, instead, aim to dive in a particular category of network dynamical systems, namely large-scale social networks, in order to capture: (i) how opinions of social groups evolve over time, (ii) how these opinions can be shaped by particular individual known as opinion leaders or influencers, and (iii) how these translate into decisions-making processes. Both works select an opinion dynamics model that is able to replicate the emergence of persistent disagreement or fragmentation that arise from a discussion on a divisive topic among numerous individuals, but the two models differ onto their level of complexity due to the ultimate goal of each paper, as described below. Then, either model is complemented by an output function that allows to model also the decision-making process relative to a certain formed opinion. Finally, they explore the potential of opinion leaders to shape the discussion in order to obtain a desired decision profile at steady state. In both papers, shaping action of influential individuals has been modeled by means of a control tool, namely pinning control, that allow to exploit the interaction structure of the social network to diffuse the leader's opinion and convince as many individuals as possible to adopt their action. Even though these papers have a lot of similarities, they tackle different methodological issues: in [136], we aimed to unveil the theoretical conditions under which a certain alternative, the one sponsored by an influencer, namely the pinner, can be preferred by the majority of networked individuals. They are assumed to discuss a topic, such as the political elections, the acceptance of a vaccine, the adoption of a product, according to a cutting-edge nonlinear opinion dynamics model that accounts for self-opinion formation and goes beyond linear diffusive coupling [137]. This work enable to discover the potentiality of influencers in diffusing an opinion in a social network with a strategy rooted in theoretical findings. However, the high complexity of this model, as many parameters are needed to capture sophisticated opinion formation mechanisms, hinders the capability of solving another crucial problem in control theory that is identifiability. For this reason, in [138] we select a simpler

model, the Friedkin-Johnsen [43], that allow us to capture heterogeneity of opinions due to intrinsic biases but keeping the number of parameters, and thus the complexity of the model, limited in order to enable us tuning it on survey data, providing a validation of the what-if scenarios proposed to compare the effectiveness of different pro-vaccination initiatives of government bodies captured by means of an external influence, a pinner node, that resemble an awareness campaign. In fact, from a critical overview of the state of the art of opinion dynamics literature, we can assess that most of the existing studies have been focused on attempting to mathematically capture some typical phenomena of opinion formation process such as the emergence of consensus [42, 56], the raise of extremism [57], the persistency of opinions heterogeneity [46, 139]. From a modelling point of view, agents' characterization translates into defining one or few parameters per agent that describe their attitude during the opinion formation process.

Even though these models have been acknowledged to be able to qualitatively capture the aforementioned phenomena observable in society, the so-called *stylised facts*, the scientific community itself admits that the majority of opinion dynamics models have been not validated yet. Indeed, a so-called *replicative validity* intended as the mere ability of matching what can be qualitatively observed in real experiments and the results of simulations, is not enough to assess the robustness of quantitative outcomes of the simulations. The ultimate goal is to make these models decision-making support tools able to quantitatively capture and predict the factual emerging behaviors in social groups. A first attempt in this direction has been made in the work [138].

4.1 Paper C - Influencing Opinions in a Nonlinear Pinning Control Model

Introduction

In today's world, technology has changed dramatically the way how people acquire and share information, but more importantly the way in which information are conveyed by companies or public authorities. The opinion formation process occurs especially on social media platforms where users with provided with high visibility, the influencers, becomes key players in shaping the beliefs towards societal issues in education [140], health [141], politics [142], or consumer preferences [143]. Thus, the need for a deep understanding of how opinions form and can be influenced to lead to a certain decision, an aspect that has been overlooked in the literature of opinion dynamics in favor of consensus emergence or mitigating polarization because most of the works are linked to modeling small social groups. However, capturing the mechanisms that make influencers opinion leaders and unveiling their persuading effect on the opinion formation process of the others, namely the followers, is crucial and remains only partially unrevealed [144, 145]. If we interpret these influences as control inputs and the followers as a group of interconnected individuals, the analogy with pinning control is crystal clear, where the *influencer* is modeled as the pinner and influence the state (or opinion) of the other nodes in a leader-follower scheme [138, 146–150].

The action of similar individuals like zealots (stubborn agents that do not consider the others' opinions and thus do not update theirs) has been analyzed when referring to classic opinion dynamics models, based on averaging updating rules that imply that the more divergent two agents' opinions are, the more they tend to get closer [42, 43, 56]. But, in this work, we wanted to add the effect of external influences introducing the pinning control formalism in the modeling framework proposed in [74, 151], where the influence an agent has on the opinion of the others is capped by a saturation, overcoming the paradox of averaging linear models.

We complemented the model with an output function describing the action, that is a choice between two alternative options, associated to the opinion pf each individual, as typically done in CODA models [70]. Then, we add a virtual node, the pinner, which corresponds to (one or more) influencers trying to steer the action of the group towards one of the two options, the one preferred by itself. In this framework the control goal, thus the pinner's one, is that of selecting the individuals to directly influence in order to maximize the number of agents that will align with its action, by exploiting its topological centrality in the network.

By breaking down the network into distinct layers, we can provide sufficient conditions for the interaction structure, the selection of pinned nodes, and the control gain ensuring that a designated group of agents within the network will align their actions with the pinner. Leveraging these theoretical insights, we design a heuristic control strat-

egy aimed at identifying the optimal set of pinned nodes to maximize the number of nodes aligned with the pinner's action. Our experiments reveal that this novel heuristic strategy outperforms traditional pinning strategies based on centrality metrics [152,153].

Uncontrolled dynamics and parameter setting

We consider a group of N interconnected agents discussing on a given topic to finally take a decision, one per individual, between two alternative actions $\mathcal{A}_{-1}$ and $\mathcal{A}_{+1}$. We assume that the opinion diffusion process occurs on a weighted directed graph $\mathcal{G} = \{\mathcal{V}, \mathcal{E}, \mathcal{W}\}$, where nodes in $\mathcal{V}$ represent the N individuals, an edge $(i, j) \in \mathcal{E}$ implies that node i influences node j, whereas the matrix $\mathcal{W}$ is the matrix of weights whose i-th entry $w_{ij} > 0$ identify the strength of interaction between two individuals.

Inspired by the two-option model in [154], we describe the evolution over time of the opinion of agent i as its scalar state $x_i(t) \in \mathbb{R}$, and model the corresponding action $y_i(t) \in \{-1, 1\}$ that agent i would take given its opinion at time t as a discrete variable. In the absence of external influences, our model is described by

$$\dot{x}_i(t) = -dx_i(t) + c \tanh\left(\alpha x_i(t) + \sum_{k=1}^{N} a_{ik} x_k(t)\right), \tag{4.1a}$$

$$y_i(t) = \text{sgn}(x_i(t)), \tag{4.1b}$$

where a_{ij} is the ij-th entry of the adjacency matrix A associated to $\mathcal{G}$ ($a_{ij} \neq 0$ if j influences i), $d > 0$ captures the resistance each agent has to change opinion, the attention parameter $c \geq 0$ weighs the opinion exchange term, thus, the larger it is, the more agent i will give credit to the opinions of the neighbors, and $\alpha > 0$ modulates how much agent i reinforces its own opinion, that is the attachment towards its own opinion;

$y_i(t) = -1$ corresponds to agent i preferring $\mathcal{A}_{-1}$ (respectively, ($y_i(t) = 1$) corresponds to ($\mathcal{A}_{+1}$) at time t, whereas $y_i(t) = 0$ corresponds to agent i being undecided. We say that agent i has a stronger opinion than j at time t if the magnitude of his/her opinion is larger than that of agent j $|x_i(t)| > |x_j(t)|$. Note that the strength of an opinion is measured by its distance from the undecided state 0, and thus it is possible to compare strengths of opinions corresponding to discordant actions.

In this study, we set the parameters c, d, and α in (4.1) so that $c > d/\alpha$. This ensures that the single-agent dynamics in the absence of interactions (i.e., when $a_{ik} = 0$ for all k), has an unstable fixed point at 0 and two stable fixed points in $\bar{x}$ and $-\bar{x}$, which are the two solutions of the implicit equation

$$\frac{x}{\tanh(\alpha x)} = \frac{c}{d}, \tag{4.2}$$

and, for any finite α, have magnitude smaller than c/d [74]. Note that as the opinion of an individual may evolve also in the absence of interactions, this model (4.1) lends itself to take into account the personal opinion formation process, where an agent may modulate the strength of its opinion based on the acquisition of new information or

critical thinking [154]. A reinforcement effect is observed when, as in our study, c is selected to be larger than d/α: the left panel of Figure 4.1 shows that, when the agents at time 0 share similar opinions towards the action to prefer $\mathcal{A}_{-1}$ (that is, $x_i(0) < 0$ for all i), the sharing of opinions leads to amplify the conviction towards this choice, thus they would asymptotically take the same action, but with a stronger opinion.

Pinning control to influence opinions

Different from [154], here we consider the case where (one or more) influencers, labeled with the Greek letter ι, try to steer the decision towards one of the two options. This enables us to mimic the action of a high-profile agent that voluntarily wants to convince its audience to be aligned with his preference. To capture this scenario, we model the effect of the influencers through a virtual node ι with no incoming edges that, in agreement with the literature on consensus and synchronization in network systems, is called pinner and is unidirectionally coupled to a subset $\mathcal{D}_1 \subseteq \mathcal{V}$ of so-called *pinned nodes* [31, 35, 106, 146, 155, 156]. We assume that its opinion, independent of that of the other agents as there is no incoming edges that connects the pinner to the other agents, is already formed (or formed on a much shorter timescale), so that $x_\iota(t) = \bar{x}_\iota$ for all t, with $\bar{x}_\iota$ corresponding to one of the two equilibria $\pm\bar{x}$ of the decoupled single-agent dynamics. This means that the pinner had a fully-formed and convinced opinion that had already led to prefer a certain alternative. The action associated to the constant opinion of the pinner is $\bar{y}_\iota(t) = \text{sgn}(\bar{x}_\iota)$ for all t.

The pinner influences the decision process of the other agents by directly affecting the opinions of a subset of agents, namely the pinned nodes, and exploiting the network structure to diffuse its effect on the rest of the network. The presence of the control action from the pinner to the pinned nodes modifies model (4.1) as

$$\dot{x}_i(t) = -dx_i(t) + c\tanh\Big(\alpha x_i(t) + \sum_{k=1}^{N} a_{ik}x_k(t) + h_i\kappa_\iota\bar{x}_\iota\Big),$$

$$y_i(t) = \text{sgn}(x_i(t)), \tag{4.3}$$

for $i = 1, \ldots, N$, where the control gain $\kappa_\iota > 0$ modulates the influence that the pinner has on the dynamics of the pinned nodes; and, $\forall i = 1, \ldots, N$, $h_i = 1$ if i is pinned, i.e. $i \in \mathcal{D}_1$, whereas $h_i = 0$ otherwise. The right panel of Figure 4.1 shows the persuading effect of a pinner on a group of interconnected agent that at time 0 would take the opposite action of the pinner, with the pinner able to convince a fraction of them to change their opinion and subsequent action.

Control objectives

The aim of the control input $h_i\kappa_\iota\bar{x}_\iota$ in (4.3) is to select the set of pinned nodes $\mathcal{D}_1$ that maximizes the number of individuals that, after a sufficient amount of time, will take the
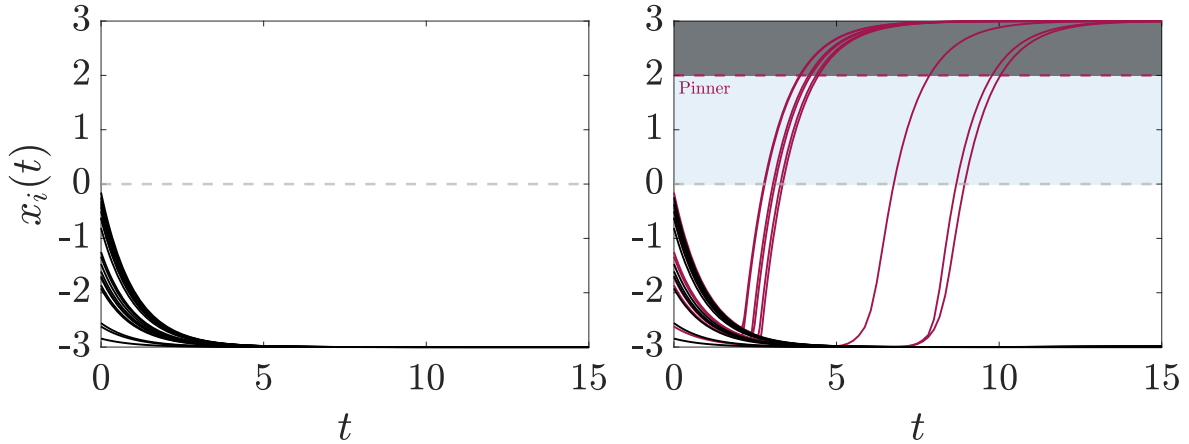
Figure 4.1. The left panel displays the opinion dynamics of $N = 30$ agents coupled on an Erdös-Rényi graph with probability $p = 0.6$, and evolving according to (4.1) with $c = 3, d = \alpha = 1$, and initial conditions uniformly randomly selected in $[-3, 0]$. The right panel depicts the dynamics of the same network in the presence of a pinner (in dashed red) that is connected to 3 agents according to (4.3) and steers the other agents towards a positive opinion. When the agents enter the blue shaded area, they will always take the same action as the pinner, thus belonging to the set $\mathcal{Q}$ defined in (4.4). Also, their opinion will become stronger than that of the pinner: as they enter the gray shaded area, that they also belong to the set $\mathcal{Q}_{\mathrm{str}}$ defined in (4.6). In both panels, black and red lines identify the opinion dynamics of agents opting for $\mathcal{A}_{-1}$ and $\mathcal{A}_{+1}$ at the end of the simulation, respectively.

same action as the pinner. To formally define this control design problem, we introduce the set

$$
\mathcal{Q} = \{i \in \mathcal{V} : \text{there exists } \bar{t} \text{ such that} \\
y(t) = \bar{y}_\iota \text{ for all } t > \bar{t} \},
\tag{4.4}
$$

whose composition will depend on the choice of κ_ι and $\mathcal{D}_1$. For any κ_ι, we can state the following optimization problem:

$$
\max_{\mathcal{D}_1} |\mathcal{Q}(\kappa_\iota, \mathcal{D}_1)|
\tag{4.5a}
$$

subject to

$$
|\mathcal{D}_1| = M,
\tag{4.5b}
$$

with $M < N$ as the number of nodes that are directly controlled may be limited by physical or economic constraints.

Depending on the context, one may be interested not only in convincing agents to take the same action as the pinner, but also to make their opinion at least as strong as that of the pinner. For instance, this is the case in which, agents deliberately starts to incite the crowd to maintain ferment in a certain discussion to exaggerate their effect [157, 158].

In such case, we can define the set $\mathcal{Q}_{\mathrm{str}} \subseteq \mathcal{Q}$ as

$$
\mathcal{Q}_{\mathrm{str}} = \{i \in \mathcal{V} : \text{there exists } \bar{t} \text{ such that} \\
y(t) = \bar{y}_\iota \text{ and } |x(t)| \geq |x_\iota| \text{ for all } t > \bar{t} \},
\tag{4.6}
$$

and state the following problem:

$$
\max_{\mathcal{D}_1} |\mathcal{Q}_{\mathrm{str}}(\kappa_\iota, \mathcal{D}_1)|
\tag{4.7a}
$$

subject to

$$
|\mathcal{D}_1| = M.
\tag{4.7b}
$$

The right panel of Figure 4.1 reports an instance where, for a given choice of κ_ι and $\mathcal{D}_1$, $\mathcal{Q}_{\mathrm{str}}$ and $\mathcal{Q}$ coincide. If this happens for all possible choices of κ_ι and $\mathcal{D}_1$, then problems (4.5) and (4.7) would also coincide.

Main results

We first show that the proposed opinion dynamics model is well-posed, as the controlled dynamics (4.3) are bounded to ensure that the modeling framework encompasses only realistic scenarios. Then, we provide sufficient conditions so that an agent forms an opinion that is coherent with the one of the pinner and more intense with respect to the influencer's opinion, that is, it belongs to Q_{str} (and therefore to $\mathcal{Q}$ as well).

The following lemma ensures that the opinions at steady-state are bounded by finite values that depend on the model's parameters.

Lemma 2. *Under the dynamics (4.3), the absolute value of the agents' opinion is asymptotically bounded by c/d, that is, for all $i = 1, \ldots, N$,*

$$
\limsup_{t \to +\infty} |x_i(t)| \leq \frac{c}{d}.
\tag{4.8}
$$

If, additionally, $|x_i(0)| \leq c/d$, then, for all $t \in \mathbb{R}_{\geq 0}$,

$$
|x_i(t)| \leq \frac{c}{d}.
\tag{4.9}
$$

Proof. Let us define two auxiliary dynamical systems

$$
\dot{\bar{x}}_i = -d\bar{x}_i + c, \qquad \bar{x}_i(0) = x_i(0).
\tag{4.10a}
$$
$$
\dot{\underline{x}}_i = -d\underline{x}_i - c, \qquad \underline{x}_i(0) = x_i(0).
\tag{4.10b}
$$

As $\tanh(\cdot) \in [-1, 1]$, from (4.3) and the Comparison Theorem for ordinary differential equations [159], we have that

$$
\underline{x}_i(t) \leq x_i(t) \leq \bar{x}_i(t), \quad \forall t \geq 0.
\tag{4.11}
$$

As $\lim_{t \to +\infty} \bar{x}_i(t) = c/d$ and $\lim_{t \to +\infty} \underline{x}_i(t) = -c/d$, inequality (4.8) follows. Next, note that $\underline{x}_i(t) = (x_i(0) + c/d) \exp\{(-dt)\} - c/d$ and $\bar{x}_i(t) = (x_i(0) - c/d) \exp\{(-dt)\} + c/d$. As $|x_i(0)| \leq c/d$, from (4.11), inequality (4.9) follows. $\qquad\square$

Remark 1. *We consider opinions that are bounded in a set centered at the undecided opinion $x_i = 0$. Considering Lemma 1, from now on we will assume $|x_i(0)| \leq c/d$, so that c/d will represent the maximum strength an opinion can have at any time instant.*

We define $\lambda_i(t) = \sum_{k=1}^{N} a_{ik} x_k(t) + h_i \kappa_\iota \bar{x}_\iota$ as the interaction term in (4.3), which can be rewritten as

$$\dot{x}_i(t) = -dx_i(t) + c \tanh\left(\alpha x_i(t) + \lambda_i(t)\right), \quad |x_i(0)| \leq c/d, \tag{4.12a}$$

$$y_i(t) = \mathrm{sgn}(x_i(t)). \tag{4.12b}$$

In what follows, we first provide a condition on the absolute value and sign of the social interaction term $\lambda_i(t)$ so that agent i belongs to $\mathcal{Q}$, that is, in finite time, agent i will take the same action of the pinner, and its opinion will be at least as strong as that of the pinner, so that i also belongs to $\mathcal{Q}_{\mathrm{str}}$. Then, we provide conditions on the control gain κ_ι and on the network topology such that the sufficient condition on $\lambda_i(t)$ is fulfilled.

Let us define $t_{1,i}$ as the first instant such that the action of agent i coincide with the one of the pinner, namely $y_i(t) \in \{\bar{y}_\iota, 0\}$, with $t_{1,i} = +\infty$ if such an instant does not exist, and

$$\tilde{\lambda} := -\tanh^{-1}\left(\sqrt{1 - d/c\alpha}\right) + \frac{c\alpha}{d}\sqrt{1 - d/c\alpha}. \tag{4.13}$$

Next, we define the set $\mathcal{T}_i := \{\tau : \forall t > \tau, \ y_i(t) = \bar{y}_\iota \text{ and } |x_i(t)| \geq |\bar{x}_\iota|\}$ and the scalar

$$t_{2,i} := \begin{cases} \min \mathcal{T}_i, & \text{if } \mathcal{T}_i \neq \varnothing, \\ +\infty, & \text{otherwise.} \end{cases} \tag{4.14}$$

In simple words, $t_{2,i}$, when finite, is the smallest time instant such that node i takes the same action as the pinner with an at least as strong opinion, thereby guaranteeing that $i \in \mathcal{Q}_{\mathrm{str}}$.

The following theorem provides sufficient conditions on the magnitude of the coupling term so that agent i will align its decision to the one of the pinner, with a stronger opinion towards that preference, if they are fulfilled.

Theorem 5. *Under the dynamics described by Eqs.* (4.12)*, if*

$$\exists \epsilon > 0 : |\lambda_i(t)| \geq |\tilde{\lambda}| + \epsilon, \tag{4.15}$$

$$\mathrm{sgn}(\lambda_i(t)) = \mathrm{sgn}(\bar{x}_\iota), \tag{4.16}$$

for all $t \geq 0$, then

$$\exists t_{1,i} < +\infty : y_i(t) = \bar{y}_\iota, \forall t > t_{1,i}, \tag{4.17a}$$

$$\exists t_{2,i} \in [t_{1,i}, +\infty[\ : |x_i(t)| \geq |\bar{x}_\iota|, \forall t > t_{2,i}. \tag{4.17b}$$

Proof. For clarity, in the proof we consider $\bar{y}_\iota = 1$, but the derivations hold *ceteris paribus* for $\bar{y}_\iota = -1$.

Existence of a finite $t_{1,i}$: Let us start by showing that if $x_i(0) < 0$ then there exists a time instant $\tilde{t}$ such that $x_i(\tilde{t}) = 0$. Note that, as the hyperbolic tangent is strictly monotone increasing, assumptions (4.15)-(4.16) imply that

$$\dot{x}_i(t) \geq f(x_i, \epsilon) := -dx_i + c \tanh\left(\alpha x_i + \tilde{\lambda} + \epsilon\right), \tag{4.18}$$

for all $x_i \in [-c/d, 0]$. Function f has two stationary points, whereby setting $\partial f(x_i, \epsilon)/\partial x_i = 0$, one obtains

$$x_{i,1}^\star = \frac{-c\alpha/d\sqrt{1 - d/c\alpha} - \epsilon}{\alpha},$$

$$x_{i,2}^\star = \frac{2\tanh^{-1}(\sqrt{1 - d/c\alpha}) - c\alpha/d\sqrt{1 - d/c\alpha} - \epsilon}{\alpha}.$$

Evaluating the function at $x_{i,1}^\star$ and $x_{i,2}^\star$, respectively, yields

$$f(x_{i,1}^\star, \epsilon) = \epsilon d/\alpha > 0, \tag{4.19}$$

$$f(x_{i,2}^\star, \epsilon) = 2\phi(c) + \epsilon d/\alpha > \epsilon d/\alpha > 0, \tag{4.20}$$

where we used that, for all $c > d/\alpha$, $\phi(c) = (c\sqrt{1 - d/c\alpha} - d/\alpha \tanh^{-1}(\sqrt{1 - d/c\alpha}) > 0$. Noting that

1. f is continuous and differentiable;

2. f is positive at the extrema of the interval $[-c/d, 0]$, whereby $f(0, \epsilon) = c\tanh\left(\tilde{\lambda} + \epsilon\right) > 0$, and $f(-\frac{c}{d}, \epsilon) = c + c\tanh\left(-\alpha\frac{c}{d} + \tilde{\lambda} + \epsilon\right) > 0$ as $\tanh(\cdot) > -1$;

3. f is positive and lower bounded by $\epsilon d/\alpha$ at both its stationary points;

we obtain $f(x_i, \epsilon) \geq \varepsilon$, for all $x_i \in [-c/d, 0]$, with

$$\varepsilon = \min\{c\tanh\left(\tilde{\lambda} + \epsilon\right), c + c\tanh\left(-\alpha c/d + \tilde{\lambda} + \epsilon\right), \epsilon d/\alpha\} > 0.$$

Therefore, from (4.18) we then have

$$\dot{x}_i(t) \geq f(x_i, \epsilon) \geq \varepsilon > 0, \ \forall t : x_i(t) \in [-c/d, 0]. \tag{4.21}$$

In turn, this implies that $x_i(t) > x_i(0) + t\varepsilon$ for all t such that $x_i(t) < 0$. As $x_i(0) \geq -c/d$, we can then conclude that $\tilde{t} \leq c/d\varepsilon$. Then, from the continuity of $f(\cdot)$ and as $f(0, \epsilon) \geq \varepsilon > 0$ we have $t_{1,i} = \tilde{t}$ (4.17a). Note that this also proves the existence of $t_{1,i}$ when $x_i(0) = 0$.

Finally, if $x_i(0) > 0$, then $t_{1,i} = 0$ follows from the continuity of $f(\cdot)$. Indeed, as $f(0, \epsilon) \geq \varepsilon > 0$, then there exists a finite $\tilde{x}_i$ such that $0 < \tilde{x}_i \leq x_i(0)$ and $f(\tilde{x}_i, \epsilon) > 0$.

Existence of a finite $t_{2,i}$: Now, let us study the dynamics (4.12) for $t > t_{1,i}$. As $x_i(t) > 0$ for all $t > t_{1,i}$, to prove (4.17b), consider that

$$\dot{x}_i(t) > -dx_i + c\tanh\left(\alpha x_i + \tilde{\lambda}\right)$$
$$> g(x_i) := -dx_i + c\tanh(\alpha x_i). \tag{4.22}$$

As $\dot{x}_i = g(x_i)$ is a bistable dynamical system with the stable fixed points at $\pm \bar{x}_\iota$, and starting at $x_i(\tilde{t}) > 0$, the dynamics governed by $g(x_i)$ monotonically converge to $\bar{x}_\iota$, thus from (4.22) the existence of a finite $t_{2,i}$ follows. $\qquad\square$

Next, we leverage the result of Theorem 5 to guarantee that a given agent will belong to $\mathcal{Q}_{\mathrm{str}}$. To do so, we define the extended graph $\widetilde{\mathcal{G}}$ obtained by adding the pinner and its ingoing edges to $\mathcal{G}$. Let $\mathcal{D} \subseteq \mathcal{V}$ be the set that includes all nodes that are destination of a directed path originating from s in $\widetilde{\mathcal{G}}$, and let $q \leq N$ be the maximum length of the shortest path from s to a node in $\mathcal{D}$. We focus on $\mathcal{D}$ as the opinion dynamics of the nodes in $\mathcal{V} \setminus \mathcal{D}$ cannot be affected either directly or indirectly by the pinner as there not exists a path connecting them to the pinner.

Next, we relabel the nodes in $\mathcal{V}$ so that the nodes belonging to $\mathcal{D}$ are the first $|\mathcal{D}|$, and decompose $\mathcal{D}$ in q disjoint subsets (layers) $\mathcal{D}_1, \ldots, \mathcal{D}_q$, so that $i \in \mathcal{D}_l$ if the shortest path in $\widetilde{\mathcal{G}}$ that connects s to i has length l, for $l = 1, \ldots, q$ (the first layer $\mathcal{D}_1$ coincides with the set of pinned nodes). Finally, we define the set $\mathcal{B}_l := \{j \in \cup_{k=1}^{l} \mathcal{D}_k : j \in \mathcal{Q}_{\mathrm{str}}\} \subseteq \cup_{k=1}^{l} \mathcal{D}_k$ of nodes in the layers $1, \ldots, l$ that in finite time will take the same action as the pinner with an at least as strong opinion.

Now, let us study the behavior of the nodes belonging to $\mathcal{D}_1$, that is, the pinned nodes. Denoting $\delta_i^{\mathrm{in}} = \sum_{k=1}^{N} a_{ik}$ the weighted in-degree of node i, we can give the following Corollary of Theorem 5 on the magnitude of control gain so that the pinned nodes will take the same action of the pinner:

Corollary 4. *For any $i \in \mathcal{D}_1$, if*

$$\kappa_\iota > \frac{|\tilde{\lambda}| + \epsilon + \frac{c}{d}\delta_i^{\mathrm{in}}}{|\bar{x}_\iota|}, \qquad (4.23)$$

then $i \in \mathcal{B}_1$.
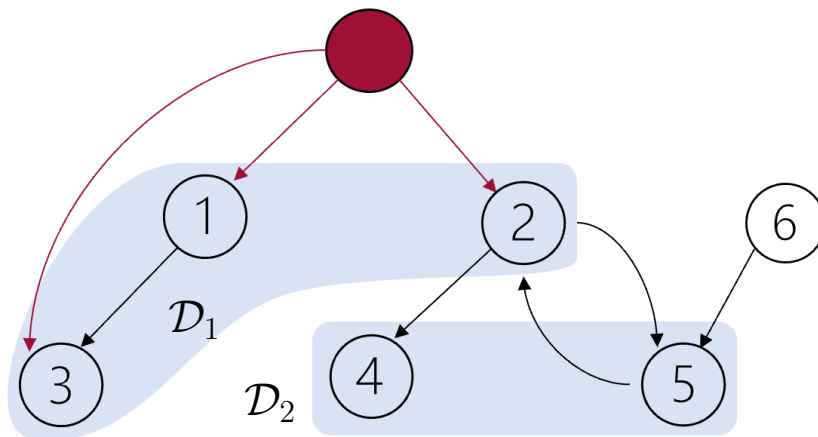
Figure 4.2. Decomposition in layers of a sample graph $\mathcal{G} = \{\mathcal{V}, \mathcal{E}\}$: the pinner (in red) has 3 outgoing edges that point to the nodes in $\mathcal{D}_1 = \{1, 2, 3\}$, whereas the set $\mathcal{D}_2$ is composed by nodes 4 and 5 that are at two steps away from the pinner. Note that $\mathcal{D} = \mathcal{D}_1 \cup \mathcal{D}_2$ does not encompass node 6, which is not influenced by the pinner, and therefore in this case $\mathcal{D} \subset \mathcal{V}$.

Proof. Let us recall that $\lambda_i(t) = \sum_{k=1}^{N} a_{ik}x_k + \kappa_\iota \bar{x}_\iota$. Then, as $|x_k| \leq c/d$ from Lemma 2 and Remark 1, and as $\sum_{k=1}^{N} a_{ik} = \delta_i^{\mathrm{in}}$ by definition, then from (4.23) we have that (4.16) holds. Furthermore, the same arguments imply that

$$|\lambda_i(t)| \geq \kappa_\iota |\bar{x}_\iota| - \sum_{k=1}^{N} a_{ik}|x_k| \geq \kappa_\iota |\bar{x}_\iota| - \frac{c}{d}\delta_i^{\mathrm{in}}.$$

Hence, also (4.15) holds, and therefore from Theorem 5 the thesis follows. $\qquad\square$

We can now study the dynamics of a generic node $i \in \mathcal{D}_l$, $l \geq 2$, that is, the ones who are indirectly connected to the pinner. Let us define b_i as the sum of the weights of the edges entering node i from every node $j \in \mathcal{B}_{l-1}$, that is, $b_i := \sum_{j \in \mathcal{B}_{l-1}} a_{ij}$, which implies that $0 \leq b_i \leq \delta_i^{\mathrm{in}}$. Then, we can give the following sufficient condition for a node i to belong to the set $\mathcal{B}_q \subseteq \mathcal{Q}_{\mathrm{str}}$ of nodes in $\mathcal{D}$ that take the same action with an at least as strong opinion as the pinner.

Corollary 5. *For any $i \in \mathcal{D}_l$, and $l \geq 2$, if $\mathcal{B}_{l-1} \neq \varnothing$, and there exists $\epsilon > 0$ such that*

$$b_i > \frac{|\tilde{\lambda}| + \epsilon + \frac{c}{d}(\delta_i^{\mathrm{in}} - b_i)}{|\bar{x}_\iota|}, \tag{4.24}$$

then $i \in \mathcal{B}_q$.

Proof. Let us note that

$$\lambda_i(t) = \sum_{j \in \mathcal{B}_{l-1}} a_{ij}x_j(t) + \sum_{j \notin \mathcal{B}_{l-1}} a_{ij}x_j(t). \tag{4.25}$$

Moreover, consider that, from Lemma 2, we have

$$\left| \sum_{j \notin \mathcal{B}_{l-1}} a_{ij}x_j(t) \right| \leq \frac{c}{d}(\delta_i^{\mathrm{in}} - b_i) \tag{4.26}$$

and from Theorem 5 and the definition of $\mathcal{B}_{l-1}$ we have that

$$\left| \sum_{j \in \mathcal{B}_{l-1}} a_{ij}x_j(t) \right| \geq |\bar{x}_\iota|b_i, \tag{4.27}$$

for all $t \geq t_l := \max_{j \in \mathcal{B}_{l-1}} t_{2,j}$. Hence, combining Eqs. (4.26)-(4.27), and from (4.24), $\lambda_i(\tau)$, with $\tau = t - t_l$, satisfies (4.15)-(4.16), and thus the thesis follows from Theorem 5. $\qquad\square$

Note that in (4.24) the lower bound of b_i is given in implicit form to underline the analogy with (4.23).

Corollaries 4 and 5 hold for any initial opinion in the set $[-c/d, c/d]$. Hence, they allow exploring layer by layer the part of the network whose dynamics is affected by the persuading action of the pinner and determine which agent we can guarantee will belong

to $\mathcal{Q}_{\text{str}}$. In particular, condition (4.23) of Corollary 4 guarantees that, even in the worst case where all the agents (except for the pinner) influencing agent i have the opposite opinion of the pinner with maximum strength c/d, the control gain κ_ι is strong enough to ensure assumption (14) of Theorem 1 is fulfilled. Condition (4.24) of Corollary 5 shows that, different from layer 1, in the other layers the control gain has only an indirect influence. Indeed, for a given level l, κ_ι may affect the cardinality $|\mathcal{B}_{l-1}|$ of the set of neighbors of node i that take the same action and have an opinion at least as strong as that of the pinner. The larger $|\mathcal{B}_{l-1}|$, the more nodes in layer l will belong to $\mathcal{Q}_{\text{str}}$, since b_i in (4.24) will be larger.

Pinning selection strategies

Once derived the mathematical conditions that guarantee the belonging of a certain node to the set of nodes that represent the agents that will be aligned with the pinner's decision, corollaries 4 and 5 can be used in an algorithmic fashion to identify a set of nodes $\widetilde{\mathcal{B}}_q$ that we can guarantee will belong to $\mathcal{B}_q$, that is, the set of nodes in the layer q that will take the same action as the pinner with an at least as strong opinion, for any $|x_i(0)| \leq c/d$. More specifically, condition (4.23) can be used to compute the pinned nodes that belong to $\widetilde{\mathcal{B}}_1$, and then condition (4.24) can be iteratively applied to sequentially compute $\widetilde{\mathcal{B}}_2, \ldots, \widetilde{\mathcal{B}}_q$ among the nodes that are indirectly influenced by the pinner.

Noting that the set of nodes that we prove to take the same action as the pinner with an opinion at least as strong as the one of the pinner is a subset $\mathcal{B}_q \subseteq \mathcal{Q}_{\text{str}}$, we can then use the cardinality of the estimation of this set $\tilde{q}(\mathcal{D}_1, \kappa_\iota) := |\widetilde{\mathcal{B}}_q|$, evaluated algorithmically through the two corollaries 4 and 5, as a proxy for the effectiveness of the choice of the set of pinned nodes $\mathcal{D}_1$ with a given cardinality M in solving problem (4.7), for a given selection of the control gain κ_ι. In what follows, assuming we do not consider any restriction on the control gain κ_ι, we propose a greedy heuristic that solves in polynomial time the NP-hard problem of selecting $\mathcal{D}_1$ with the goal of maximizing $\tilde{q}_\infty(\mathcal{D}_1) := \lim_{\kappa_\iota \to +\infty} \tilde{q}(\mathcal{D}_1, \kappa_\iota)$. We compare the effectiveness of the solution with respect to both Problems (4.5) and (4.7) against alternative choices of the pinned nodes based on centrality metrics, similar to what has been done in [152, 153].

Heuristic strategy for selecting $\mathcal{D}_1$

Starting from an empty set of pinned nodes, namely $\mathcal{D}_1 = \varnothing$, our greedy strategy sequentially adds nodes so that, at every iteration, $\tilde{q}_\infty$ is maximized given the current cardinality of $\mathcal{D}_1$. The heuristic stops as soon as $|\mathcal{D}_1| = M$. Defining

$$\bar{\kappa}_\iota := \max_{i \in \mathcal{V}} \frac{|\tilde{\lambda}| + \epsilon + \frac{c}{d}\delta_i^{\text{in}}}{|\bar{x}_\iota|},$$

as the control gain ensuring, from Corollary 4, that any pinned node belongs to $\mathcal{Q}_{\text{str}}$ the steps of our algorithm are:

1. initialize $\mathcal{D}_1 = \varnothing$, and set $\kappa_\iota > \bar{\kappa}_\iota$;

2. using Corollaries 4 and 5 compute $\tilde{q}(\mathcal{D}_1 \cup \{i\}, \kappa_\iota)$ for all $i \in \mathcal{V} \setminus \mathcal{D}_1$;

3. randomly select $i^\star$ in the set

$$\arg \max_{i \in \mathcal{V} \setminus \mathcal{D}_1} \tilde{q}(\mathcal{D}_1 \cup \{i\}, \kappa_\iota), \tag{4.28}$$

   and update $\mathcal{D}_1 = \mathcal{D}_1 \cup \{i^\star\}$;

4. if $|\mathcal{D}_1| < M$, go to step 2, otherwise stop the algorithm.

Performance in a sample retweet network from Twitter

We compare the proposed heuristic both against chance, that is, a random selection of the set $\mathcal{D}_1$, and alternative topological strategies, which consist in encompassing in $\mathcal{D}_1$ the nodes with maximum (or minimum) outdegree, indegree, and betweenness centrality [160]. To do so, we extracted a directed unweighted subgraph of 580 nodes of a retweet graph from [2]. Then, we set the number of pinned nodes to $M = 0.05N$, and evaluated the following metrics to assess the performance of the proposed heuristic:

- $m_1 = |\mathcal{Q} \cap \mathcal{D}|/|\mathcal{D}|$ and $m_2 = |\mathcal{Q}|/|\mathcal{V}|$, that is, the fraction of nodes in $\mathcal{D}$ and in $\mathcal{V}$, respectively, that take the same action of the pinner;

- $m_3 = |\mathcal{Q}_{\mathrm{str}} \cap \mathcal{D}|/|\mathcal{D}|$ and $m_4 = |\mathcal{Q}_{\mathrm{str}}|/|\mathcal{V}|$, that is, the fraction of nodes in $\mathcal{D}$ and $\mathcal{V}$, respectively, that take the same action of the pinner and have an opinion that is at least as strong as that of the pinner;

Note that m_1 and m_3 focus on the nodes that, given the selection $\mathcal{D}_1$, are directly affected by the pinner, whereas m_2 and m_4 evaluate the effectiveness of $\mathcal{D}_1$ for all the agents in $\mathcal{V}$. We evaluated these metrics for initial opinions

1. drawn from a uniform distribution in $[-c/d, c/d]$,

2. furthest from that of the pinner, i.e. $x_i(0) = -c/d$ as we set $\bar{y}_\iota = 1$.

For case 1), the results are averaged over 1000 random selections of the initial conditions. Table 4.1 shows that the proposed heuristic outperforms the alternative strategies. Also, metrics $m_{1,2}$ and $m_{3,4}$ are equivalent when all agents start with opinions that are furthest from the pinner, and the ranking of the strategies does not change depending on the metric. Moreover, we observe that the maximization of the out-degree is the topological strategy that more closely matches the performance of the proposed heuristic.

Table 4.1. Comparison of our strategy (heur) against a random selection, the maximization or minimization of the out-degree δ_{out}, in-degree δ_{in}, or the betweenness centrality bc for two alternative choices of initial conditions.

				Strategy					
Initial conditions	Metrics	heur	rand	$\delta_{\text{out}}^{\max}$	$\delta_{\text{out}}^{\min}$	$\delta_{\text{in}}^{\max}$	$\delta_{\text{in}}^{\min}$	$\text{bc}^{\max}$	$\text{bc}^{\min}$
	m_1	0.92	0.65	0.90	0.54	0.90	0.58	0.90	0.57
$x_i(0) \sim U(-\frac{c}{d}, \frac{c}{d})$	m_2	0.92	0.63	0.90	0.53	0.89	0.57	0.90	0.56
	m_3	0.81	0.61	0.80	0.53	0.79	0.57	0.80	0.56
	m_4	0.7	0.5	0.68	0.41	0.68	0.47	0.68	0.45
	m_1	0.30	0.081	0.27	0.070	0.14	0.070	0.22	0.050
$x_i(0) = -\frac{c}{d}, \forall i$	m_2	0.30	0.081	0.27	0.070	0.14	0.070	0.22	0.050
	m_3	0.22	0.061	0.20	0.050	0.11	0.050	0.16	0.050
	m_4	0.22	0.061	0.20	0.050	0.11	0.050	0.16	0.050

Performance in synthetic networks

As pinning the nodes with maximum out-degree leads to performance close to the proposed heuristic strategy, we performed a comprehensive numerical analysis on Erdös-Rényi (ER) and Scale Free (SF) graphs, generated by means of the configuration model, to assess whether the proposed heuristic yielded a significant improvement. For both ER and SF topologies, and for each value of the average degree, varied between 1 and 5 with step 1, we generated 100 graphs of $N = 500$ nodes, and we computed the average values of $m_1, \ldots, m_4$ setting $x_i(0) = -c/d$ for all i. As shown in Figure 4.3, in all synthetic networks the proposed heuristic outperforms pinning the nodes with maximum out-degree, and a t-test confirms that the difference is significant, with a p-value smaller than 0.001.

In the following, are presented additional topological considerations that have not been published for the sake of brevity.

Topological features of pinned nodes

The existing algorithms for solving the minimum input problems, that is for selecting the minimum number of nodes to directly control, namely the driver nodes, to ensure both controllability or to pinning control either the whole network or the largest sub-network, prescribe to avoid hubs [8], or more in general, very central nodes. This kind of selection is counterintuitive, as centrality has been extensively used as a proxy to identify influential nodes. Our heuristic driver node selection strategy, leveraging the realistically saturated dynamics of [137], allow to smartly select the most influential nodes to maximize their capability of diffusing their opinions in the network. In Table 4.2 we can appreciate how the average in-degree, out-degree and betweenness centrality are substantially higher than the average of the whole network nodes. This finding has
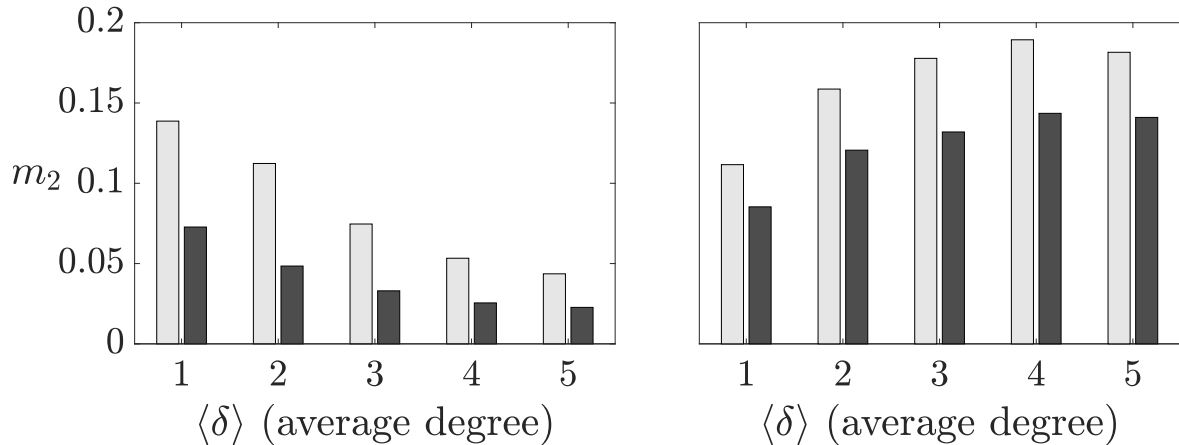
Figure 4.3. Comparing the proposed heuristic against pinning the nodes with maximum out-degree in terms of the fraction m_2 of nodes taking the same action of the pinner. The left and right panel refer to ER and SF networks, respectively. The probability of ER graphs is equal to $\langle \delta \rangle / N$, the exponent of the power law of SF network is equal to 2.6. Each data point is averaged over 100 realizations of the graph topology.

	Network metrics	Pinned nodes metrics
average in-degree	8.03	25.62
average out-degree	8.03	26.31
average betweenness	1022	6303

Table 4.2. Comparison between network centrality metrics and pinned nodes centrality metrics for the Twitter network used in the previous example.

also been confirmed by repeating the same analysis on ER and SF datasets as shown in Figures 4.4, 4.5.

Conclusions

In this work, we deployed pinning control as a mean to enhance the impact of an influencer within social groups engaged in interactions governed by a nonlinear opinion dynamics model. We established specific conditions regarding the network's structure and control parameters to ensure that individuals not only adopt the same action but also possess opinions that are at least as influential as those of the influencer. Our findings guided the development of a heuristic approach for strategically selecting the nodes where inputs should be introduced to maximize the influencer's reach, while adhering to a constraint on the number of nodes to be pinned. Future research endeavors should focus on validating our results using real-world data sourced from online social media platforms and exploring scenarios that incorporate heterogeneous agent parameters or involve multiple influencers vying for influence over other agents.
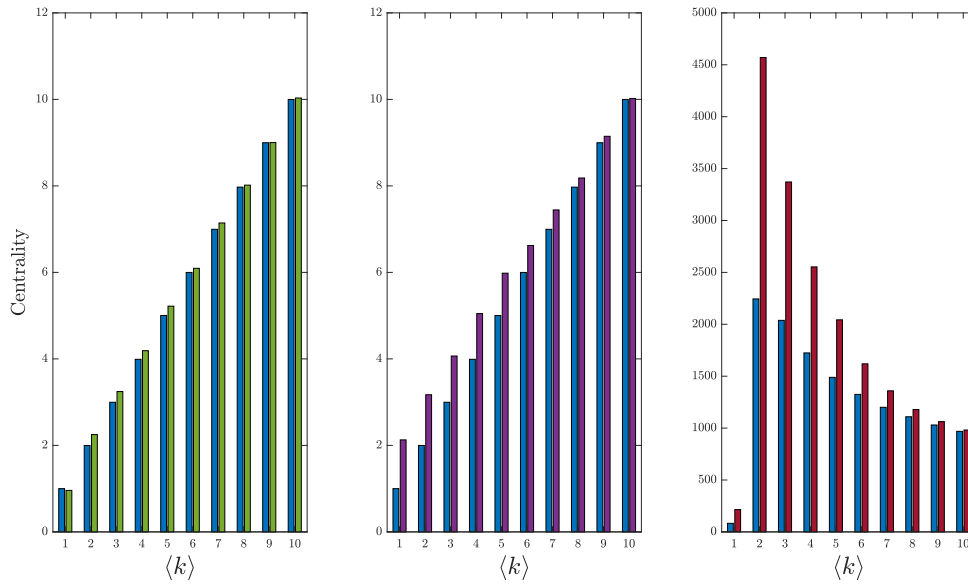
Figure 4.4. Comparison of network centrality metrics of ER dataset (in blue) with the pinned nodes' centrality metrics (from the left, average in degree (in green), average out degree(in violet) and average betweenness (in red)) at varying the average degree.
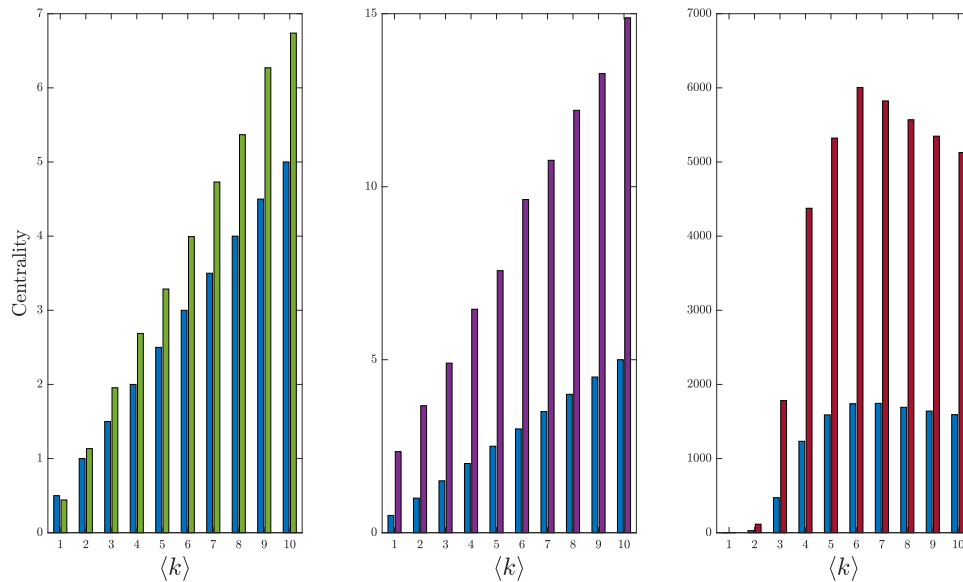
Figure 4.5. Comparison of network centrality metrics of SF dataset (in blue) with the pinned nodes' centrality metrics (from the left, average in degree (in green), average out degree (in violet) and average betweenness (in red)) at varying the average degree.

4.2   Paper D - A model-based opinion dynamics approach to tackle vaccine hesitancy

Introduction

Vaccine hesitancy has long been a subject of debate within the scientific community and the society in general, as it could heavily hinder our ability to fight viruses, see the recent revival of measles both in Europe and US [161–163]. A hesitant attitude in a non-negligible part of the population has always been observed world-wide [164–166]. Tackling this issue has become even more crucial during the COVID-19 pandemic due to the pervasive use of social media, which favored a radicalization of the opinions [167], and transformed a subset of vaccine hesitant into fierce no-vax, causing subsequent delays in our race towards herd immunity [168]. In this context, unveiling the underlying mechanisms by which opinions on vaccines form and translates into getting a jab or not could be essential to promote vaccination, and keeping the pandemic under control. Indeed, opinion formation is not only affected by the social pressure exerted through traditional media outlets such as newspapers or TV, but also by peer-to-peer interactions on social networks. We capture this opinion diffusion on large groups of networked individuals by means of an opinion dynamics model, tuned on survey data on vaccine willingness in the Italian population. Our ultimate goal is that of allowing to simulate what-if scenarios and compare the effectiveness of specifically designed pro-vaccine campaigns aimed at diffusing the vaccine literacy and boosting immunization acceptance [169]. Namely, we consider the willingness of getting vaccinated among a sample of Italian citizen, whose diffusion in a social group can be shaped over time by the influence of intrinsic biases, peer pressure and other exogenous actions, representing awareness campaigns. Such promoting actions were traditionally enforced by the government by means of general mass media such as newspapers or TV. However, given the current capillarity of social networks, they are becoming the main means for pro-vaccine awareness campaigns.

Our goal in [138] has been to capture opinion diffusion on large groups of networked individuals by means of an opinion dynamics model and to endow it of a predictive capability, thereby enabling proactive interventions [170]. This paper made a first step in this direction, proposing a scaled model and tuning it on a survey, and hypothesizing different targeted vaccine promotion campaigns to finally compare their effectiveness on the basis of the expected fraction of the population that, subject to each different campaign, will decide to take the vaccine, mathematically backing the decisions of government bodies on how devote the limited resources available in the most smartly way.

Opinion dynamics modeling of vaccine acceptance

Vaccine hesitant individuals are defined by WHO as "a heterogeneous group that are indecisive in varying degrees about specific vaccines or vaccination in general". Hence, vaccine willingness is a "fluid" opinion on vaccination that can be molded by social interaction and external stimuli.

Our modelling assumption is that the vaccine willingness of the i-th of a population of N networked individuals, $x_i(k)$, is shaped in time by social interactions according to the Friedkin-Johnsen model [43], i.e.,

$$x_i(k+1) = \lambda_i \sum_{j \in \mathcal{N}_i} w_{ij} x_j(k) + (1 - \lambda_i) x_i(0). \qquad (4.29)$$

Here, the so-called *susceptibility* $\lambda_i \in [0, 1]$ modulates the convex combination between agent i's innate opinion $x_i(0)$ and the social pressure modeled as the average of the current willingnesses $x_j(k)$ of its neighbors in the network (the agents in the set $\mathcal{N}_i$). The complement to 1 of λ_i captures the agent's *stubbornness*. In model (4.29), vaccine willingness diffuses along an undirected connected graph $\mathcal{G} = \{\mathcal{V}, \mathcal{E}\}$ with self-loops at each node, where $\mathcal{V}$ is the set of the N individuals, and $\mathcal{E} = \{(i, j) \subseteq \mathcal{V} \times \mathcal{V}\}$ is the set of edges connecting neighboring individuals. Departing from the consideration that radical views generally translate into foreseeable (unsurprising) actions, while actions related to moderate opinions are far more uncertain, we posit that the probability of an individual accepting a jab at a certain time k, $p_i(k)$, depends linearly on its willingness $x_i(k)$. Hence, we can extend the model of $x_i(k)$ to $p_i(k)$ obtaining

$$p_i(k+1) = \lambda_i \sum_{j \in \mathcal{N}_i} w_{ij} p_j(k) + (1 - \lambda_i) p_i(0). \qquad (4.30)$$

According to our model, the binary decision of taking or refusing a jab becomes a Bernoulli random variable whose parameter is $p_i(k)$.

Equation (4.30) can be rewritten in compact matrix form as

$$p(k+1) = \Lambda W p(k) + (I_N - \Lambda) p(0), \qquad (4.31)$$

where $\Lambda = \text{diag}\{[\lambda_1, \ldots, \lambda_n]^{\mathrm{T}}\}$ encodes the susceptibilities of each individual and I_N is the identity matrix of size n. Moreover, W is a row-stochastic matrix that captures the structure of the graph $\mathcal{G}$, whereby its ij-th entry w_{ij} is $w_{ij} = 1/|\mathcal{N}_i|$ if $(i, j) \in \mathcal{E}$ and zero otherwise, with $|\cdot|$ denoting the cardinality of a set. Finally, $p(0)$ encodes the initial willingness of being vaccinated. Note that $\lambda_i = 0$ corresponds to *zealot* [171, 172], who never changes its opinion while actively trying to convince the others. Assuming that $\Lambda \neq I_N$, that is, there exists at least an agent i such that $\lambda_i < 1$, the vaccination probabilities will converge at steady-state toward [173]

$$\bar{p} = (I_n - \Lambda W)^{-1} (I_N - \Lambda) p(0), \qquad (4.32)$$

where $\bar{p} = [\bar{p}_1, \ldots, \bar{p}_N]^{\mathrm{T}}$. Knowing the distribution of all individual vaccination probabilities $p(k)$ allows computing the probability that, at time k, a given fraction of the

population is willing to be vaccinated. Indeed, this event can be viewed as the outcome of a Poisson binomial experiment, which is a collection of N independent yes/no experiments with success probabilities $p_1(k), \ldots, p_n(k)$. The same consideration holds for the steady-state distribution $\bar{p}$.

A scaled model of vaccine willingness in the Italian population.
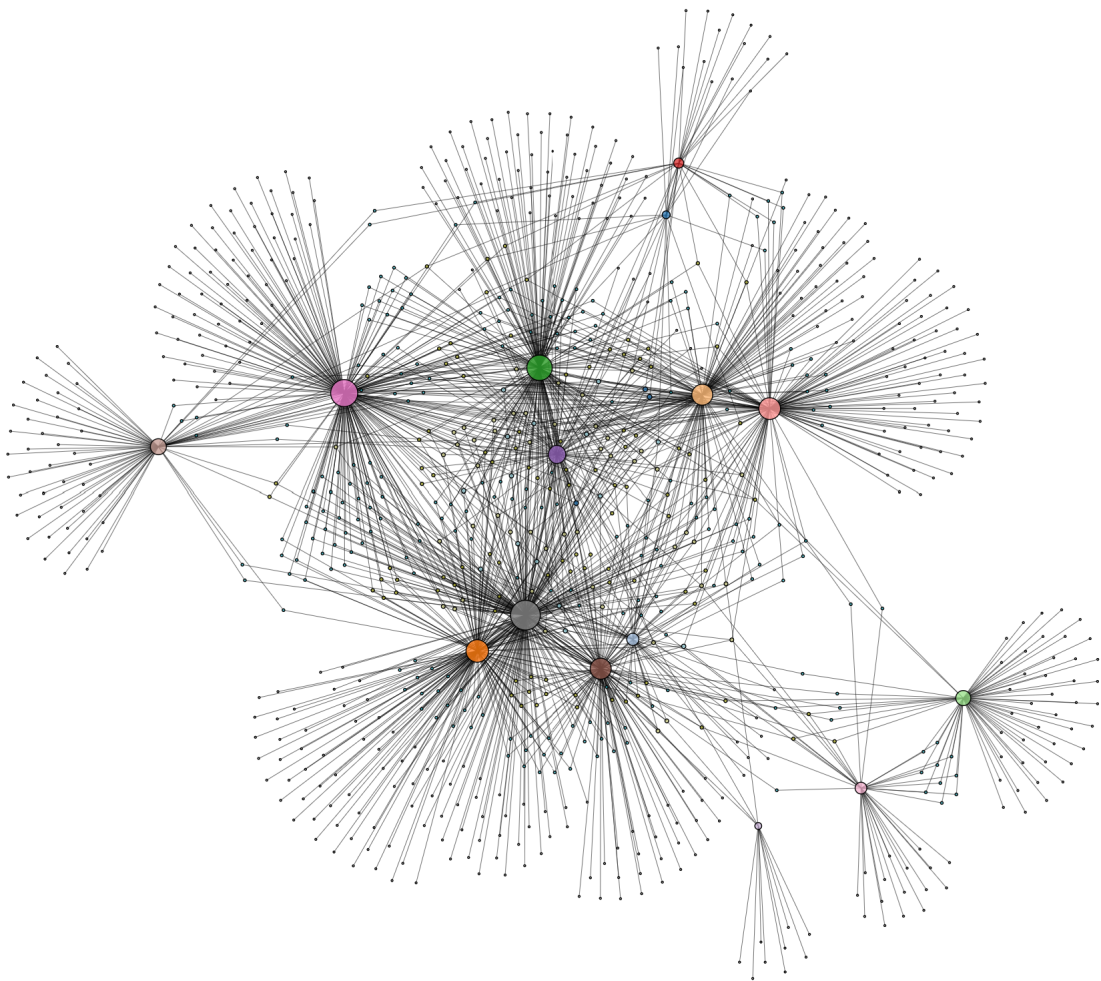
Figure 4.6. Topology of the Facebook friendship network in [2].

We exploit our modeling framework to build a scaled representation of vaccine willingness in the Italian population. Since we focus on interactions taking place through *online* social media, we borrowed the graph describing social interactions among the individuals from a Facebook friendship network [2], see Figure 4.6. We associate to the

individuals of our scaled model vaccine willingnesses (see section 4.2 below for details) whose distribution is compatible with the outcome of a survey conducted on a sample of the Italian adult population at the end of the first lockdown [165], when the vaccine availability was long to come. From these data we were able to estimate the susceptibilities λ_i so as to preserve, at steady-state, the aforementioned association, see the section 4.2 for details and the Figure 4.7 for a graphical representation.

The steady-state distribution of the vaccine willingness enables the evaluation of the probability that any given fraction of the population gets vaccinated, which in turn allows computing the expected fraction of the population that, at the time of the survey, would have taken a jab had this opportunity been given.

Tuning the model parameters on real data.

The parameters that need to be selected in model (4.31) are related to i) how individuals are connected, which is encapsulated by the network topology, described by matrix W, and ii) the inherent characteristics of each individual, captured by the susceptibilities $\lambda_1, \ldots, \lambda_n$, and by the initial probabilities $p_1(0), \ldots, p_n(0)$, a measure of their pre-existing attitude towards vaccines. The network matrix W has been borrowed from a Facebook social friendship network [2], composed by $n = 1446$ nodes, with $|\mathcal{E}| = 59600$ edges describing their mutual interactions. We have chosen the individual parameters so that the steady-state probabilities $\overline{p}$ in (4.32) are compatible with the outcome of a survey administered to a sample of Italian citizens [165]. Toward this goal, we first translated the survey outcome into target steady-state values $p^\star$, to then tune the susceptibilities λ_i and find a set of initial attitudes $p_i(0)$ so to obtain the $\overline{p}$ that best matches $p^\star$ in the least square sense (see Figure 4.7 for a visualization of $\overline{p}$ and $p^\star$). *Description of the dataset from [165] and choice of $p^\star$.* The authors of [165] tested the beliefs and attitudes of Italian citizens towards a possible COVID-19 vaccine through the administration of surveys, based on the Likert scale, to a stratified sample of 1004 individuals, representative of the Italian adult population aged between 18 and 70 years old. The respondents filled the survey during the first days following the end of Italy's strict lockdown begun in March 2020, when no vaccine was available yet. The survey contained general questions about their lives and health habits, as well as specific questions related to the COVID-19 pandemic. In this work, we focused on the 5th Likert item of the survey, which reads *'I am willing to vaccinate, if a vaccine against COVID-19 were to be found'*, with five options, ranging from $1 = $ *'not likely at all'* to $5 = $ *'absolutely'*, and computed the fraction f_j of agents choosing answer j to question 5, for $j = 1, \ldots, 5$. Accordingly, we partitioned our social network of $n = 1446$ nodes into 5 classes, where the j-th class is populated by the $c_j = f_j n$ agents expected to choose option i. As $f_j n$ is not necessarily an integer, it is rounded so that $\sum_{i=1}^{5} c_j = n$, and each agent is randomly assigned to each class. We then converted the categorical values of the Likert scale into continuous values in the interval $[0, 1]$ following the approach in [174], and splitting it in 5 sub-intervals, one for each class (alternative approaches have been proposed e.g. in [175, 176]). Namely, the
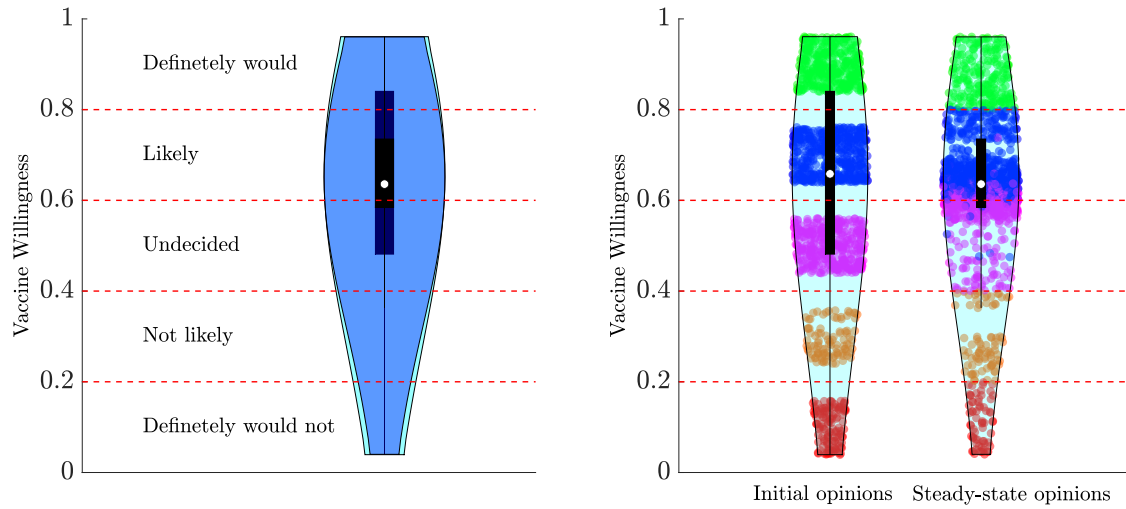
Figure 4.7. Violin plots of the steady-state opinion distribution from the model calibrated as described in the main text (light blue), with that obtained from the survey data (blue), respectively. On the right, the violin plots of the initial and final opinions' distribution of vaccine willingness, respectively. Data points corresponding to agents' opinions in the two endpoints are colored accordingly to their Likert score on the vaccine willingness survey.

jth class was associated to a range $r_j = [0.2(j-1), 0.2j]$, $j = 1, \ldots, 5$, where the steady-state vaccination probabilities $p^\star$ should lie, see Table 4.3. Given an agent i assigned to class j, the steady-state vaccination probability $p_i^\star$ has been extracted from a uniform distribution in r_j.

Likert item point	Probability range r_j
(1) Not likely at all.	0 - 0.2
(2) A little likely.	0.2 - 0.4
(3) Not likely nor unlikely.	0.4 - 0.6
(4) Very likely.	0.6 - 0.8
(5) Absolutely.	0.8 - 1

Table 4.3. Conversion of discrete vaccine willingness Likert score to continuous probability of getting vaccinated.

*Selection of the behavioral parameters λ and $p(0)$. Once we generated target steady-state probabilities $p^\star$ as explained above, we selected the individual parameters in our network so that the network dynamics converge to the steady-state vaccination

probability $\bar{p}$ that is the closest possible to $p^\star$ in the least square sense. Namely,

$$\min_{\lambda, p(0)} \|\bar{p} - p^\star\|^2 \tag{4.33a}$$

subject to

$$0 \le p_i(0) \le 1, \qquad\qquad i = 1, \ldots, n, \tag{4.33b}$$

$$\lambda^{\mathrm{T}} \mathbb{1}_n = \rho n, \quad 0 \le \lambda_i \le 1, \quad i = 1, \ldots, n, \tag{4.33c}$$

$$\frac{\lfloor 5p_i^\star \rfloor}{5} < \bar{p}_i \le \frac{\lceil 5p_i^\star \rceil}{5}, \qquad\qquad i = 1, \ldots, n, \tag{4.33d}$$

$$\bar{p} = (I_n - \Lambda W)^{-1}(I_n - \Lambda)p(0), \tag{4.33e}$$

where $\lfloor \cdot \rfloor$ and $\lceil \cdot \rceil$ map a real number to its previous or next integer, respectively, and $\mathbb{1}_n$ is the vector of all ones. Notice that the set of enforced constraints (4.33b)-(4.33e) guarantee that the outcome of the optimization is meaningful. Indeed, constraint (4.33b) guarantees that the probabilities lie in $[0, 1]$, (4.33c) that the average susceptibility to the neighbors' opinion is $0 < \rho < 1$ and the individual susceptibilities belong to $[0, 1]$, whereas (4.33d) enforces that if $p_i^\star \in r_j$, then also $\bar{p}_i \in r_j$, that is, each agents stays in the target class identified by $p^\star$. Finally, constraint (4.33e) ensures that the steady-state values $\bar{p}$ are compatible with the dynamics (4.31). In Figure 4.8 the distribution of the susceptibilities inferred is shown. In all our numerical analysis, we selected the largest value of ρ for which problem (4.33) admits a solution, that is, $\rho = 0.58$. However, our main results would still hold for lower values of ρ, see Section 4.2.1 for further details.
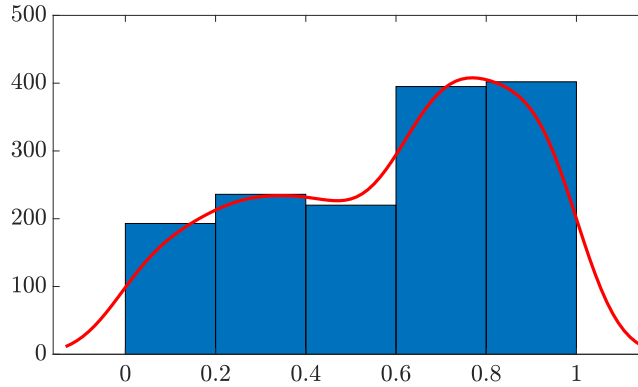
Figure 4.8. Histogram of estimated stubbornness $\hat{\lambda}_i$ and its estimated PDF.

Incorporating pro-vaccine campaigns into the model.

According to the Friedkin-Johnsen model, the individuals can neither change their own belief nor their susceptibility, thereby in the time-scale of a campaign we can only act on the social interaction term $\lambda W p(k)$ in (4.31). Exploiting tools from network control [106, 177], we incorporate a pro-vaccine campaign in model (4.29)-(4.30) as an additional

virtual node, an *influencer agent*, whose willingness is $x_l(k)$ and associated probability of accepting a jab $p_l(k) = 1 \ \forall k$. The influencer agent is connected through a directed link to a fraction ϕ of targeted individuals. Agent i will weigh the opinion of this virtual agent proportionally to the intensity of the vaccination campaign. Hence, the dynamics of the targeted agents becomes

$$p_i(k+1) = \left((1-\alpha)\lambda_i \sum_{j \in \mathcal{N}_i} p_j(k) + \alpha p_l(k) \right) + (1-\lambda_i)p_i(0). \tag{4.34}$$

where $\alpha \in [0,1]$ quantifies the *effort per target individual*. Hence, we characterize the *overall effort* $0 \le \eta \le 1$ of a campaign as the product of the two parameters α and ϕ.

In compact terms, Equation (4.31) modifies as

$$p(k+1) = \Lambda \left((I_n - \alpha\Delta)Wp(k) + \alpha\delta p_l \right) + (I_n - \Lambda)p(0), \tag{4.35}$$

where $\delta = [\delta_1, \ldots, \delta_n]^{\mathrm{T}}$, with δ_i being 1 if node i is targeted by the campaign, and 0 otherwise, $\Delta = \mathrm{diag}\{\delta\}$, $0 \le \alpha \le 1$ quantifies the intensity of the vaccination campaign, $p_l = 1$ is the vaccination probability the campaign is targeting, and we set $p(0) = \bar{p}$. Namely, $\alpha = 0$ corresponds to no effect, whereas $\alpha = 1$ to the agents disregarding the opinion of the other neighbors, and only considering the that of the virtual neighbor l. The same approach can be used to incorporate the effect of hoaxes and misinformation, just by setting p_l to zero.

During the ongoing pandemic, health authorities of most countries have conducted traditional pro-vaccine campaigns through mass media to fight vaccine hesitancy [178–180]. In our modeling framework, this means that the influencer (in this case, the health authority) is connected to all the network agents, that is, $\phi = 1$. However, in the era of online social media and targeted marketing, one could argue that a targeted pro-vaccine campaign, where the influencer devotes a larger individual effort α to a small fraction ϕ of the agents, could outperform traditional mass campaigns given the same overall effort η.

To dispel this doubt, we exploit our scaled model to design three alternative targeted campaigns, differing for the selection of the targeted agents, denoted in the following as Strategies 1, 2, and 3, respectively. Strategy 1, as in classical network science approaches, targets the most connected agents, i.e. the agents that have the greatest topological advantage for spreading opinions favorable to vaccination. Strategy 2 mitigates the effect of the antivax by targeting their neighbors, whereas Strategy 3 directly targets the most susceptible agents.

Comparing pro-vaccine campaigns.

Leveraging our scaled model, we conducted a numerical analysis to compare the effectiveness of targeted and mass campaigns on our synthetic population. Our simulations show that i) the targeted campaigns outperform a general mass-media campaign, and ii) the best strategy for targeting individuals depends on the overall effort η of the campaign.

Indeed, for all possible selections of η, it is possible to find a targeted strategy that yields an advantage compared with general mass-media campaigns, with an increase of the expected number of vaccinated individuals that reaches a maximum 5% for $\eta = 0.25$, see the left panel of Figure 4.9. Interestingly, for low efforts ($\eta < 0.1$), any strategy is capable of increasing the effectiveness of the vaccination campaign, with the merely topological approach of Strategy 1 being the most effective. When more resources can be devoted to the campaign, our model predicts that a finer characterization of the individuals is required to substantially increase the expected vaccinated population, see the right panel of Figure 4.9. In particular, for all $\eta \geq 0.1$, Strategy 3, which relies on the estimation of the individual susceptibility, proves to be the best campaign. One could argue that the expected advantage of targeted strategies over the general alternative could be irrelevant, should the variance be high. However, as shown in Section 4.2.1, the variance of the distribution of the fraction of vaccinated individuals tends to 0 as the size of the populations increases, and is negligible when we consider the population of a country like Italy. These results are robust to changing the graph underlying our scaled model, see Section 4.2.1.
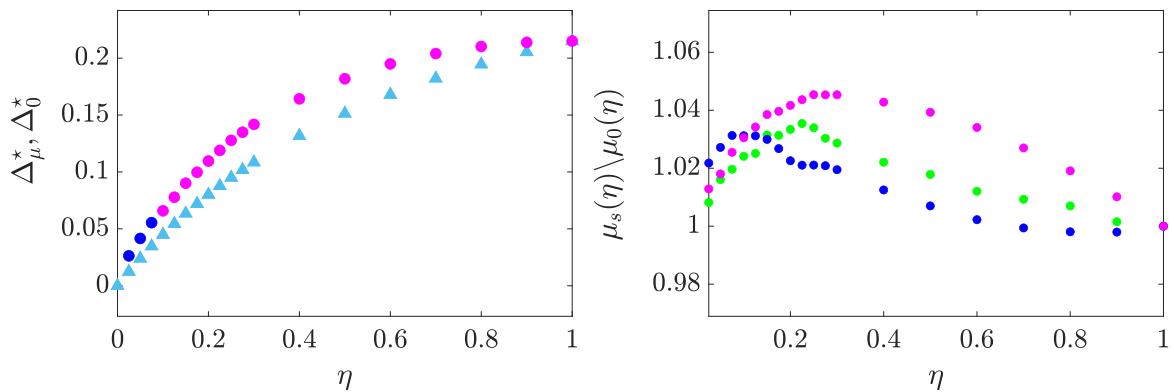
Figure 4.9. Comparison of targeted and traditional provax mass campaigns. The left panel depicts, for each effort η, the additional population fraction $\Delta_\mu^\star$ and Δ_μ^0 that is expected to be vaccinated when the best targeted campaign (identified by circles) or the mass provax campaign (identified by triangles) are employed, respectively. The right panel displays for each effort η and targeted strategy s, the ratio between the fractions of the population $\mu_s(\eta)$ and $\mu_0(\eta)$ that are expected to be vaccinated when strategy s and the traditional campaign are employed, respectively. In both panels, Strategy 1, 2, and 3 are depicted in blue, green, and magenta, respectively, the intensity of the vaccination campaign is set to $\alpha = 1$ and for the maximum effort $\eta = 1$, all points are superimposed since all strategies would be equivalent.

Impact of antivax campaigns.

Our model can also be used to assess the possible impact of antivax campaigns. Analogously to the provax case, we incorporate the role of antivax campaigns attempting to polarize the vaccination probabilities towards zero by setting $p_l(k) = 0$ for all k. Moreover, we assume that the selection of the agents targeted by the antivax influencer is made according to the same criteria defining the provax strategies. As illustrated in Figure 4.10, antivax campaigns can be even more impactful than their provax counterparts, and thus can represent a serious hindrance in our quest to stem the transmission of the virus.

Figure 4.10. Comparison of the targeted and traditional mass antivax campaigns. The left panel depicts, for each effort η, the additional population fraction $\Delta_\mu^\star$ and Δ_μ^0 that is expected to be vaccinated when the best targeted (identified by circles) or the mass (identified by triangles) antivax campaigns are employed, respectively. The right panel displays, for each effort η and targeted strategy s, the ratio between the fractions of the population $\mu_s(\eta)$ and $\mu_0(\eta)$ that are expected to be vaccinated when strategy s and the mass antivax campaign are employed, respectively. In both panels, Strategy 1, 2, and 3 are depicted in blue, green, and magenta, respectively, the intensity of the vaccination campaign is set to $\alpha = 1$, and, for the maximum effort $\eta = 1$, all points are superimposed since all strategies would be equivalent.

4.2.1   Additional analyses

Consideration on the variance of the Poisson Bernoulli distribution of the population

The model presented interprets each agent's opinion as its probability p_i of getting vaccinated. We can then associate to each agent $i = 1, \ldots, n$ independent Bernoulli

variables $X_1, \ldots, X_N$, with *heterogeneous* probability of success $p_1, \ldots, p_N$, respectively. As our ultimate goal is to estimate the expected *fraction* of the population that will get vaccinated, we define the stochastic variable

$$Y_N = \frac{1}{N} \sum_{i=1}^{N} X_i,$$

whose expected value and variance can be computed as

$$E[Y_N] = \frac{1}{N} \sum_{i=1}^{N} p_i, \quad \text{Var}[Y_N] = \frac{1}{N^2} \sum_{i=1}^{N} p_i(1 - p_i), \tag{4.36}$$

respectively. Its variance is, instead,

$$\text{Var}[Y_N] = \mathcal{E}[Y_N^2] - \mathcal{E}^2[Y_N] = \mathcal{E}\left[\left(\frac{\sum_{i=1}^{N}[X_i]}{N}\right)^2\right] - \left(\frac{1}{N} \sum_{i=1}^{N} p_i\right)^2 =$$

$$\frac{1}{N^2} \sum_{i=1}^{N} p_i - \left(\frac{1}{N} \sum_{i=1}^{N} p_i\right)^2 = \frac{1}{N^2} \sum_{i=1}^{N} (p_i - p_i^2),$$
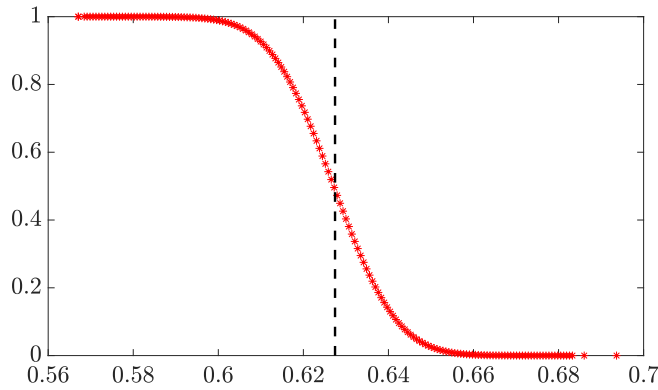
Figure 4.11. Complementary CDF of the fraction of population that will get vaccinated Y_n in free evolution.

Scaling the Poisson Binomial distribution

Note that Y_i is a Poisson binomial distribution (scaled by the factor $1/N$), that is the sum of N independent Bernoulli distributions. Here, we study how its moments scale with the population size N. Denoting $N_0 = 1446$ the number of participants to the survey on which the opinion dynamics model is parametrized in the main text, we scale the population as multiples of N_0, so that we can always associate a vaccination probability p_i to a fraction $1/N_0$ of the total population N, for all $i = 1, \ldots, N_0$. Specifically, we

introduce the parameter $\beta_k := \lfloor l_k/N_0 \rceil$ with $l_k = 10^k$, and $k = 4, \ldots, 7$. This gimmick allows us to inspect the behavior of the moments of the Poisson Binomial distribution when the size of the population is $N = \beta_k N_0$. In turn, from equation (4.36) this reflects into the following scaling behavior of the first and second moment of Y_N

$$E[Y_n] = \frac{1}{\beta_k n_0} \sum_{i=1}^{n_0} \beta_k \mathcal{E}(X_i) = \frac{1}{n_0} \sum_{i=1}^{n_0} p_i = E[Y_{n_0}]. \tag{4.37a}$$

$$\mathrm{Var}[Y_n] = \frac{1}{(\beta_k n_0)^2} \sum_{i=1}^{n_0} \beta_k p_i (1 - p_i) = \frac{1}{\beta_k} \mathrm{Var}[Y_{n_0}]. \tag{4.37b}$$

Hence,

- the expected value $\mathcal{E}[Y_N]$ of the fraction of the population that will get a shot of vaccine does not change with the population size;

- the variance $\mathrm{Var}[Y_N]$ decreases linearly with the population size.

Table 4.3 reports the mean and variance of Y_N for different orders of magnitudes for l_k, whereas Figure 4.12 the error bar of the fraction of vaccinated population as a function of the population size N.

l_k	β_k	$\mathcal{E}[Y_N]$	$\mathrm{Var}[Y_N]$
10^4	7	0.6171	1.773e-05
10^5	69	0.6171	1.799e-06
10^6	692	0.6171	1.793e-07
10^7	6916	0.6171	1.794e-08

Table 4.4. First and second moment of Y_N as the population size $N = \beta_k N_0$ varies.

Parametric analysis of ρ

In section 4.2 of the main text, we presented a constrained least square optimization problem aimed to realistically calibrate the model parameters consistently with survey data. In particular, in the main text we explained that constraint (4.33c) sets the average susceptibility to be equal to a value ρ, and that problem (4.33) admits a solution only if $\rho \leq 0.58$. In the main text, all the analysis have been performed for $\rho = 0.58$. Here, we perform a parametric analysis of the results, whereby we vary ρ in the interval $[0.18, 0.48]$ with step 0.1. Figure 4.13 illustrates that the results are qualitatively similar, the only difference being the attenuated effectiveness of all the strategies, since lower values of the λ_i correspond to a more stubborn population.
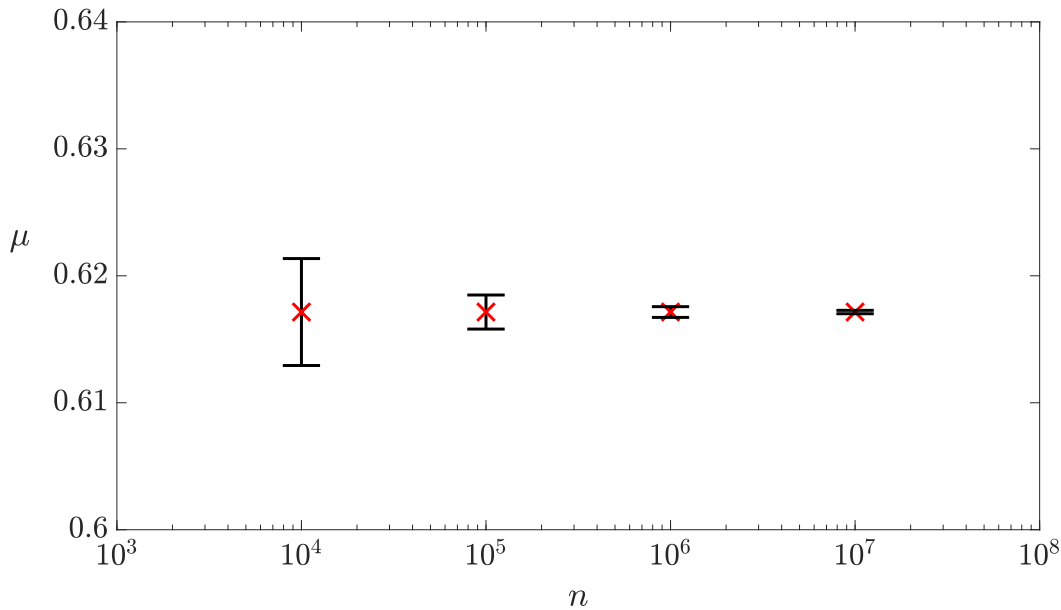
Figure 4.12. Error bar plot of the mean and standard deviation of Y_n.

Robustness analysis

To test the robustness of our results, we have run additional simulations varying the graph through which opinions diffuse. To do so, we repeated the same analysis performed in the main text on a pool of real and synthetic networks, whereby we compared the effectiveness of the targeted campaigns to that of mass campaigns. As shown in Figures 4.14-4.17, the results are consistent with the case illustrated in the main text, that is, the targeted campaigns always outperform the traditional mass-media ones.

The pool of synthetic networks is made of 10 unweighted undirected graphs of size $N = 1500$, extracted from a Scale-Free distribution with exponent $\gamma = 2.8$ and average degree $k_{av} = 80$, consistently with the properties of the real online social networks reported in [2], and repeated the same analysis performed in the main text. The 3 real networks, called soc-fbHamilton46, socfb-Simmons81 and Hamsterster, have been retrieved from the network repository [2].

Consideration on the transient

In this thesis, we have looked only at the steady-state vaccination probabilities to assess the effectiveness of the campaigns. However, capturing the evolution over time of vaccine willingness by means of an opinion dynamics model also allow investigating what happens in the transient dynamics. This can be key especially when news generate shocks in the public opinion bringing it towards another steady state, thus arising the need of readily redesign the awareness campaigns by policymakers. Establishing if the transient dynamics will be affected by an overshoot or an undershoot could be crucial in designing

Figure 4.13. Comparison of targeted and traditional mass campaigns for different values of the average susceptibility ρ (set to $0.18, 0.28, 0.38,$ and 0.48, from top to bottom). The left panels depict, for each effort η, the additional population fraction $\Delta_\mu^\star$ and Δ_μ^0 that is expected to be vaccinated when the best targeted campaign (identified by circles) or the mass campaign (identified by triangles) are employed, respectively. The right panels display for each effort η and targeted strategy s, the ratio between the fractions of the population $\mu_s(\eta)$ and $\mu_0(\eta)$ that are expected to be vaccinated when strategy s and the traditional campaign are employed, respectively. In all panels, Strategies 1, 2, 3 are depicted in blue, green, and magenta, respectively, and the intensity of the vaccination campaign is set to $\alpha = 1$.

the campaign timing, as these phenomena will translate in a boost or a decrease of the campaign effectiveness. Assuming that the discrete-time LTI system described by the FJ model used to capture opinion dynamics is completely controllable/observable, that the control action is additive and constant (e.g., a step), that the output is a linear function of the state as the expected value of the Poisson binomial distribution is the mean of the vaccine willingness there is no instantaneous relation between the inputs and the output, the system's transfer function is strictly proper.

As matrix $C = 1/N \mathbb{1}_N^{\mathrm{T}}$, the relative degree of the transfer function should be 1. We want to show that the output function $y = Cp = p/N \mathbb{1}_N^{\mathrm{T}}$ that represent the fraction of population that we expected to get the vaccination to have a first order-like transient dynamics.

Figure 4.14. Comparison of targeted and traditional mass campaigns effectiveness averaged on a pool of 10 Scale-Free synthetic networks. The left panels depict, for each effort η, the additional population fraction $\Delta_\mu^\star$ and Δ_μ^0 that is expected to be vaccinated when the best targeted campaign (identified by circles) or the mass campaign (identified by triangles) are employed, respectively. The right panels display, for each effort η and targeted strategy s, the ratio between the fractions of the population $\mu_s(\eta)$ and $\mu_0(\eta)$ that are expected to be vaccinated when strategy s and the traditional campaign are employed, respectively. In all panels, Strategies 1, 2, 3 are depicted in blue, green, and magenta, respectively, and the intensity of the vaccination campaign is set to $\alpha = 1$.

In Figure 4.18 we can observe how numerical simulations show that the behavior is compatible with the dynamics of a system with relative degree equals to 1, namely a first order-like transient dynamics, for all media campaigns, no overshoot or undershoot are observed.

Recalling that an overshoot could be generated by multiple poles that depend on the dynamics matrix and thus cannot be imposed or Left Half Plane (LHP) zeros that makes the system response faster and depends also on the structure of matrices B and C, a future work can be related to investigate if it is possible, given the matrices A and C, to choose B in such a way to induce an overshoot, thus to boost the effectiveness of awareness campaigns.

Discussion

In this paper, we proposed a model-based approach rooted in opinion dynamics to analyze the evolution over time of opinions towards vaccines within a population. To endow this model of a quantitative capability, we calibrated it on survey data on vac-
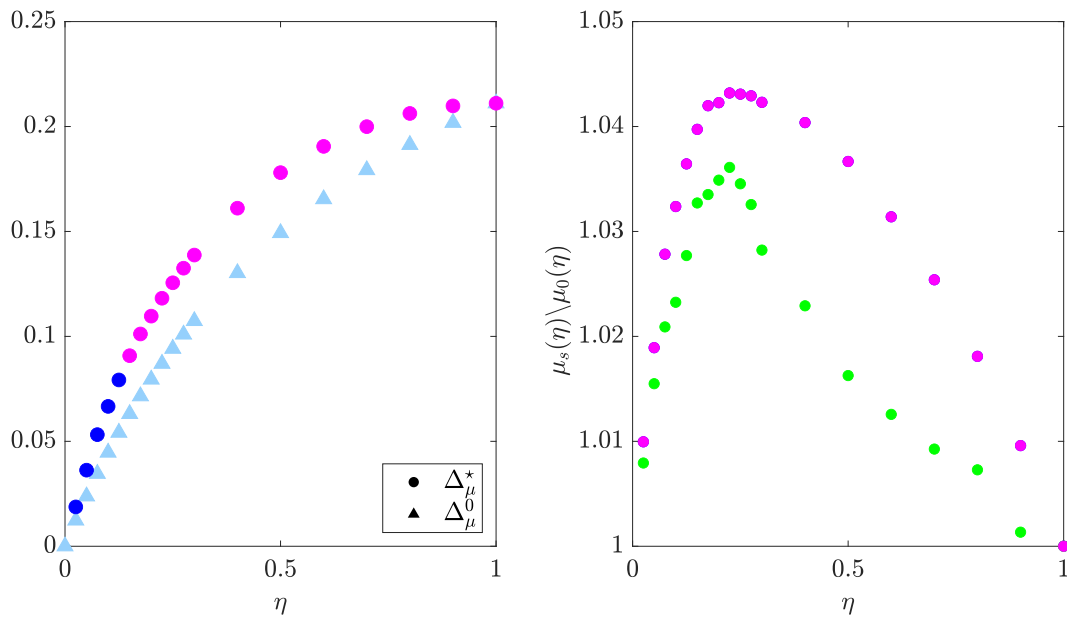
Figure 4.15. Comparison of targeted and traditional mass campaigns. The graph deployed is an unweighted, undirected network of Facebook friendships. The number of nodes $N = 2300$, the number of edges $|\epsilon| = 96400$, the average degree $k_{av} = 83$.
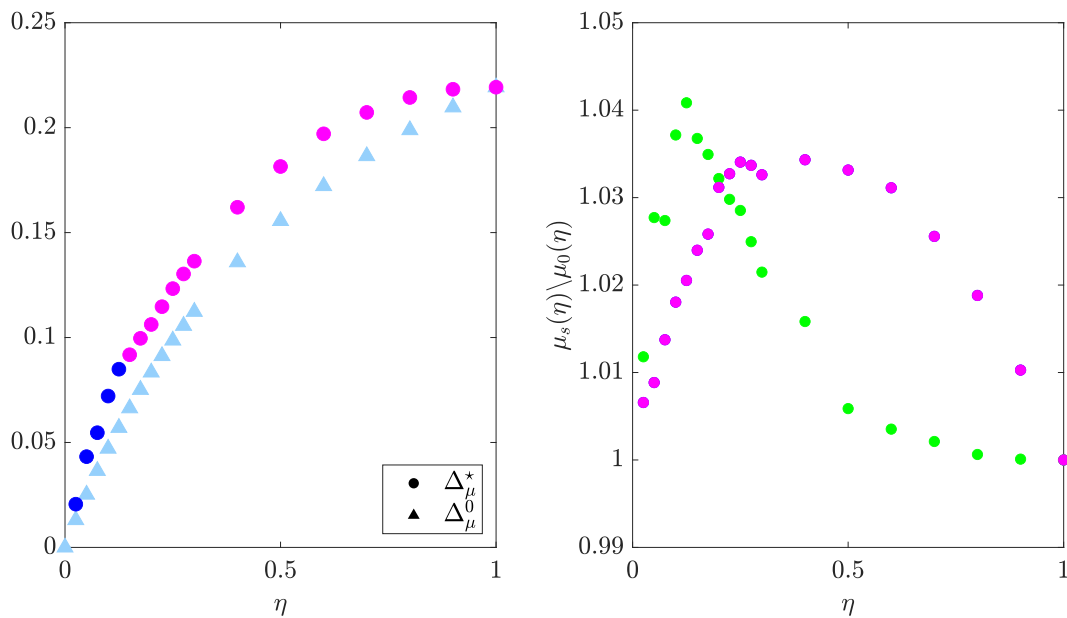
Figure 4.16. Comparison of targeted and traditional mass campaigns. The graph deployed is an unweighted undirected network of the friendships and family links between users of the website `http://www.hamsterster.com.`. The number of nodes $N = 2400$, the number of edges $|\epsilon| = 16600$, the average degree $k_{av} = 13$.
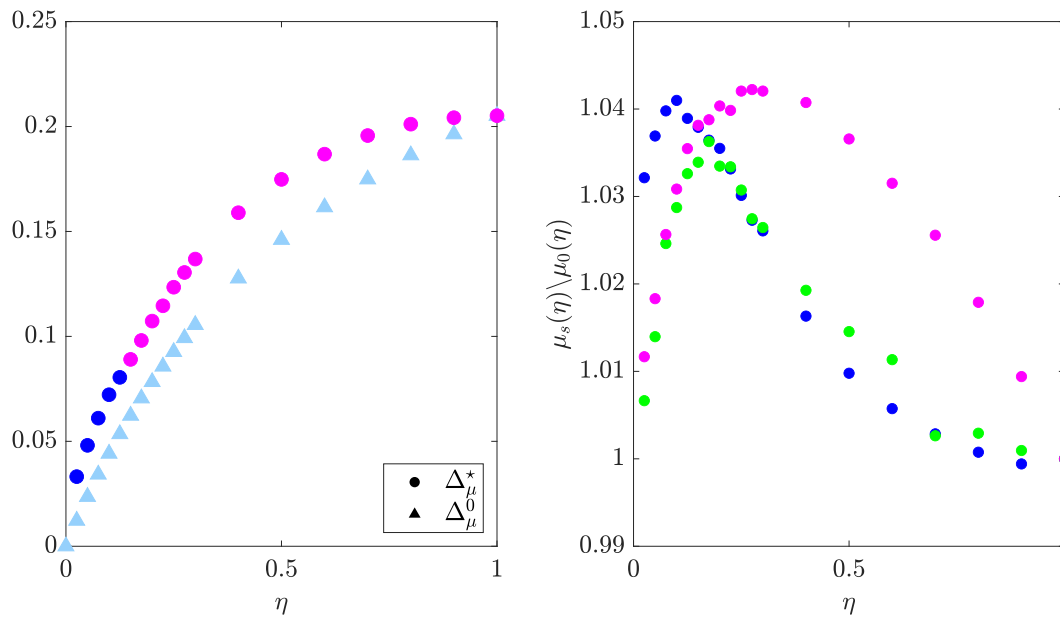
Figure 4.17. Comparison of targeted and traditional mass campaigns. The graph deployed is an unweighted undirected network of Facebook friendships. The number of nodes $N = 1500$, the number of edges $|\epsilon| = 33000$, the average degree $k_{av} = 43$.

cine willingness of a sample of Italian citizens. Having at disposal such a scaled model allow to predict, with a certain level of confidence, how many individuals of a given population will decide to get vaccinated, thus enriching the information on only a sample extracted from a population that originating from surveys on vaccine willingness. Moreover, it allows testing the effectiveness of alternative what-if scenarios simulating different awareness campaigns enacted on social platforms. Prior to their implementation, these campaigns can be designed and tested on a scaled model to maximize their effectiveness.In particular, we exploited the calibrated model to test the effectiveness of three targeted pro-vaccine campaigns against that of a traditional mass media alternative.

Our results indicate that targeted campaigns always outperform mass campaigns in convincing individuals to get vaccinated, yielding the maximum increment in the expected fraction of the population willing to be vaccinated for intermediate values of the overall effort of the campaign. Moreover, they show that media campaigns increase the expected fraction of vaccinated individuals by somewhere in between 10% and 15% with the last percentage points to be gained by designing smart, targeted social media campaigns rather than mass campaigns. This demonstrates how having at disposal a model of opinion dynamics can practical affect the decision-making process of managerial board or government bodies, that can exploit this quantitative tool to smartly invest in targeted campaigns in order to maximize the effectiveness of their (mathematically backed) initiatives.

However, one could argue if a marginal increase of vaccinated individuals can make
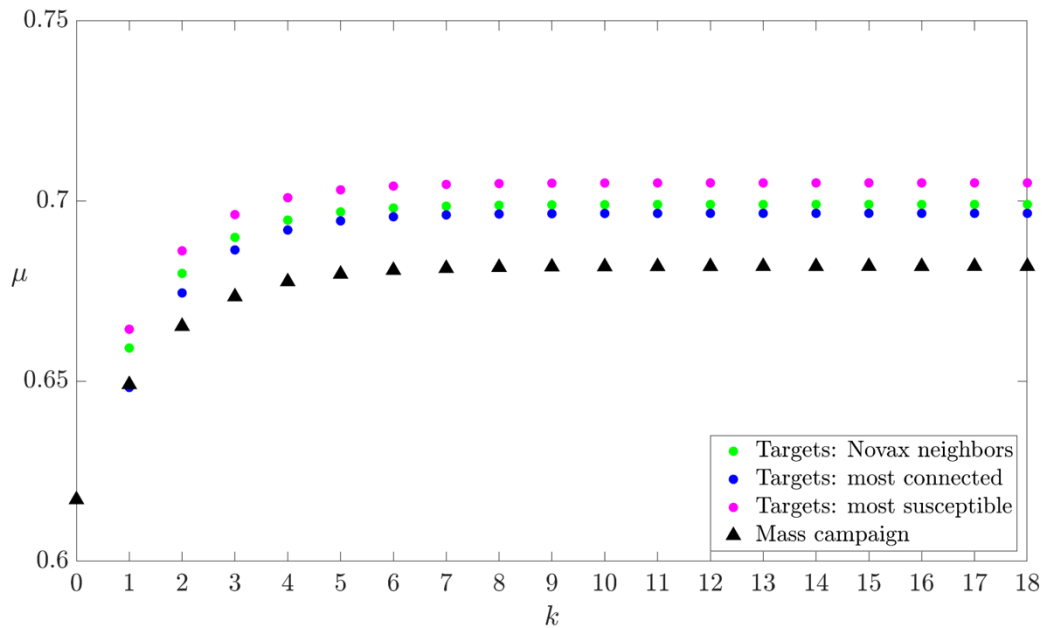
Figure 4.18. Transient dynamics of the fractions of the population $\mu_s(\eta)$ and $\mu_o(\eta)$ that are expected to be vaccinated when strategy s and the traditional campaign are employed, respectively.

a difference. From the perspective of protecting public health, the empirical answer lies in the recent data showing that avoiding saturation of the healthcare system is a matter of slight differences in the number of vaccinated individuals [181]. Modest increases in the effectiveness of a campaign can well be the difference between expecting or not to live with the virus without restrictions.

From a methodological perspective, our work represents a first step toward bridging the abstract literature on opinion dynamics with the key problem of providing easy-to-use quantitative tools to test the effectiveness of awareness campaigns to support the decision-making process. The simplicity of the selected model and of the calibration procedure we propose is one of the strengths of our approach. The reductive choice of characterizing the behavior of each individual through the Friedkin-Johnsen model allows for a first assessment of the effectiveness of pro-vaccine campaigns on the basis of data collected from a single survey. Indeed, the strength of our inherently causal model-based approach lies in the ability of teasing out the relationship between the choice of the targets of the campaign and its effectiveness. This ease of interpretation is a feature we believe should be retained even when more refined data on vaccine hesitancy are considered.

Although the results are promising, our work is not free of limitations. First, in its current incarnation, model calibration is only concerned with steady-state vaccination probabilities. This is certainly sufficient when the campaigns are planned way ahead of the administration of the vaccine. However, in the case of a new epidemic, news from media outlets may perturb the beliefs of the population, see e.g., the scientific and social

debate on the AstraZeneca vaccine [182, 183]. In such cases, the campaign should be immediately redesigned, and tailored on the basis of the response time of the population. Our model has the potential to account for these transient dynamics, provided that several snapshots of the opinions of the same cohort of the population are available. It is worth pointing out that the three strategies we propose require different information levels, thus posing different feasibility issues. Indeed, targeting the most connected agents only requires knowledge of the unweighted topology of the social network. Attempting instead at neutralizing the antivax requires complementing this structural information with that on the agents' vaccine hesitancy, which can be monitored by means of, for example, sentiment analysis on social media [184, 185]. Finally, directly influencing the most susceptible agents constitutes a psychological targeting strategy (see [186] and the references therein for alternative methods to do so) that requires assessing the personality traits of each individual.

Implementing smart, targeted campaigns entails the use of tools from artificial intelligence and data science, with higher investments needed compared to traditional campaigns. It is reasonable to ask whether this additional burden is worth carrying: from an ethical perspective, one could argue that targeting individuals based on information obtained from its online social media might surpass the borders protecting the privacy of the population. Where the optimal trade-off lies between feasibility and ethics is the subject of ongoing worldwide discussions [187].

There are also several directions along which this work can be extended: first, alternative models of opinion dynamics could be considered. In the spectrum of model complexity, we decided to opt for the simplest one, so as to minimize the number of parameters to be tuned. Should one have more data for finer calibrations, alternative, more complex models of opinion dynamics could be considered to account, e.g., for bounded confidence [46], or for the difference between private and publicly expressed opinions [188]. Finally, since it has been observed that social networks may be characterized by the presence of communities of like-minded individuals [189], which are socially well-connected and share many interests, an open research question is to evaluate how these densely connected communities may affect the effectiveness of targeted vaccination campaigns.

4.3   Preliminary results on non-conventional data sources

Conferring a predictive validity to opinion dynamics models requires a thorough collection of real data that could represent the measurements/observations of the actual opinions in the population under study. Different data sources can be deployed for this aim: one of all, traditional surveys, that are specifically designed questionnaires conducted on a representative sample of the population. This tool, while easy to administer and providing statistically accurate outcomes, is not free of limitations. One-time surveys are not suitable to follow trends in real time or over periods of time in the past, making it difficult to track changes in the population's sentiment, unless *longitudinal* surveys are available, that is two or more surveys are iterated over time on the same set of respondents. Such repetition is often expensive and time-consuming, making frequent periodic surveys impractical and rare, except for rare exceptions such [190, 191], thus hindering the modelling of cause and effect phenomena. Furthermore, especially online surveys, suffer from other limitations as they are completed only by persons who are literate and who have access to the internet, and by those who are sufficiently biased to be interested in the subject [192]. More importantly, as respondents are "forced" to answer to specific questions and do not express spontaneously their opinion, boredom and/or insincerity could be a non-negligible factor. Linked to this point, answer options to surveys questions could lead to inaccurate data because certain answer options may be interpreted differently by respondents.

These reasons motivate the usage of other sources of information for capturing opinions: social media. The extreme penetration of social networks in our daily life has drawn the attention of the scientific community in considering posts on Facebook, tweets on Twitter or discussions on blogs such as Reddit as proxies for retrieving information on opinion trends. These data, being shared voluntarily and publicly and being intrinsically available over time, could overcome the aforementioned limitations of surveys. However, exploiting textual data for retrieving information implies data handling procedures capable of converting text into quantitative data.

In the following, we present preliminary results on the extension of the analysis made in [138]. In this work, we retrieve textual data from Twitter to extract an opinion distribution of Italian Twitter users's vaccine willingness in order to i) verify if the opinion distributions of two different sources of information are comparable or not and motivate the outcomes; ii) check if, as stated in the literature, the opinions retrieved from social networks are more polarized; iii) assess the robustness of the aforementioned strategies proposed in [138] starting from different opinion distributions with respect to the one reported in [193].

4.3.1   Data collection

Several public datasets of tweets related to the coronavirus pandemic are available in English, including the ones presented in [194], however almost none is available in Italian.

#novaccino #iovaccino #libertadiscelta #vaccinocovid19
#iiononmivaccino #iomivaccino #novax
#provax #iononsonounacavia #dittaturasanitaria

vaccino covid-19 vaccinazione covid-19
vaccino covid vaccinazione
vaccini

Table 4.5. Keywords and Hashtags used for the queries.

Thus, we took advantage of the fact that Twitter (now X) made available their Application Programming Interface (API) to collect public data from their sites from 2021 to 2022. Indeed, even though Twitter has always provided Twitter REST API to get static data like user profile information, and streaming API2 to get streaming data like tweets, for a short period of time had allowed to access the complete archive of tweets thorough the option *full archive*, which allows to download data in any time window for free. In order to collect a tweets' dataset on COVID-19 vaccination in Italy, we queried Twitter's Streaming API searching for Italian tweets from April 1st 2020 to December 31-th 2020 containing at least one of the keywords reported in . We collected 128434 tweets in Italian language matching the specific set of keywords regarding COVID-19 vaccine, that were posted during April 2020, that is almost at the end of the first lockdown, when the vaccine availability was long to come. In order to build a less possible biased data set, we generated several random subsample of tweets: in particular, we selected 500 tweets from each day of April where more than 1000 tweets were posted, obtaining 7000 tweets; then we sampled 3 random sample of 1446 tweets, to match the size of the network considered in [138]. We preprocessed tweets by removing URLs, lowering, and removing special Twitter specific characters. Emoji has been maintained because most of the advanced tools of Natural Language Processing (NLP) are capable to learn also by them the overall meaning of a textual dataset.

4.3.2   Experimental analysis

Recently, some surveys on Deep Learning methods for Natural Language Processing have been published, see [195–198]. They encompass the most important articles in text analytics of the last years, and all agree on showing that methods based on neural networks and transformers outperform other machine learning methods in text analytics tasks. Furthermore, among the numerous works that focus on sentiment analysis, there are few that attempt to solve very challenging tasks such as multilingual classification or multi-label classification using transfer learning paradigm of BERT-based architecture [199, 200] and zero-shot classification [201–204], but the works that combine more

than two of the above-mentioned tasks together are rare [205]. In particular, our work positions itself in transfer learning framework [206]. The process of transfer learning provides the exploitation of a pre-trained model as a starting point, and a second phase of fine-tuning it on a new task by updating its weights. By leveraging the knowledge gained through transfer learning and fine-tuning, the training process can be improved and made faster compared to starting from scratch. Moreover, our case-study of COVID-19 vaccination, has been commonly used as test bed in the literature, [207–210], as it is well suited for opinion mining provided the social media hype on this relevant societal topic.

Our goal has been to evaluate vaccine willingness of a sample of Italian Twitter users by implementing a fine-grained sentiment analysis on tweets via a deep learning language model called BERT (for more information on NLP techniques, see Appendix B. To do so, we had to face two different challenges: first, we needed a labeled dataset of Italian tweets, second, we wanted to classify the tweets on a 5-point scale (from 1 to 5 corresponding to strongly disagree to strongly agree) regarding Covid-19 vaccine willingness. In the literature, there are some works as [208, 209, 211] that perform a similar task, namely a fine-grained sentiment analysis 5 classes with the help of the SST-5 English dataset, however, being in another language it has not been suitable for our purpose. Previous work that tried to form a baseline dataset of Italian tweets is [212] where BERT is adjusted to perform NPL tasks including sentiment analysis in Italian, however this model is pretrained to give as output a binary sentiment detection, whereas our goal was to capture the intensity of the opinions towards vaccination in a scale from 1 to 5, similarly to the Likert one used in [165].

Hence, we used a sequence of two different BERT versions: one trained on a 5-star product reviews and a BERT version pretrained on plain text, that is able to get contextual meaning of words across different domains, exploiting the potential of transfer and in-context learning typical of transformers architectures [199, 213]. This choice was made following the proposed approach showed in [214], tested on the most famous Italian dataset for sentiment analysis that exists in the literature, the SENTIPOLC 2016. There are two reasons for this choice: first, the pre-trained models are widely available in many languages, avoiding the time-consuming and resource-intensive model training on tweets from scratch that requires manual labelling and thus could inject some bias or subjectivities; second, available plain text corpora are larger than tweet-only ones, allowing for better performance.

We started from the complete dataset retrieved by querying the API according to Table 4.5 made of 128434 tweets, then we balanced it in order to have classes of the same frequency, obtaining a dataset of 38150 tweets (7630 for each class). We deployed a pipeline encompassing two transformer-based models for fine-grained sentiment detection of Italian tweets: in details, we pre-labelled tweets to fine-tune a plain version of BERT. We first assigned a label to each tweet, performing unsupervised classification using a variant of BERT pretrained on more than 500000 product reviews for sentiment analysis in six languages, including Italian. It classifies the sentiment of each review as a number of stars between 1 and 5 with an accuracy of 59% and an accuracy off-by-one of 95%. We checked that the model performs well on the vaccine topic by visual inspection

on simple trial sentences.

We then used this prelabelled tweets to perform the fine-tune phase in a supervised manner of a basic variant of BERT, that comes with 12 layers with hidden size 768 and was trained on multilingual plain text in order to obtain a multi-classifier for our specific task.

Average accuracy	0.90
Average accuracy off-by-one	0.93
Macro F1-Score 0.67	

Table 4.6. Fine-tuning performances.

Table 4.7. Confusion matrix of the fine-tuning phase.

Fine-tuning has been performed with both hold out and k-fold validation, with the latter achieving better performances. We have fine-tuned the model for 3 epochs, using a learning rate of $2e-5$ [207] suitable for text classification on tweets. Performances of the fine-tuning phase are shown in Table 4.7.

4.3.3   Polarization in social networks

Since the Seventies, social experiments [215] on a group of people stated the emergence of polarization in social groups: keeping track of individuals' attitude before and after a discussion over a topic, they have shown that the average post-discussion attitude in a group moved away from the mid-point, becoming more extreme. [216] Group polarization can be defined as the tendency for groups to show more extreme opinions or actions when compared to the ones made by individuals. In particular, in [217], has been stressed the interdependency between choice shift and group polarization: choice shifts occur when, after a social interaction, the average attitude of the group members differs from the

members' average initial attitudes; group polarization instead occurs when the choice shift exaggerates the initial attitudes. One of the reason of this behavior has been exposed by the Social Comparison Theory: at first people enter a discussion sharing moderate opinions with respect to their true ones due to fear of being judged, however, when group discussion reveals that other people have similar but more extreme attitudes, moderate positions are eroded by discussions and extreme positions encouraged as more recognizable [217].

Sociological theory agrees on some factors or cognitive biases that may favor polarization in a social networks: homophily and biased assimilation. Homophily is defined in [63] as the fact that people's personal networks are homogeneous with regard to many sociodemographic, behavioral, and intrapersonal characteristics. Biased assimilation is the tendency to interpret information in a way that supports a desired conclusion. Supporting facts may seem overwhelmingly strong, and negating facts may seem automatically weak. This view of humans as biased information processors has led to the formulation of the echo chamber hypothesis [218]. According to this hypothesis, people's tendency to prefer congenial information and disregard uncongenial information leads to the creation of attitudinally homogeneous networks, also called *echo chambers* where group members mutually validate and perpetuate their worldviews, becoming immune to other viewpoints, that is enforcing their stubbornness and prejudices, leading to polarization.

Hence, to capture these emerging collective behaviors, new models of opinion formation have been proposed in the last 10 years. It has been studied that these cognitive biases, naturally present in interacting humans, have been used in recommendation algorithms in online social media and networks, and they are the main reason why online discussions result in opinions extremism. Ideally, social networks, and the Internet in general, should increase the diversity of information and opinions that individuals are exposed to. Counterintuitively, social networks have also been widely associated to increased polarization in divisive topics in politics, science, and healthcare. Somehow, despite the exposure to a wide variety of opinions and perspectives, individuals form different clusters, unable to reach consensus with one another.

According to [219], social media companies encourages the exposure of content similar to our views to increase engagement and ad revenue. Such recommendations can be direct: friend or follow suggestions on social platforms, or they can be based on historical data of each user to filter and sort their feeds with posts that they are most likely to engage with. By recommending such content, it has been argued that social network companies create "filter bubbles" of similar-minded users. Many attempts have been done to experimental support these reasonable theories [220]. The danger of filter bubbles was recently highlighted by Apple CEO Tim Cook in a commencement speech at Tulane University [220]. Filter bubbles have been blamed for the spread of fake news during the Brexit referendum and the 2016 U.S. presidential election, protests against immigration in Europe, and even measles outbreaks in 2014 and 2015.

Further findings have shown that biased assimilation is not the only cause of polarization: also the exposure to opposing views might lead to polarization, for example in [221] have established a relationship between network heterogeneity and polarization called

backfire effect in which users exposed to radically different views end up being more polarized to their own opinions. In [222] argued that network negativity bias, a negative valence in the tone of discussions, might fuel polarization both in selective exposure and in backfire contexts. Studies on social media language use have reported that negativity outweighs positivity, particularly for controversial topics [223–226]. "Negative language is shared more frequently, and it is used to express feelings towards rival groups, these dynamics are likely to perpetuate more intergroup hostility, which plays a role in affective polarization and sectarianism" [227]. In [228] it has been shown that radical users seeking wider audiences and more followers may have an incentive to ramp up the vitriolic rhetoric, increasing negative attitudes about vaccine and potentially driving a larger gap in favor of vaccine hesitancy, which might further increase polarization.

Summarizing, it emerges that social media enable dysfunctional collective behaviors as homophily and biased assimilation are favored by social media algorithms, as well as negativity bias, fueling polarization as a result of the combination of weak regulation and lack of ethical design. With these additional experiments, we wanted to verify if the phenomenon of polarization also emerges in Italian tweets on vaccine willingness.

4.3.4   Comparison between survey data and Twitter data
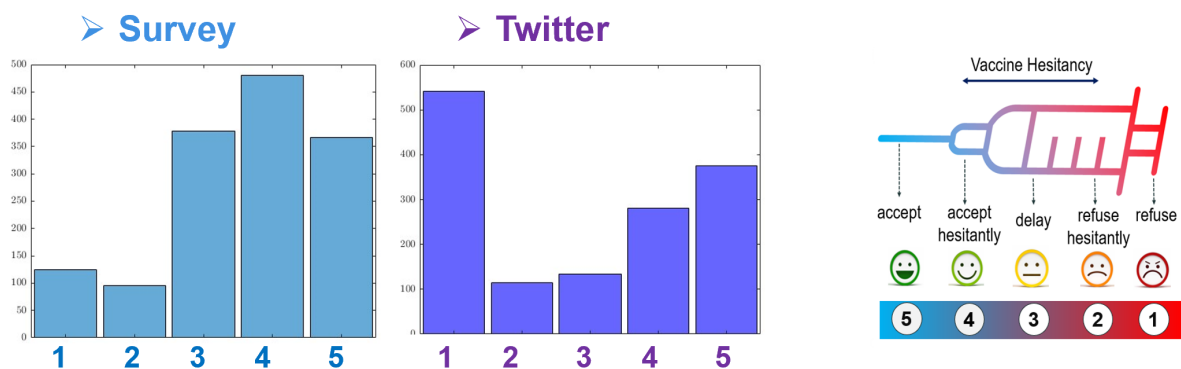
Figure 4.19. Comparison between survey and Twitter data distribution among 5 classes.

Our results in Figure 4.19 show a stance position regarding willingness to take the vaccine among Twitter users' (on the right) that is very different from the one obtained from survey data [193] (on the left), confirming what we expected by the current literature.

Given these findings, we wondered, given this great difference between the distribution of the opinions of online users and those reported by a statistically representative survey, if the control strategies proposed in [138] are still effective and thus robust in the case of polarization of opinions.

4.3.5   Results

We simulated and compared the outcome of the 3 different strategies of implementing awareness campaigns proposed in [138] starting from the opinion distributions compatible with the Twitter data (similarly with what we have done for survey data) for the same parameter selection of [138].

Our simulations show that: *(i)* targeted campaigns outperform a general mass-media campaign.
(ii) the best strategy for targeting individuals depends on the overall effort η of the campaign.
Indeed, for all possible selections of η, it is possible to find a targeted strategy that yields an advantage compared with general mass-media campaigns, with an increase of the expected number of vaccinated individuals that reaches a maximum 5% for $\eta = 0.3$. Interestingly, for low efforts ($\eta < 0.1$), strategy 1 and 3 are capable of increasing the effectiveness of the vaccination campaign, with the merely topological approach of Strategy 1 being the most effective.
In particular, for all $\eta \geq 0.1$, Strategy 3, which relies on the estimation of the individual susceptibility, proves to be the best campaign.
Surprisingly, Strategy 2 for small effort values in $(0.1, 0.3)$ seems to be less advantageous in respect to a traditional mass campaign for all the three choices of susceptibilities of the agents.
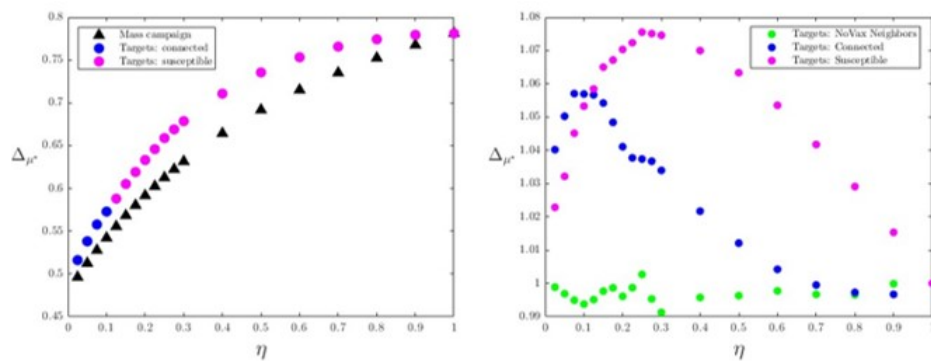
Figure 4.20. Comparison of targeted and traditional mass campaigns.

The left panel depicts, for each effort η, the additional population fraction Δ_μ^* that is expected to be vaccinated when the best targeted campaign (identified by circles) or the mass campaign (identified by triangles) are employed, respectively. The right panel displays, for each effort η and targeted strategy s, the ratio between the fractions of the population $\mu_s(\eta)$ and $\mu_o(\eta)$ that are expected to be vaccinated when strategy s and the traditional campaign are employed, respectively. In both panels, Strategy $1, 2, 3$ are depicted in blue, green, and magenta, respectively, and the intensity of the vaccination campaign is set to $\alpha = 1$.

From the results obtained, the control strategies are robust even in the case in which there are extremely opinionated individuals. In particular, all the pro-vaccine campaigns implemented lead to an increase in the expected fraction of users to be vaccinated, and the most beneficial strategy is the one that targets the most susceptible users.

4.3.6   Conclusions

In this analysis on social media data, we showed that the opinions' distribution that can be retrieved from Twitter data of a random sample of Italian citizen is substantially different from the one obtained by administering a survey to a stratified sample of Italian citizens. Then, as expected, we detected an increment in the opinions belonging to more extreme classes, showing the phenomenon of polarization. Finally, we have shown that although Twitter users have more extreme and convinced views, the strategies we have implemented to enact pro-vaccine campaigns are robust and can influence also these extremist users' decision-making by incentivizing them to get vaccinated.

This is a preliminary step in tuning the parameters of opinion dynamics models by means of non-conventional data gathered automatically and for free from social media. Exploiting massive available social network data could allow acting more readily in planning effective strategies among policymakers.

Conclusion

In this thesis, we showed how complex network dynamical systems can be used to model, analyze, monitor and influence real-world collective behaviors that may emerge in large-scale networks, with a focus on opinion dynamics. Namely, we studied the mechanisms that determine decision-making processes in social groups of interconnected individuals discussing on a given topic. The ultimate goal of this thesis was to provide mathematical tools to make policymakers and relevant stakeholders (such as government bodies or management groups) able to better comprehend social phenomena and their root causes to then devise efficient control strategies that help diffuse social norms or market preferences, depending on the target application.

Toward this overarching goal, we started by performing a comprehensive taxonomy of most of the opinion dynamics models in the literature, providing a critical overview that highlights gaps and limitations, emphasizing those that have been addressed in this thesis, that is, (i) simultaneously modeling the evolution over time of opinions and their associated decisions, (ii) using control theory to gauge the effect of opinion leaders on opinion dynamics in social groups and pinpoint influence mechanisms, and (iii) bridging the gap between opinion dynamics mathematical models and real data of opinion evolution.

To model the role of influencers and policymakers in social groups, we moved in two parallel directions. On one hand, we developed theoretical tools to endow a network of controllability and observability properties that are compatible with the limitations that typically arise in the context of social interactions. Namely, we considered the case where control inputs are constrained, for instance in sign, and only some network nodes can be directly affected by control signals or sensed as is typical in social groups where only the opinion of agents that express their opinions can be monitored. In turn, these limitations hinder our ability to control/observe the whole network, hence the need to study under which (sufficient) conditions and devise algorithms to find the maximal controllable/observable subnetwork.

In paper A, we tackled the problem of select the network nodes where to inject the control inputs to ensure the unilateral controllability of the largest subnetwork of dynamical systems. We considered a realistic scenario in which the set of available control inputs were limited both in number and in sign, hindering our ability of controlling the whole network. Thus, after having defined the properties of controllability and reachability for subsystems and subnetwork, and having highlighted the similarities and the differences, we derived a heuristic strategy to maximize the number of nodes unilaterally controllable given a fixed number of control inputs.

In paper B, we focused to make observable the maximum number of nodes in a

complex network of dynamical system in case the number of sensors was not enough to ensure complete observability of the whole network. We derived an ad hoc solution to this problem, since the duality with controllability could not be leveraged due to the considered constraints. Namely, we devised a heuristic procedure that the specificity of this constrained observability problem to optimize the sensor node selection procedure. Tackling these problems with rigorous fashion to enable us to deploy in a more efficient and effective way the limited resources at disposal to achieve a desired collective behavior.

The rigorous solution of constrained controllability and observability problem can support the design of a campaign in government bodies or companies when policymakers or marketing department must decide whether to invest in some activities or not.

The next step is then to understand how they can smartly optimize their effort to get the most out of their initiatives. Towards this goal, we have studied how the opinion dynamics occur in social groups translate into actions. We considered that the collective behaviors go beyond classical consensus, different from engineered systems, due to cognitive biases, antagonistic ties, extremism, external influences, typical of human nature.Therefore, we revisited the classical models to capture the heterogeneity of opinions, persistent disagreement and polarization that we observe in the real world settings to explore some what-if scenarios, investigate the beneficial or detrimental effects of some external actions carried out by peculiar individuals, resembling opinion leaders or influencers.

In paper C, we incorporated the influence effect of an influencer in a network of interconnected individuals exchanging opinions according to a nonlinear opinion dynamics model that accounts for the fact that, due to intrinsic beliefs and cognitive biases, the influence of the neighbors in the opinion formation of the individual is capped by a certain threshold. We assumed that this peculiar agent, a so-called pinner in control theory, exerted a shaping action on a select subset of individuals, exploiting the network structure to diffuse and thus convince the largest number of individuals to take its same action, strictly correlated to its opinion. Indeed, we complemented this model with an output function that allows to link how opinion translates in decisions. We derived sufficient conditions on the control gains and on the network structure to achieve its goal, namely convincing as many individuals as possible to take the same action of the pinner, resembling the persuading effect that high-profile people has on the majority of the society on divisive topics like political propaganda, costumers preferences and ethical debates.

In paper D, we made a first step towards bridging the models of opinion dynamics and data available of the opinion of social groups. Specifically, we used pinning control to study the problem of vaccine hesitancy, which became a key issue during the controversial debate on COVID-19 pandemic in Italy. Namely, we selected a simplistic model that still enables us to take into account the heterogeneity of opinions and capture the spectrum of opinion regarding the propensity towards vaccines, and we introduced the effect of influencers as pinning control strategies to replicate the effect of awareness campaigns implemented by government bodies during the health emergency. Given this set-up, the main goal has been tuning the parameters of this model of vaccine willingness and decision-making of vaccine acceptance on real data, specifically survey data on

vaccine willingness of a sample of Italian citizens. With a parameter identification in the least square sense, we calibrated the model parameters, in particular the susceptibilities to social pressure, to match the opinion distributions recast from the survey. This analysis shown how smartly selecting a certain set of individuals to be directly targeted in awareness campaign can provide a substantial increment in the vaccination acceptance, resulting in a practical advantage to exploit mathematically backed strategies in decision-making processes.

The analyses presented in this thesis represent a step toward bridging the gap among complex theory, network science and control theory in order to provide a deeper and rigorous understanding of opinion formation and decision-making process in social systems. However, the framework proposed in this thesis is not free of limitations: for instance, the problems of finding the largest controllable or observable subnetworks addressed in Chapter 3 are NP-hard constrained optimization problem cannot be efficiently solved. We have proposed heuristic approaches that could be solved in polynomial time, but without any guarantee on the optimality of the solution. Hence, the suboptimality of the results can be further investigated, and alternative heuristic approaches could be proposed and tested against the ones illustrated in this thesis.

In Chapter 4, we dealt with a specific application, that is, complex networks of social systems, thus the future steps are strictly linked to the intensive use of social media to exchange opinions that is complementing, when not substituting, face-to-face interactions. The use of non-conventional data, e.g., the ones originated by means of sentiment analysis, will enable to consider a larger number of interconnected individuals with respect to traditional surveys which are cost and time-consuming. These data sources will allow accounting for transient dynamics, provided that several snapshots of the opinions' distribution of the same group of users are available, enabling the reconstruction of the salient features of the interaction network. The availability of huge datasets of opinion expression can potentially enable both finer calibrations of simplistic models or, alternatively, the possibility of pinpointing the psychological phenomena that emerges from the analysis of textual data to build more complex but realistic models of opinion dynamics. This is still a challenge in the field of opinion dynamics due to intrinsic noisy process of automated translating words in numerical quantities, but NLP techniques are becoming more and more sophisticated, raising good hopes that soon online posts will be a goldmine for the validation of opinion dynamics models.

Appendices

APPENDIX A
Journal articles

Partial controllability of network dynamical systems with unilateral inputs

Camilla Ancona, Francesco Lo Iudice, Antonio Coppola, Pietro De Lellis and Franco Garofalo

Abstract— **Our ability to control network dynamical systems is often hindered by constraints on the number and nature of the available control actions, which make controlling the whole network unfeasible. In this manuscript, we focus on the case where unilateral inputs are exerted on a subset of the network nodes. Leveraging the observation that, different from the case of subsystems, unilateral node reachability and controllability are equivalent, we provide conditions for a given node subset to be unilaterally controllable. The theoretical findings are then employed to develop a computationally efficient heuristic to select the nodes where the unilateral inputs should be injected.**

I. Introduction

Modeling, analyzing, and controlling network dynamical systems is of interest for applications as diverse as formation control [1], multicellular control in biology [2], [3], power systems [4], and financial market dynamics [5], [6]. In the last decades, control engineers have focused on designing distributed protocols capable of inducing the emergence of collective behaviors, such as e.g. consensus and synchronization [7]–[10]. More recently, the ambition to systematically tackle more general network control problems has brought to specify the classical concept of controllability to the case of network systems [11]. It has been pointed out that, when studying network dynamical systems, (i) controllability should be conferred through an appropriate choice of the nodes where the inputs should be injected, thereby several input selection algorithms have been developed [12], [13], (ii) existing controllability tests may be misleading since, when the number of inputs is much smaller than the number of network nodes, controlling a network can be energetically unfeasible [14]–[16], and (iii) achieving complete network controllability can turn out being unnecessary or unfeasible, and thus one should rather focus on controlling selected subnetworks [17].

When studying controllability, a crucial difference exists between large scale dynamical systems and network systems, whereby subsytem controllability differs from controllability of a node subset for a subtle, yet critical, aspect [18]. Although in general the choice of the reference frame for the state variables of the controllable subsystem is irrelevant, this is not true for node subsets, as we need to preserve the association between nodes and network state variables. This in turn has several relevant consequences, such as the fact that, whereas the controllable subsystem is unique, there can be multiple controllable node subsets.

A further challenge, typically overlooked in the literature on network control, is that in real-world systems the input signals are constrained. A relevant case in applications is when the inputs are constrained to be unilateral, that is, the sign of each signal cannot change over time [19], [20]. Practical examples where such constraints arise include the optimal power flow problem in power grids, where nodes are either loads or generators [21], [22], the inhibition or activation or genes in biological networks [23], control of wire-driven parallel robots [24], [25], or marketing campaigns where comparative advertising is forbidden [26], see [20, Table 1] for further practical instances of unilateral control. The literature on controllability under constrained inputs can be traced back to the Seventies [27], [28], but only recently the problem has been tackled for network dynamical systems. Specifically, Lindmark and Altafini have derived conditions for finding the minimal set of inputs that render the whole network controllable [20].

To the best of our knowledge, none of the existing work tackled the controllability problem of a subset of the network nodes with unilateral inputs, and this is the gap we aim at filling in this manuscript. Different from the case of unconstrained inputs, when the inputs are constrained to be unilateral, the controllability of a network cannot be studied through structural approaches, nor through the controllability gramian. This in turn restricts the theoretical tools available to design optimal input placement strategies, making the unilateral case much more challenging than the unconstrained case. We tackle this problem by first characterizing the convex cone containing the unilaterally controllable states of a linear dynamical system, which we show to differ from the one containing the unilaterally reachable states. Then, by means of a suitable projection, we translate these results for network systems, and obtain the conditions for unilateral reachability and controllability of a node subset that, different from the general case of systems, we observe to be equivalent. The theoretical findings are then used to develop a greedy heuristic to decide where to inject the unilateral inputs, which provides a suboptimal solution to the problem of maximizing the number of controllable nodes.

II. Preliminaries

Given a set $\mathcal{H}$, we denote by $|\mathcal{H}|$ its cardinality, and given a vector space, we denote by 0 its origin. Given a real vector space $\mathbb{R}^n$, we denote by $\mathbb{R}^n_{\geq 0}$ ($\mathbb{R}^n_{\leq 0}$) the set of vectors in $\mathbb{R}^n$ with nonnegative (nonpositive) entries. Let $\mathcal{D}$ be a set of $|\mathcal{D}| = k$ vectors $d_1, \ldots, d_k$ in $\mathbb{R}^n$, $\mathrm{Span}(\mathcal{D})$ is the set of all

linear combinations of the vectors in $\mathcal{D}$. The *positive span* $\mathrm{Span}^+(\mathcal{D})$ of $\mathcal{D}$ is the set of all linear combinations with nonnegative coefficients, that is, $\mathrm{Span}^+(\mathcal{D}) = \{\sum_{i=1}^k \alpha_i d_i : \alpha_i \in \mathbb{R}_{\geq 0}\}$, which constitutes a polyhedral convex cone [29]. If $\mathcal{D}$ is a singleton then $\mathrm{Span}^+(\mathcal{D})$ is called a ray. All the rays and the singleton $\mathcal{O} = \{0\}$ are degenerate cones. Given a convex polyhedral cone $\mathcal{C}$, we define its dimension $|\mathcal{C}|$ as the number of vectors required to generate it. The lineality space of a convex cone $\mathcal{C}$ is defined as the largest subspace $\mathcal{X}^l := \mathcal{C} \cap -\mathcal{C}$ contained in $\mathcal{C}$, whose dimension is the lineality of $\mathcal{C}$ [30].

Next, let us denote by $\mathfrak{e}_i$ the i-th versor in $\mathbb{R}^n$. Given an index set $\mathcal{K}$, we define $\mathcal{X}_\mathcal{K}$ as the subspace linearly spanned by $\cup_{i \in \mathcal{K}} \{\mathfrak{e}_i\}$. Furthermore, given a vector $d \in \mathbb{R}^n$, we denote by $\mathrm{proj}_{\mathcal{X}_\mathcal{K}}(d) = \sum_{i \in \mathcal{K}} (d^\mathrm{T}\mathfrak{e}_i)\mathfrak{e}_i$ the orthogonal projection of d along $\mathcal{X}_\mathcal{K}$. Given a complex vector $c \in \mathbb{C}^n$, we denote by $\Re(c)$ and $\Im(c)$ its real and imaginary parts, respectively. The operators $\vee$ and $\wedge$ denote the logical disjunction and conjunction, respectively, whereas the symbol $\setminus$ denotes a set difference. Finally, the big-O notation $O(\cdot)$ describes the order of magnitude of the algorithm execution time with respect to the number of steps required to complete it.

III. Problem Formulation

Let us consider a linear dynamical network on a graph $\mathcal{G} = \{\mathcal{V}, \mathcal{E}\}$, where $\mathcal{V}$ and $\mathcal{E} \subseteq (\mathcal{V} \times \mathcal{V})$ are the sets of its nodes and edges, respectively. Defining the network state $x = [x_1, \ldots, x_n]^\mathrm{T}$, with $x_i \in \mathbb{R}$ being the state of the i-th node, the network dynamics are given by

$$\dot{x}(t) = Ax(t) + Bu(t), \tag{1}$$

where $A \in \mathbb{R}^{n \times n}$ is the adjacency matrix of $\mathcal{G}$, whose ij-th entry $a_{ij} \neq 0$ if $(i,j) \in \mathcal{E}$ and $a_{ij} = 0$ otherwise. Matrix A encapsulates both the individual dynamics and the interaction between the network nodes, which are encoded by the diagonal and off-diagonal elements of A, respectively. Matrix $B \in \mathbb{R}^{n \times m}$ is the input matrix, whose ij-th element modulates the effect the input u_j has on the dynamics of node i. Here, we consider the case of unilateral inputs.

Definition 1. *The input $u(t)$ to network (1) is called unilateral if $(u(t) \in \mathbb{R}_{\geq 0}^m, \forall t) \vee (u(t) \in \mathbb{R}_{\leq 0}^m, \forall t)$.*

In what follows, without loss of generality, we consider only nonnegative inputs for the sake of clarity, whereby their sign will be determined by the sign of the entries of B. More formally, we make the following assumption.

Assumption 1. *Inputs are nonnegative, that is $u(t) \in \mathbb{R}_{\geq 0}^m$ for all t and each column of matrix B belongs to the set $\mathcal{B} = \{\mathfrak{e}_i, -\mathfrak{e}_i, i = 1, \ldots, n\}$ [20].*

Here, we focus on the case in which unilateral controllability of the whole network is not feasible, whereby the conditions given in [20] do not hold. The problem then arises of selecting the input so that the state of a subset of the network nodes can be steered towards any desired value. Before stating this problem, we need to define unilateral

controllability of a node subset $\mathcal{V}_s$, whose associated state x_s is the vector stacking the states of all nodes in $\mathcal{V}_s$.

Definition 2. *A node subset $\mathcal{V}_s \subseteq \mathcal{V}$ is unilaterally reachable if the state of its nodes x_s can be steered from 0 to any target value in finite time through an appropriate selection of the unilateral input $u(t)$.*

Definition 3. *A node subset $\mathcal{V}_s \subseteq \mathcal{V}$ is unilaterally controllable if, for all initial conditions $x_s(0)$, the state of its nodes can be steered towards any target value in finite time through an appropriate selection of the unilateral input $u(t)$.*

Given the adjacency matrix A, the controllability problem we consider is that of designing the input matrix B fulfilling Assumption 1 that maximizes the cardinality of the set $\mathcal{V}_s = \mathcal{V}_s(B)$ of unilaterally controllable nodes, that is,

$$\max_{B \subset \mathcal{B}} \quad |\mathcal{V}_s| \tag{2a}$$

$$\text{subject to}$$

$$\sum_{i,j} |b_{ij}| = m \tag{2b}$$

$$\mathcal{V}_s \text{ unilaterally controllable} \tag{2c}$$

Solving (2) requires finding the conditions such that, given a set of control inputs, a set of nodes is unilaterally controllable, and then devising an input placement algorithm that finds a unilaterally controllable node subset of maximal dimension.

IV. Unilateral Reachability and Controllability of a Node Subset

Let J be the Jordan normal form of matrix A and μ the number of its blocks. We associate to each Jordan block J_i, whose size we denote by ν_i, the corresponding eigenvalue λ_i, for $i = 1, \ldots, \mu$. Next, let $\mathcal{L} := \{l_{i,k}, i = 1, \ldots, \mu, k = 1, \ldots, \nu_i\}$ be a set of μ chains of unit norm linearly independent (generalized) left eigenvectors of A with the maximal number of elements orthogonal to the columns of matrix B. Finally, let us denote by T the matrix obtained by juxtaposing row-wise the elements of $\mathcal{L}$. We can now define the set $\gamma_{i,k}(l_{i,k}^\mathrm{T}B)$ as

$$\gamma_{i,k} = \begin{cases} \varnothing, & \text{if } l_{i,k'}^\mathrm{T}B = 0 + j0 \; \forall k' \geq k \quad (3a) \\ \{r_{i,k}, -r_{i,k}\}, & \text{if } \exists \, k', k'' \geq k : l_{i,k'}^\mathrm{T}B \in (\mathbb{R}_{\geq 0}^m \setminus \mathcal{O}) \wedge \\ & \quad l_{i,k''}^\mathrm{T}B \in \mathbb{R}_{\leq 0}^m \setminus \mathcal{O}), \Im(l_{i,k}) = 0, \quad (3b) \\ \{r_{i,k}\} & \text{if } \exists \, k' \geq k : l_{i,k'}^\mathrm{T}B \in (\mathbb{R}_{\geq 0}^m \setminus \mathcal{O}) \wedge \\ & \quad \nexists \, k'' \geq k : l_{i,k''}^\mathrm{T}B \in (\mathbb{R}_{\leq 0}^m \setminus \mathcal{O}), \Im(l_{i,k}) = 0, \quad (3c) \\ \{-r_{i,k}\}, & \text{if } \exists \, k' \geq k : l_{i,k'}^\mathrm{T}B \in (\mathbb{R}_{\leq 0}^m \setminus \mathcal{O}) \wedge \\ & \quad \nexists \, k'' \geq k | l_{i,k''}^\mathrm{T}B \in (\mathbb{R}_{\geq 0}^m \setminus \mathcal{O}), \Im(l_{i,k}) = 0, \quad (3d) \\ \{\Re(r_{i,k}), -\Re(r_{i,k}), \Im(r_{i,k}), -\Im(r_{i,k})\}, & \text{otherwise} \quad (3e) \end{cases}$$

for $i = 1, \ldots, \mu$. Additionally, we denote by $\mathcal{C}_r(B)$ the positive span of the set of all $\gamma_{i,k}$-s, that is,

$$\mathcal{C}_r(B) := \mathrm{Span}^+\left(\bigcup_{i=1}^\mu \bigcup_{k=1}^{\nu_i} \{\gamma_{i,k}\} \right) \tag{4}$$

Theorem 1. *If Assumption 1 holds, then*

> *(i) the cone $\mathcal{C}_r(B)$ is the set of unilaterally reachable states of the pair (A, B);*
>
> *(ii) the lineality space $\mathcal{X}^l$ of $\mathcal{C}_r(B)$ is the largest unilaterally reachable subspace of the pair (A, B).*

Proof. *Statement (i)*: Let us consider the transformation $z = Tx$. As $J = TAT^{-1}$, the dynamics of network (1) become $\dot{z}(t) = Jz(t) + TBu(t)$. By setting $z(0) = 0$, we obtain its forced dynamics as $z(t) = \int_0^t \exp(J(t-\tau))TBu(\tau)d\tau$ or, in scalar form,

$$z_{i,k}(t) = \sum_{k' \geq k} \sum_{j=1}^m l_{i,k'}^{\mathrm{T}} b_j \eta_j(u_j) d\tau, \qquad (5)$$

for all $i = 1, \dots, \mu$, $k = 1, \dots, \nu_i$, where

$$\eta_j(u_j) = \int_0^t (t-\tau)^{k'-k} \exp(\lambda_i(t-\tau)) u_j(\tau) d\tau.$$

Since $x = T^{-1}z$, and as the columns of T^{-1} are right generalized eigenvectors of A, $z_{i,k}(t)$ represents the dynamics along the right eigenvector $r_{i,k}$ of each Jordan block J_i, for all $i = 1, \dots, \mu$. Let us now distinguish the case in which $r_{i,k}$ is associated to a real or to a complex eigenvalue

Case (a): $\Im(\lambda_i) = 0$. From Assumption 1 (i.e., nonnegative inputs), we have that $\eta_j(u_j) \geq 0$ for all j. Hence, from (5) we have that

- if $l_{i,k'}^{\mathrm{T}} B = 0 + j0 \; \forall k' \geq k$, then any $\tilde{x} \in \mathrm{Span}(r_{i,k})$ is unreachable;
- if there exist $\exists \; k', k'' \geq k$ such that $l_{i,k'}^{\mathrm{T}} b_j \geq 0, l_{i,k''}^{\mathrm{T}} b_j \leq 0$, any $\tilde{x} \in \mathrm{Span}(r_{i,k})$ is unilaterally reachable;
- if $\exists \; k' \geq k : l_{i,k'}^{\mathrm{T}} \in (\mathbb{R}_{\geq 0}^m \setminus \mathcal{O})$ and $\nexists \; k'' \geq k : l_{i,k''}^{\mathrm{T}} B \in (\mathbb{R}_{\leq 0}^m \setminus \mathcal{O})$, then any $\tilde{x} \in \mathrm{Span}^+(r_{i,k})$ is unilaterally reachable;
- if $\exists \; k' \geq k : l_{i,k'}^{\mathrm{T}} B \in (\mathbb{R}_{\leq 0}^m \setminus \mathcal{O})$ and $\nexists \; k'' \geq k : l_{i,k''}^{\mathrm{T}} B \in (\mathbb{R}_{\geq 0}^m \setminus \mathcal{O})$, then any $\tilde{x} \in \mathrm{Span}^+(\text{-}r_{i,k})$ is unilaterally reachable.

Case (b): $\Im(\lambda_i) \neq 0$. As A is a real matrix, each complex eigenvalue will have a complex conjugate. Therefore, the modal dynamics associated to each of the ν_i pairs of complex conjugate eigenvalues $(\lambda_{i,k}, \lambda_{i,k}^*)$, $k = 1, \dots, \nu_i$ occur along the plane $\widetilde{\mathcal{X}} = \mathrm{Span}(\{\Re(r_{i,k}), \Im(r_{i,k})\})$ of $\mathbb{R}^n$ and, according to Euler's formula, can be expressed as a sum of sinusoidal functions. Hence, all the states belonging to $\widetilde{\mathcal{X}}$ are unilaterally reachable if there exists an index j such that $\mathrm{proj}_{\widetilde{\mathcal{X}}} l_{i,k'}^{\mathrm{T}} b_j \neq 0, \forall k' \geq k$. If, instead, such an index did not exist, then no state would be unilaterally reachable. Finally, considering that (i) if two (or more) states are unilaterally reachable, then any positive combination of the these states is also unilaterally reachable, and (ii) any linear combination involving an unreachable state defines another unreachable state, Statement (i) follows.

Statement (ii). From Statement (i), no state outside $\mathcal{C}_r(B)$ is reachable. Therefore, Statement (ii) follows. $\qquad\square$

Lemma 1. *Let Assumption 2 hold, then the set of controllable states is $\mathcal{C}_c(B) := \mathcal{X}^l(B) \cup \{x \in \mathbb{R}^n : \text{-}\exp(At)x \in \mathcal{C}_r(B)\}$.*

Proof. The thesis follows from the consideration that a point $\bar{x}$ is controllable if and only if $\text{-}\exp(At)\bar{x}$ is reachable. $\quad\square$

A. Node subset unilateral reachability

When studying partial unilateral controllability of network dynamical systems, we need to preserve the association between state variables and network nodes. Therefore, we now provide the following theorems and corollaries characterizing the unilateral reachability and controllability of a node subset.

Theorem 2. *Given network (1) and a node subset $\mathcal{V}_s \subset \mathcal{V}$, if Assumption 1 holds and $\mathrm{proj}_{\mathcal{X}_{\mathcal{V}_s}}(\mathcal{C}_r(B)) = \mathcal{X}_{\mathcal{V}_s}$, then $\mathcal{V}_s$ is unilaterally reachable.*

Proof. From Definition 2, for a node subset $\mathcal{V}_s$ to be reachable, for all $\bar{x}_s \in \mathbb{R}^{|\mathcal{V}_s|}$ and $x(0) : x_s(0) = 0$ there must exists a unilateral input $u(t)$ that steers the network towards a state $\bar{x}$ such that the projection of $\bar{x}$ on the subspace $\mathcal{X}_{\mathcal{V}_s}$ spanned by the versors $\{\mathfrak{e}_i : i \in \mathcal{V}_s\}$, is $\bar{x}_s$. This is equivalent to the existence of a point $\bar{\bar{x}} \in \mathcal{C}_r(B)$ such that

$$\mathrm{proj}_{\mathcal{X}_{\mathcal{V}_s}} \bar{\bar{x}} = \bar{x}_s - \mathrm{proj}_{\mathcal{X}_{\mathcal{V}_s}} \exp(At)x(0). \qquad (6)$$

As from Theorem 1 $\mathcal{C}_r(B)$ is the unilaterally reachable cone, and $\mathrm{proj}_{\mathcal{X}_{\mathcal{V}_s}}(\mathcal{C}_r(B)) = \mathcal{X}_{\mathcal{V}_s}$ by hypothesis, a point $\bar{\bar{x}}$ fulfilling (6) exists for all $\bar{x}_s$ and $x(0) : x_s(0) = 0$, and thus the thesis follows. $\qquad\square$

Interestingly, we note that the number of unilaterally reachable nodes may be larger than the dimension of the largest unilaterally reachable subspace.

B. Node subset unilateral controllability

Theorem 3. *Given network (1), if Assumption 1 holds, then a node subset $\mathcal{V}_s$ is unilaterally reachable if and only if it is unilaterally controllable.*

Proof. Unilateral controllability of a node subset trivially implies its unilateral reachability, see Definitions 2 and 3. Hence, let us focus on proving that unilateral reachability of a node implies its unilateral controllability. From Definition 3, for a node subset $\mathcal{V}_s$ to be unilaterally controllable, for all $\bar{x}_s$ and $x(0)$ there must exists a unilateral input $u(t)$ that steers the network towards a state $\bar{x}$ such that the projection of $\bar{x}$ on the subspace $\mathcal{X}_{\mathcal{V}_s}$ is $\bar{x}_s$. This is equivalent to the existence of a point $\bar{\bar{x}} \in \mathcal{C}_r(B)$ such that

$$\mathrm{proj}_{\mathcal{X}_{\mathcal{V}_s}} \bar{\bar{x}} = \bar{x}_s - \mathrm{proj}_{\mathcal{X}_{\mathcal{V}_s}} \exp(At)x(0). \qquad (7)$$

As from Theorem 2 if $\mathcal{V}_s$ is unilaterally reachable then $\mathrm{proj}_{\mathcal{X}_{\mathcal{V}_s}} \mathcal{C}_r(B) = \mathcal{X}_{V_s}$, by hypothesis a point $\bar{\bar{x}}$ fulfilling (7) exists for all $\bar{x}_s$ and $x(0)$. Hence, $\mathcal{V}_s$ is unilaterally controllable. $\qquad\square$

The equivalence between unilateral reachability and controllability of node subsets allows to derive a set of corollaries that characterize partial unilateral controllability of network systems.

Corollary 1. *Given network* (1) *and a node subset* $\mathcal{V}_s \subseteq \mathcal{V}$, *if Assumption 1 holds and* $\mathrm{proj}_{\mathcal{X}_{\mathcal{V}_s}}(\mathcal{C}_r(B)) = \mathcal{X}_{\mathcal{V}_s}$, *then* $\mathcal{V}_s$ *is unilaterally controllable.*

Proof. Combining Theorems 2 and 3, the thesis follows. □

Corollary 2. *Let* $\mathcal{C}_r(B)$ *be the unilaterally reachable set of the pair* (A, B). *There exists a controllable node subset* $\mathcal{V}_s$ *such that* $|\mathcal{V}_s| \geq |\mathcal{X}^l(B)|$.

Proof. From Theorem 1 we know that if $\mathcal{C}_r(B)$ is the unilaterally reachable set, this implies that $\mathcal{X}^l(B)$ is its lineality space of dimension $|\mathcal{X}^l(B)|$. Moreover, considering that, for a given subspace $\mathcal{X}$ there always exists a set of indices $\mathcal{K}$ and the associated subspace $\bar{\mathcal{X}} = \mathrm{Span}(\cup_{i \in \mathcal{K}} \{\mathfrak{e}_i\})$ such that $\mathrm{proj}_{\bar{\mathcal{X}}} \mathcal{X} = \bar{\mathcal{X}}$, this holds also for $\mathcal{X} = \mathcal{X}^l(B)$. Therefore, from Theorem 2 there exists a unilaterally reachable node subset $\mathcal{V}_s$ of dimension at least equal to $|\mathcal{V}_s| = |\mathcal{X}^l(B)|$ that, from Theorem (3), is also unilaterally controllable. □

The next corollary provides a sufficient condition guaranteeing that there exists a unilaterally controllable node subset $\mathcal{V}_s$ that contains a given node i.

Corollary 3. *Given a node, say* i, *if there exists a quadruplet* $\{h, j, k, m\}$ *such that* $r_{j,k}^{\mathrm{T}} \mathfrak{e}_i > 0$, $r_{m,h}^{\mathrm{T}} \mathfrak{e}_i < 0$, *and* $\{r_{j,k}, r_{m,h}\} \in \mathcal{C}_r(B)$, *then there exists a unilaterally controllable node subset* $\mathcal{V}_s$ *such that* $i \in \mathcal{V}_s$.

Proof. Considering that $\mathrm{proj}_{\mathfrak{e}_i} \mathcal{C}_r(B) = \mathfrak{e}_i$, the thesis follows from Corollary 1. □

Remark 1. *The mathematical treatment of this section substantially differs from the analyses that are performed when seeking complete unilateral controllability [20]. First, when the network is not completely unilaterally controllable, the set of reachable states is a convex cone instead of a vector space. Second, we needed to show and consider that, albeit the set of reachable states differs from that of controllable states (Lemma 1), the reachable and controllable node subsets do coincide (Theorem 3). Finally, we had to account for the fact that the number of unilaterally reachable nodes can be larger than the maximal dimension of a unilaterally reachable subspace, as remarked after Theorem 2.*

V. GREEDY ALGORITHM

In what follows, we shall leverage the theoretical findings of Section IV to design a heuristic for solving problem (2). Before illustrating the derivation of the algorithm, we need to introduce the spanning set $\mathcal{W}(B)$ of the lineality space $\mathcal{X}^l(B) \in \mathcal{C}_r(B)$, which can be computed as

$$\mathcal{W}(B) = \{r_{i,k}, i, k : \{r_{i,k}, -r_{i,k}\} \in \mathcal{C}_r(B) \wedge \Im(r_{i,k}) = 0\}$$
$$\cup \{\{\Re(r_{i,k}), \Im(r_{i,k})\}, i, k : \Im(r_{i,k}) \in \mathcal{C}_r(B)\}, \quad (8)$$

where $i = 1, \ldots, \mu$, $k = 1, \ldots, v_i$. Furthermore, let $\mathcal{S}$ be the set of all subspaces of $\mathbb{R}^n$ such that $\mathrm{proj}_{\mathcal{X}} \mathcal{C}_r(B) = \mathcal{X}, \forall \mathcal{X} \in \mathcal{S}$. From Theorem 1, solving problem (2), that is, finding a maximal unilaterally controllable node subset, is equivalent

to finding the matrix $B^\star$ that maximizes the cardinality of the largest subspace in $\mathcal{S}$. Namely,

$$B^\star := \arg \max_B \left(\max_{\mathcal{X} \in \mathcal{S}} |\mathrm{proj}_{\mathcal{X}} \mathcal{C}_r(B)| \right). \quad (9)$$

Unfortunately, (9) is a combinatorial problem with time computational complexity of order $O(n!)$ that can only be solved through extensive search, which is unfeasible even for a network of a handful of nodes.

Since finding an exact solution of (9) is typically unfeasible, we propose a two-step procedure for the selection of matrix B whose computational complexity is determined by that of finding the Jordan form J, that is, $O(n^4)$. In Step 1, we seek for a heuristic approach that tries to maximize the lineality $|\mathcal{X}^l(B)|$, which from Corollary 2 is a lower bound for the cardinality $|\mathcal{V}_s|$ of the unilaterally controllable node subset $\mathcal{V}_s$. Then, Step 2 attempts to add to $\mathcal{V}_s$ the nodes fulfilling the sufficient condition for node unilateral controllability given in Corollary 3.

Step 1. Heuristic maximizing $|\mathcal{X}^l(B)|$.

Here, we seek for the suboptimal solution

$$\widetilde{B}^\star := \arg \max |\mathcal{X}^l|, \quad \mathcal{X}_l \subseteq \mathcal{C}_r(B) \quad (10)$$

to problem (9). The heuristic we propose (Step 1) takes as inputs the matrix A and the number of available inputs m. Denoting B_k the $\widetilde{B}$ selected at the k-th iteration, the algorithm starts with $B_0 = 0_{n \times m}$. Then, at each iteration, one or two columns are added to $\widetilde{B}$. Defining $\Delta(\beta) := |\mathcal{X}^l([B_{k-1}, \beta])| - |\mathcal{X}^l(B_{k-1})|$, where $\beta \in \mathcal{B}$, we can now distinguish two different cases:

1) If there exists $\beta \in \mathcal{B}$ such that $\Delta(\beta) > 0$, a single column is added at step k, that is, $B_k = [B_{k-1}, \beta^\star]$, where

$$\beta^\star = \begin{cases} \arg \max_{\beta \in \mathcal{B}} |\mathcal{X}^l(B_k)|, \text{if } \exists! \arg \max_{\beta \in \mathcal{B}} |\mathcal{X}^l(B_k)|, & (11a) \\ \arg \max_{\beta \in \mathcal{B}} |\mathcal{C}_r(B_k)|, \text{if } \nexists! \arg \max_{\beta \in \mathcal{B}} |\mathcal{X}^l(B_k)|^1. & (11b) \end{cases}$$

2) If, instead, a $\beta \in \mathcal{B}$ such that $\Delta(\beta) > 0$ does not exist, we add two columns to B_{k-1} at step k, that is, $B_k = [B_{k-1}, \beta^{\star\star}, -\beta^{\star\star}]$, where

$$\beta^{\star\star} = \arg \max_{\beta \in \mathcal{B}} |\mathcal{X}^l([B_{k-1}, \beta, -\beta])|. \quad (12)$$

Summing up, at each step k our updating rule attempts to add the input that maximizes the lineality $|\mathcal{X}^l(B_k)|$. When such an input is not unique, it selects the input that adds the largest number of rays in $\mathcal{C}_r(B_k)$. If instead we cannot find a β such that $\Delta(\beta)$ is positive, then we add the two inputs that maximize $|\mathcal{X}^l(B_k)|$. The algorithm stops when $B_k \in \mathbb{R}^{n \times m}$. Note that this first step has a computational complexity of $O(n^4)$, due to the evaluation of the Jordan form of A.

Once we have computed $\widetilde{B} = B_m$, we need to identify one of the unilaterally controllable node subsets $\mathcal{V}_s^1$ corresponding to $\widetilde{B}$. To this aim, we leverage Corollary 2, which

---

[1]With a slight abuse of notation, here we mean that such a β exists but is not unique.

states that there exists a unilaterally controllable node subset $\mathcal{V}_s^1$ with $|\mathcal{V}_s^1|=|\mathcal{X}^l(\widetilde{B})|$ such that $\mathrm{proj}_{\mathcal{X}_{\mathcal{V}_s^1}}\mathcal{X}^l(\widetilde{B})=\mathcal{X}_{\mathcal{V}_s^1}$. To identify such a node subset, we compute the set $\mathcal{W}(\widetilde{B})$ according to (8). Then, we build the set $\mathcal{V}_s^1$ so that the elements of the sets $\mathcal{V}_s^1$ and $\mathcal{W}(\widetilde{B})$ can be associated into $|\mathcal{V}_s^1|$ pairs (v_j,w_i) such that (i) no pairs share a common element and (ii) each pair (v_j,w_i) is such that $\mathfrak{e}_{v_j}^\mathrm{T}w_i\neq 0$. Finding this association can be recast as the problem of finding the maximum matching [31] of an unbalanced bipartite graph $\mathcal{G}_b=(\mathcal{V}_b,\mathcal{E}_b)$. Here, $\mathcal{V}_b:=\mathcal{V}_w\cup\mathcal{V}_s$ is the set of vertexes and each node in $\mathcal{V}_w$ represents an element of $\mathcal{W}(\widetilde{B})$. The set of edges $\mathcal{E}_b=\{(i,j)|\mathfrak{e}_i^\mathrm{T}w_j\neq 0 \wedge w_j\in\mathcal{W}(\widetilde{B})\}$ defines all the possible associations, by appriopriately connecting the nodes in $\mathcal{V}_w$ to those in $\mathcal{V}_s$. Finding a maximum matching is possible by means of the Hopcroft-Karp algorithm [32] and thus the computational complexity of this sub-step is $O(\sqrt{|\mathcal{V}_b|}|\mathcal{E}_b|)\leq O(n^{5/2})$.

Step 2. Enlarging the unilaterally controllable node subset.

In the second step, we enrich the unilaterally controllable node subset $\mathcal{V}_s^1$ by exploiting the set $\mathcal{C}_r(\widetilde{B})\setminus\mathcal{X}^l(\widetilde{B})$. To do so, let us define the set

$$\mathcal{Q}(\widetilde{B}):=\{r_{i,j},i,j:r_{i,j}\in\mathcal{C}_r(\widetilde{B})\wedge\text{-}r_{i,j}\notin\mathcal{C}_r(\widetilde{B})\}\cup \tag{13}$$
$$\{r_{i,j},i,j:\text{-}r_{i,j}\in\mathcal{C}_r(\widetilde{B})\wedge r_{i,j}\notin\mathcal{C}_r(\widetilde{B})\},$$

whose positive span is $\mathcal{C}_r(\widetilde{B})\setminus\mathcal{X}^l(\widetilde{B})$. Then, let us define the matrix Q as the matrix obtained by juxtaposing the elements of $\mathcal{Q}(\widetilde{B})$ column-wise. Exploiting Corollary 3, we then add a node to $\mathcal{V}_s^1$ whenever the i-th row of Q encompasses two

---

Step 1 Maximizing the lineality $|\mathcal{X}^l(B)|$.

Inputs: A, m
procedure INITIALIZATION($B_0=\varnothing$, $\mathcal{X}^l(B_0)=\mathcal{O}$, $\mathcal{W}(B_0)=\varnothing$)
    while $k\leq m-1$ **do**
        if $\exists\beta\in\mathcal{B}:|\mathcal{X}^l([B_{k-1},\beta])|>|\mathcal{X}^l(B_{k-1})|$ **then**
            compute $\beta^\star$ as in (11a), (11b)
            set $B_k=[B_{k-1},\ \beta^\star]$
            compute $\mathcal{W}(B_k)$
            $k=k+1$
        else
            compute $\beta^{\star\star}$ as in (12)
            set $B_k=[B_{k-1},\ \beta^{\star\star},\ -\beta^{\star\star}]$ and
            compute $\mathcal{W}(B_k)$
            $k=k+2$
        end if
    end while
    if $k=m$ **then**
        compute $\beta^\star$ as in (11a), (11b)
        set $B_k=[B_{k-1},\beta^\star]$
        compute $\mathcal{W}(B_k)$
    end if
end procedure
Outputs: $\widetilde{B}=B_m$, $\mathcal{W}(\widetilde{B})$

---

nonzero entries, say q_{ij} and q_{im}, that are such that $\mathrm{sgn}(q_{ij})=-\mathrm{sgn}(q_{im})$. Let us note that the computational complexity of this step of the algorithm is $O(n^3)$.

Step 2 Enlarging the unilaterally controllable node subset associated to $\widetilde{B}$

Inputs: $Q,\mathcal{V}_s^1$
for i = 1, …, n **do**
    if $\exists\ l,m:\mathrm{sgn}(q_{i,m})=-\mathrm{sgn}(q_{i,l})$ **then**
        Set $\mathcal{V}_s^1=\mathcal{V}_s^1\cup\{i\}$
        Remove the l-th and m-th columns from Q
    end if
end for
Output: $\mathcal{V}_s=\mathcal{V}_s^1$.

Application on a sample network

To illustrate our heuristic, we consider a linear network dynamical system on the graph $\mathcal{G}$ depicted in Fig. 1, whose dynamics is described by matrix

$$A=\begin{bmatrix} 1 & -4 & 0 & 0 & 0 & 0 & 0 \\ 4 & 1 & 0 & 0 & 0 & 0 & 0 \\ 1 & 0 & 3 & 0 & -1 & 0 & -1 \\ 0 & 0 & 1 & 4 & 1 & 0 & 4 \\ 0 & 0 & 0 & 0 & 2 & -3 & 0 \\ 0 & 0 & 0 & 0 & 3 & 2 & 0 \\ 0 & 0 & 0 & 0 & -3 & 0 & 0 \end{bmatrix},$$

with spectrum $\{4,3,0,1+4i,1-4i,2+3i,2-3i\}$. Let us assume that we can inject $m=2$ unilateral controls. The input matrix $\widetilde{B}$ is designed following Step 1, that is, by maximizing the lineality $|\mathcal{X}^l(\widetilde{B})|$. At time instant $k=1$, four possible selections of β ($\mathfrak{e}_2$, $\mathfrak{e}_6$, $-\mathfrak{e}_2$ and $-\mathfrak{e}_6$) yield the same (positive) $\Delta(\beta)$. Hence, $\beta^\star$ should be selected among these four according to (11b). However, since all choices would yield the same $|\mathcal{C}(B_1)|$, the selection is performed randomly, and we elect $B_1=-\mathfrak{e}_6$, with the set $\mathcal{W}(B_1)$ being $[r_6,r_7]$. At $k=2$, $-\mathfrak{e}_2$ is the unique β returning $\Delta(\beta)>0$. Hence, we select node 2 as the second and last node where a control signal is injected, i.e., we set $\widetilde{B}=B_2=[-\mathfrak{e}_6;-\mathfrak{e}_2]$ and $\mathcal{W}(\widetilde{B})=[r_1,r_4,r_5,r_6,r_7]$.

Having selected the matrix B, we now turn to finding one of the possibly multiple unilaterally controllable node subsets $\mathcal{V}_s^1$ such that $|\mathcal{V}_s^1|=|\mathcal{X}^l(\widetilde{B})|$ by solving the maximum matching problem. Among the multiple equivalent solutions to this problem, we randomly pick $\mathcal{V}_s^1=\{v_1,v_2,v_4,v_5,v_6\}$. Finally, we compute, from (13), $\mathcal{Q}(\widetilde{B})=\{-r_2,r_3\}$, and from Step 2 of the proposed heuristic we can enlarge the unilaterally controllable node subset with node 3, that is $\mathcal{V}_s=\{v_1,v_2,v_3,v_4,v_5,v_6\}$. Interestingly, in this simple example, we find that $|\mathcal{V}_s|>|\mathcal{X}^l|$, that is, the number of unilaterally controllable nodes is greater than the largest unilaterally controllable subspace.

VI. CONCLUSIONS

In this letter, we have studied controllability of linear network dynamical systems when the inputs are unilateral.
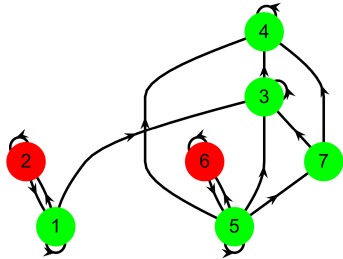
Fig. 1. Network topology: the nodes in red are the driver nodes where, according to the proposed heuristic, the negative unilateral control inputs are injected.

Specifically, we focused on the case where the constraint on the number and type of inputs prevents the achievement of complete controllability of the network system, whereby only a node subset can be made controllable. In this setting, we have identified conditions for unilateral reachability and controllability of a node set, which we found to be equivalent, different from the general case of subsystems, where we have proved that reachability does not imply controllability. After showing that maximizing the size of a controllable nodes subset is a combinatorial problem, we have leveraged the theoretical findings on unilateral controllability to build an heuristic that can find a suboptimal solution to this problem in polynomial time, as illustrated on a sample network.

Our work has laid the foundations of partial controllability under unilateral inputs, thus paving the ways for future studies in this area of research. First, alternative heuristic approaches may be developed and tested against the one proposed in this manuscript. Moreover, once partial controllability has been guaranteed, the problem of evaluating the energy associated to the control action arises, thereby minimum energy control problems could be formulated in this setting.

REFERENCES

[1] P. DeLellis, F. Garofalo, F. Lo Iudice, and G. Mancini, "Decentralised coordination of a multi-agent system based on intermittent data," *International Journal of Control*, vol. 88, no. 8, pp. 1523–1532, 2015.

[2] D. Fiore, D. Salzano, E. Cristòbal-Cóppulo, J. M. Olm, and M. di Bernardo, "Multicellular feedback control of a genetic toggle-switch in microbial consortia," *IEEE Control Systems Letters*, vol. 5, no. 1, pp. 151–156, 2020.

[3] P. A. Iglesias and B. P. Ingalls, *Control theory and systems biology.* MIT press, 2010.

[4] M. Hommelberg, C. Warmer, I. Kamphuis, J. Kok, and G. Schaeffer, "Distributed control concepts using multi-agent technology and automatic markets: An indispensable feature of smart power grids," in *2007 IEEE Power Engineering Society General Meeting.* IEEE, 2007, pp. 1–7.

[5] G. Caldarelli, S. Battiston, D. Garlaschelli, and M. Catanzaro, "Emergence of complexity in financial networks," in *Complex Networks.* Springer, 2004, pp. 399–423.

[6] P. De Lellis, A. Di Meglio, and F. Lo Iudice, "Overconfident agents and evolving financial networks," *Nonlinear Dynamics*, vol. 92, no. 1, pp. 33–40, 2018.

[7] W. Yu, G. Chen, and M. Cao, "Some necessary and sufficient conditions for second-order consensus in multi-agent dynamical systems," *Automatica*, vol. 46, no. 6, pp. 1089–1095, 2010.

[8] C. W. Wu and L. O. Chua, "Synchronization in an array of linearly coupled dynamical systems," *IEEE Transactions on Circuits and Systems I: Fundamental Theory and Applications*, vol. 42, no. 8, pp. 430–447, 1995.

[9] Q. Song, J. Cao, and W. Yu, "Second-order leader-following consensus of nonlinear multi-agent systems via pinning control," *Systems & Control Letters*, vol. 59, no. 9, pp. 553–562, 2010.

[10] Z. Li, Z. Duan, G. Chen, and L. Huang, "Consensus of multiagent systems and synchronization of complex networks: A unified viewpoint," *IEEE Transactions on Circuits and Systems I: Regular Papers*, vol. 57, no. 1, pp. 213–224, 2009.

[11] Y.-Y. Liu, J.-J. Slotine, and A.-L. Barabási, "Controllability of complex networks," *Nature*, vol. 473, no. 7346, pp. 167–173, 2011.

[12] J. Gao, Y.-Y. Liu, R. M. D'souza, and A.-L. Barabási, "Target control of complex networks," *Nature Communications*, vol. 5, no. 1, pp. 1–8, 2014.

[13] L.-Z. Wang, Y.-Z. Chen, W.-X. Wang, and Y.-C. Lai, "Physical controllability of complex networks," *Scientific Reports*, vol. 7, no. 1, pp. 1–14, 2017.

[14] F. Pasqualetti, S. Zampieri, and F. Bullo, "Controllability metrics, limitations and algorithms for complex networks," *IEEE Transactions on Control of Network Systems*, vol. 1, no. 1, pp. 40–52, 2014.

[15] G. Lindmark and C. Altafini, "Minimum energy control for complex networks," *Scientific Reports*, vol. 8, no. 1, pp. 1–14, 2018.

[16] P. De Lellis, A. Di Meglio, F. Garofalo, and F. Lo Iudice, "The inherent uncertainty of temporal networks is a true challenge for control," *Scientific Reports*, vol. 11, no. 1, pp. 1–7, 2021.

[17] P. DeLellis, F. Garofalo, and F. Lo Iudice, "The partial pinning control strategy for large complex networks," *Automatica*, vol. 89, pp. 111–116, 2018.

[18] F. Lo Iudice, F. Sorrentino, and F. Garofalo, "On node controllability and observability in complex dynamical networks," *IEEE Control Systems Letters*, vol. 3.4, pp. 847–852, 2019.

[19] B. Goodwine and J. Burdick, "Controllability with unilateral control inputs," in *Proceedings of 35th IEEE Conference on Decision and Control*, vol. 3, 1996, pp. 3394–3399.

[20] G. Lindmark and C. Altafini, "Controllability of complex networks with unilateral inputs," *Scientific Reports*, vol. 7.1, pp. 1–14, 2017.

[21] S. Frank, I. Steponavice, and S. Rebennack, "Optimal power flow: a bibliographic survey I," *Energy Systems*, vol. 3, no. 3, pp. 221–258, 2012.

[22] ——, "Optimal power flow: a bibliographic survey II," *Energy systems*, vol. 3, no. 3, pp. 259–289, 2012.

[23] D. McDonald, L. Waterbury, R. Knight, and M. Betterton, "Activating and inhibiting connections in biological network dynamics," *Biology Direct*, vol. 3, no. 1, pp. 1–14, 2008.

[24] J.-P. Merlet, "Wire-driven parallel robot: open issues," in *Romansy 19–Robot Design, Dynamics and Control.* Springer, 2013, pp. 3–10.

[25] A. Alamdari, R. Haghighi, and V. Krovi, "Stiffness modulation in an elastic articulated-cable leg-orthosis emulator: Theory and experiment," *IEEE Transactions on Robotics*, vol. 34, no. 5, pp. 1266–1279, 2018.

[26] P. Miskolczi-Bodnár *et al.*, "Definition of comparative advertising," *European Integration Studies*, vol. 3, no. 1, pp. 25–44, 2004.

[27] S. H. Saperstone and J. A. Yorke, "Controllability of linear oscillatory systems using positive controls," *SIAM Journal on Control*, vol. 9, no. 2, pp. 253–262, 1971.

[28] R. F. Brammer, "Controllability in linear autonomous systems with positive controllers," *SIAM Journal on Control*, vol. 10.2, pp. 339–353, 1972.

[29] A. Schrijver, *Theory of linear and integer programming*. John Wiley & Sons, 1998.

[30] L. Sandgren, "On convex cones," *Mathematica Scandinavica*, vol. 2, no. 1, pp. 19–28, 1954.

[31] J. Edmonds, "Maximum matching and a polyhedron with 0, 1-vertices," *Journal of research of the National Bureau of Standards B*, vol. 69, no. 125-130, pp. 55–56, 1965.

[32] J. E. Hopcroft and R. M. Karp, "An n^5/2 algorithm for maximum matchings in bipartite graphs," *SIAM Journal on computing*, vol. 2, no. 4, pp. 225–231, 1973.

Influencing Opinions in a Nonlinear Pinning Control Model

Camilla Ancona, Pietro De Lellis, and Francesco Lo Iudice, *Member, IEEE*

Abstract—This letter studies how opinions and subsequent actions of groups of individuals are shaped by opinion leaders, nowadays denoted influencers. We model an influencer as a pinner that exerts a control input on a small subset of individuals, and leverages the interaction network to affect the action of a large fraction of individuals. We provide sufficient conditions so that a given agent takes the same action as the pinner. Based on these conditions, we design a heuristic for the pinned node selection that maximizes the number of nodes taking the action elected by the pinner. The performance of the heuristic is then numerically tested against standard pinning strategies.

Index Terms—Control of networks, network analysis and control, control applications.

I. Introduction

FROM understanding how to protect democracy against foreign cyber interference [1] to the design of awareness campaigns enhancing health literacy and trust in vaccinations [2], several pressing societal challenges require a deeper understanding of how opinions can be shaped and manipulated. While opinion dynamics models have shed light on some essential mechanisms for the emergence of consensus, the role of external influences on the opinion shaping process has only been partially unravelled [3], [4].

Control theory has recently attempted to contribute in this area, as the actions of an external entity in a social group can be viewed as a control signal acting on select nodes of the network that describes the interactions within the group [5], [6], [7]. A glaring analogy has been established with pinning control [8], [9], whereby an opinion leader (or *influencer*) is

identified as the pinner and affects the state (opinion) of the other nodes without being affected by them [10], [11], [12].

The analogy between the action of a pinner in a network system and that of an influencer has been explored in classic opinion dynamics models, based on averaging updating rules that imply that the more divergent two agents' opinions are, the more they tend to get closer [13], [14], [15]. To overcome this paradox, a discontinuous model, called bounded confidence, considered that interactions only take place when the opinion difference between neighboring nodes is below a given threshold [16], [17]. An alternative model has been recently presented in [18], [19], where the influence an agent has on the opinion of the others is capped by a saturation.

Here, we introduce the pinning control formalism in the modeling framework proposed in [18], [19] to describe a two-options problem. We complement the model with an output function describing the action (choice between the alternative options) associated to the opinion, as typically done in continuous opinion and discrete actions (CODA) models [20]. Then, we add a virtual node, the pinner, which corresponds to (one or more) influencers trying to steer the action of the group towards one of the two options. The pinner will have to decide the pinned nodes, that is, the nodes it will directly attempt to influence. The rest of the network will be instead indirectly affected by the pinner through the interaction topology.

Decomposing the network in layers, we are able to provide sufficient conditions on the interaction topology, the set of pinned nodes, and the pinning control gain guaranteeing that a given subset of agents in the network will take the same action as the pinner. On the basis of our theoretical findings, we design a heuristic control strategy that aims to select the set of pinned nodes maximizing the number of nodes that will agree with the pinner on the action to take. We observe that the proposed heuristic outperforms classic pinning strategies based on centrality metrics [21], [22].

Graph notation: A weighted directed graph is the triplet $\mathcal{G} = \{\mathcal{V}, \mathcal{E}, \mathcal{W}\}$, where $\mathcal{V}$ is the set of nodes, $\mathcal{E} \subseteq \mathcal{V} \times \mathcal{V}$ is the set of edges, and $\mathcal{W}$ is the set weight function that associates to every edge $(i, j) \in \mathcal{E}$ a positive weight w_{ji}. Following the notation used, e.g., in [23], the ij-th element of the adjacency matrix A associated to $\mathcal{G}$ is defined as $a_{ij} = w_{ij}$, if $(j, i) \in \mathcal{E}$, whereas it is zero otherwise. Given a node i, its weighted in-degree is the sum of the weights of its incoming edges, that is, $\delta_i^{\text{in}} = \sum_{j:(j,i) \in \mathcal{E}} a_{ij} = \sum_{j=1}^{N} = a_{ij}$. An illustration of the notation used in this letter is given in Figure 1.
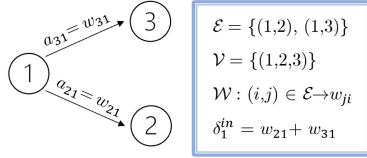
Fig. 1. Illustration of the graph notation used in the manuscript on a sample 3-node graph $\mathcal{G}$.

II. THE OPINION DYNAMICS MODEL

A. Uncontrolled Dynamics and Parameter Setting

We consider an ensemble of N interconnected agents discussing a topic and assume that the opinion diffusion process occurs on a weighted directed graph $\mathcal{G} = \{\mathcal{V}, \mathcal{E}, \mathcal{W}\}$, where nodes in $\mathcal{V}$ represent the N individuals, an edge $(i, j) \in \mathcal{E}$ implies that node i influences node j, whereas the function $\mathcal{W}$ associates to each edge a positive scalar modulating the strength of the interaction. Based on their opinion on the topic under discussion, each agent has to take a decision between two alternative actions $\mathcal{A}_{-1}$ and $\mathcal{A}_{+1}$.

Following [24], we identify the evolution over time of the opinion of agent i as its scalar state $x_i(t)$, and model the corresponding action $y_i(t)$ that agent i would take given its opinion at time t as a discrete variable. In the absence of external influences, our model is described by

$$\dot{x}_i(t) = -dx_i(t) + c \tanh\left(\alpha x_i(t) + \sum_{k=1}^{N} a_{ik} x_k(t)\right), \quad (1a)$$

$$y_i(t) = \text{sgn}(x_i(t)), \quad (1b)$$

where a_{ij} is the ij-th entry of the adjacency matrix A associated to $\mathcal{G}$ ($a_{ij} \neq 0$ if j influences i), $d > 0$ captures the resistance each agent has to changing opinion, the attention parameter $c \geq 0$ weighs the opinion exchange term, and $\alpha > 0$ modulates how much agent i reinforces its own opinion;

$y_i(t) = -1$ ($y_i(t) = 1$) corresponds to agent i preferring $\mathcal{A}_{-1}$($\mathcal{A}_{+1}$) at time t, whereas $y_i(t) = 0$ corresponds to agent i being undecided. We say that agent i has a stronger opinion than j at time t if $|x_i(t)| > |x_j(t)|$. Note that the strength of an opinion is measured by its distance from the undecided state 0, and thus it is possible to compare strengths of opinions corresponding to discordant actions.

In this letter, we set the parameters c, d, and α in (1) so that $c > d/\alpha$. This ensures that the single-agent dynamics in the absence of interactions (i.e., when $a_{ik} = 0$ for all k), has an unstable fixed point at 0 and two stable fixed points in $\bar{x}$ and $-\bar{x}$, which are the two solutions of the implicit equation

$$\frac{x}{\tanh(\alpha x)} = \frac{c}{d}, \quad (2)$$

and, for any finite α, have magnitude smaller than c/d [18]. Note that the agent opinion may change also in the absence of interactions, whereby model (1) mimics the opinion formation process, where an agent may modulate the strength of its opinion based on collected information or critical thinking [24]. A reinforcement effect is observed when, as in our study, c is selected to be larger than d/α: the left panel of Figure 2 shows
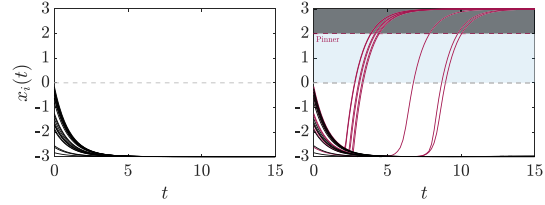
Fig. 2. The left panel displays the opinion dynamics of $N = 30$ agents coupled on an Erdös-Rényi graph with probability $p = 0.6$, and evolving according to (1) with $c = 3$, $d = \alpha = 1$, and initial conditions uniformly randomly selected in $[-3, 0]$. The right panel depicts the dynamics of the same network in the presence of a pinner (in dashed red) that is connected to 3 agents according to (3) and steers the other agents towards a positive opinion. When the agents enter the blue shaded area, they will always take the same action as the pinner, thus belonging to the set $\mathcal{Q}$ defined in (4). Also, their opinion will become stronger than that of the pinner: as they enter the gray shaded area, that they also belong to the set $\mathcal{Q}_{\text{str}}$ defined in (6). In both panels, black and red lines identify the opinion dynamics of agents opting for $\mathcal{A}_{-1}$ and $\mathcal{A}_{+1}$ at the end of the simulation, respectively.

that, when the agents at time 0 would all take the same action $\mathcal{A}_{-1}$ (that is, $x_i(0) < 0$ for all i), they would asymptotically take the same action, but with a stronger opinion.

B. Pinning Control to Influence Opinions

Different from [24], here we consider the case where (one or more) influencers, labeled with the greek letter ι, try to steer the decision towards one of the two options. To capture this scenario, we model the effect of the influencers through a virtual node ι with no incoming edges that, in agreement with the literature on consensus and synchronization in network systems, is called pinner and is unidirectionally coupled to a subset $\mathcal{D}_1 \subseteq \mathcal{V}$ of so-called *pinned nodes* [8], [9], [10], [25], [26], [27]. We assume that its opinion, independent of that of the other agents, is already formed (or formed on a much shorter timescale), so that $x_\iota(t) = \bar{x}_\iota$ for all t, with $\bar{x}_\iota$ corresponding to one of the two equilibria $\pm\bar{x}$ of the decoupled single-agent dynamics. The action associated to the constant opinion of the pinner is $\bar{y}_\iota(t) = \text{sgn}(\bar{x}_\iota)$ for all t.

The pinner influences the decision process of the other agents by directly affecting the opinions of the pinned nodes, and exploiting the network structure to diffuse its effect on the rest of the network. The presence of the control action from the pinner to the pinned nodes modifies model (1) as

$$\dot{x}_i(t) = -dx_i(t) + c \tanh\left(\alpha x_i(t) + \sum_{k=1}^{N} a_{ik} x_k(t) + h_i \kappa_\iota \bar{x}_\iota\right),$$

$$y_i(t) = \text{sgn}(x_i(t)), \quad (3)$$

for $i = 1, \ldots, N$, where the control gain $\kappa_\iota > 0$ modulates the influence that the pinner has on the dynamics of the pinned nodes; and, $\forall i = 1, \ldots, N$, $h_i = 1$ if i is pinned, i.e., $i \in \mathcal{D}_1$, whereas $h_i = 0$ otherwise. The right panel of Figure 2 shows the effects of a pinner on a group of interconnected agent that at time 0 would take the opposite action of the pinner, with the pinner able to convince a fraction of them to change their opinion and subsequent action.

C. Control Objectives

The aim of the control input $h_i \kappa_\iota \bar{x}_\iota$ in (3) is to select the set of pinned nodes $\mathcal{D}_1$ that maximizes the number of individuals that, after a sufficient amount of time, will take the same action as the pinner. To formally define this control design problem, we introduce the set

$$\mathcal{Q} = \{i \in \mathcal{V} : \text{there exists } \bar{t} \text{ such that}$$
$$y(t) = \bar{y}_\iota \text{ for all } t > \bar{t}\}, \qquad (4)$$

whose composition will depend on the choice of κ_ι and $\mathcal{D}_1$. For any κ_ι, we can state the following optimization problem:

$$\max_{\mathcal{D}_1} |\mathcal{Q}(\kappa_\iota, \mathcal{D}_1)| \qquad (5a)$$
$$\text{subject to}$$
$$|\mathcal{D}_1| = M, \qquad (5b)$$

with $M < N$ as the number of nodes that are directly controlled may be limited by physical or economic constraints.

Depending on the context, one may be interested not only in convincing agents to take the same action as the pinner, but also to make their opinion at least as strong as that of the pinner. In such case, we can define the set $\mathcal{Q}_{\text{str}} \subseteq \mathcal{Q}$ as

$$\mathcal{Q}_{\text{str}} = \{i \in \mathcal{V} : \text{there exists } \bar{t} \text{ such that}$$
$$y(t) = \bar{y}_\iota \text{ and } |x(t)| \geq |x_\iota| \text{ for all } t > \bar{t}\}, \quad (6)$$

and state the following problem:

$$\max_{\mathcal{D}_1} |\mathcal{Q}_{\text{str}}(\kappa_\iota, \mathcal{D}_1)| \qquad (7a)$$
$$\text{subject to}$$
$$|\mathcal{D}_1| = M. \qquad (7b)$$

The right panel of Figure 2 reports an instance where, for a given choice of κ_ι and $\mathcal{D}_1$, $\mathcal{Q}_{\text{str}}$ and $\mathcal{Q}$ coincide. If this happens for all possible choices of κ_ι and $\mathcal{D}_1$, then problems (5) and (7) would also coincide.

III. MAIN RESULTS

We first show that the proposed opinion dynamics model is well-posed, as the controlled dynamics (3) are bounded. Then, we provide sufficient conditions so that an agent belongs to Q_{str} (and therefore to $\mathcal{Q}$ as well).

Lemma 1: Under the dynamics (3), the absolute value of the agents' opinion is asymptotically bounded by c/d, that is, for all $i = 1, \ldots, N$,

$$\limsup_{t \to +\infty} |x_i(t)| \leq \frac{c}{d}. \qquad (8)$$

If, additionally, $|x_i(0)| \leq c/d$, then, for all $t \in \mathbb{R}_{\geq 0}$,

$$|x_i(t)| \leq \frac{c}{d}. \qquad (9)$$

Proof: Let us define two auxiliary dynamical systems

$$\dot{\bar{x}}_i = -d\bar{x}_i + c, \qquad \bar{x}_i(0) = x_i(0). \qquad (10a)$$
$$\dot{\underline{x}}_i = -d\underline{x}_i - c, \qquad \underline{x}_i(0) = x_i(0). \qquad (10b)$$

As $\tanh(\cdot) \in [-1, 1]$, from (3) and the Comparison Theorem for ordinary differential equations [28], we have that

$$\underline{x}_i(t) \leq x_i(t) \leq \bar{x}_i(t), \quad \forall t \geq 0. \qquad (11)$$

As $\lim_{t \to +\infty} \bar{x}_i(t) = c/d$ and $\lim_{t \to +\infty} \underline{x}_i(t) = -c/d$, inequality (8) follows. Next, note that $\underline{x}_i(t) = (x_i(0) + c/d) \exp(-dt) - c/d$ and $\bar{x}_i(t) = (x_i(0) - c/d) \exp(-dt) + c/d$. As $|x_i(0)| \leq c/d$, from (11), inequality (9) follows. ∎

Remark 1: We consider opinions that are bounded in a set centered at the undecided opinion $x_i = 0$. Considering Lemma 1, from now on we will assume $|x_i(0)| \leq c/d$, so that c/d will represent the maximum strength an opinion can have at any time instant.

We define $\lambda_i(t) = \sum_{k=1}^{N} a_{ik} x_k(t) + h_i \kappa_\iota \bar{x}_\iota$ as the interaction term in (3), which can be rewritten as

$$\dot{x}_i(t) = -dx_i(t) + c \tanh(\alpha x_i(t) + \lambda_i(t)), \quad |x_i(0)| \leq c/d, \quad (12a)$$
$$y_i(t) = \text{sgn}(x_i(t)). \qquad (12b)$$

In what follows, we first provide a condition on the absolute value and sign of $\lambda_i(t)$ so that agent i belongs to $\mathcal{Q}$, that is, in finite time, agent i will take the same action of the pinner, and its opinion will be at least as strong as that of the pinner, so that i also belongs to $\mathcal{Q}_{\text{str}}$. Then, we provide conditions on the control gain κ_ι and on the network topology such that the sufficient condition on $\lambda_i(t)$ is fulfilled.

Let us define $t_{1,i}$ as the first instant such that $y_i(t) \in \{\bar{y}_\iota, 0\}$, with $t_{1,i} = +\infty$ if such an instant does not exist, and

$$\tilde{\lambda} := -\tanh^{-1}(\sqrt{1 - d/c\alpha}) + \frac{c\alpha}{d}\sqrt{1 - d/c\alpha}. \qquad (13)$$

Next, we define the set $\mathcal{T}_i := \{\tau : \forall t > \tau, y_i(t) = \bar{y}_\iota \text{ and } |x_i(t)| \geq |\bar{x}_\iota|\}$ and the scalar

$$t_{2,i} := \begin{cases} \min \mathcal{T}_i, & \text{if } \mathcal{T}_i \neq \varnothing, \\ +\infty, & \text{otherwise.} \end{cases} \qquad (14)$$

In simple words, $t_{2,i}$, when finite, is the smallest time instant such that node i takes the same action as the pinner with an at least as strong opinion, thereby guaranteeing that $i \in \mathcal{Q}_{\text{str}}$.

Theorem 1: Under the dynamics described by Eqs. (12), if

$$\exists \epsilon > 0 : |\lambda_i(t)| \geq |\tilde{\lambda}| + \epsilon, \qquad (15)$$
$$\text{sgn}(\lambda_i(t)) = \text{sgn}(\bar{x}_\iota), \qquad (16)$$

for all $t \geq 0$, then

$$\exists t_{1,i} < +\infty : y_i(t) = \bar{y}_\iota, \forall t > t_{1,i}, \qquad (17a)$$
$$\exists t_{2,i} \in [t_{1,i}, +\infty[\, |x_i(t)| \geq |\bar{x}_\iota|, \forall t > t_{2,i}. \qquad (17b)$$

Proof: For clarity, in the proof we consider $\bar{y}_\iota = 1$, but the derivations hold *ceteris paribus* for $\bar{y}_\iota = -1$.

Existence of a finite $t_{1,i}$: Let us start by showing that if $x_i(0) < 0$ then there exists a time instant $\bar{t}$ such that $x_i(\bar{t}) = 0$. Note that, as the hyperbolic tangent is strictly monotone increasing, assumptions (15)-(16) imply that

$$\dot{x}_i(t) \geq f(x_i, \epsilon) := -dx_i + c \tanh(\alpha x_i + \tilde{\lambda} + \epsilon), \qquad (18)$$

for all $x_i \in [-c/d, 0]$. Function f has two stationary points, whereby setting $\partial f(x_i, \epsilon)/\partial x_i = 0$, one obtains

$$x_{i,1}^\star = \frac{-c\alpha/d\sqrt{1 - d/c\alpha} - \epsilon}{\alpha},$$
$$x_{i,2}^\star = \frac{2\tanh^{-1}(\sqrt{1 - d/c\alpha}) - c\alpha/d\sqrt{1 - d/c\alpha} - \epsilon}{\alpha}.$$
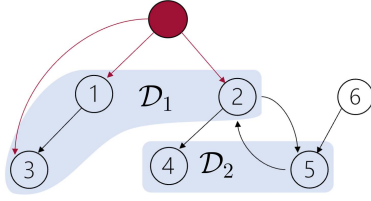
Fig. 3. Decomposition in layers of a sample graph $\mathcal{G} = \{\mathcal{V}, \mathcal{E}\}$: the pinner (in red) has 3 outgoing edges that point to the nodes in $\mathcal{D}_1 = \{1, 2, 3\}$, whereas the set $\mathcal{D}_2$ is composed by nodes 4 and 5 that are at two steps away from the pinner. Note that $\mathcal{D} = \mathcal{D}_1 \cup \mathcal{D}_2$ does not encompass node 6, which is not influenced by the pinner, and therefore in this case $\mathcal{D} \subset \mathcal{V}$.

Evaluating the function at $x_{i,1}^\star$ and $x_{i,2}^\star$, respectively, yields

$$f(x_{i,1}^\star, \epsilon) = \epsilon d/\alpha > 0, \qquad (19)$$

$$f(\bar{x}_{i,2}^\star, \epsilon) = 2\phi(c) + \epsilon d/\alpha > \epsilon d/\alpha > 0, \qquad (20)$$

where we used that, for all $c > d/\alpha$, $\phi(c) = c\sqrt{1 - d/c\alpha} - d/\alpha \tanh^{-1}(\sqrt{1 - d/c\alpha}) > 0$. Noting that
1) f is continuous and differentiable;
2) f is positive at the extrema of the interval $[-c/d, 0]$, whereby $f(0, \epsilon) = c \tanh(\tilde{\lambda} + \epsilon) > 0$, and $f(-\frac{c}{d}, \epsilon) = c + c \tanh(-\alpha\frac{c}{d} + \tilde{\lambda} + \epsilon) > 0$ as $\tanh(\cdot) > -1$;
3) f is positive and lower bounded by $\epsilon d/\alpha$ at both its stationary points;
we obtain $f(x_i, \epsilon) \geq \epsilon$, for all $x_i \in [-c/d, 0]$, with

$$\varepsilon = \min\{c \tanh(\tilde{\lambda} + \epsilon), c + c \tanh(-\alpha c/d + \tilde{\lambda} + \epsilon), \epsilon d/\alpha\} > 0.$$

Therefore, from (18) we then have

$$\dot{x}_i(t) \geq f(x_i, \epsilon) \geq \varepsilon > 0, \quad \forall t : x_i(t) \in [-c/d, 0]. \qquad (21)$$

In turn, this implies that $x_i(t) > x_i(0) + t\varepsilon$ for all t such that $x_i(t) < 0$. As $x_i(0) \geq -c/d$, we can then conclude that $\tilde{t} \leq c/d\varepsilon$. Then, from the continuity of $f(\cdot)$ and as $f(0, \epsilon) \geq \varepsilon > 0$ we have $t_{1,i} = \tilde{t}$ (17a). Note that this also proves the existence of $t_{1,i}$ when $x_i(0) = 0$.

Finally, if $x_i(0) > 0$, then $t_{1,i} = 0$ follows from the continuity of $f(\cdot)$. Indeed, as $f(0, \epsilon) \geq \varepsilon > 0$, then there exists a finite $\tilde{x}_i$ such that $0 < \tilde{x}_i \leq x_i(0)$ and $f(\tilde{x}_i, \epsilon) > 0$.

Existence of a finite $t_{2,i}$: Now, let us study the dynamics (12) for $t > t_{1,i}$. As $x_i(t) > 0$ for all $t > t_{1,i}$, to prove (17b), consider that

$$\dot{x}_i(t) > -dx_i + c \tanh(\alpha x_i + \tilde{\lambda})$$
$$> g(x_i) := -dx_i + c \tanh(\alpha x_i). \qquad (22)$$

As $\dot{x}_i = g(x_i)$ is a bistable dynamical system with the stable fixed points at $\pm\bar{x}_i$, and starting at $x_i(\tilde{t}) > 0$, the dynamics governed by $g(x_i)$ monotonically converge to $\bar{x}_i$, thus from (22) the existence of a finite $t_{2,i}$ follows. ∎

Next, we leverage the result of Theorem 1 to guarantee that a given agent will belong to $\mathcal{Q}_{str}$. Namely, we define the extended graph $\widetilde{\mathcal{G}}$ obtained by adding the pinner and its ingoing edges to $\mathcal{G}$. Let $\mathcal{D} \subseteq \mathcal{V}$ be the set that includes all nodes that are destination of a directed path originating from s in $\widetilde{\mathcal{G}}$, and let $q \leq N$ be the maximum length of the shortest path

from s to a node in $\mathcal{D}$. We focus on $\mathcal{D}$ as the opinion dynamics of the nodes in $\mathcal{V} \setminus \mathcal{D}$ cannot be affected either directly or indirectly by the pinner.

Next, we relabel the nodes in $\mathcal{V}$ so that the nodes belonging to $\mathcal{D}$ are the first $|\mathcal{D}|$, and partition $\mathcal{D}$ in q disjoint subsets (layers) $\mathcal{D}_1, \ldots, \mathcal{D}_q$, so that $i \in \mathcal{D}_l$ if the shortest path in $\widetilde{\mathcal{G}}$ that connects s to i has length l, for $l = 1, \ldots, q$ (the first layer $\mathcal{D}_1$ coincides with the set of pinned nodes). Finally, we define the set $\mathcal{B}_l := \{j \in \cup_{k=1}^l \mathcal{D}_k : j \in \mathcal{Q}_{str}\} \subseteq \cup_{k=1}^l \mathcal{D}_k$ of nodes in the layers $1, \ldots, l$ that in finite time will take the same action as the pinner with an at least as strong opinion.

Now, let us study the behavior of the nodes belonging to $\mathcal{D}_1$, that is, the pinned nodes. Denoting $\delta_i^{in} = \sum_{k=1}^N a_{ik}$ the weighted in-degree of node i, we can give

Corollary 1: For any $i \in \mathcal{D}_1$, if

$$\kappa_\iota > \frac{|\tilde{\lambda}| + \epsilon + \frac{c}{d}\delta_i^{in}}{|\bar{x}_\iota|}, \qquad (23)$$

then $i \in \mathcal{B}_1$.

Proof: Let us recall that $\lambda_i(t) = \sum_{k=1}^N a_{ik}x_k + \kappa_\iota\bar{x}_\iota$. Then, as $|x_k| \leq c/d$ from Lemma 1 and Remark 1, and as $\sum_{k=1}^N a_{ik} = \delta_i^{in}$ by definition, then from (23) we have that (16) holds. Furthermore, the same arguments imply that

$$|\lambda_i(t)| \geq \kappa_\iota|\bar{x}_\iota| - \sum_{k=1}^N a_{ik}|x_k| \geq \kappa_\iota|\bar{x}_\iota| - \frac{c}{d}\delta_i^{in}.$$

Hence, also (15) holds, and therefore from Theorem 1 the thesis follows. ∎

We can now study the dynamics of a generic node $i \in \mathcal{D}_l$, $l \geq 2$. Let us define b_i as the sum of the weights of the edges entering node i from every node $j \in \mathcal{B}_{l-1}$, that is, $b_i := \sum_{j \in \mathcal{B}_{l-1}} a_{ij}$, which implies that $0 \leq b_i \leq \delta_i^{in}$. Then, we can give the following sufficient condition for a node i to belong to the set $\mathcal{B}_q \subseteq \mathcal{Q}_{str}$ of nodes in $\mathcal{D}$ that take the same action with an at least as strong opinion as the pinner.

Corollary 2: For any $i \in \mathcal{D}_l$, and $l \geq 2$, if $\mathcal{B}_{l-1} \neq \varnothing$, and there exists $\epsilon > 0$ such that

$$b_i > \frac{|\tilde{\lambda}| + \epsilon + \frac{c}{d}(\delta_i^{in} - b_i)}{|\bar{x}_\iota|}, \qquad (24)$$

then $i \in \mathcal{B}_q$.

Proof: Let us note that

$$\lambda_i(t) = \sum_{j \in \mathcal{B}_{l-1}} a_{ij}x_j(t) + \sum_{j \notin \mathcal{B}_{l-1}} a_{ij}x_j(t). \qquad (25)$$

Moreover, consider that, from Lemma 1, we have

$$\left| \sum_{j \notin \mathcal{B}_{l-1}} a_{ij}x_j(t) \right| \leq \frac{c}{d}(\delta_i^{in} - b_i) \qquad (26)$$

and from Theorem 1 and the definition of $\mathcal{B}_{l-1}$ we have that

$$\left| \sum_{j \in \mathcal{B}_{l-1}} a_{ij}x_j(t) \right| \geq |\bar{x}_\iota|b_i, \qquad (27)$$

for all $t \geq t_l := \max_{j \in \mathcal{B}_{l-1}} t_{2,j}$. Hence, combining Eqs. (26)-(27), and from (24), $\lambda_i(\tau)$, with $\tau = t - t_l$, satisfies (15)-(16), and thus the thesis follows from Theorem 1. ∎

COMPARISON OF OUR STRATEGY (HEUR) AGAINST A RANDOM SELECTION, THE MAXIMIZATION OR MINIMIZATION OF THE OUT-DEGREE δ_{out}, IN-DEGREE δ_{in}, OR THE BETWEENNESS CENTRALITY bc FOR TWO ALTERNATIVE CHOICES OF INITIAL CONDITIONS

Initial conditions	Metrics	heur	rand	$\delta_{\text{out}}^{\max}$	$\delta_{\text{out}}^{\min}$	$\delta_{\text{in}}^{\max}$	$\delta_{\text{in}}^{\min}$	$\text{bc}^{\max}$	$\text{bc}^{\min}$
$x_i(0) \sim U(-\frac{c}{d}, \frac{c}{d})$	m_1	0.92	0.65	0.90	0.54	0.90	0.58	0.90	0.57
	m_2	0.92	0.63	0.90	0.53	0.89	0.57	0.90	0.56
	m_3	0.81	0.61	0.80	0.53	0.79	0.57	0.80	0.56
	m_4	0.7	0.5	0.68	0.41	0.68	0.47	0.68	0.45
$x_i(0) = -\frac{c}{d}, \forall i$	m_1	0.30	0.081	0.27	0.070	0.14	0.070	0.22	0.050
	m_2	0.30	0.081	0.27	0.070	0.14	0.070	0.22	0.050
	m_3	0.22	0.061	0.20	0.050	0.11	0.050	0.16	0.050
	m_4	0.22	0.061	0.20	0.050	0.11	0.050	0.16	0.050

Note that in (24) the lower bound of b_i is given in implicit form to underline the analogy with (23).

Corollaries 1 and 2 hold for any initial opinion in the set $[-c/d, c/d]$. Hence, they allow exploring layer by layer the part of the network whose dynamics is affected by the control signals and determine which agent we can guarantee will belong to $\mathcal{Q}_{\text{str}}$. In particular, condition (23) of Corollary 1 guarantees that, even in the worst case where all the agents (except for the pinner) influencing agent i have the opposite opinion of the pinner with strength c/d, the control gain κ_ι is strong enough to ensure assumption (14) of Theorem 1 is fulfilled. Condition (24) of Corollary 2 shows that, different from layer 1, in the other layers the control gain has only an indirect influence. Indeed, for a given level l, κ_ι may affect the cardinality $|\mathcal{B}_{l-1}|$ of the set of neighbors of node i that take the same action and have an opinion at least as strong as that of the pinner. The larger $|\mathcal{B}_{l-1}|$, the more nodes in layer l will belong to $\mathcal{Q}_{\text{str}}$, since b_i in (24) will be larger.

IV. PINNING SELECTION STRATEGIES

Corollaries 1 and 2 can be used in an algorithmic fashion to identify a set of nodes $\widehat{\mathcal{B}}_q$ that we can guarantee will belong to $\mathcal{B}_q$ for any $|x_i(0)| \leq c/d$. More specifically, condition (23) can be used to compute $\widetilde{\mathcal{B}}_1$, and then condition (24) can be iteratively applied to sequentially compute $\widetilde{\mathcal{B}}_2, \ldots, \widetilde{\mathcal{B}}_q$.

Noting that $\mathcal{B}_q \subseteq \mathcal{Q}_{\text{str}}$, we can then use $\tilde{q}(\mathcal{D}_1, \kappa_\iota) := |\widehat{\mathcal{B}}_q|$, evaluated algorithmically through the two corollaries, as a proxy for the effectiveness of the choice of the set of pinned nodes $\mathcal{D}_1$ with a given cardinality M in solving problem (7), for a given selection of the control gain κ_ι. In what follows, assuming we can freely select κ_ι, we propose a greedy heuristic that solves in polynomial time the NP-hard problem of selecting $\mathcal{D}_1$ with the goal of maximizing $\tilde{q}_\infty(\mathcal{D}_1) := \lim_{\kappa_\iota \to +\infty} \tilde{q}(\mathcal{D}_1, \kappa_\iota)$. We compare the effectiveness of the solution with respect to both Problems (5) and (7) against alternative choices of the pinned nodes based on centrality metrics, similar to what has been done in [21], [22].

A. Heuristic Strategy for Selecting $\mathcal{D}_1$

Starting from an empty set of pinned nodes, namely $\mathcal{D}_1 = \varnothing$, our greedy strategy sequentially adds nodes so that, at every iteration, $\tilde{q}_\infty$ is maximized given the current cardinality

of $\mathcal{D}_1$. The heuristic stops as soon as $|\mathcal{D}_1| = M$. Defining

$$\bar{\kappa}_\iota := \max_{i \in \mathcal{V}} \frac{|\tilde{\lambda}| + \epsilon + \frac{c}{d}\delta_i^{\text{in}}}{|\bar{x}_\iota|},$$

as the control gain ensuring, from Corollary 1, that any pinned node belongs to $\mathcal{Q}_{\text{str}}$ the steps of our algorithm are:
1) initialize $\mathcal{D}_1 = \varnothing$, and set $\kappa_\iota > \bar{\kappa}_\iota$;
2) using Corollaries 1 and 2 compute $\tilde{q}(\mathcal{D}_1 \cup \{i\}, \kappa_\iota)$ for all $i \in \mathcal{V} \setminus \mathcal{D}_1$;
3) randomly select $i^\star$ in the set

$$\arg\max_{i \in \mathcal{V} \setminus \mathcal{D}_1} \tilde{q}(\mathcal{D}_1 \cup \{i\}, \kappa_\iota), \tag{28}$$

and update $\mathcal{D}_1 = \mathcal{D}_1 \cup \{i^\star\}$;
4) if $|\mathcal{D}_1| < M$, go to step 2, otherwise stop the algorithm.

B. Performance in a Sample Retweet Network From Twitter

We compare the proposed heuristic both against chance, that is, a random selection of the set $\mathcal{D}_1$, and alternative topological strategies, which consist in encompassing in $\mathcal{D}_1$ the nodes with maximum (or minimum) outdegree, indegree, and betweenness centrality [29]. To do so, we extracted a directed unweighted subgraph of 580 nodes of a retweet graph from [30]. Then, we set the number of pinned nodes to $M = 0.05N$, and evaluated the following metrics to assess the performance of the proposed heuristic:
- $m_1 = |\mathcal{Q} \cap \mathcal{D}|/|\mathcal{D}|$ and $m_2 = |\mathcal{Q}|/|\mathcal{V}|$, that is, the fraction of nodes in $\mathcal{D}$ and in $\mathcal{V}$, respectively, that take the same action of the pinner;
- $m_3 = |\mathcal{Q}_{\text{str}} \cap \mathcal{D}|/|\mathcal{D}|$ and $m_4 = |\mathcal{Q}_{\text{str}}|/|\mathcal{V}|$, that is, the fraction of nodes in $\mathcal{D}$ and $\mathcal{V}$, respectively, that take the same action of the pinner and have an opinion that is at least as strong as that of the pinner;

Note that m_1 and m_3 focus on the nodes that, given the selection $\mathcal{D}_1$, are directly affected by the pinner, whereas m_2 and m_4 evaluate the effectiveness of $\mathcal{D}_1$ for all the agents in $\mathcal{V}$. We evaluated these metrics for initial opinions
1) drawn from a uniform distribution in $[-c/d, c/d]$,
2) furthest from that of the pinner, i.e., $x_i(0) = -c/d$ as we set $\bar{y}_\iota = 1$.

For case 1), the results are averaged over 1000 random selections of the initial conditions. Table I shows that the proposed heuristic outperforms the alternative strategies. Also, metrics $m_{1,2}$ and $m_{3,4}$ are equivalent when all agents start with
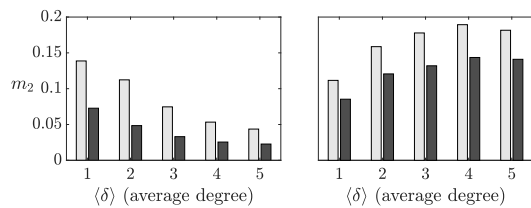
Fig. 4. Comparing the proposed heuristic against pinning the nodes with maximum out-degree in terms of the fraction m_2 of nodes taking the same action of the pinner. The left and right panel refer to ER and SF networks, respectively. The probability of ER graphs is equal to $\langle\delta\rangle/N$, the exponent of the power law of SF network is equal to 2.6. Each data point is averaged over 100 realizations of the graph topology.

opinions that are furthest from the pinner, and the ranking of the strategies does not change depending on the metric. Moreover, we observe that the maximization of the out-degree is the topological strategy that more closely matches the performance of the proposed heuristic.

C. Performance in Synthetic Networks

As pinning the nodes with maximum out-degree leads to performance close to the proposed heuristic strategy, we performed a comprehensive numerical analysis on Erdös-Rényi (ER) and Scale Free (SF) graphs, generated by means of the configuration model, to assess whether the proposed heuristic yielded a significant improvement. For both ER and SF topologies, and for each value of the average degree, varied between 1 and 5 with step 1, we generated 100 graphs of $N = 500$ nodes, and we computed the average values of $m_1, \ldots, m_4$ setting $x_i(0) = -c/d$ for all i. As shown in Figure 4, in all synthetic networks the proposed heuristic outperforms pinning the nodes with maximum out-degree, and a t-test confirms that the difference is significant, with a p-value smaller than 0.001.

V. Conclusion

In this letter, we used pinning control to maximize the effect of an influencer in social groups interacting according to a nonlinear opinion dynamics model. We derived sufficient conditions on the topology and control gain so that individuals take the same action and have an opinion at least as strong as that of the pinner. We leveraged our results to design a heuristic to select the nodes where inputs should be injected so to maximize the influence of the pinner, given a constraint on the number of nodes to pin. Future work should be devoted to test our results on real world data borrowed from online social media, and investigating the more realistic cases where the agents' parameters are heterogeneous or there is more than one pinner competing for influencing the other agents.

References

[1] I. Hansen and D. J. Lim, "Doxing democracy: Influencing elections via cyber voter interference," *Contemp. Polit.*, vol. 25, no. 2, pp. 150–171, 2019.

[2] N. Puri, E. A. Coomes, H. Haghbayan, and K. Gunaratne, "Social media and vaccine hesitancy: New updates for the era of COVID-19 and globalized infectious diseases," *Human Vaccin Immunother.*, vol. 16, no. 11, pp. 2586–2593, 2020.

[3] E. Yildiz, A. Ozdaglar, D. Acemoglu, A. Saberi, and A. Scaglione, "Binary opinion dynamics with stubborn agents," *ACM Trans. Econ. Comput.*, vol. 1, no. 4, pp. 1–30, 2013.

[4] T. Li and H. Zhu, "Effect of the media on the opinion dynamics in online social networks," *Physica A, Stat. Mech. Appl.*, vol. 551, Aug. 2020, Art. no. 124117.

[5] Z. Zhao, L. Shi, T. Li, J. Shao, and Y. Cheng, "Opinion dynamics of social networks with intermittent-influence leaders," *IEEE Trans. Computat. Social Syst.*, vol. 10, no. 3, pp. 1073–1082, Jun. 2023.

[6] W. Su, X. Chen, Y. Yu, and G. Chen, "Noise-based control of opinion dynamics," *IEEE Trans. Autom. Control*, vol. 67, no. 6, pp. 3134–3140, Jun. 2022.

[7] L. Shi, Y. Cheng, J. Shao, X. Wang, and H. Sheng, "Leader–follower opinion dynamics of signed social networks with asynchronous trust/distrust level evolution," *IEEE Trans. Netw. Sci. Eng.*, vol. 9, no. 2, pp. 495–509, Mar./Apr. 2022.

[8] W. Yu, G. Chen, J. Lü, and J. Kurths, "Synchronization via pinning control on general complex networks," *SIAM J. Control Optim.*, vol. 51, no. 2, pp. 1395–1416, 2013.

[9] P. De Lellis, M. di Bernardo, and M. Porfiri, "Pinning control of complex networks via edge snapping," *Chaos*, vol. 21, no. 3, 2011, Art. no. 33119.

[10] F. Lo Iudice, F. Garofalo, and P. De Lellis, "Bounded partial pinning control of network dynamical systems," *IEEE Trans. Control Netw. Syst.*, vol. 10, no. 1, pp. 238–248, Mar. 2023.

[11] F. Dietrich, S. Martin, and M. Jungers, "Control via leadership of opinion dynamics with state and time-dependent interactions," *IEEE Trans. Autom. Control*, vol. 63, no. 4, pp. 1200–1207, Apr. 2018.

[12] C. Ancona, F. Lo Iudice, F. Garofalo, and P. De Lellis, "A model-based opinion dynamics approach to tackle vaccine hesitancy," *Sci. Rep.*, vol. 12, no. 1, pp. 1–8, 2022.

[13] C. Altafini, "Consensus problems on networks with antagonistic interactions," *IEEE Trans. Autom. Control*, vol. 58, no. 4, pp. 935–946, Apr. 2013.

[14] M. H. DeGroot, "Reaching a consensus," *J. Amer. Stat. Assoc.*, vol. 69, no. 345, pp. 118–121, 1974.

[15] N. E. Friedkin and E. C. Johnsen, "Social influence and opinions," *J. Math. Sociol.*, vol. 15, nos. 3–4, pp. 193–206, 1990.

[16] R. Hegselmann and U. Krause, "Opinion dynamics and bounded confidence models, analysis, and simulation," *J. Artif. Soc. Soc. Simul.*, vol. 5, no. 3, pp. 1–33, 2002.

[17] G. Weisbuch, "Bounded confidence and social networks," *Eur. Phys. J. B*, vol. 38, no. 2, pp. 339–343, 2004.

[18] A. Bizyaeva, A. Franci, and N. E. Leonard, "Nonlinear opinion dynamics with tunable sensitivity," *IEEE Trans. Autom. Control*, vol. 68, no. 3, pp. 1415–1430, Mar. 2023.

[19] R. Gray, A. Franci, V. Srivastava, and N. E. Leonard, "Multiagent decision-making dynamics inspired by honeybees," *IEEE Trans. Control Netw. Syst.*, vol. 5, no. 2, pp. 793–806, Jun. 2018.

[20] A. C. R. Martins, "Continuous opinions and discrete actions in opinion dynamics problems," *Int. J. Mod. Phys. C*, vol. 19, no. 4, pp. 617–624, 2008.

[21] M. Jalili, O. A. Sichani, and X. Yu, "Optimal pinning controllability of complex networks: Dependence on network structure," *Phys. Rev. E, Stat. Phys. Plasmas Fluids Relat. Interdiscip. Top.*, vol. 91, no. 1, 2015, Art. no. 12803.

[22] Y. Orouskhani, M. Jalili, and X. Yu, "Optimizing dynamical network structure for pinning control," *Sci. Rep.*, vol. 6, no. 1, pp. 1–13, 2016.

[23] Y.-Y. Liu, J.-J. Slotine, and A.-L. Barabási, "Controllability of complex networks," *Nature*, vol. 473, no. 7346, pp. 167–173, 2011.

[24] N. E. Leonard, K. Lipsitz, A. Bizyaeva, and Y. Lelkes, "The nonlinear feedback dynamics of asymmetric political polarization," *Proc. Nat. Acad. Sci. USA*, vol. 118, no. 50, 2021, Art. no. e2102149118.

[25] X. F. Wang and G. Chen, "Pinning control of scale-free dynamical networks," *Physica A*, vol. 310, nos. 3–4, pp. 521–531, 2002.

[26] P. DeLellis, F. Garofalo, and F. Lo Iudice, "The partial pinning control strategy for large complex networks," *Automatica*, vol. 89, pp. 111–116, Mar. 2018.

[27] A. Arenas, A. Díaz-Guilera, J. Kurths, Y. Moreno, and C. Zhou, "Synchronization in complex networks," *Phys. Rep.*, vol. 469, no. 3, pp. 93–153, 2008.

[28] A. McNabb, "Comparison theorems for differential equations," *J. Math. Anal. Appl.*, vol. 119, nos. 1–2, pp. 417–428, 1986.

[29] M. Barthélemy, "Betweenness centrality in large complex networks," *Eur. Phys. J. B*, vol. 38, no. 2, pp. 163–168, 2004.

[30] R. A. Rossi and N. K. Ahmed, "The network data repository with interactive graph analytics and visualization," in *Proc. AAAI*, 2015, pp. 4292–4293. [Online]. Available: https://networkrepository.com

scientific reports

OPEN

A model-based opinion dynamics approach to tackle vaccine hesitancy

Camilla Ancona[1,2,3], Francesco Lo Iudice[1,3], Franco Garofalo[1✉] & Pietro De Lellis[1✉]

Uncovering the mechanisms underlying the diffusion of vaccine hesitancy is crucial in fighting epidemic spreading. Toward this ambitious goal, we treat vaccine hesitancy as an opinion, whose diffusion in a social group can be shaped over time by the influence of personal beliefs, social pressure, and other exogenous actions, such as pro-vaccine campaigns. We propose a simple mathematical model that, calibrated on survey data, can predict the modification of the pre-existing individual willingness to be vaccinated and estimate the fraction of a population that is expected to adhere to an immunization program. This work paves the way for enabling tools from network control towards the simulation of different intervention plans and the design of more effective targeted pro-vaccine campaigns. Compared to traditional mass media alternatives, these model-based campaigns can exploit the structural properties of social networks to provide a potentially pivotal advantage in epidemic mitigation.

The ongoing COVID-19 pandemic has put the phenomenon of vaccine hesitancy back under the spotlight for the subsequent delays in our race to stem the transmission of the virus[1–3]. Prior to this global emergency, the reluctance that a fraction of the population has in getting vaccinated already proved to be a global threat for human health, see the recent resurgence of measles both in Europe and the US[4–6]. Since the first vaccines were developed, a hesitant attitude in a relevant fraction of the population has been constantly observed at every latitude and across all socio-economic classes[7–9]. Public concerns about vaccines can potentially resonate on social platforms, triggering skepticism towards a recommended vaccination, which in turn translates into delaying or refusing to take the jab. The spectrum of hesitants ranges from fierce antivax, to people who accept vaccines but still remain uncertain about their use. In this social environment, being the vaccination based on voluntary compliance, the fear is that some people might play a wait-and-see game, whereby individuals who choose to wait enjoy the benefits generated by those who do opt for vaccination. This triggers a collective threat that has been highlighted through game theory: rational vaccination decisions based on individual self-interest bring to vaccination levels that are below the optimum for the community[10]. However, rational arguments are seldom at the basis of vaccine hesitancy, which is typically amplified by the rumors spreading on social media[11]. Indeed, opinion formation is not only affected by the social pressure exerted through traditional media outlets such as newspapers or tv, but also by peer-to-peer interactions on social networks. The latter should then probably be the main means for effective promotion campaigns aimed at diffusing the vaccine literacy and boosting immunization acceptance[12].

An incisive campaign to promote vaccination over a social network requires a suitable selection of the target subjects, and should be tailored to the specific concerns they have on vaccination. Doing so demands the contribution of diverse scientific communities. The large literature on behavioral motivation in medical and social sciences is a precious source of effective communication strategies and arguments to tackle any kind of concern[13–16]. Artificial intelligence and data science may help detect misinformation flowing on social platforms and assess the public confidence in vaccination, see[17] and references therein. In this context, the contribution of network control[18–20] could be crucial, since model-based approach may enable the simulation of what-if scenarios corresponding to different promotion campaigns. Here, we show that a network model of opinion diffusion can (i) capture the dynamics of vaccine hesitancy in large groups of individuals and (ii) inform the design of pro-vaccine social media campaigns targeting select individuals within these groups.

[1]Department of Electrical Engineering and Information Technology, University of Naples Federico II, Naples 80125, Italy. [2]Department of Management, Information and Production Engineering, University of Bergamo, Bergamo 24127, Italy. [3]These authors contributed equally: Camilla Ancona and Francesco Lo Iudice ✉email: franco.garofalo@unina.it; pietro.delellis@unina.it

Most of the existing models of opinion dynamics have an explanatory character and derive the basic mechanisms of social influence from analogies with diffusion processes in physical systems. Different rules for updating the opinions in the group have been considered, which include imitation[21,22], averaging over people with similar opinions[23–25], following the majority[26,27], and cooperative versus competitive interactions[28–31]. Feeding the huge amount of data that artificial intelligence and data science can mine from social networks to an opinion dynamics model can help unleash the predictive power of these explanatory models under external stimuli, thereby enabling proactive interventions[32]. This paper tries to make a first step in this direction, bridging opinion dynamics and vaccine willingness in a scaled model, which is calibrated on a survey conducted on a sample of the Italian population. This enables us to hypothesize different targeted vaccine promotion campaigns and compare their effectiveness on the basis of the expected fraction of the population that, subject to the each different campaign, will decide to take the vaccine.

Results

A dynamic model of vaccine willingness Vaccine hesitant individuals are defined by WHO as "a heterogeneous group that are indecisive in varying degrees about specific vaccines or vaccination in general". Hence, vaccine willingness is a "fluid" opinion on vaccination that can be molded by social interaction and external stimuli. Our modelling assumption is that the vaccine willingness of the i-th of a population of n networked individuals, $x_i(k)$, is shaped in time by social interactions according to the Friedkin-Johnsen model[33], i.e.,

$$x_i(k+1) = \lambda_i \sum_{j \in \mathcal{N}_i} w_{ij} x_j(k) + (1 - \lambda_i) x_i(0). \tag{1}$$

Here, the so-called *susceptibility* $\lambda_i \in [0, 1]$ modulates the convex combination between agent i's innate opinion $x_i(0)$ and the social pressure modeled as the average of the current willingnesses $x_j(k)$ of its neighbors in the network (the agents in the set $\mathcal{N}_i$). The complement to 1 of λ_i captures the agent's *stubbornness*.

Departing from the consideration that radical views generally translate into foreseeable (unsurprising) actions, while actions related to moderate opinions are far more uncertain, we posit that the probability of an individual accepting a jab at a certain time k, $p_i(k)$, depends linearly on its willingness $x_i(k)$. Hence, we can extend the model of $x_i(k)$ to $p_i(k)$ obtaining

$$p_i(k+1) = \lambda_i \sum_{j \in \mathcal{N}_i} w_{ij} p_j(k) + (1 - \lambda_i) p_i(0). \tag{2}$$

According to our model, the binary decision of taking or refusing a jab becomes a Bernoulli random variable whose parameter is $p_i(k)$.

Incorporating pro-vaccine campaigns into the model Exploiting tools from network control[34,35], we incorporate a pro-vaccine campaign in model (1)–(2) as an additional virtual node, an *influencer agent*, whose willingness is $x_l(k)$ and associated probability of accepting a jab $p_l(k)$. The influencer agent is connected through a directed link to a fraction ϕ of targeted individuals. Hence, the dynamics of the targeted agents becomes

$$p_i(k+1) = \left((1 - \alpha) \lambda_i \sum_{j \in \mathcal{N}_i} p_j(k) + \alpha p_l(k) \right) + (1 - \lambda_i) p_i(0), \tag{3}$$

where $\alpha \in [0, 1]$ quantifies the *effort per target individual*. Hence, we characterize the *overall effort* $0 \le \eta \le 1$ of a campaign as the product of the two parameters α and ϕ. During the ongoing pandemic, health authorities of most countries have conducted traditional pro-vaccine campaigns through mass media to fight vaccine hesitancy[36–38]. In our modeling framework, this means that the influencer (in this case, the health authority) is connected to all the network agents, that is, $\phi = 1$. However, in the era of online social media and targeted marketing, one could argue that a targeted pro-vaccine campaign, where the influencer devotes a larger individual effort α to a small fraction ϕ of the agents, could outperform traditional mass campaigns given the same overall effort η.

To dispel this doubt, we exploit our scaled model to design three alternative targeted campaigns, differing for the selection of the targeted agents, denoted in the following as Strategies 1, 2, and 3, respectively. Strategy 1, as in classical network science approaches, targets the most connected agents, i.e. the agents that have the greatest topological advantage for spreading opinions favourable to vaccination. Strategy 2 mitigates the effect of the antivax by targeting their neighbors, whereas Strategy 3 directly targets the most susceptible agents. The details on the implementation of these campaigns are provided in the Methods.

It is worth pointing out that the three strategies we propose require different information levels, thus posing different feasibility issues. Indeed, targeting the most connected agents only requires knowledge of the unweighted topology of the social network. Attempting instead at neutralizing the antivax requires to complement this structural information with that on the agents' vaccine hesitancy, which can be monitored by means e.g. of sentiment analysis on social media[39,40]. Finally, directly influencing the most susceptible agents constitutes a psychological targeting strategy (see[41] and the references therein for alternatives methods to do so) that requires assessing the personality traits of each individual.

A scaled model of vaccine willingness in the Italian population We exploit our modeling framework to build a scaled representation of vaccine willingness in the Italian population. Since we focus on interactions taking place through *online* social media, we borrowed the graph describing social interactions among the individuals from a Facebook friendship network[42]. We associate to the individuals of our scaled model vaccine willingnesses whose distribution is compatible with the outcome of a survey conducted on a sample of the Italian adult population at the end of the first lockdown[8], when the vaccine availability was long to come. From these data
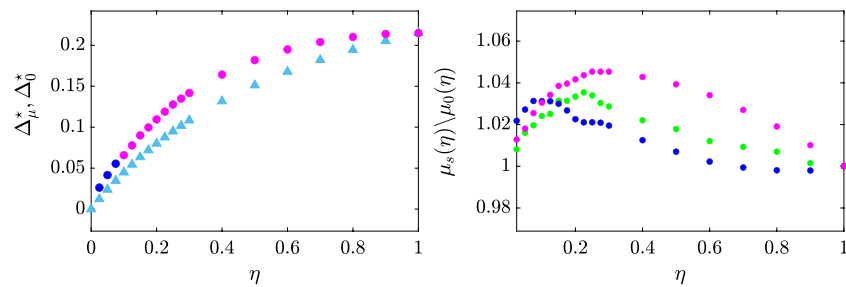
Figure 1. Comparison of targeted and traditional provax mass campaigns. The left panel depicts, for each effort η, the additional population fraction $\Delta_\mu^\star$ and Δ_μ^0 that is expected to be vaccinated when the best targeted campaign (identified by circles) or the mass provax campaign (identified by triangles) are employed, respectively. The right panel displays for each effort η and targeted strategy s, the ratio between the fractions of the population $\mu_s(\eta)$ and $\mu_0(\eta)$ that are expected to be vaccinated when strategy s and the traditional campaign are employed, respectively. In both panels, Strategy 1, 2, and 3 are depicted in blue, green, and magenta, respectively, the intensity of the vaccination campaign is set to $\alpha = 1$ and for the maximum effort $\eta = 1$, all points are superimposed since all strategies would be equivalent.

we were able to estimate the susceptibilities λ_i so as to preserve, at steady-state, the aforementioned association, see the Methods for details and the Supplementary Information, Figure S7, for a graphical representation. The steady-state distribution of the vaccine willingness enables the evaluation of the probability that any given fraction of the population gets vaccinated (see Section S1 of the Supplementary Information), which in turn allows to compute the expected fraction of the population that, at the time of the survey, would have taken a jab had this opportunity been given.

Comparing pro-vaccine campaigns Leveraging our scaled model, we conducted a numerical analysis to compare the effectiveness of targeted and mass campaigns on our synthetic population. Our simulations show that i) the targeted campaigns outperform a general mass-media campaign, and ii) the best strategy for targeting individuals depends on the overall effort η of the campaign. Indeed, for all possible selections of η, it is possible to find a targeted strategy that yields an advantage compared with general mass-media campaigns, with an increase of the expected number of vaccinated individuals that reaches a maximum 5% for $\eta = 0.25$, see the left panel of Fig. 1. Interestingly, for low efforts ($\eta < 0.1$), any strategy is capable of increasing the effectiveness of the vaccination campaign, with the merely topological approach of Strategy 1 being the most effective. When more resources can be devoted to the campaign, our model predicts that a finer characterization of the individuals is required to substantially increase the expected vaccinated population, see the right panel of Fig. 1. In particular, for all $\eta \geq 0.1$, Strategy 3, which relies on the estimation of the individual susceptibility, proves to be the best campaign. One could argue that the expected advantage of targeted strategies over the general alternative could be irrelevant, should the variance be high. However, as shown in the Supplementary Information, the variance of the distribution of the fraction of vaccinated individuals tends to 0 as the size of the populations increases, and is negligible when we consider the population of a country like Italy. These results are robust to changing the graph underlying our scaled model, see Section S3 of the Supplementary Information.

Impact of antivax campaigns Our model can also be used to assess the possible impact of antivax campaigns. Analogously to the provax case, we incorporate the role of antivax campaigns attempting to polarize the vaccination probabilities towards zero by setting $p_l(k) = 0$ for all k. Moreover, we assume that the selection of the agents targeted by the antivax influencer is made according to the same criteria defining the provax strategies. As illustrated in Fig. 2, antivax campaigns can be even more impactful than their provax counterparts and thus can represent a serious hindrance in our quest to stem the transmission of the virus.

Discussion

In this paper, we proposed a model-based approach, grounded in opinion dynamics, which identifies the patterns through which the vaccine hesitancy/willingness diffuses in a population. The availability of such a model offers, potentially, two major benefits. The first is the possibility of predicting the fraction of a given population that, with a certain confidence level, will decide to get vaccinated, thus enriching the information that can be drawn from the numerous surveys on vaccine willingness. The second and more crucial benefit consists in the possibility of simulating alternative scenarios where different pro-vaccine media campaigns over social media are enacted. Prior to their implementation, the campaigns can then be designed and tested on a scaled model, so that their effectiveness can be maximized.

Our results indicate that targeted campaigns always outperform mass campaigns, yielding the maximum increment in the expected vaccinated population for intermediate values of the overall effort of the campaign. For such values, the gain of electing smart, targeted campaigns rather than mass campaigns is to increase the expected vaccinated population by an additional 5%. Implementing targeted campaigns entails the use of tools from artificial intelligence and data science, with higher investments needed compared to traditional campaigns.
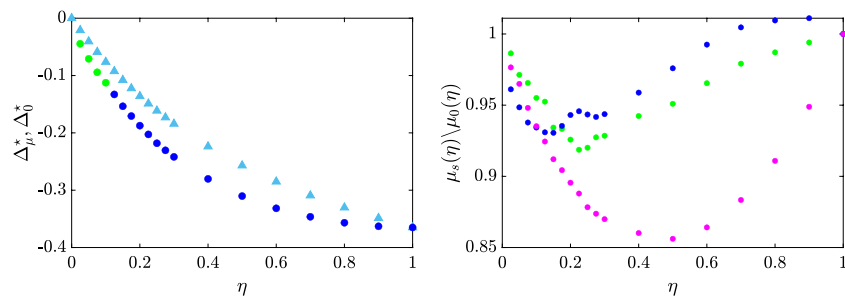
Figure 2. Comparison of the targeted and traditional mass antivax campaigns. The left panel depicts, for each effort η, the additional population fraction $\Delta_\mu^\star$ and $\Delta_0^\star$ that is expected to be vaccinated when the best targeted (identified by circles) or the mass (identified by triangles) antivax campaigns are employed, respectively. The right panel displays for each effort η and targeted strategy s, the ratio between the fractions of the population $\mu_s(\eta)$ and $\mu_0(\eta)$ that are expected to be vaccinated when strategy s and the mass antivax campaign are employed, respectively. In both panels, Strategy 1, 2, and 3 are depicted in blue, green, and magenta, respectively, the intensity of the vaccination campaign is set to $\alpha = 1$, and, for the maximum effort $\eta = 1$, all points are superimposed since all strategies would be equivalent.

It is reasonable to ask whether this additional burden is worth carrying: can a marginal increase of vaccinated individuals make a difference? From the perspective of protecting public health, the empirical answer lies in the recent data showing that avoiding saturation of healthcare sys is a matter of slight differences in the number of vaccinated individuals[43]. Modest increases in the effectiveness of a campaign can well be the difference between expecting or not to live with the virus without restrictions. However, from an ethical perspective one could argue that targeting individuals based on information obtained from its online social media might surpass the borders protecting the privacy of the population. Where the optimal trade-off lies between feasibility and ethics is subject of ongoing worldwide discussions[44].

From a methodological perspective our work represents a first step toward bridging the abstract literature on opinion dynamics with the pressing open problem of fighting vaccine hesitancy. Although the results are promising, our work is not free of limitations, and there are several directions along which it can be extended. First, in its current incarnation, model calibration is only concerned with steady-state vaccination probabilities. This is certainly sufficient when the campaigns are planned way ahead the administration of the vaccine. However, in the case of a new epidemic, news from media outlets may perturb the beliefs of the population, see e.g. the scientific and social debate on the AstraZeneca COVID-19 vaccine[45,46]. In such cases, the campaign should be immediately redesigned, and tailored on the basis of the response time of the population. Our model has the potential to account for these transient dynamics, provided that several snapshots of the opinions of the same cohort of the population are available. Having access to additional snapshots would also allow considering weighted networks. Second, alternative models of opinion dynamics could be considered. In the spectrum of model complexity, we decided to opt for the simplest one, so as to minimize the number of parameters to be tuned. Should one have more data for finer calibrations, alternative, more complex models of opinion dynamics could be considered to account e.g. for bounded confidence[24], or for the difference between private and publicly expressed opinions[22]. Third, our assumption that vaccination decisions were grounded on steady-state willingness was justified by the fact that the COVID-19 pandemic was characterized by a one year delay between the first prospect and mass availability of vaccines. As this could not be the case in the future, it could be interesting to evaluate the effectiveness of provax campaigns when removing this assumption. In this vein, the model could be reworked so to consider the influence of an individual's decision on the willingness of its peers. Finally, since it has been observed that social networks may be characterized by the presence of communities of like-minded individuals[47], which are socially well connected and share many interests, an open research question is to evaluate how these densely connected communities may affects the effectiveness of targeted vaccination campaigns.

The reductive choice of characterizing the behavior or each individual through the Friedkin-Johnsen model allows for a first assessment of the effectiveness of pro-vaccine campaigns on the basis of data collected from a single survey. Indeed, the strength of our inherently causal model-based approach lies in the ability of teasing out the relationship between the choice of the targets of the campaign and its effectiveness. This ease of interpretation is a feature we believe should be retained even when more refined data on vaccine hesitancy are considered.

Methods

Opinion dynamics modeling of vaccine acceptance. In model (1), vaccine willingness diffuses along an undirected connected graph $\mathcal{G} = \{\mathcal{V}, \mathcal{E}\}$ with self-loops at each node, where $\mathcal{V}$ is the set of the n individuals, and $\mathcal{E} = \{(i,j) \subseteq \mathcal{V} \times \mathcal{V}\}$ is the set of edges connecting neighboring individuals. We posit that an individual's probability of accepting a jab is linearly proportional to its vaccine willingess leading to Eq. (2), that can be rewritten in compact matrix form as

Likert item point	Probability range r_j
(1) Not likely at all.	0 – 0.2
(2) A little likely.	0.2 – 0.4
(3) Not likely nor unlikely.	0.4 – 0.6
(4) Very likely.	0.6 – 0.8
(5) Absolutely.	0.8 – 1

Table 1. Conversion of discrete vaccine willingness Likert score to continuous probability of getting vaccinated.

$$p(k + 1) = \Lambda W p(k) + (I_n - \Lambda)p(0), \tag{4}$$

where $\Lambda = \text{diag}\{[\lambda_1, \ldots, \lambda_n]^\text{T}\}$ encodes the susceptibilities of each individual and I_n is the identity matrix of size n. Moreover, W is a row-stochastic matrix that captures the structure of the graph $\mathcal{G}$, whereby its ij-th entry w_{ij} is $w_{ij} = 1/|\mathcal{N}_i|$ if $(i, j) \in \mathcal{E}$ and zero otherwise, with $|\cdot|$ denoting the cardinality of a set. Finally, $p(0)$ encodes the initial willingness of being vaccinated. Note that $\lambda_i = 0$ corresponds to a *zealot*[48,49], who never changes its opinion while actively trying to convince the others. Assuming that $\Lambda \neq I_n$, that is, there exists at least an agent i such that $\lambda_i < 1$, the vaccination probabilities will converge at steady-state toward[50]

$$\bar{p} = (I_n - \Lambda W)^{-1}(I_n - \Lambda)p(0), \tag{5}$$

where $\bar{p} = [\bar{p}_1, \ldots, \bar{p}_n]^\text{T}$. Knowing the distribution of all individual vaccination probabilities $p(k)$ allows computing the probability that, at time k, a given fraction of the population is willing to be vaccinated. Indeed, this event can be viewed as the outcome of a Poisson binomial experiment, which is a collection of n independent yes/no experiments with success probabilities $p_1(k), \ldots, p_n(k)$. The same consideration holds for the steady-state distribution $\bar{p}$.

Tuning the model parameters on real data. The parameters that need to be selected in model (4) are related to i) how individuals are connected, which is encapsulated by the network topology, described by matrix W, and ii) the inherent characteristics of each individual, captured by the susceptibilities $\lambda_1, \ldots, \lambda_n$, and by the initial probabilities $p_1(0), \ldots, p_n(0)$, a measure of their pre-existing attitude towards vaccines. The network matrix W has been borrowed from a Facebook social friendship network[42], composed by $n = 1446$ nodes, with $|\mathcal{E}| = 59600$ edges describing their mutual interactions. We have chosen the individual parameters so that the steady-state probabilities $\bar{p}$ in (5) are compatible with the outcome of a survey administered to a sample of Italian citizens[8]. Toward this goal, we first translated the survey outcome into target steady-state values $p^\star$, to then tune the susceptibilities λ_i and find a set of initial attitudes $p_i(0)$ so to obtain the $\bar{p}$ that best matches $p^\star$ in the least square sense (see Figure S7 of the Supplementary Information for a visualization of $\bar{p}$ and $p^\star$).

Description of the dataset from[8] and choice of $p^\star$. The authors of[8] tested the beliefs and attitudes of Italian citizens towards a possible COVID-19 vaccine through the administration of surveys, based on the Likert scale, to a stratified sample of 1004 individuals, representative of the Italian adult population aged between 18 and 70 years old. The respondents filled the survey during the first days following the end of Italy's strict lockdown begun in March 2020, when no vaccine was available yet. The survey contained general questions about their lives and health habits, as well as specific questions related to the COVID-19 pandemic. In this work, we focused on the 5th Likert item of the survey, which reads *'I am willing to vaccinate, if a vaccine against COVID-19 were to be found'*, with five options, ranging from 1 = *'not likely at all'* to 5 = *'absolutely'*, and computed the fraction f_j of agents choosing answer j to question 5, for $j = 1, \ldots, 5$.

Accordingly, we partitioned our social network of $n = 1446$ nodes into 5 classes, where the j-th class is populated by the $c_j = f_j n$ agents expected to choose option i. As $f_j n$ is not necessarily an integer, it is rounded so that $\sum_{i=1}^5 c_j = n$, and each agent is randomly assigned to each class. We then converted the categorical values of the Likert scale into continuous values in the interval [0, 1] following the approach in[51], and splitting it in 5 sub-intervals, one for each class (alternative approaches have been proposed e.g. in[52,53]). Namely, the jth class was associated to a range $r_j = [0.2(j - 1), 0.2j]$, $j = 1, \ldots, 5$, where the steady-state vaccination probabilities $p^\star$ should lie, see Table 1. Given an agent i assigned to class j, the steady-state vaccination probability $p_i^\star$ has been extracted from a uniform distribution in r_j.

Selection of the behavioral parameters λ and $p(0)$. Once we generated target steady-state probabilities $p^\star$ as explained above, we selected the individual parameters in our network so that the network dynamics converge to the steady-state vaccination probability $\bar{p}$ that is the closest possible to $p^\star$ in the least square sense. Namely,

$$\min_{\lambda, p(0)} \left\| \bar{p} - p^\star \right\|^2 \tag{6a}$$

subject to

$$0 \le p_i(0) \le 1, \qquad\qquad i = 1, \ldots, n, \tag{6b}$$

$$\lambda^{\mathrm{T}} \mathbb{1}_n = \rho n, \quad 0 \le \lambda_i \le 1, \quad i = 1, \ldots, n, \tag{6c}$$

$$\frac{\lfloor 5p_i^{\star} \rfloor}{5} < \bar{p}_i \le \frac{\lceil 5p_i^{\star} \rceil}{5}, \qquad i = 1, \ldots, n, \tag{6d}$$

$$\bar{p} = (I_n - \Lambda W)^{-1} (I_n - \Lambda) p(0), \tag{6e}$$

where $\lfloor \cdot \rfloor$ and $\lceil \cdot \rceil$ map a real number to its previous or next integer, respectively, and $\mathbb{1}_n$ is the vector of all ones. Notice that the set of enforced constraints (6b)–(6e) guarantee that the outcome of the optimization is meaningful. Indeed, constraint (6b) guarantees that the probabilities lie in [0, 1], (6c) that the average susceptibility to the neighbors' opinion is $0 < \rho < 1$ and the individual susceptibilities belong to [0, 1], whereas (6d) enforces that if $p_i^{\star} \in r_j$, then also $\bar{p}_i \in r_j$, that is, each agents stays in the target class identified by $p^{\star}$. Finally, constraint (6e) ensures that the steady-state values $\bar{p}$ are compatible with the dynamics (4). In all our numerical analysis, we selected the largest value of ρ for which problem (6) admits a solution, that is, $\rho = 0.58$. However, our main results would still hold for lower values of ρ, see Supplementary Information S2 for further details.

Incorporating the effect of pro-vaccine campaigns. Once the model has been tuned following the steps described above, we used it to test the effect of alternative pro-vaccine campaigns. According to the Friedkin-Johnsen model, the individuals can neither change their own belief nor their susceptibility, thereby in the time-scale of a campaign we can only act on the social interaction term $\lambda W p(k)$ in (4). Specifically, we model the effect of the vaccination campaign on agent i as the addition of a virtual neighbor l whose probability p_l of being vaccinated is equal to 1 for all k. Agent i will weigh the opinion of this virtual agent proportionally to the intensity of the vaccination campaign. In formal terms, Eq. (4) modifies as

$$p(k + 1) = \Lambda \left((I_n - \alpha \Delta) W p(k) + \alpha \delta p_l \right) + (I_n - \Lambda) p(0), \tag{7}$$

where $\delta = [\delta_1, \ldots, \delta_n]^{\mathrm{T}}$, with δ_i being 1 if node i is targeted by the campaign, and 0 otherwise, $\Delta = \mathrm{diag}\{\delta\}$, $0 \le \alpha \le 1$ quantifies the intensity of the vaccination campaign, $p_l = 1$ is the vaccination probability the campaign is targeting, and we set $p(0) = \bar{p}$. Namely, $\alpha = 0$ corresponds to no effect, whereas $\alpha = 1$ to the agents disregarding the opinion of the other neighbors, and only considering the that of the virtual neighbor l. The same approach can be used to incorporate the effect of hoaxes and misinformation, just by setting p_l to zero.

Data availability
The survey raw data on vaccine willingness are publicly accessible from the Supplementary Information of[8] available online. The network topology that we have used as reference in this work is publicly available from the repository[42] under the name "Socfb-Haverford-76".

Code availability
ll code for the model is publicly available on Open Science Framework (OSF) https://osf.io/7ndmx/?view_only=e0afacbe567147b0ad72ee1fce416c45.

References
1. Dror, A. A. *et al.* Vaccine hesitancy: the next challenge in the fight against COVID-19. *Eur. J. Epidemiol.* **35**, 775–779 (2020).
2. Aschwanden, C. Five reasons why COVID herd immunity is probably impossible. *Nature* **591**, 520–522 (2021).
3. Ophir, Y. et al. Vaccine hesitancy under the magnifying glass: A systematic review of the uses and misuses of an increasingly popular construct. Health Commun., 1–15 (2022).
4. Feemster, K. A. & Szipszky, C. Resurgence of measles in the United States: how did we get here?. *Curr. Opin. Pediatr.* **32**, 139–144 (2020).
5. Wilder-Smith, A. B. & Qureshi, K. Resurgence of measles in Europe: a systematic review on parental attitudes and beliefs of measles vaccine. *J. Epidemiol. Glob. Health* **10**, 46 (2020).
6. Dimala, C. A., Kadia, B. M., Nji, M. A. M. & Bechem, N. N. Factors associated with measles resurgence in the United States in the post-elimination era. *Sci. Rep.* **11**, 1–10 (2021).
7. Lazarus, J. V. *et al.* A global survey of potential acceptance of a COVID-19 vaccine. *Nat. Med.* **27**, 225–228 (2021).
8. Graffigna, G., Palamenghi, L., Boccia, S. & Barello, S. Relationship between citizens' health engagement and intention to take the COVID-19 vaccine in Italy: a mediation analysis. Vaccines **8** (2020).
9. Peretti-Watel, P. et al. A future vaccination campaign against COVID-19 at risk of vaccine hesitancy and politicisation. *Lancet. Infect. Dis* **20**, 769–770 (2020).
10. Bauch, C. T. & Earn, D. J. D. Vaccination and the theory of games. *Proc. Natl. Acad. Sci.* **101**, 13391–13394 (2004).
11. Islam, M. S. *et al.* COVID-19 vaccine rumors and conspiracy theories: The need for cognitive inoculation against misinformation to improve vaccine adherence. *PLoS ONE* **16**, e0251605 (2021).
12. Steffens, M. S., Dunn, A. G., Leask, J. & Wiley, K. E. Using social media for vaccination promotion: Practices and challenges. *Digital Health* **6**, 2055207620970785 (2020).
13. MacDonald, N. E. *et al.* Vaccine hesitancy: Definition, scope and determinants. *Vaccine* **33**, 4161–4164 (2015).

14. Chou, W.-Y.S. & Budenz, A. Considering Emotion in COVID-19 vaccine communication: addressing vaccine hesitancy and fostering vaccine confidence. *Health Commun.* **35**, 1718–1722 (2020).
15. Kestenbaum, L. A. & Feemster, K. A. Identifying and addressing vaccine hesitancy. *Pediatr. Ann.* **44**, e71–e75 (2015).
16. Amin, A. B. *et al.* Association of moral values with vaccine hesitancy. *Nat. Hum. Behav.* **1**, 873–880 (2017).
17. Hussain, A. & Sheikh, A. Opportunities for artificial intelligence–enabled social media analysis of public attitudes toward Covid-19 vaccines. NEJM Catal. Innov. Care Delivery **2** (2021).
18. Liu, Y.-Y & Barabási, A.-L. Control principles of complex systems. *Rev. Mod. Phys.* **88**, 035006 (2016).
19. Lo Iudice, F., Garofalo, F. & Sorrentino, F. Structural permeability of complex networks to control signals. Nat. Commun. **6**, 1–6 (2015).
20. Della Rossa, F. et al. A network model of Italy shows that intermittent regional strategies can alleviate the COVID-19 epidemic. Nat. Commun. **11**, 1–9 (2020).
21. Garofalo, F., LoIudice, F. & Napoletano, E. Herding as a consensus problem. *Nonlinear Dyn.* **92**, 25–32 (2018).
22. Ye, M., Qin, Y., Govaert, A., Anderson, B. D. O. & Cao, M. An influence network model to study discrepancies in expressed and private opinions. *Automatica* **107**, 371–381 (2019).
23. Weisbuch, G. Bounded confidence and social networks. *Eur. Phys. J. B* **38**, 339–343 (2004).
24. Hegselmann, R., Krause, U., et al. Opinion dynamics and bounded confidence models, analysis, and simulation. J. Artif. Soc. Soc. Simul. **5** (2002).
25. Dandekar, P., Goel, A. & Lee, D. T. Biased assimilation, homophily, and the dynamics of polarization. *Proc. Natl. Acad. Sci.* **110**, 5791–5796 (2013).
26. Javarone, M. A. Social influences in opinion dynamics: the role of conformity. *Physica A* **414**, 19–30 (2014).
27. Krapivsky, P. L. & Redner, S. Dynamics of majority rule in two-state interacting spin systems. *Phys. Rev. Lett.* **90**, 238701 (2003).
28. Bizyaeva, A., Franci, A. & Leonard, N. E. Nonlinear opinion dynamics with tunable sensitivity. IEEE Trans. Autom. Control (2022).
29. Altafini, C. Consensus problems on networks with antagonistic interactions. *IEEE Trans. Autom. Control* **58**, 935–946 (2012).
30. Altafini, C. & Ceragioli, F. Signed bounded confidence models for opinion dynamics. *Automatica* **93**, 114–125 (2018).
31. Tangredi, D., Iervolino, R. & Vasca, F. Consensus stability in the Hegselmann-Krause model with coopetition and cooperosity. *IFAC-PapersOnLine* **50**, 11920–11925 (2017).
32. Hofman, J. M. et al. Integrating explanation and prediction in computational social science. Nature, 1–8 (2021).
33. Friedkin, N. E. & Johnsen, E. C. Social influence and opinions. *J. Math. Sociol.* **15**, 193–206 (1990).
34. DeLellis, P., Garofalo, F. & Lo Iudice, F. The partial pinning control strategy for large complex networks. *Automatica* **89**, 111–116 (2018).
35. Sorrentino, F., di Bernardo, M., Garofalo, F. & Chen, G. Controllability of complex networks via pinning. *Phys. Rev. E* **75**, 046103 (2007).
36. Guardian, T. https://www.theguardian.com/world/2021/mar/05/covid-vaccine-adsaim-to-influence-without-alienating-people (2021).
37. Department, A. G. H. https://www.health.gov.au/news/new-information-campaignto-encourage-australians-to-get-a-covid-19-vaccine (2021).
38. News, N. https://www.nbcnews.com/health/health-news/sweeping-ad-campaignwill-encourage-vaccinations-rcna309 (2021)
39. Muric, G., Wu, Y. & Ferrara, E. COVID-19 vaccine hesitancy on social media: building a public Twitter dataset of anti-vaccine content, vaccine misinformation and conspiracies. *JMIR Public Health Surveill.* **7**, e20642 (2021).
40. Piedrahita-Valdés, H. *et al.* Vaccine hesitancy on social media: Sentiment analysis from June 2011 to April 2019. *Vaccines* **9**, 28 (2021).
41. Kosinski, M., Stillwell, D. & Graepel, T. Private traits and attributes are predictable from digital records of human behavior. *Proc. Natl. Acad. Sci.* **110**, 5802–5805 (2013).
42. Rossi, R. A. & Ahmed, N. K. The network data repository with interactive graph analytics and visualization in AAAI (2015). http://networkrepository.com.
43. Trentini, F. *et al.* Pressure on the health-care system and intensive care utilization during the COVID-19 outbreak in the lombardy region of Italy: A retrospective observational study in 43,538 hospitalized patients. *Am. J. Epidemiol.* **191**, 137–146 (2022).
44. Asadi Someh, I., Breidbach, C. F., Davern, M. & Shanks, G. Ethical implications of big data analytics. Res. Progress Papers **24** (2016).
45. Østergaard, S. D., Schmidt, M., Horváth-Puhó, E., Thomsen, R. W. & Sørensen, H. T. Thromboembolism and the Oxford-Astra-Zeneca COVID-19 vaccine: Side-effect or coincidence?. *The Lancet* **397**, 1441–1443 (2021).
46. Larson, H. J. & Broniatowski, D. A. Volatility of vaccine confidence. *Science* **371**, 1289–1289 (2021).
47. Modani, N. et al. Like-minded communities: bringing the familiarity and similarity together. *World Wide Web* **17**, 899–919 (2014).
48. Cardillo, A. & Masuda, N. Critical mass effect in evolutionary games triggered by zealots. *Physical Review Research* **2**, 023305 (2020).
49. Verma, G., Swami, A. & Chan, K. The impact of competing zealots on opinion dynamics. *Physica A* **395**, 310–331 (2014).
50. Proskurnikov, A. V. & Tempo, R. A tutorial on modeling and analysis of dynamic social networks. Part I.. *Ann. Rev. Control* **43**, 65–79 (2017).
51. Polemi, N. in Securing Critical Information Infrastructures and Supply Chains (Elsevier, 2017).
52. Sullivan, G. M. & Artino, A. R. Jr. Analyzing and interpreting data from Likert-type scales. *J. Grad. Med. Educ.* **5**, 541 (2013).
53. Carifio, J. & Perla, R. Resolving the 50-year debate around using and misusing Likert scales. *Med. Educ.* **42**, 1150–1152 (2008).

Acknowledgements

Author contributions

F.G. conceived the research and supervised the project together with P.D.; F.L.I and P.D. devised the methods underlying the investigation; C.A. designed and performed the numerical analysis. All authors wrote the manuscript.

Competing interests

The authors declare no competing interests.

Additional information

Supplementary information The online version contains supplementary material available at https://doi.org/10.1038/s41598-022-15082-0.

Correspondence and requests for materials should be addressed to F.G. or P.L.

Reprints and permissions information is available at www.nature.com/reprints.

Publisher's note Springer Nature remains neutral with regard to jurisdictional claims in published maps and institutional affiliations.

A Model-based Opinion Dynamics Approach to Tackle Vaccine Hesitancy

Camilla Ancona[1,2,†], Francesco Lo Iudice[1,†], Franco Garofalo[1,*],
Pietro De Lellis[1,*]

[1] *Departiment of Electrical Engineering and Information
Techonology, University of Naples Federico II, Via Claudio 21,
80125 Italy*
[2] *Departiment of Management, Information and Production
Engineering, University of Bergamo, via dei Caniana 2, 24127
Italy*
[†] *These authors contributed equally*
[*] *Corresponding authors: franco.garofalo@unina.it;
pietro.delellis@unina.it*

S1   Mean and variance of Y_n as a function of n

The model presented interprets each agent's opinion as its probability p_i of getting vaccinated. We can then associate to each agent $i = 1, \ldots, n$ independent Bernoulli variables $X_1, \ldots, X_n$, with *heterogeneous* probability of success $p_1, \ldots, p_n$, respectively. As our ultimate goal is to estimate the expected *fraction* of the population that will get vaccinated, we define the stochastic variable

$$Y_n = \frac{1}{n} \sum_{i=1}^{n} X_i,$$

whose expected value and variance can be computed as

$$E[Y_n] = \frac{1}{n} \sum_{i=1}^{n} p_i, \quad \text{Var}[Y_n] = \frac{1}{n^2} \sum_{i=1}^{n} p_i(1 - p_i), \tag{S1}$$

respectively.

Note that Y_i is a Poisson binomial distribution (scaled by the factor $1/n$), that is the sum of n independent Bernoulli distributions. Here, we study how its moments scale with the population size n. Denoting $n_0 = 1446$ the number of participants to the survey on which the opinion dynamics model is parametrized in the main text, we scale the population as multiples of n_0, so that we can always associate a vaccination probability p_i to a fraction $1/n_0$ of the total population n, for all $i = 1, \ldots, n_0$. Specifically, we introduce the parameter $\beta_k := \lfloor l_k/n_0 \rceil$ with $l_k = 10^k$, and $k = 4, \ldots, 7$. This gimmick allows us to inspect the behaviour of the moments of the Poisson Binomial distribution when the size of the population is $n = \beta_k n_0$. In turn, from equation (S1) this reflects into the following scaling behavior of the first and second moment of Y_n

$$E[Y_n] = \frac{1}{\beta_k n_0} \sum_{i=1}^{n_0} \beta_k E(X_i) = \frac{1}{n_0} \sum_{i=1}^{n_0} p_i = E[Y_{n_0}]. \tag{S2a}$$

$$\mathrm{Var}[Y_n] = \frac{1}{(\beta_k n_0)^2} \sum_{i=1}^{n_0} \beta_k p_i (1 - p_i) = \frac{1}{\beta_k} \mathrm{Var}[Y_{n_0}]. \tag{S2b}$$

Hence,

- the expected value $\mathrm{E}[Y_n]$ of the fraction of the population that will get a shot of vaccine does not change with the population size;

- the variance $\mathrm{Var}[Y_n]$ decreases linearly with the population size.

Table S1 reports the mean and variance of Y_n for different orders of magnitudes for l_k, whereas Figure S1 the error bar of the fraction of vaccinated population as a function of the population size n.

l_k	β_k	$\mathrm{E}[Y_n]$	$\mathrm{Var}[Y_n]$
10^4	7	0.6171	1.773e-05
10^5	69	0.6171	1.799e-06
10^6	692	0.6171	1.793e-07
10^7	6916	0.6171	1.794e-08

Table S1: First and second moment of Y_n as the population size $n = \beta_k n_0$ varies.
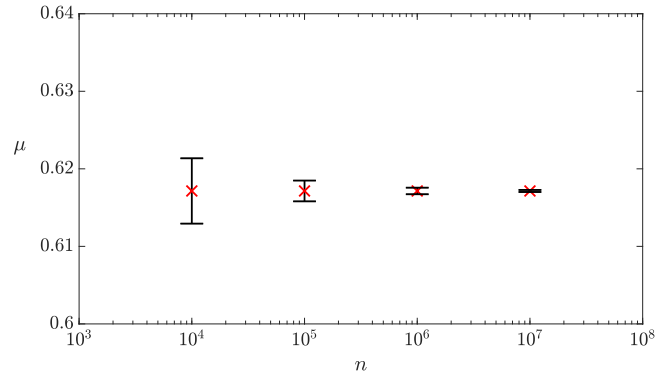
Figure S1: Error bar plot of the mean and standard deviation of Y_n.

S2   Parametric analysis of ρ

In the second subsection of the Methods section of the main text, we presented a constrained least square optimization problem aimed to realistically calibrate the model parameters consistently with survey data. In particular, in the in the main text we explained that constraint (4c) sets the average susceptibility to be equal to a value ρ, and that problem (4) admits a solution only if $\rho \leq 0.58$. In the main text, all the analysis have been performed for $\rho = 0.58$. Here, we perform a parametric analysis of the results whereby we vary ρ in the interval $[0.18, 0.48]$ with step 0.1. Figure S2 illustrates that the results are qualitatively similar, the only difference being the attenuated effectiveness of all the strategies, since lower values of the λ_i correspond to a more stubborn population.

3

Figure S2: Comparison of targeted and traditional mass campaigns for different values of the average susceptibility ρ (set to $0.18, 0.28, 0.38,$ and 0.48, from top to bottom). The left panels depict, for each effort η, the additional population fraction $\Delta_\mu^\star$ and Δ_μ^0 that is expected to be vaccinated when the best targeted campaign (identified by circles) or the mass campaign (identified by triangles) are employed, respectively. The right panels display for each effort η and targeted stra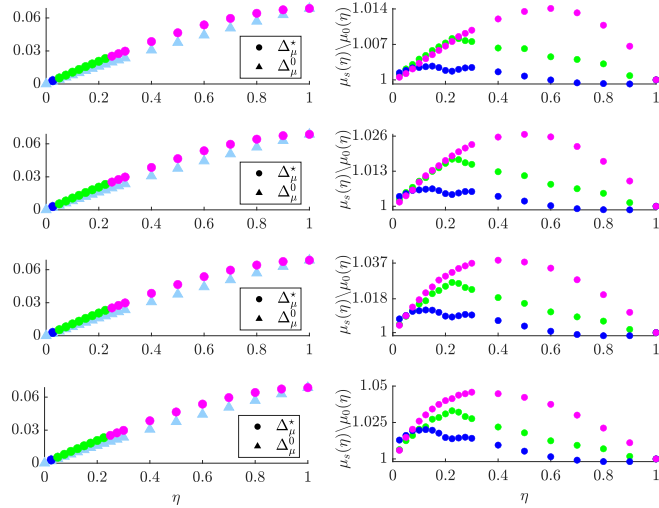tegy s, the ratio between the fractions of the population $\mu_s(\eta)$ and $\mu_0(\eta)$ that are expected to be vaccinated when strategy s and the traditional campaign are employed, respectively. In all panels, Strategies 1, 2, 3 are depicted in blue, green, and magenta, respectively, and the intensity of the vaccination campaign is set to $\alpha = 1$.

S3   Robustness analysis

To test the robustness of our results we have run additional simulations varying the graph through which opinions diffuse. To do so, we repeated the same analysis performed in the main text on a pool of real and synthetic networks, whereby we compared the effectiveness of the targeted campaigns to that of mass campaigns. As shown in Figures S3-S6, the results are consistent with the case illustrated in the main text, that is, the targeted campaigns always outperforms the traditional mass-media ones.

The pool of synthetic networks is made of 10 unweighted undirected graphs of size $N = 1500$, extracted from a Scale-Free distribution with exponent $\gamma = 2.8$ and average degree $k_{av} = 80$, consistently with the properties of the real online

social networks reported in [1], and repeated the same analysis performed in the main text. The 3 real networks, called soc-fbHamilton46, socfb-Simmons81 and Hamsterster, have been retrieved from the network repository [1].

Figure S3: Comparison of targeted and traditional mass campaigns effectiveness averaged on a pool of 10 Scale-Free synthetic networks. The left panels depict, for each effort η, the additional population fraction $\Delta_\mu^\star$ and Δ_μ^0 that is expected to be vaccinated when the best targeted campaign (identified by circles) or the mass campaign (identified by triangles) are employed, respectively. The right panels display for each effort η and targeted strategy s, the ratio between the fractions of the population $\mu_s(\eta)$ and $\mu_0(\eta)$ that are expected to be vaccinated when strategy s and the traditional campaign are employed, respectively. In all panels, Strategies 1, 2, 3 are depicted in blue, green, and magenta, respectively, and the intensity of the vaccination campaign is set to $\alpha = 1$.

Figure S4: Comparison of targeted and traditional mass campaigns. The graph deployed is an unweighted undirected network of Facebook friendships. The number of nodes $N = 2300$, the number of edges $|\epsilon| = 96400$, the average degree $k_{av} = 83$.
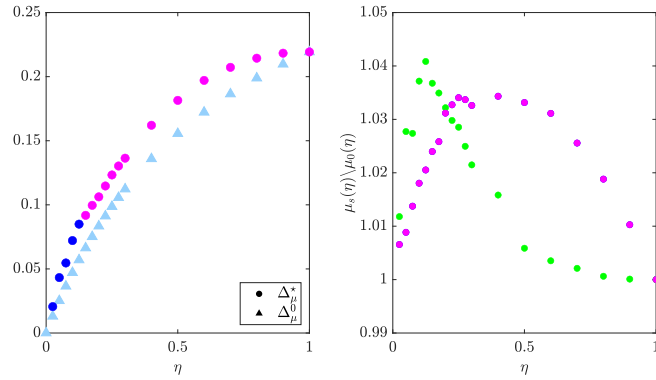
Figure S5: Comparison of targeted and traditional mass campaigns. The graph deployed is an unweighted undirected network of the friendships and family links between users of the website `http://www.hamsterster.com.`. The number of nodes $N = 2400$, the number of edges $|\epsilon| = 16600$, the average degree $k_{av} = 13$.
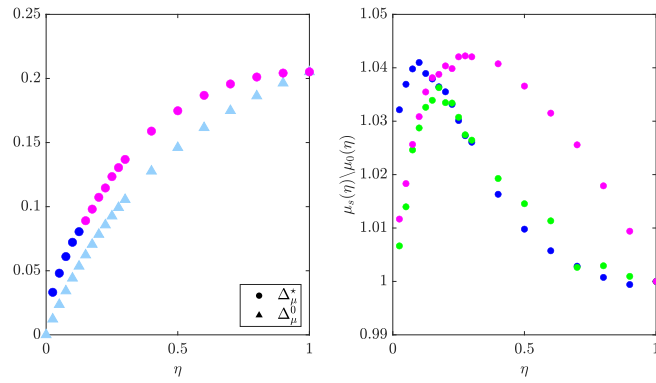
Figure S6: Comparison of targeted and traditional mass campaigns. The graph deployed is an unweighted undirected network of Facebook friendships. The number of nodes $N = 1500$, the number of edges $|\epsilon| = 33000$, the average degree $k_{av} = 43$.

7

S4   Supplementary Figure

In Figure S7, we report a graphical representation of the calibration procedure described in the Methods Section of the main text.
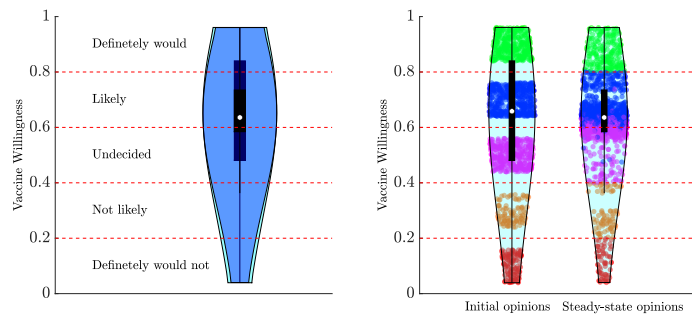
Figure S7: Violin plots of the steady-state opinion distribution from the model calibrated as described in the Methods (light blue), with that obtained from the survey data (blue), respectively. On the right, the violin plots of the initial and final opinions distribution of vaccine willingness, respectively. Data points corresponding to agents' opinions in the two endpoints are colored accordingly to their Likert score on vaccine willingness survey.

References

[1] R. A. Rossi and N. K. Ahmed, "The network data repository with interactive graph analytics and visualization," in *AAAI*, 2015. [Online]. Available: http://networkrepository.com

APPENDIX B

Natural Language Processing

Natural Language Processing NLP can be defined as the application of computational techniques to analyze natural language.

This world combines elements of both machine learning and deep learning tools to understand textual data in a human-like way (see Figure B.1). NLP has a wide range of applications across various domains

1. Language Translation: NLP enables the automatic translation of text or speech from one language to another. Systems like Google Translate use NLP algorithms to understand the meaning of sentences in one language and generate equivalent sentences in another.

2. Sentiment Analysis: NLP can be used to determine the sentiment or emotional tone expressed in text data, such as social media posts or product reviews. It helps businesses understand customer feedback, track public sentiment about their products or services, and make data-driven decisions.
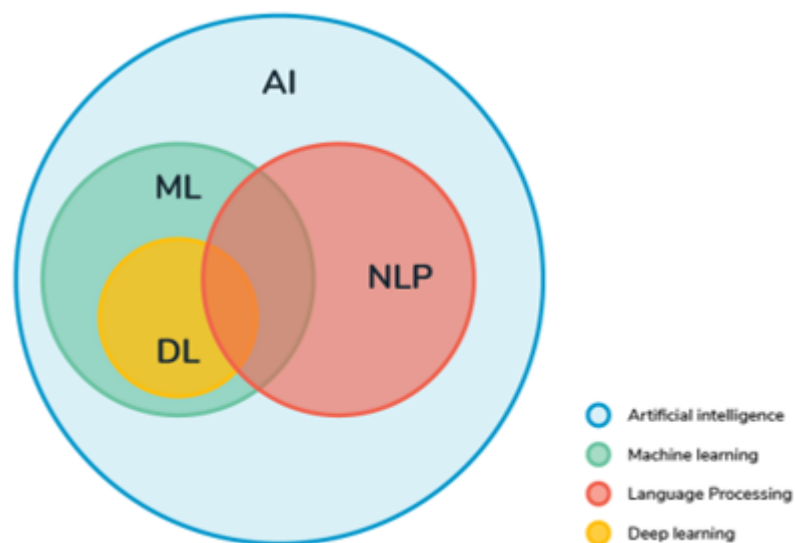
Figure B.1. Collocation of NLP in the Artificial Intelligence framework

3. Chatbots and Virtual Assistants: NLP powers chatbots and virtual assistants like Siri and Alexa, allowing them to understand and respond to natural language queries and commands. They can answer questions, perform tasks, or engage in conversations, making them useful for customer support and automation.

4. Text Summarization: NLP can automatically generate concise summaries of long texts, making it easier to grasp the key points and insights within large volumes of information. This is useful in news aggregation, document summarization, and content curation.

5. Named Entity Recognition (NER): NLP can identify and classify entities like names of people, places, organizations, and dates within text data. NER is used in information retrieval, content tagging, and data extraction for applications like news categorization and financial analysis.

6. Speech Recognition: NLP is employed in converting spoken language into written text. This technology is widely used in voice assistants, transcription services, and even in healthcare for converting doctor-patient conversations into electronic health records.

7. Language Generation: NLP models can generate human-like text, including creative writing, automated content generation, and even code generation. This is useful in content marketing, text generation for chatbots, and assisting developers in code completion.

8. Social Media Analysis: Businesses use NLP to monitor social media conversations, track brand mentions, and gauge customer sentiment. This information can inform marketing strategies and brand management.

9. Recommendation Systems: NLP is integrated into recommendation algorithms, such as those used by streaming platforms and e-commerce websites, to provide personalized content and product recommendations based on user preferences and behavior.

These applications demonstrate the versatility of NLP in improving efficiency, automation, and decision-making across numerous industries and domains. NLP continues to evolve with advancements in AI and machine learning, opening up new possibilities for natural language understanding and communication.

Opinion mining is a subfield of NLP whose goal is extracting information on individual beliefs from unstructured texts. Sentiment Analysis (SA) focuses on the sentiment detection by which the opinion of the examined text is assigned a positive or negative sentiment. Traditionally, the outcome of the classification is binary, however the refining of the techniques of text classification enabled also more sophisticated sentiment analyses, the so-called *fine-grained* ones, in which the classes are more than two, in order to also capture the intensity of the sentiment in a discrete scale, for e.g. from 1 to 5, retracing Likert scale.

B.1 Machine learning techniques

Sentiment analysis can be implemented via two main different approaches: lexicon-based approach or machine learning approach. The first one uses pre-prepared sentiment lexicon to score a document by aggregating the sentiment scores of all the words in the document. The pre-prepared sentiment lexicon should contain a word and corresponding sentiment score to it. This approach is divided into dictionary-based and corpus-based. The former involves making use of an online dictionary to tag words, while the latter relies on co-occurrence statistics or syntactic patterns embedded in text corpora, thus is more suitable for large documents. VADER (Valence Aware Dictionary and Sentiment Reasoner) and TextBlob are the most widely used NL library to analyze sentiments expressed in social media. The machine learning approach could be implemented either in an unsupervised or supervised way: in the first case it basically involves the usage of a traditional clustering algorithm, whereas for the supervised case Naive Bayes classifiers or Support Vector Machines are the most used tools. The advantage of using this approach rather than the simpler lexicon-based relies on the fact that it is more accurate as it can retain sequential dependencies among words. This is possible by means of Word Embedding: text first is preprocessed and converted into vectors. Embeddings translate large sparse vectors into a lower-dimensional space that preserves semantic relationships, modeling it in a numeric form. Word2vec [229] is a group of related models that are used to produce word embeddings. These models are two-layer neural networks that are trained to reconstruct linguistic contexts of words. Word2vec takes as its input a large corpus of text and produces a large vector space, with each unique word in the corpus being assigned a corresponding vector in the space. Word vectors are positioned in the vector space such that words that share common contexts in the corpus are located close to one another in the space. GloVe [230], aka Global Vectors, is a model for distributed word representation. The model maps words into a meaningful space, where the distance between words is related to semantic similarity. ELMo (Embeddings from Language Model) is a word embedding method for representing a sequence of words as a corresponding sequence of vectors. ELMo embeddings are context-sensitive, producing different representations for words that share the same spelling but have different meanings.
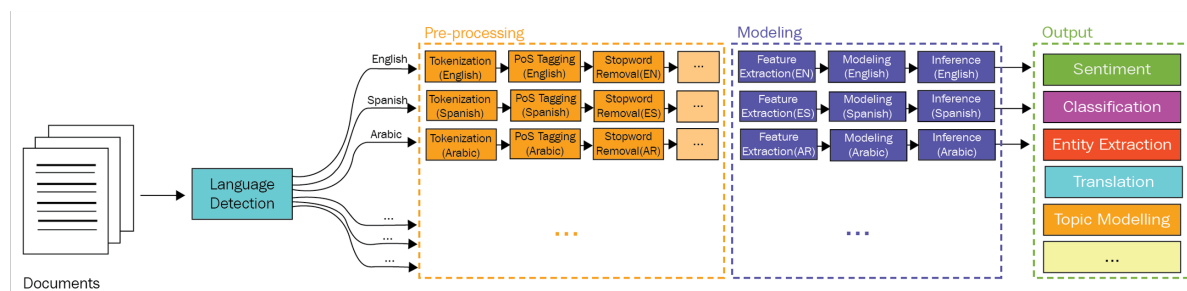

Figure B.2. Scheme of machine learning based sentiment analysis procedure

B.2   Deep learning techniques

Deep learning is an advanced machine learning method that outperforms the previous approaches that we briefly presented [231]. In recent years, NLP methods in the realm of deep learning have witnessed an unprecedented surge in advancement. These break-throughs have not merely improved our approach to working with human language; they have sparked a paradigm shift in the very fabric of linguistic analysis and comprehension. At the heart of these innovations lies the power of deep neural networks, which have emerged as the linchpin in our ability to model and process natural language text. By effectively harnessing the capabilities of deep learning, we've unlocked a host of remark-able tools and techniques that span the entire spectrum of language-related tasks, from basic text classification to nuanced language generation.

These NLP methods represent a quantum leap in our understanding of language, offering the means to extract intricate semantic nuances, detect sentiment, perform lan-guage translation, and even generate human-like text with an unprecedented level of accuracy and fluency. What's most striking is the versatility of these deep learning mod-els; they can be pre-trained on vast corpora of text and then fine-tuned for specific tasks, effectively transferring linguistic knowledge from one domain to another. This capability has not only made NLP models highly efficient but also less reliant on enormous labeled datasets, thereby democratizing access to advanced language processing technology.

Furthermore, the advent of architectures like the Transformer has ushered in a new era of context-aware language understanding. Transformers' self-attention mechanisms enable them to capture intricate relationships between words, making them exceptionally adept at tasks that require understanding context and contextually generating text. Models such as BERT and GPT have set benchmarks for a wide array of NLP tasks, from question answering to text summarization, and their pre-trained embeddings have become the cornerstone of countless NLP applications.

In summary, NLP methods in deep learning are not just a technological evolution; they represent a fundamental shift in how we interact with and understand human language. These methods, bolstered by the prowess of deep neural networks, have the potential to reshape industries, improve communication, and pave the way for innovative applications in areas like healthcare, education, and customer service. As we continue to explore the vast capabilities of NLP in deep learning, the boundaries of what we can achieve with language-driven technology are continually expanding, promising a future where human-machine interaction becomes more natural and intuitive than ever before.

We will focus on a particular deep learning framework for text analysis that is BERT. BERT represents the state-of-the-art model for a wide range of NLP tasks, including sentiment analysis.

BERT stands for Bidirectional Encoder Representations from Transformers. Trans-former is an architecture for transforming one sequence into another by means of En-coder and Decoder without any Recurrent Neural Networks. BERT generates a language model by means of an Encoder to learn contextual relations between words in a text. It reads the entire sequence of words at once (bidirectionally) learning the context of a
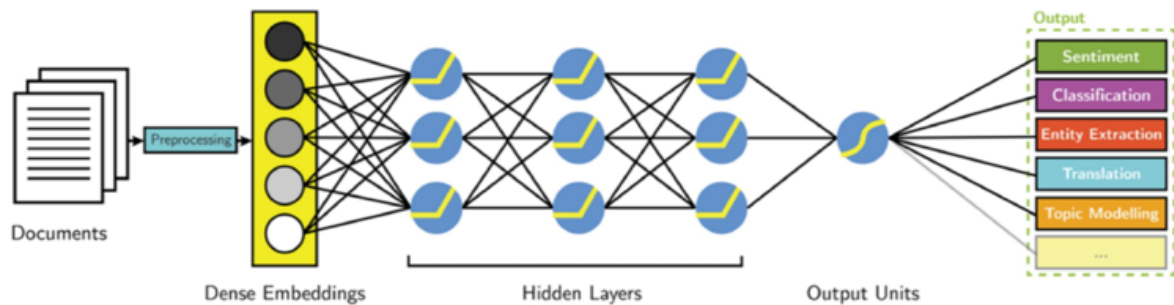
Figure B.3. Scheme of deep learning based sentiment analysis procedure

word based on all of its surroundings (left and right of the word). The contextualized embedding is achieved thanks to the idea of self-attention. Indeed, to comprehend language, it is not sufficient to understand the individual words that make up a sentence but how words relate to each other in the context. BERT approach for solving NLP tasks became a 2-step semi-supervised process:

- Train a language model on a large unlabeled text corpus (unsupervised)

- Fine-tune this large model (initialized with the pretrained parameters) to specific tasks (supervised) with labeled data

BERT is pretrained on two tasks:Masked Language Modelling (MLM) and Next Sentence Prediction (NSP). Masked language modeling is an example of autoencoding language modeling (the output is reconstructed from corrupted input) in BERT 15% of words in a sentence are typically masked and have the model predict those masked words given the other words in the sentence. By training the model with such an objective, it can essentially learn certain statistical properties of word sequences. As a result of the training process, BERT learns contextual embeddings for words. In the BERT training process, the model receives pairs of sentences as input and learns to predict if the second sentence in the pair is the subsequent sentence in the original document. To help the model distinguish between the two sentences in training, the input is processed in the following way before entering the model:

- A [CLS] token is inserted at the beginning of the first sentence and a [SEP] token is inserted at the end of each sentence.

- A sentence embedding indicating Sentence A or Sentence B is added to each token.

- A positional embedding is added to each token to indicate its position in the sequence.

First, BERT is pre-trained on a large corpus of unlabeled text, including the entire Wikipedia (2,500 million words) and Book Corpus (800 million words). Fine-tune BERT regenerates all word embeddings starting from a specific domain pre-labeled text corpus only by means of an additional feedforward layer.

Bibliography

[1] L. O. Chua, "Chua circuit," *Scholarpedia*, vol. 2, no. 10, p. 1488, 2007.

[2] R. A. Rossi and N. K. Ahmed, "The network data repository with interactive graph analytics and visualization," in *AAAI*, 2015.

[3] A. Wiek and A. I. Walter, "A transdisciplinary approach for formalized integrated planning and decision-making in complex systems," *European Journal of Operational Research*, vol. 197, no. 1, pp. 360–370, 2009.

[4] J. Beck, R. Kempener, B. Cohen, and J. Petrie, "A complex systems approach to planning, optimization and decision making for energy networks," *Energy policy*, vol. 36, no. 8, pp. 2795–2805, 2008.

[5] J. Rasmussen and M. Lind, "A model of human decision making in complex systems and its use for design of system control strategies," in *1982 American Control Conference*, pp. 270–276, IEEE, 1982.

[6] M. Lyons, I. Adjali, D. Collings, and K. Jensen, "Complex systems models for strategic decision making," *BT Technology Journal*, vol. 21, no. 2, pp. 11–27, 2003.

[7] S. H. Strogatz, "Exploring complex networks," *Nature*, vol. 410, no. 6825, pp. 268–276, 2001.

[8] A.-L. Barabási, "Network science," *Philosophical Transactions of the Royal Society A: Mathematical, Physical and Engineering Sciences*, vol. 371, no. 1987, p. 20120375, 2013.

[9] C. Godsil and G. F. Royle, *Algebraic graph theory*, vol. 207. Springer Science & Business Media, 2001.

[10] P. Erdős, A. Rényi, *et al.*, "On the evolution of random graphs," *Publ. math. inst. hung. acad. sci*, vol. 5, no. 1, pp. 17–60, 1960.

[11] D. J. Watts and S. H. Strogatz, "Collective dynamics of 'small-world' networks," *Nature*, vol. 393, pp. 440–442, June 1998.

[12] A.-L. Barabási and R. Albert, "Emergence of scaling in random networks," *science*, vol. 286, no. 5439, pp. 509–512, 1999.

[13]   K.-I. Goh, B. Kahng, and D. Kim, "Universal behavior of load distribution in scale-free networks," *Physical review letters*, vol. 87, no. 27, p. 278701, 2001.

[14]   M. E. J. Newman, "The Structure and Function of Complex Networks," *SIAM Rev.*, vol. 45, pp. 167–256, Jan. 2003.

[15]   P. Bonacich, "Power and centrality: A family of measures," *American journal of sociology*, vol. 92, no. 5, pp. 1170–1182, 1987.

[16]   L. C. Freeman *et al.*, "Centrality in social networks: Conceptual clarification," *Social network: critical concepts in sociology. Londres: Routledge*, vol. 1, pp. 238–263, 2002.

[17]   C. W. Wu, *Synchronization in complex networks of nonlinear dynamical systems*. World scientific, 2007.

[18]   P. DeLellis, M. Di Bernardo, and D. Liuzza, "Convergence and synchronization in heterogeneous networks of smooth and piecewise smooth systems," *Automatica*, vol. 56, pp. 1–11, 2015.

[19]   F. Bullo, *Lectures on network systems*, vol. 1. Kindle Direct Publishing Seattle, DC, USA, 2020.

[20]   Y. Tang, F. Qian, H. Gao, and J. Kurths, "Synchronization in complex networks and its application–a survey of recent advances and challenges," *Annual Reviews in Control*, vol. 38, no. 2, pp. 184–198, 2014.

[21]   S. Roy and N. Abaid, "Leader-follower consensus and synchronization in numerosity-constrained networks with dynamic leadership," *Chaos: An Interdisciplinary Journal of Nonlinear Science*, vol. 26, no. 11, 2016.

[22]   Y.-Y. Liu and A.-L. Barabási, "Control principles of complex systems," *Reviews of Modern Physics*, vol. 88, no. 3, p. 035006, 2016.

[23]   E. D. Sontag, *Mathematical control theory: deterministic finite dimensional systems*, vol. 6. Springer Science & Business Media, 2013.

[24]   F. Lo Iudice, F. Garofalo, and F. Sorrentino, "Structural permeability of complex networks to control signals," *Nature communications*, vol. 6, no. 1, pp. 1–6, 2015.

[25]   S. Hosoe, "Determination of generic dimensions of controllable subspaces and its application," *Automatic Control, IEEE Transactions on*, vol. 25, pp. 1192–1196, Dec 1980.

[26]   U. Forssell and L. Ljung, "Closed-loop identification revisited," *Automatica*, vol. 35, no. 7, pp. 1215–1241, 1999.

[27] M. Anguelova, *Nonlinear Observability and Identi ability: General Theory and a Case Study of a Kinetic Model for S. cerevisiae.* Chalmers Tekniska Hogskola (Sweden), 2004.

[28] Y.-Y. Liu, J.-J. Slotine, and A.-L. Barabási, "Controllability of complex networks," *Nature*, vol. 473, no. 7346, pp. 167–173, 2011.

[29] R. Shields and J. Pearson, "Structural controllability of multiinput linear systems," *IEEE Transactions on Automatic control*, vol. 21, no. 2, pp. 203–212, 1976.

[30] C.-T. Lin, "Structural controllability," *Automatic Control, IEEE Transactions on*, vol. 19, pp. 201–208, Jun 1974.

[31] X. F. Wang and G. Chen, "Pinning control of scale-free dynamical networks," *Physica A: Statistical Mechanics and its Applications*, vol. 310, no. 3-4, pp. 521–531, 2002.

[32] F. Sorrentino, M. di Bernardo, F. Garofalo, and G. Chen, "Controllability of complex networks via pinning," *Phys. Rev. E*, vol. 75, p. 046103, Apr. 2007. Publisher: American Physical Society.

[33] P. DeLellis, F. Garofalo, and F. Lo Iudice, "The partial pinning control strategy for large complex networks," *Automatica*, vol. 89, pp. 111–116, Mar. 2018.

[34] W. Lu, X. Li, and Z. Rong, "Global stabilization of complex networks with digraph topologies via a local pinning algorithm," *Automatica*, vol. 46, pp. 116–121, Jan. 2010.

[35] W. Yu, G. Chen, *et al.*, "Synchronization via pinning control on general complex networks," *SIAM Journal on Control and Optimization*, vol. 51, no. 2, pp. 1395–1416, 2013.

[36] B. Anderson and M. Ye, "Recent advances in the modelling and analysis of opinion dynamics on influence networks," *International Journal of Automation and Computing*, vol. 16, no. 2, pp. 129–149, 2019.

[37] M. Ye, Y. Qin, A. Govaert, B. D. Anderson, and M. Cao, "An influence network model to study discrepancies in expressed and private opinions," *Automatica*, vol. 107, pp. 371–381, 2019.

[38] Y. Dong, M. Zhan, G. Kou, Z. Ding, and H. Liang, "A survey on the fusion process in opinion dynamics," *Information Fusion*, vol. 43, pp. 57–65, Sept. 2018.

[39] A. Sîrbu, V. Loreto, V. D. Servedio, and F. Tria, "Opinion dynamics: models, extensions and external effects," *Participatory sensing, opinions and collective awareness*, pp. 363–401, 2017.

[40] K. Sznajd-Weron and J. Sznajd, "Opinion evolution in closed community," *International Journal of Modern Physics C*, vol. 11, no. 06, pp. 1157–1165, 2000.

[41] R. Durrett, J. P. Gleeson, A. L. Lloyd, P. J. Mucha, F. Shi, D. Sivakoff, J. E. Socolar, and C. Varghese, "Graph fission in an evolving voter model," *Proceedings of the National Academy of Sciences*, vol. 109, no. 10, pp. 3682–3687, 2012.

[42] M. H. DeGroot, "Reaching a consensus," *Journal of the American Statistical Association*, vol. 69, no. 345, pp. 118–121, 1974.

[43] N. E. Friedkin and E. C. Johnsen, "Social influence and opinions," *Journal of Mathematical Sociology*, vol. 15, no. 3-4, pp. 193–206, 1990.

[44] G. Deffuant, D. Neau, F. Amblard, and G. Weisbuch, "Mixing beliefs among interacting agents," *Advances in Complex Systems*, vol. 3, no. 01n04, pp. 87–98, 2000.

[45] G. Weisbuch, G. Deffuant, F. Amblard, and J.-P. Nadal, "Meet, discuss, and segregate!," *Complexity*, vol. 7, no. 3, pp. 55–63, 2002.

[46] R. Hegselmann, U. Krause, *et al.*, "Opinion dynamics and bounded confidence models, analysis, and simulation," *Journal of Artificial Societies and Social Simulation*, vol. 5, no. 3, 2002.

[47] V. Sood and S. Redner, "Voter model on heterogeneous graphs," *Physical review letters*, vol. 94, no. 17, p. 178701, 2005.

[48] S. Galam, "Contrarian Deterministic Effect: the "Hung Elections Scenario"," *Physica A: Statistical Mechanics and its Applications*, vol. 333, pp. 453–460, Feb. 2004. arXiv: cond-mat/0307404.

[49] R. A. Holley and T. M. Liggett, "Ergodic theorems for weakly interacting infinite systems and the voter model," *The annals of probability*, pp. 643–663, 1975.

[50] J. R. French Jr, "A formal theory of social power.," *Psychological review*, vol. 63, no. 3, p. 181, 1956.

[51] A. V. Proskurnikov and R. Tempo, "A tutorial on modeling and analysis of dynamic social networks. part i," *Annual Reviews in Control*, vol. 43, pp. 65–79, 2017.

[52] C. Altafini, "Opinion dynamics on social networks," 2023. `https://people.isy.liu.se/en/rt/claal20/OpinDynSocNet/Notes_OpinionDyn.pdf`.

[53] N. E. Friedkin, "The problem of social control and coordination of complex systems in sociology: A look at the community cleavage problem," *IEEE Control Systems Magazine*, vol. 35, no. 3, pp. 40–51, 2015.

[54] N. E. Friedkin, P. Jia, and F. Bullo, "A theory of the evolution of social power: Natural trajectories of interpersonal influence systems along issue sequences," *Sociological Science*, vol. 3, pp. 444–472, 2016.

[55] N. E. Friedkin and E. C. Johnsen, *Social influence network theory: A sociological examination of small group dynamics*, vol. 33. Cambridge University Press, 2011.

[56] C. Altafini, "Consensus problems on networks with antagonistic interactions," *IEEE Transactions on Automatic Control*, vol. 58, no. 4, pp. 935–946, 2012.

[57] C. Altafini and F. Ceragioli, "Signed bounded confidence models for opinion dynamics," *Automatica*, vol. 93, pp. 114–125, 2018.

[58] A. V. Proskurnikov, A. S. Matveev, and M. Cao, "Opinion dynamics in social networks with hostile camps: Consensus vs. polarization," *IEEE Transactions on Automatic Control*, vol. 61, no. 6, pp. 1524–1536, 2015.

[59] P. Dandekar, A. Goel, and D. T. Lee, "Biased assimilation, homophily, and the dynamics of polarization," *Proceedings of the National Academy of Sciences*, vol. 110, no. 15, pp. 5791–5796, 2013.

[60] F. Garofalo, F. Lo Iudice, and E. Napoletano, "Herding as a consensus problem," *Nonlinear Dynamics*, vol. 92, no. 1, pp. 25–32, 2018.

[61] C. Altafini, "Dynamics of opinion forming in structurally balanced social networks," *PloS one*, vol. 7, no. 6, p. e38135, 2012.

[62] C. I. Hovland, I. L. Janis, and H. H. Kelley, "Communication and persuasion. new haven: Yale uni," 1953.

[63] M. McPherson, L. Smith-Lovin, and J. M. Cook, "Birds of a feather: Homophily in social networks," *Annual review of sociology*, vol. 27, no. 1, pp. 415–444, 2001.

[64] M. Ye, M. H. Trinh, Y.-H. Lim, B. D. Anderson, and H.-S. Ahn, "Continuous-time opinion dynamics on multiple interdependent topics," *Automatica*, vol. 115, p. 108884, 2020.

[65] W. Xia, M. Ye, J. Liu, M. Cao, and X.-M. Sun, "Analysis of a nonlinear opinion dynamics model with biased assimilation," *Automatica*, vol. 120, p. 109113, 2020. Publisher: Elsevier.

[66] F. Xiong, X. Wang, S. Pan, H. Yang, H. Wang, and C. Zhang, "Social recommendation with evolutionary opinion dynamics," *IEEE Transactions on Systems, Man, and Cybernetics: Systems*, vol. 50, no. 10, pp. 3804–3816, 2018. Publisher: IEEE.

[67] K. Sugishita, M. A. Porter, M. Beguerisse-Díaz, and N. Masuda, "Opinion dynamics in tie-decay networks," *arXiv:2010.00143 [nlin, physics:physics]*, Sept. 2020. arXiv: 2010.00143.

[68] L. Zino, M. Ye, and M. Cao, "A two-layer model for coevolving opinion dynamics and collective decision-making in complex social systems," *Chaos*, vol. 30, p. 083107, Aug. 2020. Publisher: American Institute of Physics.

[69] A. Franci, "Analysis and control of agreement and disagreement opinion cascades," *Swarm Intelligence*, p. 36, 2021.

[70] A. C. Martins, "Continuous opinions and discrete actions in opinion dynamics problems," *International Journal of Modern Physics C*, vol. 19, no. 04, pp. 617–624, 2008.

[71] Z. Wu, Q. Zhou, Y. Dong, J. Xu, A. H. Altalhi, and F. Herrera, "Mixed opinion dynamics based on degroot model and hegselmann–krause model in social networks," *IEEE Transactions on Systems, Man, and Cybernetics: Systems*, vol. 53, no. 1, pp. 296–308, 2022.

[72] A. C. R. Martins, "Continuous opinions and discrete actions in opinion dynamics problems," *Int. J. Mod. Phys. C*, vol. 19, pp. 617–624, Apr. 2008. Publisher: World Scientific Publishing Co.

[73] N. R. Chowdhury, I.-C. Morărescu, S. Martin, and S. Srikant, "Continuous opinions and discrete actions in social networks: a multi-agent system approach," in *2016 IEEE 55th Conference on Decision and Control (CDC)*, pp. 1739–1744, IEEE, 2016.

[74] A. Bizyaeva, A. Franci, *et al.*, "Nonlinear opinion dynamics with tunable sensitivity," *IEEE Transactions on Automatic Control*, 2022.

[75] A. F. Peralta, J. Kertész, and G. Iñiguez, "Opinion dynamics in social networks: From models to data," *arXiv preprint arXiv:2201.01322*, 2022.

[76] H. Noorazar, K. R. Vixie, A. Talebanpour, and Y. Hu, "From classical to modern opinion dynamics," *International Journal of Modern Physics C*, vol. 31, no. 07, p. 2050101, 2020.

[77] N. Perra and L. E. Rocha, "Modelling opinion dynamics in the age of algorithmic personalisation," *Scientific Reports*, vol. 9, no. 1, pp. 1–11, 2019.

[78] L. Zhu, Q. Bao, and Z. Zhang, "Minimizing polarization and disagreement in social networks via link recommendation," *Advances in Neural Information Processing Systems*, vol. 34, 2021.

[79] C.-C. Li, Y. Dong, Y. Xu, F. Chiclana, E. Herrera-Viedma, and F. Herrera, "An overview on managing additive consistency of reciprocal preference relations for consistency-driven decision making and fusion: Taxonomy and future directions," *Information Fusion*, vol. 52, pp. 143–156, 2019.

[80] E. M. Rogers and D. G. Cartano, "Methods of measuring opinion leadership," *Public opinion quarterly*, pp. 435–441, 1962.

[81] R. Iyengar, C. Van den Bulte, J. Eichert, and B. West, "How social network and opinion leaders affect the adoption of new products," *NIM Marketing Intelligence Review*, vol. 3, no. 1, pp. 16–25, 2011.

[82] J. Lees-Marshment, "Political marketing and opinion leadership: Comparative perspectives and findings," in *Comparative political leadership*, pp. 165–185, Springer, 2012.

[83] E. Gentina, D. Kilic, and P.-F. Dancoine, "Distinctive role of opinion leaders in the social networks of school adolescents: an investigation of e-cigarette use," *Public health*, vol. 144, pp. 109–116, 2017.

[84] Y. Li, S. Ma, Y. Zhang, R. Huang, *et al.*, "An improved mix framework for opinion leader identification in online learning communities," *Knowledge-Based Systems*, vol. 43, pp. 43–51, 2013.

[85] S. Peng, Y. Zhou, L. Cao, S. Yu, J. Niu, and W. Jia, "Influence analysis in social networks: A survey," *Journal of Network and Computer Applications*, vol. 106, pp. 17–32, 2018.

[86] X. Huang, D. Chen, D. Wang, and T. Ren, "Identifying influencers in social networks," *Entropy*, vol. 22, no. 4, p. 450, 2020.

[87] C. Castellano, S. Fortunato, and V. Loreto, "Statistical physics of social dynamics," *Rev. Mod. Phys.*, vol. 81, pp. 591–646, May 2009.

[88] P. Sobkowicz, "Whither Now, Opinion Modelers?," *Frontiers in Physics*, vol. 8, p. 461, 2020.

[89] F. L. Iudice, F. Sorrentino, and F. Garofalo, "On node controllability and observability in complex dynamical networks," *IEEE Control Systems Letters*, vol. 3, no. 4, pp. 847–852, 2019.

[90] C. Ancona, F. L. Iudice, A. Coppola, P. De Lellis, and F. Garofalo, "Partial controllability of network dynamical systems with unilateral inputs," *IEEE Control Systems Letters*, vol. 6, pp. 2252–2257, © 2022 IEEE.

[91] P. DeLellis, F. Garofalo, F. Lo Iudice, and G. Mancini, "Decentralised coordination of a multi-agent system based on intermittent data," *International Journal of Control*, vol. 88, no. 8, pp. 1523–1532, 2015.

[92] D. Fiore, D. Salzano, E. Cristòbal-Cóppulo, J. M. Olm, and M. di Bernardo, "Multicellular feedback control of a genetic toggle-switch in microbial consortia," *IEEE Control Systems Letters*, vol. 5, no. 1, pp. 151–156, 2020.

[93] P. A. Iglesias and B. P. Ingalls, *Control theory and systems biology.* MIT press, 2010.

[94] M. Hommelberg, C. Warmer, I. Kamphuis, J. Kok, and G. Schaeffer, "Distributed control concepts using multi-agent technology and automatic markets: An indispensable feature of smart power grids," in *2007 IEEE Power Engineering Society General Meeting*, pp. 1–7, IEEE, 2007.

[95] G. Caldarelli, S. Battiston, D. Garlaschelli, and M. Catanzaro, "Emergence of complexity in financial networks," in *Complex Networks*, pp. 399–423, Springer, 2004.

[96] P. De Lellis, A. Di Meglio, and F. Lo Iudice, "Overconfident agents and evolving financial networks," *Nonlinear Dynamics*, vol. 92, no. 1, pp. 33–40, 2018.

[97] W. Yu, G. Chen, and M. Cao, "Some necessary and sufficient conditions for second-order consensus in multi-agent dynamical systems," *Automatica*, vol. 46, no. 6, pp. 1089–1095, 2010.

[98] C. W. Wu and L. O. Chua, "Synchronization in an array of linearly coupled dynamical systems," *IEEE Transactions on Circuits and Systems I: Fundamental Theory and Applications*, vol. 42, no. 8, pp. 430–447, 1995.

[99] Q. Song, J. Cao, and W. Yu, "Second-order leader-following consensus of nonlinear multi-agent systems via pinning control," *Systems & Control Letters*, vol. 59, no. 9, pp. 553–562, 2010.

[100] Z. Li, Z. Duan, G. Chen, and L. Huang, "Consensus of multiagent systems and synchronization of complex networks: A unified viewpoint," *IEEE Transactions on Circuits and Systems I: Regular Papers*, vol. 57, no. 1, pp. 213–224, 2009.

[101] J. Gao, Y.-Y. Liu, R. M. D'souza, and A.-L. Barabási, "Target control of complex networks," *Nature Communications*, vol. 5, no. 1, pp. 1–8, 2014.

[102] L.-Z. Wang, Y.-Z. Chen, W.-X. Wang, and Y.-C. Lai, "Physical controllability of complex networks," *Scientific Reports*, vol. 7, no. 1, pp. 1–14, 2017.

[103] F. Pasqualetti, S. Zampieri, and F. Bullo, "Controllability metrics, limitations and algorithms for complex networks," *IEEE Transactions on Control of Network Systems*, vol. 1, no. 1, pp. 40–52, 2014.

[104] G. Lindmark and C. Altafini, "Minimum energy control for complex networks," *Scientific Reports*, vol. 8, no. 1, pp. 1–14, 2018.

[105] P. De Lellis, A. Di Meglio, F. Garofalo, and F. Lo Iudice, "The inherent uncertainty of temporal networks is a true challenge for control," *Scientific Reports*, vol. 11, no. 1, pp. 1–7, 2021.

[106] P. DeLellis, F. Garofalo, *et al.*, "The partial pinning control strategy for large complex networks," *Automatica*, vol. 89, pp. 111–116, 2018.

[107] B. Goodwine and J. Burdick, "Controllability with unilateral control inputs," in *Proceedings of 35th IEEE Conference on Decision and Control*, vol. 3, pp. 3394–3399, 1996.

[108] G. Lindmark and C. Altafini, "Controllability of complex networks with unilateral inputs," *Scientific Reports*, vol. 7.1, pp. 1–14, 2017.

[109] S. Frank, I. Steponavice, and S. Rebennack, "Optimal power flow: a bibliographic survey I," *Energy Systems*, vol. 3, no. 3, pp. 221–258, 2012.

[110] S. Frank, I. Steponavice, and S. Rebennack, "Optimal power flow: a bibliographic survey II," *Energy systems*, vol. 3, no. 3, pp. 259–289, 2012.

[111] D. McDonald, L. Waterbury, R. Knight, and M. Betterton, "Activating and inhibiting connections in biological network dynamics," *Biology Direct*, vol. 3, no. 1, pp. 1–14, 2008.

[112] J.-P. Merlet, "Wire-driven parallel robot: open issues," in *Romansy 19–Robot Design, Dynamics and Control*, pp. 3–10, Springer, 2013.

[113] A. Alamdari, R. Haghighi, and V. Krovi, "Stiffness modulation in an elastic articulated-cable leg-orthosis emulator: Theory and experiment," *IEEE Transactions on Robotics*, vol. 34, no. 5, pp. 1266–1279, 2018.

[114] P. Miskolczi-Bodnár *et al.*, "Definition of comparative advertising," *European Integration Studies*, vol. 3, no. 1, pp. 25–44, 2004.

[115] S. H. Saperstone and J. A. Yorke, "Controllability of linear oscillatory systems using positive controls," *SIAM Journal on Control*, vol. 9, no. 2, pp. 253–262, 1971.

[116] R. F. Brammer, "Controllability in linear autonomous systems with positive controllers," *SIAM Journal on Control*, vol. 10.2, pp. 339–353, 1972.

[117] A. Schrijver, *Theory of linear and integer programming*. John Wiley & Sons, 1998.

[118] L. Sandgren, "On convex cones," *Mathematica Scandinavica*, vol. 2, no. 1, pp. 19–28, 1954.

[119] Y.-Y. Liu, J.-J. Slotine, and A.-L. Barabasi, "Controllability of complex networks," *Nature*, vol. 473, no. 7346, pp. 167–173, 2011.

[120] Y.-Y. Liu, J.-J. Slotine, and A.-L. Barabási, "Observability of complex systems," *Proceedings of the National Academy of Sciences*, vol. 110, no. 7, pp. 2460–2465, 2013.

[121] F. L. Iudice, F. Sorrentino, and F. Garofalo, "On node controllability and observability in complex dynamical networks," *IEEE Control Systems Letters*, vol. 3, no. 4, pp. 847–852, 2019.

[122] T. Chen, X. Liu, and W. Lu, "Pinning complex networks by a single controller," *IEEE Transactions on Circuits and Systems I: Regular Papers*, vol. 54, no. 6, pp. 1317–1326, 2007.

[123] A. J. Whalen, S. N. Brennan, T. D. Sauer, and S. J. Schiff, "Observability and controllability of nonlinear networks: The role of symmetry," *Physical Review X*, vol. 5, no. 1, p. 011005, 2015.

[124] T. H. Summers, F. L. Cortesi, and J. Lygeros, "On submodularity and controllability in complex dynamical networks," *IEEE Transactions on Control of Network Systems*, vol. 3, no. 1, pp. 91–101, 2015.

[125] Z. Yuan, C. Zhao, Z. Di, W.-X. Wang, and Y.-C. Lai, "Exact controllability of complex networks," *Nature communications*, vol. 4, 2013.

[126] G. Ramos, A. P. Aguiar, and S. Pequito, "An overview of structural systems theory," *Automatica*, vol. 140, p. 110229, 2022.

[127] J. Gao, Y.-Y. Liu, R. M. D'Souza, and A.-L. Barabási, "Target control of complex networks," *Nature communications*, vol. 5, 2014.

[128] F. L. Iudice, F. Sorrentino, and F. Garofalo, "Structural permeability of complex networks to control signals," *Nature Communications*, Sep 2015.

[129] S. Poljak, "On the generic dimension of controllable subspaces," *Automatic Control, IEEE Transactions on*, vol. 35, pp. 367–369, Mar 1990.

[130] E. Barabási, Albert-Lászlóand Bonabeau, "Scale-free networks," *Scientific American*, vol. 288, no. 5, pp. 60–69, 2003.

[131] K.-I. Goh, B. Kahng, and D. Kim, "Universal behavior of load distribution in scale-free networks," *Phys. Rev. Lett.*, vol. 87, p. 278701, Dec 2001.

[132] K. Börner, S. Sanyal, and A. Vespignani, "Network science," *Annual review of information science and technology*, vol. 41, no. 1, pp. 537–607, 2007.

[133] M. Molloy and B. Reed, "A critical point for random graphs with a given degree sequence," *Random structures & algorithms*, vol. 6, no. 2-3, pp. 161–180, 1995.

[134] N. Schwartz, R. Cohen, D. Ben-Avraham, A.-L. Barabási, and S. Havlin, "Percolation in directed scale-free networks," *Physical Review E*, vol. 66, no. 1, p. 015104, 2002.

[135] R. Tarjan, "Depth-first search and linear graph algorithms," *SIAM journal on computing*, vol. 1, no. 2, pp. 146–160, 1972.

[136] C. Ancona, P. De Lellis, and F. L. Iudice, "Influencing opinions in a nonlinear pinning control model," *IEEE Control Systems Letters*, 2023.

[137] A. Bizyaeva, A. Franci, and N. E. Leonard, "Nonlinear opinion dynamics with tunable sensitivity," *arXiv preprint arXiv:2009.04332*, 2020.

[138] C. Ancona, F. Lo Iudice, *et al.*, "A model-based opinion dynamics approach to tackle vaccine hesitancy," *Scientific Reports*, vol. 12, no. 1, pp. 1–8, 2022.

[139] G. Weisbuch, "Bounded confidence and social networks," *The European Physical Journal B*, vol. 38, no. 2, pp. 339–343, 2004.

[140] J. P. Carpenter, C. C. Shelton, and S. E. Schroeder, "The education influencer: A new player in the educator professional landscape," *Journal of Research on Technology in Education*, pp. 1–16, 2022.

[141] N. Puri, E. A. Coomes, *et al.*, "Social media and vaccine hesitancy: new updates for the era of covid-19 and globalized infectious diseases," *Human Vaccines & Immunotherapeutics*, vol. 16, no. 11, pp. 2586–2593, 2020.

[142] M. Riedl, C. Schwemmer, S. Ziewiecki, and L. M. Ross, "The rise of political influencers—perspectives on a trend towards meaningful content," *Frontiers in Communication*, vol. 6, p. 752656, 2021.

[143] M. Sudha and K. Sheena, "Impact of influencers in consumer decision process: the fashion industry," *SCMS Journal of Indian Management*, vol. 14, no. 3, pp. 14–30, 2017.

[144] E. Yildiz, A. Ozdaglar, *et al.*, "Binary opinion dynamics with stubborn agents," *ACM Transactions on Economics and Computation (TEAC)*, vol. 1, no. 4, pp. 1–30, 2013.

[145] T. Li and H. Zhu, "Effect of the media on the opinion dynamics in online social networks," *Physica A: Statistical Mechanics and its Applications*, vol. 551, p. 124117, 2020.

[146] F. L. Iudice, F. Garofalo, and P. De Lellis, "Bounded partial pinning control of network dynamical systems," *IEEE Transactions on Control of Network Systems*, vol. 10, no. 1, pp. 238–248, 2022.

[147] F. Dietrich, S. Martin, *et al.*, "Control via leadership of opinion dynamics with state and time-dependent interactions," *IEEE Transactions on Automatic Control*, vol. 63, no. 4, pp. 1200–1207, 2017.

[148] Z. Zhao, L. Shi, *et al.*, "Opinion dynamics of social networks with intermittent-influence leaders," *IEEE Transactions on Computational Social Systems*, pp. 1–10, 2022.

[149] W. Su, X. Chen, *et al.*, "Noise-based control of opinion dynamics," *IEEE Transactions on Automatic Control*, vol. 67, no. 6, pp. 3134–3140, 2021.

[150] L. Shi, Y. Cheng, *et al.*, "Leader-follower opinion dynamics of signed social networks with asynchronous trust/distrust level evolution," *IEEE Transactions on Network Science and Engineering*, vol. 9, no. 2, pp. 495–509, 2021.

[151] R. Gray, A. Franci, *et al.*, "Multiagent decision-making dynamics inspired by honeybees," *IEEE Transactions on Control of Network Systems*, vol. 5, no. 2, pp. 793–806, 2018.

[152] M. Jalili, O. A. Sichani, *et al.*, "Optimal pinning controllability of complex networks: Dependence on network structure," *Physical Review E*, vol. 91, no. 1, p. 012803, 2015.

[153] Y. Orouskhani, M. Jalili, *et al.*, "Optimizing dynamical network structure for pinning control," *Scientific reports*, vol. 6, no. 1, pp. 1–13, 2016.

[154] N. E. Leonard, K. Lipsitz, *et al.*, "The nonlinear feedback dynamics of asymmetric political polarization," *Proceedings of the National Academy of Sciences*, vol. 118, no. 50, 2021.

[155] P. De Lellis, M. di Bernardo, *et al.*, "Pinning control of complex networks via edge snapping," *Chaos: An Interdisciplinary Journal of Nonlinear Science*, vol. 21, no. 3, p. 033119, 2011.

[156] A. Arenas, Díaz-Guilera, *et al.*, "Synchronization in complex networks," *Physics Reports*, vol. 469, no. 3, pp. 93–153, 2008.

[157] S. A. Haslam, S. D. Reicher, H. P. Selvanathan, A. M. Gaffney, N. K. Steffens, D. Packer, J. J. Van Bavel, E. Ntontis, F. Neville, S. Vestergren, *et al.*, "Examining the role of donald trump and his supporters in the 2021 assault on the us capitol: A dual-agency model of identity leadership and engaged followership," *The Leadership Quarterly*, vol. 34, no. 2, p. 101622, 2023.

[158] X. Zheng, H. Tian, Z. Wan, X. Wang, D. D. Zeng, and F.-Y. Wang, "Game starts at gamestop: Characterizing the collective behaviors and social dynamics in the short squeeze episode," *IEEE Transactions on Computational Social Systems*, vol. 9, no. 1, pp. 45–58, 2021.

[159] A. McNabb, "Comparison theorems for differential equations," *Journal of mathematical analysis and applications*, vol. 119, no. 1-2, pp. 417–428, 1986.

[160] M. Barthelemy, "Betweenness centrality in large complex networks," *The European Physical Journal B*, vol. 38, no. 2, pp. 163–168, 2004.

[161] K. A. Feemster and C. Szipszky, "Resurgence of measles in the united states: how did we get here?," *Current Opinion in Pediatrics*, vol. 32, no. 1, pp. 139–144, 2020.

[162] A. B. Wilder-Smith and K. Qureshi, "Resurgence of measles in Europe: a systematic review on parental attitudes and beliefs of measles vaccine," *Journal of Epidemiology and Global Health*, vol. 10, no. 1, p. 46, 2020.

[163] C. A. Dimala, B. M. Kadia, M. A. M. Nji, and N. N. Bechem, "Factors associated with measles resurgence in the united states in the post-elimination era," *Scientific Reports*, vol. 11, no. 1, pp. 1–10, 2021.

[164] J. V. Lazarus, S. C. Ratzan, A. Palayew, L. O. Gostin, H. J. Larson, K. Rabin, S. Kimball, and A. El-Mohandes, "A global survey of potential acceptance of a COVID-19 vaccine," *Nature Medicine*, vol. 27, pp. 225–228, Feb. 2021. Number: 2 Publisher: Nature Publishing Group.

[165] G. Graffigna, L. Palamenghi, S. Boccia, and S. Barello, "Relationship between Citizens' Health Engagement and Intention to Take the COVID-19 Vaccine in Italy: A Mediation Analysis," *Vaccines (Basel)*, vol. 8, Oct. 2020.

[166] P. Peretti-Watel, V. Seror, S. Cortaredona, O. Launay, J. Raude, P. Verger, L. Fressard, F. Beck, S. Legleye, O. L'Haridon, D. Léger, and J. K. Ward, "A future vaccination campaign against COVID-19 at risk of vaccine hesitancy and politicisation," *The Lancet Infectious Diseases*, vol. 20, pp. 769–770, July 2020. Publisher: Elsevier.

[167] M. S. Islam, A.-H. M. Kamal, A. Kabir, D. L. Southern, S. H. Khan, S. M. Hasan, T. Sarkar, S. Sharmin, S. Das, T. Roy, *et al.*, "Covid-19 vaccine rumors and conspiracy theories: The need for cognitive inoculation against misinformation to improve vaccine adherence," *PloS One*, vol. 16, no. 5, p. e0251605, 2021.

[168] A. A. Dror, N. Eisenbach, S. Taiber, N. G. Morozov, M. Mizrachi, A. Zigron, S. Srouji, and E. Sela, "Vaccine hesitancy: the next challenge in the fight against COVID-19," *Eur J Epidemiol*, vol. 35, pp. 775–779, Aug. 2020.

[169] M. S. Steffens, A. G. Dunn, J. Leask, and K. E. Wiley, "Using social media for vaccination promotion: Practices and challenges," *Digital Health*, vol. 6, p. 2055207620970785, 2020.

[170] J. M. Hofman, D. J. Watts, S. Athey, F. Garip, T. L. Griffiths, J. Kleinberg, H. Margetts, S. Mullainathan, M. J. Salganik, S. Vazire, *et al.*, "Integrating explanation and prediction in computational social science," *Nature*, pp. 1–8, 2021.

[171] A. Cardillo and N. Masuda, "Critical mass effect in evolutionary games triggered by zealots," *Physical Review Research*, vol. 2, no. 2, p. 023305, 2020.

[172] G. Verma, A. Swami, and K. Chan, "The impact of competing zealots on opinion dynamics," *Physica A: Statistical Mechanics and its Applications*, vol. 395, pp. 310–331, 2014.

[173] A. V. Proskurnikov and R. Tempo, "A tutorial on modeling and analysis of dynamic social networks. part i," *Annual Reviews in Control*, vol. 43, pp. 65–79, 2017.

[174] N. Polemi, "Port cybersecurity," in *Securing Critical Information Infrastructures and Supply Chains*, Elsevier, 2017.

[175] G. M. Sullivan and A. R. Artino Jr, "Analyzing and interpreting data from likert-type scales," *Journal of Graduate Medical Education*, vol. 5, no. 4, p. 541, 2013.

[176] J. Carifio and R. Perla, "Resolving the 50-year debate around using and misusing likert scales," *Medical Education*, vol. 42, no. 12, pp. 1150–1152, 2008.

[177] F. Sorrentino, M. di Bernardo, F. Garofalo, and G. Chen, "Controllability of complex networks via pinning," *Physical Review E*, vol. 75, no. 4, p. 046103, 2007.

[178] T. Guardian. `https://www.theguardian.com/world/2021/mar/05/covid-vaccine-ads-aim-to-influence-without-alienating-people`, Feb. 2021.

[179] A. G. H. Department. `https://www.health.gov.au/news/new-information-campaign-to-encourage-australians-to-get-a-covid-19-vaccine`, Feb. 2021.

[180] N. News. `https://www.nbcnews.com/health/health-news/sweeping-ad-campaign-will-encourage-vaccinations-rcna309`, Feb. 2021.

[181] F. Trentini, V. Marziano, G. Guzzetta, M. Tirani, D. Cereda, P. Poletti, R. Piccarreta, A. Barone, G. Preziosi, F. Arduini, *et al.*, "Pressure on the health-care system and intensive care utilization during the covid-19 outbreak in the lombardy region of italy: A retrospective observational study in 43,538 hospitalized patients," *American Journal of Epidemiology*, vol. 191, no. 1, pp. 137–146, 2022.

[182] S. D. Østergaard, M. Schmidt, E. Horváth-Puhó, R. W. Thomsen, and H. T. Sørensen, "Thromboembolism and the oxford–astrazeneca covid-19 vaccine: side-effect or coincidence?," *The Lancet*, vol. 397, no. 10283, pp. 1441–1443, 2021.

[183] H. J. Larson and D. A. Broniatowski, "Volatility of vaccine confidence," *Science*, vol. 371, no. 6536, pp. 1289–1289, 2021.

[184] G. Muric, Y. Wu, and E. Ferrara, "COVID-19 vaccine hesitancy on social media: building a public twitter dataset of anti-vaccine content, vaccine misinformation and conspiracies," *JMIR Public Health and Surveillance*, vol. 7, p. e20642, 2021.

[185] H. Piedrahita-Valdés, D. Piedrahita-Castillo, J. Bermejo-Higuera, P. Guillem-Saiz, J. R. Bermejo-Higuera, J. Guillem-Saiz, J. A. Sicilia-Montalvo, and F. Machío-Regidor, "Vaccine hesitancy on social media: Sentiment analysis from june 2011 to april 2019," *Vaccines*, vol. 9, no. 1, p. 28, 2021.

[186] M. Kosinski, D. Stillwell, and T. Graepel, "Private traits and attributes are predictable from digital records of human behavior," *Proceedings of the National Academy of Sciences*, vol. 110, no. 15, pp. 5802–5805, 2013.

[187] I. Asadi Someh, C. F. Breidbach, M. Davern, and G. Shanks, "Ethical implications of big data analytics," *Research-in-Progress Papers*, vol. 24, 2016.

[188] M. Ye, Y. Qin, A. Govaert, B. D. O. Anderson, and M. Cao, "An influence network model to study discrepancies in expressed and private opinions," *Automatica*, vol. 107, pp. 371–381, Sept. 2019.

[189] N. Modani, S. Nagar, S. Shannigrahi, R. Gupta, K. Dey, S. Goyal, and A. A. Nanavati, "Like-minded communities: bringing the familiarity and similarity together," *World Wide Web*, vol. 17, no. 5, pp. 899–919, 2014.

[190] U. D. Service. `https://ukdataservice.ac.uk/help/data-types/longitudinal-data-studies/`.

[191] U.S.Bureau. `https://www.bls.gov/nls/cohorts.htm`.

[192] C. Andrade, "The limitations of online surveys," *Indian journal of psychological medicine*, vol. 42, no. 6, pp. 575–576, 2020.

[193] G. Graffigna, L. Palamenghi, S. Boccia, and S. Barello, "Relationship between citizens' health engagement and intention to take the covid-19 vaccine in italy: a mediation analysis," *Vaccines*, vol. 8, no. 4, p. 576, 2020.

[194] L.-A. Cotfas, C. Delcea, I. Roxin, C. Ioanăş, D. S. Gherai, and F. Tajariol, "The longest month: Analyzing covid-19 vaccination opinions dynamics from tweets in the month following the first vaccine announcement," *IEEE Access*, vol. 9, pp. 33203–33223, 2021.

[195] S. Singh and A. Mahmood, "The nlp cookbook: Modern recipes for transformer based deep learning architectures," *IEEE Access*, vol. 9, pp. 68675–68702, 2021.

[196] Q. Li, H. Peng, J. Li, C. Xia, R. Yang, L. Sun, P. S. Yu, and L. He, "A survey on text classification: From shallow to deep learning," *arXiv preprint arXiv:2008.00364*, 2020.

[197] S. Minaee, N. Kalchbrenner, E. Cambria, N. Nikzad, M. Chenaghlu, and J. Gao, "Deep learning–based text classification: a comprehensive review," *ACM Computing Surveys (CSUR)*, vol. 54, no. 3, pp. 1–40, 2021.

[198] Q. Liu, M. J. Kusner, and P. Blunsom, "A survey on contextual embeddings," *arXiv preprint arXiv:2003.07278*, 2020.

[199] Y. Pruksachatkun, J. Phang, H. Liu, P. M. Htut, X. Zhang, R. Y. Pang, C. Vania, K. Kann, and S. R. Bowman, "Intermediate-task transfer learning with pretrained models for natural language understanding: When and why does it work?," *arXiv preprint arXiv:2005.00628*, 2020.

[200] F. Zhuang, Z. Qi, K. Duan, D. Xi, Y. Zhu, H. Zhu, H. Xiong, and Q. He, "A comprehensive survey on transfer learning," *Proceedings of the IEEE*, vol. 109, no. 1, pp. 43–76, 2020.

[201] A. Sarkar, S. Reddy, and R. S. Iyengar, "Zero-shot multilingual sentiment analysis using hierarchical attentive network and bert," in *Proceedings of the 2019 3rd International Conference on Natural Language Processing and Information Retrieval*, pp. 49–56, 2019.

[202] S. G. Tesfagergish, J. Kapočiūtė-Dzikienė, and R. Damaševičius, "Zero-shot emotion detection for semi-supervised sentiment analysis using sentence transformers and ensemble learning," *Applied Sciences*, vol. 12, no. 17, p. 8662, 2022.

[203] Z. Ye, Y. Geng, J. Chen, J. Chen, X. Xu, S. Zheng, F. Wang, J. Zhang, and H. Chen, "Zero-shot text classification via reinforced self-training," in *Proceedings of the 58th Annual Meeting of the Association for Computational Linguistics*, pp. 3014–3024, 2020.

[204] P. Kumar, K. Pathania, and B. Raman, "Zero-shot learning based cross-lingual sentiment analysis for sanskrit text with insufficient labeled data," *Applied Intelligence*, pp. 1–18, 2022.

[205] S. Prabhu, M. Mohamed, and H. Misra, "Multi-class text classification using bert-based active learning," *arXiv preprint arXiv:2104.14289*, 2021.

[206] L. E. Dor, A. Halfon, A. Gera, E. Shnarch, L. Dankin, L. Choshen, M. Danilevsky, R. Aharonov, Y. Katz, and N. Slonim, "Active learning for bert: an empirical study," in *Proceedings of the 2020 Conference on Empirical Methods in Natural Language Processing (EMNLP)*, pp. 7949–7962, 2020.

[207] C. Sun, X. Qiu, Y. Xu, and X. Huang, "How to fine-tune bert for text classification?," in *China national conference on Chinese computational linguistics*, pp. 194–206, Springer, 2019.

[208] E. D'Andrea, P. Ducange, A. Bechini, A. Renda, and F. Marcelloni, "Monitoring the public opinion about the vaccination topic from tweets analysis," *Expert Systems with Applications*, vol. 116, pp. 209–226, 2019.

[209] M. T. J. Ansari and N. A. Khan, "Worldwide covid-19 vaccines sentiment analysis through twitter content.," *Electronic Journal of General Medicine*, vol. 18, no. 6, 2021.

[210] N. Alturayeif and H. Luqman, "Fine-grained sentiment analysis of arabic covid-19 tweets using bert-based transformers and dynamically weighted loss function," *Applied Sciences*, vol. 11, no. 22, p. 10694, 2021.

[211] M. Munikar, S. Shakya, and A. Shrestha, "Fine-grained sentiment classification using bert," in *2019 Artificial Intelligence for Transforming Business and Society (AITB)*, vol. 1, pp. 1–5, IEEE, 2019.

[212] M. Polignano, V. Basile, P. Basile, M. de Gemmis, and G. Semeraro, "Alberto: Modeling italian social media language with bert," *IJCoL. Italian Journal of Computational Linguistics*, vol. 5, no. 5-2, pp. 11–31, 2019.

[213] E. Akyürek, D. Schuurmans, J. Andreas, T. Ma, and D. Zhou, "What learning algorithm is in-context learning? investigations with linear models," *arXiv preprint arXiv:2211.15661*, 2022.

[214] M. Pota, M. Ventura, R. Catelli, and M. Esposito, "An effective bert-based pipeline for twitter sentiment analysis: a case study in italian," *Sensors*, vol. 21, no. 1, p. 133, 2021.

[215] D. G. Myers and H. Lamm, "The group polarization phenomenon.," *Psychological bulletin*, vol. 83, no. 4, p. 602, 1976.

[216] C. Nickerson, "What is deindividuation in psychology? definition and examples," *Simply Psychology*, 2021.

[217] N. E. Friedkin, "Choice shift and group polarization," *American Sociological Review*, pp. 856–875, 1999.

[218] C. R. Sunstein, *# Republic.* Princeton university press, 2018.

[219] E. Pariser, *The filter bubble: What the Internet is hiding from you.* Penguin UK, 2011.

[220] U. Chitra and C. Musco, "Analyzing the impact of filter bubbles on social network polarization," in *Proceedings of the 13th International Conference on Web Search and Data Mining*, pp. 115–123, 2020.

[221] C. A. Bail, L. P. Argyle, T. W. Brown, J. P. Bumpus, H. Chen, M. F. Hunzaker, J. Lee, M. Mann, F. Merhout, and A. Volfovsky, "Exposure to opposing views on social media can increase political polarization," *Proceedings of the National Academy of Sciences*, vol. 115, no. 37, pp. 9216–9221, 2018.

[222] J. Buder, L. Rabl, M. Feiks, M. Badermann, and G. Zurstiege, "Does negatively toned language use on social media lead to attitude polarization?," *Computers in Human Behavior*, vol. 116, p. 106663, 2021.

[223] J. A. Fine and M. F. Hunt, "Negativity and elite message diffusion on social media," *Political Behavior*, pp. 1–19, 2021.

[224] A. Rudat and J. Buder, "Making retweeting social: The influence of content and context information on sharing news in twitter," *Computers in Human Behavior*, vol. 46, pp. 75–84, 2015.

[225] A. Chmiel, P. Sobkowicz, J. Sienkiewicz, G. Paltoglou, K. Buckley, M. Thelwall, and J. A. Hołyst, "Negative emotions boost user activity at bbc forum," *Physica A: statistical mechanics and its applications*, vol. 390, no. 16, pp. 2936–2944, 2011.

[226] F. Zollo, P. K. Novak, M. Del Vicario, A. Bessi, I. Mozetič, A. Scala, G. Caldarelli, and W. Quattrociocchi, "Emotional dynamics in the age of misinformation," *PloS one*, vol. 10, no. 9, p. e0138740, 2015.

[227] J. P. Schöne, B. Parkinson, and A. Goldenberg, "Negativity spreads more than positivity on twitter after both positive and negative political situations," *Affective Science*, vol. 2, no. 4, pp. 379–390, 2021.

[228] P. Rossini, J. Hemsley, S. Tanupabrungsun, F. Zhang, and J. Stromer-Galley, "Social media, opinion polls, and the use of persuasive messages during the 2016 us election primaries," *Social Media+ Society*, vol. 4, no. 3, p. 2056305118784774, 2018.

[229] K. W. Church, "Word2vec," *Natural Language Engineering*, vol. 23, no. 1, pp. 155–162, 2017.

[230] Y. Sharma, G. Agrawal, P. Jain, and T. Kumar, "Vector representation of words for sentiment analysis using glove," in *2017 international conference on intelligent communication and computational techniques (icct)*, pp. 279–284, IEEE, 2017.

[231] L. Zhang, S. Wang, and B. Liu, "Deep learning for sentiment analysis: A survey," *Wiley Interdisciplinary Reviews: Data Mining and Knowledge Discovery*, vol. 8, no. 4, p. e1253, 2018.